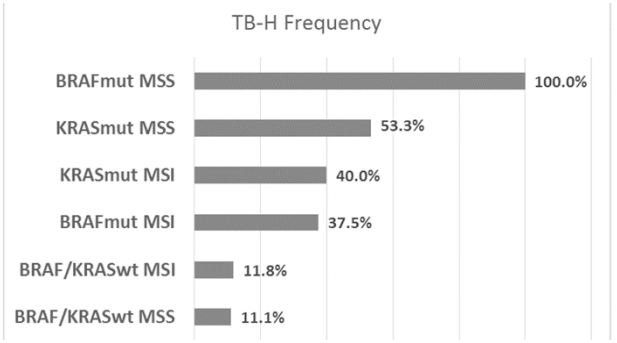

Conclusions: Mutation of BRAF or KRAS is strongly associated with TB-H in CRC, independently of MSI/MSS status. The findings suggest the hypothesis that RAS-RAF MAPK signalling may be directly related to the epithelial–mesenchymal transition that underlies TB in CRC.

Genitourinary Pathology (including Renal tumors)

803 Analysis of Presence and Extent of Adverse Pathologic Characteristics in Small Clear Cell Renal Cell Carcinomas

Adebowale Adeniran, Brian Shuch, Maria Serrano, Adam Kibel, Cayce Nawaf, Robin Vollmer, Peter Humphrey. Yale University School of Medicine, New Haven, CT; Kaiser Permanente, San Francisco, CA; Brigham & Women's Hospital, Boston, MA; Veteran Affairs Medical Center, Durham, NC.

Background: Tumor size has been used for decision making in the management of patients with Renal Cell Carcinoma (RCC). Active surveillance in selected patients is now increasingly common and tumor size is being used as threshold for enrollment. Adverse pathologic features have been described in renal tumors and these features correlate well with prognosis in RCC. The aim of this study was to determine the frequency and extent of adverse pathologic characteristics in small RCC.

Design: A computer search of a single institution database for partial and radical nephrectomies performed for RCC identified a total of 898 consecutive cases of RCC with available clinical follow-up. Tumor slides were reviewed for histologic correlation for the following adverse conditions: presence and proportion of high nuclear grade, necrosis, rhabdoid features, sarcomatoid features and lymphovascular invasion (LVI). Relationships between the variables were examined by Kruskal-Wallis tests, Wilcoxon tests, Chi-square tests and logistic regression.

Results: Every tumor characteristic evaluated was significantly related to size in all RCC. The frequency of adverse tumor histopathologic characteristics based on size of 629 cases of clear cell RCC is provided in Table 1 (p values by Chi-square test). 15% of cases of clear cell RCC ≤ 4 cm have some component of high grade nuclear features compared with 45% in cases > 4cm. 21% of cases ≤ 4 cm have areas of necrosis compared with 46% in cases > 4cm. 3% of cases ≤ 4 cm have LVI compared with 17% in cases > 4cm.

	Size ≤4cm(n=288)	Size >4cm(n=341)	p value
High grade	43 (15%)	153 (45%)	~ 0
Necrosis	60 (21%)	157 (46%)	~ 0
Rhabdoid	3 (1%)	27 (8%)	.0001
Sarcomatoid	3 1%)	21 (6%)	.01
LVI	9 (3%)	58 (17%)	~ 0

Conclusions: Adverse histopathologic characteristics in small clear cell RCC may have clinical implications for tumor sampling and clinical management, especially in patients with tumors ≤ 4cm for whom active surveillance is considered.

804 A Prospective Investigation of PTEN Loss and ERG Expression in Lethal Prostate Cancer

Thomas Ahearn, Andreas Pettersson, Travis Gerke, Carlos Morais, Jessica Hicks, Massimo Loda, Meir Stampfer, Angelo De Marzo, Lorelei Mucci, Tamara Lotan. Harvard School of Public Health, Boston, MA; Johns Hopkins School of Medicine, Baltimore, MD; Harvard Medical School, Boston, MA.

Background: PTEN is a tumor suppressor frequently deleted in prostate cancer that may be a useful prognostic biomarker. However, the association of PTEN loss with lethal disease has not been tested in a large, predominantly surgically-treated cohort.

Design: We studied 1045 men in the Physicians' Health Study and Health Professionals Follow-up Study diagnosed with prostate cancer from 1986 – 2009, treated with radical prostatectomy (95%) and followed through 2012 for biochemical recurrence and cancer and all-cause mortality. Genetically validated and dichotomously scored PTEN and ERG immunohistochemistry (IHC) assays were performed on tumor tissue microarrays (TMA). Cox proportional hazards models adjusting for age and BMI at diagnosis, Gleason grade, and clinical/pathologic stage were used to estimate hazard ratios (HR) and 95% confidence intervals (CI) of the association with lethal disease.

Results: On average, men were followed 11.6 years, during which there were 81 lethal events. 16% of tumors had homogeneous PTEN loss in all TMA cores, 9% had heterogeneous PTEN loss, and the remaining 75% had intact PTEN expression. Homogeneous PTEN loss was significantly associated with ERG expression, higher Gleason grade, and higher pathologic stage. In multivariate analysis, cases with homogeneous PTEN loss (HR=1.9; 95% CI=1.2-3.0), but not cases with heterogeneous PTEN loss (HR=1.2; 95% CI=0.5-2.6), were associated with lethal progression. Homogeneous PTEN loss was more strongly associated with lethal progression among tumors with Gleason score ≤ 7 (HR=2.7; 95% CI=1.4-5.5) compared to Gleason score 8-10 (HR=1.6; 95% CI=0.9-3.1). Finally, any PTEN loss (homogeneous or heterogeneous) was significantly associated with lethal progression only in ERG negative tumors (HR=2.8; 95% CI=1.5-5.2) in multivariate analysis.

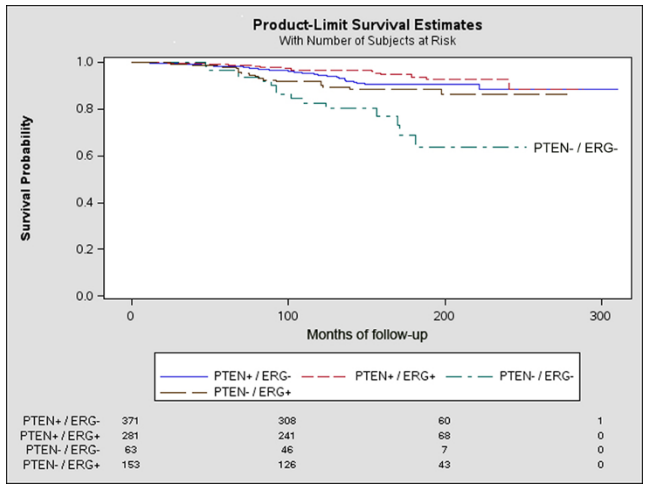

Conclusions: PTEN loss is associated with increased risk of lethal progression in prostatectomy samples independent of clinical-pathologic parameters, particularly in the ERG negative subgroup. These validated and inexpensive IHC assays may be useful for routine risk stratification in low and intermediate risk prostate cancer.

805 A Retrospective Analysis of the Outcome for Patients With ASAP Diagnosis in the Trans-Rectal Ultrasound (TRUS)-Guided Prostate Biopsies at Pennine Acute Hospitals

Khalid Ahmed, Stefano Sioletic. Pennine Acute Hospitals - Royal Oldham Hospital, Oldham, Greater Manchester, Lancashire, United Kingdom.

Background: In patients with high PSA or clinically suspicious patients the trans rectal ultrasound (TRUS)-guided prostate biopsy became the gold standard in the diagnosis of the tumours. In a small percentage of cases the pathologist has insufficient data to make a definitive diagnosis. This entity called ASAP, is defined as a "focus of small acinar structures formed by atypical epithelial cells". According to the literature the cancer detection rate in the second biopsy after a first diagnosis of ASAP varies between 21% and 60%. The reason of the conflicting results found by different authors is the subjectivity of the diagnostic criteria.

Design: We retrospectively reviewed all the TRUS-guided biopsy reports of patients that underwent to TRUS-guided biopsy in Pennine Acute Trust between 2007 and 2012. Of the 4631 cases 270 (5.8%) were diagnosed as ASAP, 215 (4.6%) of which were reported in the first biopsy specimen. All cases were stained for racemase (AMCR), p63 and high-molecular weight cytokeratin.

Results: The mean age of the patients that were diagnosed with ASAP was 66.8 (39-86). 98 (45.6 %) patients with persistent clinical suspicion underwent another TRUS-guided biopsy. 59 (60%) of the subsequent biopsies showed a hyperplastic process or prostatitis with no tumour. In 8 (13.7%) of this patients a High Grade PIN has been identified. 39 (39.8%) of the subsequent biopsies showed a primary adenocarcinoma. In 3 cases the tumour was diagnosed only in the third biopsies after 2 to 3 years from the first diagnoses. The median time elapsed (MET) between the first and second biopsy was 13.6 month for the cases subsequently reported as tumour and 9 month for the one with no tumour. 23 ASAP cases were subsequently reported as Gleason 6 (MET: 14.34 month), 12 as Gleason 7 (7 cases 3+4 and 5 cases 4+3) (MET: 14.58 months), four cases as Gleason ≥ 8 (MET: 9.5 months) (3 cases 4+4 and 1 case 5+4).

Conclusions: In our data the prostate cancer has been found subsequently in 18.1% of all the cases with an ASAP diagnosis. This rate is increasing to 39.8 % in ASAP cases when a repeat biopsy had been performed. This results together with the relatively shorter MET in patients diagnosed as tumour in the repeat biopsy are suggesting that a multidisciplinary approach involving the clinicians and the radiologist are extremely important to identify rapidly the patients that needs a subsequent biopsy for a definitive diagnosis of tumour.

806 Renal Oncocytic Neoplasms Diagnosed By Image-Guided Core Needle Biopsy: A Morphologic and Immunophenotypic Study of 145 Cases With Clinical Follow-Up at a Single Academic Institution

Megan Alderman, Lakshmi Kunju, Ritu Bhalla, Ganesh Palapattu, Elaine Caoili, Khaled Hafez, J Stuart Wolf, Angela Wu. University of Michigan Health System, Ann Arbor, MI; Louisiana State University Health Sciences Center, New Orleans, LA.

Background: Core needle biopsies (CNB) of renal masses are becoming common; however, oncocytic neoplasms (ON) are challenging to accurately classify due to histologic overlap among several benign and malignant oncocytic tumors. There is limited literature documenting accuracy, immunohistochemistry and clinical follow-up of renal ON on CNB.

Design: All renal ON on CNB (hematoxylin and eosin slides) from 2006-2013 at the University of Michigan were retrospectively reviewed by two genitourinary pathologists and preliminarily categorized as favor oncocytoma; favor renal cell carcinoma (RCC) with subtype; or cannot exclude RCC. Immunohistochemistry (IHC) composed of at least CK7, C-KIT, and S100A1 was scored as diffusely positive, single cells/clusters positive or negative and a final (post IHC) diagnosis was made. Concordance between final CNB and resection was determined by assessing a change from a benign to malignant diagnosis or vice-versa. Clinical follow-up included resection, active surveillance (AS), ablation, or no treatment. Tumor interval growth (mm/year) was compared among diagnostic categories for patients on AS. Adverse outcomes including metastases, death of disease, or recurrence were recorded.

Results: Incidence of ON was 16% (145/909 CNB) and final diagnoses included: favor oncocytoma (85); favor RCC (19); and cannot exclude RCC (40). The diagnosis was revised following IHC in 8% (11) (predominantly conversion of favor oncocytoma to cannot exclude RCC with 3 cases confirmed as RCC on excision). Resection was performed in 20% (29) with 97% concordance; ablation in 22%; and AS in 54% cases. Of 40 cases of cannot exclude RCC, 25% underwent resection with a diagnosis of RCC in all but one (hybrid oncocytic tumor). Patients on AS showed no statistical interval growth difference among diagnostic categories (p=0.85). No adverse outcomes occurred.

Conclusions: ON comprise a significant subset (16%) of CNB. Selective IHC in conjunction with morphology are essential for accurate diagnosis. The vast majority (72%) of ON could be classified as favor oncocytoma or favor RCC. The majority (90%) of cannot exclude RCC on CNB were RCC on excision. There was high concordance between CNB and resection diagnoses. No adverse outcomes were identified.

807 Is Ki-67 a Reliable Marker To Differentiate Between Nested Variant of Urothelial Carcinoma and Proliferation of Von Brunn's Nests (VBN)?

Fatima Al-Hashimi, Wei Tian, Jonathan Epstein. Johns Hopkins Medicine, Baltimore, MD.

Background: Usual nested UC (NVUC) is an uncommon variant of UC, characterised by small nests with a bland cytology and an aggressive behavior. Due to the tumour's minimally atypical cytology it may be misdiagnosed as a benign lesion. The leading differential diagnosis is a florid proliferation of VBN which can also make a tumor-like mass. Large nested variant of urothelial carcinoma (LNVUC) is a relatively new entity and can even be harder to differentiate from florid VBN. This study aims to establish whether Ki-67 is a reliable marker, which can be used as an aid in making a diagnosis. To date, only two studies addressed this topic; both of which with a smaller number of cases and none of which included LNVUC.

Design: We retrieved 34 NVUC, 11 LNVUC and 14 florid proliferation of VBN from one of the author's consult files. The International Breast Group method for interpreting Ki-67 staining was used by defining a hot spot and manually counting the positive cells within a nest of at least 500 epithelial cells.

Results: The mean age of the patients for the urothelial carcinoma was 67.5 yrs, with a male predominance. The mean age of the benign counterpart was 54.0, with an even gender distribution. The mean positive Ki-67 percentage for NVUC was 16.5%, LNVUC 25.2% and VBN 4.3%. Ki-67 rate was different between combined NVUC/LNVUC (18.6%) versus florid VBN (4.3%), p=0.0006. The difference in Ki-67 rate between NVUC and LNVUC was not statistically significant, p=0.08. With a Ki-67 rate of ≤15%, the diagnosis is consistent with florid VBN, as 13/14 cases (93%) of the cases had this low Ki-67 rate; the single outlier showed an 18.2% proliferation. However, a low Ki-67 rate is not specific for florid VBN as NVUC and LNVUC can have similar low values. However, a Ki-67 of >30% is useful as it is not seen in VBN proliferations and is present in a minority of NVUC (15%, 5/34) and more frequently in LNVUC (40%, 5/34).

Conclusions: While a Ki-67 of ≤15% should be present before diagnosing florid VBN, this low proliferation rate does not rule out nested urothelial carcinoma. Although in most cases IHC for Ki-67 is not helpful in distinguishing between these two entities and requires morphological distinction, a Ki-67>30% is helpful in establishing the diagnoses of LNVUC and NVUC in 45% and 15% of cases, respectively. It is, however, important to establish that these percentages were obtained quantitatively by manual counting of cells rather than a subjective estimation.

808 Comprehensive Genomic Profiling of Papillary Renal Cell Carcinoma Reveals Clinically Relevant Genomic Alterations

Siraj Ali, Kai Wang, Norma Palma, James Sun, Roman Yelensky, Julia Elvin, Juliann Chmielecki, Doron Lipson, Vincent Miller, Philip Stephens, Jeffrey Ross. Foundation Medicine Inc, Cambridge, MA.

Background: Papillary Renal Cell Carcinoma (PRCC) originates from the epithelium of the proximal tubules with unique histologic and clinicopathologic features. Given the often aggressive nature of this tumor and its failure to respond to systemic therapy, we performed comprehensive genomic profiling (CGP) on PRCC to identify clinically relevant genomic alterations (CRGA) that may suggest benefit from the use of targeted therapy.

Design: DNA was extracted from 40 microns of FFPE sections from 34 PRCC. CGP was performed on hybridization-captured, adaptor ligation based libraries to a mean coverage depth of >680X for 3,769 exons of 236 cancer-related genes plus 47 introns from 19 genes frequently rearranged in cancer. The results were evaluated for all classes of genomic alterations (GA). CRGA were defined as GA linked to drugs on the market or under evaluation in mechanism driven clinical trials.

Results: There were 24 male and 10 female patients, with a median age of 56 (range 23-75). Stage: Stage I (n=3), II (n=2), III (n=6), IV (n=22), unknown (n=1). Ten (30%) cases were low grade (Fuhrman 1-2), and 23 (70%) were high grade (Fuhrman 3-4), with histology unavailable for one case. There were 65 GAs identified in 34 PRCC cases (1.9 per tumor) with 82% of the cases containing at least one GA. 29 clinically relevant GAs (0.9 per tumor) involving 17 different genes were identified in 18/34 (53%) of the cases. The most common CRGA were *CDKN2A* (15%), *ARID1A* (12%), *NF2* (9%), *MET*, *KRAS, FLT4, CDK6,* and *BRAF*(each at 6%). The common GA were *SMARCB1*, *SETD2 (*each at *9%), TP53, CDKN2B,* and *ATM* (each at 6%). Responses of PRCC with CRGA to targeted therapies will be presented.

Conclusions: Despite the known association of germline *MET* alterations with PRCC, the frequency of somatic *MET* CRGA in this study was low. Further analysis will be performed to define histology (Type I/II) and correlation to CRGA, particularly *MET* alterations. PRCC harbors a broad range of CRGA that may provide options for targeted treatment.

809 Bladder and Prostate Tumors Following Radiation Therapy for Prostate Cancer

Lindsay Alpert, Jerome Taxy, Tatjana Antic. University of Chicago, Chicago, IL; North Shore University Health System, Evanston, IL.

Background: Prostate cancer (PC) is the 2nd most common cancer in men worldwide, and many cases of PC are definitively treated with radiation therapy (RT). While rates of secondary malignancies in post-RT PC patients have been assessed in epidemiologic studies, the pathologic features and distribution of these tumors compared to those in non-radiated patients are not well-documented.

Design: Patients with a history of RT for PC who underwent cystoprostatectomy, prostatectomy, or cystectomy between 1/2005 and 7/2013 were retrieved from the pathology archives. Clinical features, pathology reports, and all slides were reviewed. The total numbers and diagnoses of prostates and bladders resected during this period were also reviewed.

Results: Sixty-five post-RT patients were identified. Most patients had a history of smoking, and on average there was a 7.5-year interval between primary RT and organ resection. Urothelial carcinoma was the most common tumor in post-RT cystectomies and cystoprostatectomies, followed by recurrent or persistent prostatic adenocarcinoma (PA). PA was also present in 14 of the 15 post-RT prostatectomies and in 3,181 of the 3,190 non-RT prostatectomies. There was 1 primary angiosarcoma in a post-RT patient and no primary bladder or prostate sarcomas in the non-RT patients.

Table 1. Clinical characteristics

Age, mean±SD, years (n=65)	70.8±8.2
Smoking history (n=61)	73.8%
Years from RT to surgery, mean±SD (n=61)	7.5±4.7
Type of RT (n=65)	
Brachytherapy	33.8%
External beam	38.5%
Combined RT	27.7%
Specimen (n=65)	
Cystoprostatectomy	69.2%
Prostatectomy	23.1%
Cystectomy	7.7%

Table 2. Cystectomy & Cystoprostatectomy Diagnoses at Surgery

	Post-RT (n=50)	No RT (n=730)*
UC	30.0%	43.2%
PA	22.0%	9.2%
Both UC & PA	22.0%	29.7%
Non-prostatic adenocarcinoma	8.0%	3.0%
No residual UC	8.0%	11.8%
Squamous cell carcinoma (SCC)	2.0%	2.7%
Other tumor	2.0%	1.2%
Benign (cystitis/fistula)	6.0%	0.5%
*Total>100% - 10 cases had both PA & non-prostatic adenocarcinoma or SCC		

Conclusions: UC accounts for the majority of bladder tumors following RT for PC. The distribution of bladder and prostate tumors is similar in resection specimens from post-RT and non-RT patients. The only primary sarcoma was a post-RT angiosarcoma, which is known to be associated with RT in other organ systems.

810 High Nodal Density (HND) Is Associated With Aggressive Pathologic Features and Predicts Outcome in Patients with Penile Squamous Cell Carcinoma (PeCa) Treated By Penectomy and Inguinal Lymphadenectomy

Isabel Alvarado-Cabrero, Cesar Aponte, Diana Piedras, Adriana Rodriguez-Gomez, Diego Sanchez, Narciso Hernandez-Toriz, Antonio Cubilla, Alcides Chaux. Hopsital de Oncologia Centro Medico Nacional Siglo XXI, México, DF, Mexico; Office of Scientific Research, Norte University, Asunción, Paraguay; Instituto de Patología e Investigación & Facultad de Ciencias Médicas, UNA, Asunción, Paraguay.

Background: Clinical management of patients with PeCa is hampered by its rarity in developed nations and by the lack of large series with adequate follow-up. Aimed to solve this issue several pathologic features have been proposed as prognostic factors. Recently, nodal density (defined as the ratio of positive inguinal lymph nodes over the total number of resected nodes) has been identified as a promising tool to define the outcome of patients with PeCa. In this study, we evaluated the usefulness of nodal density as a predictor of aggressive pathologic features and outcome.

Design: 154 patients with PeCa treated by penectomy, of whom 133 received a bilateral inguinal lymphadenectomy, were studied. The number of lymph nodes per patient that were pathologically evaluated ranged from 1 to 27 for each side, with a median of 8 lymph nodes per side per patient. Clinical endpoints included cancer-free survival and cancer-specific death. Patients were followed from 11 to 82 months (mean of 54.2 ± 16.5 months). Associations were evaluated using the Mann-Whitney U/Kruskal-Wallis test. A 2-sided p<0.05 was required for statistical signficance.

Results: HND was significantly associated with: invasion of multiple anatomical sites (P=1.36e-4), tumor size > 4 cm (P=1.02e-11), high grade (P=5.97e-13), thickness > 13 mm (P=2.75e-20), lymphovascular invasion (P=1.68e-17), perineural invasion (P=2.48e-9), invasion of corpora cavernosa (P=2.29e-15), prognostic index > 4 (P=2.12e-15), > pT1b (P=2.43e-6), > pN1 (P=1.07e-27), pM (P=4.14e-19), > stage II (P=2.14e-20), and invasion of distal urethra (P=2.35e-6). HND was associated with cancer-free survival (P=1.38e-18) and cancer-specific death (P=2.32e-12).

Conclusions: HND was significantly associated with aggressive pathologic features in the primary tumor, a lower proportion of cancer-free survival and a higher proportion of cancer-specific death.

811 Prognostic Risk Groups in Subtypes of Penile Squamous Cell Carcinomas (SCC) According To the New WHO Classification (2015)

Isabel Alvarado-Cabrero, Diego Sanchez, Diana Piedras, Adriana Rodriguez-Gomez, Ingrid Rodriguez, Cecilia Lezcano, Narciso Hernandez-Toriz, Antonio Cubilla. Hopsital de Oncologia Centro Medico Nacional Siglo XXI, México, DF, Mexico; Instituto de Patología e Investigación & Facultad Ciencias Médicas, UNA, Asunción, Paraguay; University of Pittsburgh Medical Center, Pittsburgh, PA.

Background: The prognostic spectrum of penile carcinomas, variable from excellent to dismal, is in part related to the histological architecture of the various tumors.

Design: 126 Patients had penectomies and bilateral groin dissections at the Hospital Oncológico, Mexico City. After pathological classification in 13 subtypes, 3 prognostic risk groups were determined: 1- low risk (Usual grade 1, Verrucous, Verrucous Hybrid, Cuniculatum, Pseudohyperplastic, Pseudoglandular, and Papillary NOS carcinomas), 2- Intermediate risk (Usual grade 2, Mixed, and Warty), 3- High risk (Usual grade 3, Warty-basaloid, Papillary-basaloid, Basaloid, and Sarcomatoid).

Results: Table 1 shows 126 patients with follow up and nodal dissection distributed by histologic risk groups.

Risk Group	Cases	Positive Nodes (%)	DOD (%)
Low	31	3 (10)	0
Intermediate	48	14 (29)	4 (8)
High	47	35 (74)	30 (64)
p		0.0005	0.0005

DOD: dead of disease

Patients' survival by groups is shown in Figure 1 (p<0.00005).

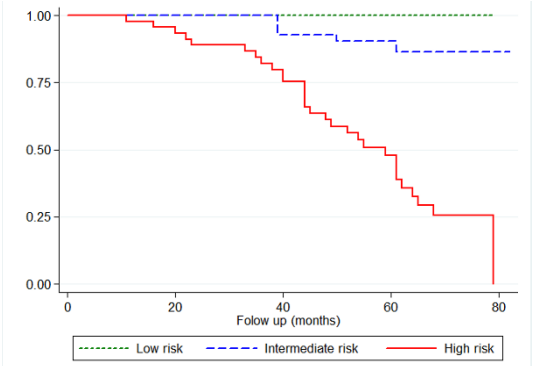

Conclusions: Although other pathological risk factors need to be considered (grade, depth and perineural invasion), histological subtyping and risk grouping of penile carcinomas are strong indicators of the potential for nodal metastasis and final outcome.

812 Leydig Cell Tumors of the Testis May Express c-KIT Without KIT or PDGFRA Mutation

Antonio Alves, Marco Ferreira, Eduardo Gavin, Carla Matos, Federico Rojo, Maria Gabriela Gasparinho. Centro Hospitalar Lisboa Norte, Lisbon, Portugal; Hospital CUF Descobertas, Lisbon, Portugal; Fundacion Jimenez Diaz, Madrid, Spain.

Background: Immunohistochemical (IHC) demonstration of c-KIT (CD117) protein is useful in the diagnosis of several neoplasms, namely GIST, and can prove to have therapeutic utility in cases associated with *KIT* or *PDGFRA* mutation. Concerning testicular neoplasms, it is said to be a specific marker for seminoma, and expression in Leydig cell tumors has not been reported. Our objective was to assess c-KIT protein IHC expression and mutational status of *KIT* and *PDGFRA* in testicular Leydig cell tumors.

Design: Multi-institutional Pathology Department databases were reviewed from 2004 to 2013. Slides of Leydig cell tumors were reviewed and CD117 extension and intensity of immunostaining was recorded. Tumors were classified as benign or malignant according to WHO criteria. Tumor size, necrosis, vascular invasion, cytologic atypia and mitosis were recorded. CD117 positive tumors were assessed for mutations in exons 9 and 11 of the *KIT* gene and in exons 12 and 18 of the *PDGFRA* gene. Exon analysis was carried out by pyrosequencing using specific primers.

Results: We identified 12 patients with Leydig cell tumors. Eleven cases were classified as benign. Necrosis and significant cellular atypia were identified only in the malignant tumor. No vascular invasion was recognized. CD117 expression was detected in two benign cases (17% of all cases), in 10% and 90% of the neoplastic cells, with strong cytoplasmatic and membranous staining. No mutations in exons of *KIT* or *PDGFRA* were identified.

Conclusions: CD117 expression in Leydig cell tumors is reported for the first time. The existence of CD117-positive Leydig cell tumors is important in the differential diagnosis of testicular neoplasms. However, no KIT-activating mutations in exon 9 or 11 of *KIT*, or exons 12 and 18 of the *PDGFRA* gene were found. Therefore, these tumors are unlikely to respond to imatinib mesylate therapy.

813 Tumor-Infiltrating Lymphocytes and PD-L1 Expression in Renal Cell Carcinomas: Correlation With Interleukin-2 Treatment Response

Nicole Andeen, Nadia Giannakopoulos, Khanh Doan, Scott Tykodi, Maria Tretiakova. University of Washington, Seattle, WA.

Background: Qualitative and quantitative methods of assessing immunologic responses to neoplasms have gained increasing interest due to their potential prognostic value; however, studies assessing correlations between tumor-infiltrating lymphocytes (TILs) in renal cell carcinoma (RCC) and clinical outcomes have mixed results. Cytokine-inducible RCC expression of PD-L1 results in diminished T-cell effector function (PMID: 24714771) and is associated with poor prognosis (PMID: 16585157). Anti-PD-1 immunotherapy is thought to exert its effect by facilitating anti-tumoral activity of effector T-cells. Since cytokine therapy is a mainstay of treatment for advanced RCC, we sought to assess the relationship between CD8 TILs, PD-L1 expression, and clinical outcome in patients with metastatic RCC treated with interleukin-2 (IL-2).

Design: A tissue microarray was constructed from 21 nephrectomies from patients with metastatic clear cell RCC who received post-operative therapy with IL-2 (n=20) or anti-PD-1 antibody (n=1). A 1mm diameter punch was made from 4 separate tumor regions: highest Fuhrman grade, highest density of TILs (HD), infiltrative margin, and central tumor. A cutoff of ≥ 5% for RCC PD-L1 staining was considered positive. The carcinoma was considered CD8 high if the mean for the 4 points exceeded that for the group (mean CD8 TIL = 44/400x field), or if the CD8 TILs in the HD area exceeded the HD area mean. Findings were correlated with outcome data.

Results: Overall, 12/21 (57%) RCCs were CD8 high, and 5/21 (24%) were PD-L1-positive; most PD-L1-positive cases were also CD8 high (4/5). At a median follow up time of 24 months, 3/20 patients receiving IL-2 therapy had partial remission and 4 had complete remission (35% responders); 12/20 (60%) had progressive disease and 1 was lost to follow up. Of the 7 patients who responded to IL-2 therapy, 5 (71%) had a CD8 high RCC and 3 (43%) had a PD-L1-positive RCC. The patient treated with anti-PD-L1 antibody had partial remission; no PD-L1 immunoreactivity was detected in his tumor.

Conclusions: In contrast to studies of all-comers with RCC, in patients with metastatic RCC treated with IL-2, PD-L1 expression does not appear to be a poor prognostic indicator. Response to IL-2 therapy and "no evidence of disease" status were associated with greater numbers of CD8 TILs. The findings suggest that response to IL-2 therapy may in part reflect a pre-existing immunologic milieu that has already recognized the carcinoma and generated tumor-infiltrating lymphocytes.

814 Metastatic Renal Cell Carcinoma: Correlation With Grade, Stage and Histologic Characteristics of the Primary Renal Mass – A 15-Year Study

Javier Arias-Stella, Omar Rayes, David Saulino, Sean Williamson, Nilesh Gupta. Henry Ford Health System, Detroit, MI; Michigan State University College of Osteopathic Medicine, Lansing, MI.

Background: Most adult kidney tumors are renal cell carcinomas (RCC), which can be associated with significant morbidity and mortality, including distant metastasis even many years after resection. Occasional reports of metastases from low-stage, low-grade tumors are well-known. We investigated our institutional experience with metastatic renal cell carcinoma, correlating histopathologic characteristics of the primary tumor and metastases.

Design: Retrospective electronic database search was performed for patients with metastatic RCC from 2000 to 2014. We assessed metastatic site(s), primary tumor morphology, grade and stage, and time between primary diagnosis and first metastasis.

Results: A total of 120 patients were identified, of whom 76 (63%) were men and 44 (37%) women with a mean age of 65.5 years (range 14-87). Eighty-three (69%) were Caucasian, 22 (18%) African American, 1 (1%) Asian, 1 (1%) American Indian, 1

(1%) Hispanic and 12 (10%) unknown. Metastatic sites were lung 41 (35%), bone 17 (14%), lymph node 14 (12%), liver 12 (10%), adrenal gland 11 (9%), soft tissue 9 (8%), pancreas 6 (5%), central nervous system 5 (4%), gastrointestinal tract 2 (2%), frontal sinus 1 (<1%), trachea 1 (<1%), and thyroid 1 (<1%). Metastasis size mean was 3.1 cm (range 0.3-13). Mean time between primary and metastasis was 45 months (range 0-273). Morphologic sub types of metastatic tumors were clear cell 112 (93%), papillary 5 (4%), sarcomatoid 2 (2%), and chromophobe RCC 1 (<1%).
Primary tumors were available in 57 cases; 44 (77%) clear cell, 5 (9%) papillary, 6 (11%) sarcomatoid, and 2 (4%) unclassified. One patient had RCC associated with Xp11.2 translocation/TFE3 gene fusion. Mean primary tumor size was 8.6 cm (range 0.7-18.8). Two (4%) Fuhrman grade 1, 12 (21%) grade 2, 30 (53%) grade 3 and 13 (23%) grade 4. Two (4%) stage T1a, 11 (19%) T1b, 7 (12%) T2a, 4 (7%) T2b, 17 (30%) T3a, 12 (21%) T3b, and 4 (7%) T4. Seven (12%) N0, 9 (16%) N1, 3 (5%) N2 and 38 (67%) Nx.
Conclusions: This study provides a single institution experience and contributes to the epidemiologic data of metastatic RCC and confirms the assertion that some tumors of small size, with low grade, and low stage do have metastatic potential. Nonetheless, none of the metastatic tumors were identified from our partial nephrectomy patient population.

815 MDM2 Labeling Is Seen in a Subset of Fat-Predominant Angiomyolipomas: A Potential Diagnostic Pitfall

Rebecca Asch-Kendrick, Rajni Sharma, Jonathan Epstein, Pedram Argani, Ashley Cimino-Mathews. Johns Hopkins Hospital, Baltimore, MD.
Background: Angiomyolipomas (AML) are mesenchymal tumors with a predominantly benign behavior and variable histologic composition. Fat-predominant AMLs are composed primarily of adipose tissue and can mimic well-differentiated liposarcomas (WDLS) radiographically as well as histologically, due to the abundance of fat with admixed atypical cells resembling lipoblasts. However, the treatment and prognosis of AML and WDLS are vastly different. Immunohistochemistry (IHC) for MDM2 has been used to support a diagnosis of WDLS, however MDM2 labeling has not been evaluated in fat-predominant AMLs. Here, we evaluate the immunolabeling pattern of MDM2 and HMB45 and calponin/actin (standard IHC markers for AMLs) in a series of AMLs and WDLS.
Design: Retrospective review of the pathology archives identified 13 fat-predominant AMLs (defined here as containing >90% adipose component) and 6 fat rich AMLs (defined here as containing 50-90% adipose component). Additional consecutively identified cases of conventional AML (n=14), epithelioid AML (n=3), and WDLS (n=10) were also included for study. Whole sections of all cases were labeled by IHC for MDM2, HMB45, calponin or smooth muscle actin. Any extent of moderate to strong nuclear MDM2 labeling was considered positive, with <5% labeling considered focal and >5% labeling considered diffuse.
Results:

MDM2, HMB45 and Calponin/Actin Labeling in Angiomyolipomas (AML) and Well-differentiated Liposarcomas

Lesion	Number	MDM2	HMB45	Calponin or Actin
All AML	36	5 (14%)	36 (100%)	26 (100%)
Fat-predominant AML	13	3 (23%)	13 (100%)	13 (100%)
Fat-rich AML	6	0	6 (100%)	6 (100%)
Conventional AML	14	1 (7%)	14 (100%)	14 (100%)
Epithelioid AML	3	1 (33%)	3 (100%)	3 (100%)
Well-differentiated liposarcoma	10	9 (90%)	0	8 (80%)

Conclusions: Although uncommon, MDM2 labeling is seen in 23% of fat-predominant AMLs and is a potential diagnostic pitfall in the evaluation of fatty tumors of the retroperitoneum. In our study, immunolabeling for HMB45 is 100% sensitive and specific for AML, and an immunopanel containing both HMB45 and MDM2 may be warranted to distinguish between fat-predominant AML and WDLS in diagnostically ambiguous cases.

816 Assessment of Circumferential Margins, Extraprostatic Extension and Gleason Score in Radical Prostatectomy Specimens – Comparison of a Partial Embedding Method With Supplementary Total Inclusion of Peripheral Tissues

Daniel Athanazio, Luiza Fadul, Mariana Silva, Andreia Santos. Federal University of Bahia, Salvador, Brazil; Hospital Universitário Professor Edgard Santos, Salvador, Brazil.
Background: There is no consensus on the merits and drawbacks of total and partial embedding of radical prostatectomy specimens. However, a recent study has suggested that up to 21% of positive circumferential margins (PCM) and 47% of extraprostatic extension (EPE) may be missed when partial embedding methods are employed. Kim (Arch Pathol Lab Med 133:1278–84) suggested that total inclusion of the periphery (3 mm rim) of the prostate prevents the failure to detect PCM and EPE.
Design: Radical prostatectomy specimen (n=109) slides were reviewed after adoption of a protocol with the inclusion of a 3 mm rim of peripheral tissues in two Pathology Services of Salvador, Bahia, Brazil: IMAGEPAT (Private Laboratory) and HUPES (Public/Academic Hospital).

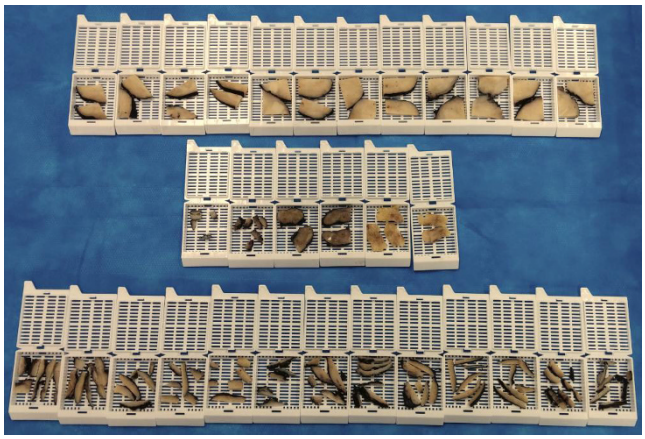

Results: Total inclusion of prostatic periphery (TIPP) resulted in 10 ± 5 slides per case, in addition to the standard 16 slides from 12 regions, apical and basal margins, and seminal vesicles. TIPP increased the detection of PCM from 26 (24%) to 38 (35%). From 13 cases registered as focal PCM at partial embedding alone, 7 (54%) were determined to be non-focal PCM after analysis of the TIPP slides. TIPP increased the detection of EPE from 15 (14%) to 20 (18%). From 10 cases registered as focal PCM at partial embedding alone, 3 (30%) were determined to be non-focal EPE after analysis of TIPP slides. In four cases (3%), the Gleason score changed due to analysis of TIPP slides. In one case, only supplementary sections of the prostatic periphery had detectable carcinoma.
Conclusions: Partial sampling resulted in missing 32% of PCM and 25% of EPE. Changes in Gleason score were uncommon. These results indicate the importance of inclusion of all prostate periphery for microscopic analysis when partial embedding methods are adopted.

817 mTOR: A New Sensitive and Specific Marker for Prostatic Cells, Is Useful in Distinguishing Between Carcinomas of Prostatic and Other Origins

Sabina Babayeva, Judy Sarungbam, Ximing Yang, Minghao Zhong. New York Medical College at Westchester Medical Center, Valhalla, NY; Memorial Sloan Kettering Cancer Center, New York, NY; Northwestern University, Feinberg School of Medicine, Chicago, IL.
Background: The origin of a primary or metastatic carcinoma is sometimes difficult to establish and is critical for patient management, in particular the distinction between those originating in the bladder and the prostate. By analyzing "human protein atlas" (http://www.proteinatlas.org) data, we found that mTOR could be a biomarker for prostatic cells. Therefore, we would like to validate the clinical utility of mTOR IHC stain.
Design: Tissue micro arrays (TMA) were constructed from 115 cases of prostatic adenocarcinoma (PCa); 93 cases of urothelial carcinoma (UC); and 128 cases of other common carcinoma (lung, colon, kidney, head/neck, breast, endometrium and ovary). The full section slides containing all different tissues also have been used. The IHC stains of mTOR, PSA, AMACR and cocktail have been applied to those slides.
Results: All benign prostate glands and prostatic carcinomas (100%) are positive for mTOR. All 10 (100%) cases of metastatic PCa are positive for mTOR. High grade (Gleason 8-10) PCa usually present with weaker mTOR stain than lower (Gleason <8) grade PCa and benign prostatic glands. Comparing to PSA stain, mTOR stain usually are stronger than PSA stain with diffuse pattern. All other tissues and carcinomas (100%) are negative for mTOR; including basal cells of prostatic glands and seminal vesicles, which are positive for PSA.
Conclusions: In this study, we demonstrate that:
1. mTOR IHC is a sensitive marker for prostatic cell origin: Positivity rate is as the same as PSA, however, mTOR show much stronger and diffuse pattern than PSA; and mTOR is much more sensitive than AMACR.
2. mTOR is specific marker for prostatic cells origin: all tested normal tissues and (>200 cases) different common carcinoma cases are negative for mTOR, including 93 cases of UC which is one of the most important differential diagnosis; also, basal cells and seminal vesicles which positive for PSA.
3. The biological meaning of this observation is not clear. mTOR protein expression and activation in prostatic gland and carcinoma (PCa) warrant for further investigations which may yield a novel target therapy for prostatic carcinoma.

818 Identical ERG Expression in "Early PIN-Like and Other Non-Classic Patterns" of Intraductal Carcinoma of the Prostate (IDC-P) and Concomitant "Classic" IDC-P

Bridget Banach, Gladell Paner. University of Chicago, Chicago, IL.
Background: We have previously shown that non-classical patterns of IDC-P including PIN-like patterns exist which may represent the advancing edge of IDC-P. The ERG status of these non-classical IDC-P patterns relative to the concomitant classic IDC-P is unknown.
Design: A representative section from 98 radical prostatectomies (mostly >GS7) that showed prostate promontory were examined and immunostained for PIN4 and PTEN. Proximal ducts (PDs) were identified as elongated ducts that converged toward the prostatic promontory/urethra. IDC-P identified based on published criteria were labeled

as classic IDC-P. Non-classic IDC-P was accepted if all the following criteria were met: 1)neoplasia present within PDs confirmed by PIN4, 2)neoplasia contiguous with classic IDC-P in PDs or peripheral ducts/acini, 3)loss of PTEN and 4)exhibits architecture that does not conform to those described in classic IDC-P. ERG immunostaining was performed on all cases with non-classic IDC-P.

Results: Of 98 cases IDC-P was identified in 62 (63%) and extension into the PD in 25 (26%) cases. Non-classic patterns of IDC-P were identified in the PD including partial duct involvement (18/25, 72%), overriding of duct urothelium (4/25, 16%), flat/tufted PIN-like (14/25, 56%), micropapillary PIN-like (4/25, 16%), and inverted PIN-like (1/25, 4%) patterns. As per definition, all non-classical IDC-P exhibit PTEN loss. ERG positivity was seen in 14/25 (56%) of non-classic IDC-P. ERG expression in all non-classic and adjacent classic IDC-P correlated, either as positive or negative staining for both. ERG staining was concordant to invasive carcinoma at the immediate vicinity of the PD. This concordance was maintained in cases with heterogeneity in ERG staining in invasive carcinoma (distant invasive carcinoma foci showed opposite reactivity). Interestingly in 4 cases, the IDC-P extended into the prostatic urethra. In 2/4, ERG highlighted the IDC-P cells mingled with the urethral urothelium.

Conclusions: Our study shows that non-classic IDC-P including PIN-like patterns exists in the PD in continuum with the classic IDC-P and demonstrate the characteristic PTEN loss. We show that ERG expression of these non-classic IDC-P patterns positively correlates with the ERG expression in the associated classical IDC-P and invasive carcinoma, further supporting our hypothesis that these PIN-like patterns represent the advancing edge of IDC-P. Further, ERG has a potential utility as an ancillary tool in identifying prostate carcinoma spread in urethral biopsies.

819 Gleason Scores 3+5=8 and 5+3=8 at Biopsy Exhibit a Wide Spectrum of Gleason Scores at Prostatectomy

Alexander Baras, Jonathan Epstein. Johns Hopkins, Baltimore, MD.

Background: Gleason score (GS) 3+5=8 and 5+3=8 on biopsy (Bx) are uncommon and there is scant data on their correlation with GS at radical prostatectomy (RP). This study seeks to characterize the spectrum of GS at RP in cases of 3+5=8 and 5+3=8 on Bx and assess the biochemical recurrence free survival (BRFS) of GS 3+5=8 and 5+3=8 at RP.

Design: We conducted a retrospective review of all paired Bx & RP cases from our institution over the last decade (2004 to 2014) using the modified GS. The total number of cases was 9,811.

Results: In biopsies with GS other than 3+5=8 and 5+3=8, the most common GS of the RP was consistent with the biopsy GS; however, for biopsy GS 3+5=8 and 5+3=8 a wide spectrum of RP GS is observed, ranging predominantly from GS 7 to GS 9-10, Table 1. The proportion of GS containing a higher tertiary Gleason pattern 5 (t5) was higher in RPs whose Bx were GS 3+5=8 and 5+3=8 (56%) as compared to the other possible GS on Bx (12%), Figure 1A.

The BRFS of 3+5=8 and 5+3=8 at RP did not statistically differ from each other. The combined BRFS of GS 3+5=8 and 5+3=8 is in between GS 4+3=7 and GS 4+4=8 (both without t5) and is similar to GS 4+3=7 with t5, Figure 1B.

***Table 1.** Gleason scores at prostatectomy stratified by Gleason score at biopsy*

	Biopsy							
Prostatectomy	3+3=6	3+4=7	4+3=7	3+5=8	5+3=8	4+4=8	GS 9,10	
3+3=6	72%	21%	9%	**4%**	**5%**	3%	1%	4609
3+4=7	22%	56%	32%	**36%**	**30%**	11%	7%	2968
4+3=7	4%	18%	40%	**36%**	**20%**	26%	10%	1246
3+5=8	0%	1%	1%	**13%**	**10%**	1%	4%	86
5+3=8	0%	0%	0%	**0%**	**15%**	0%	2%	18
4+4=8	1%	1%	9%	**2%**	**0%**	38%	8%	364
GS 9,10	1%	2%	9%	**9%**	**20%**	21%	67%	520
	5610	2216	1136	55	20	436	338	9811

Percentages are based on biopsy grouping (i.e. column wise).

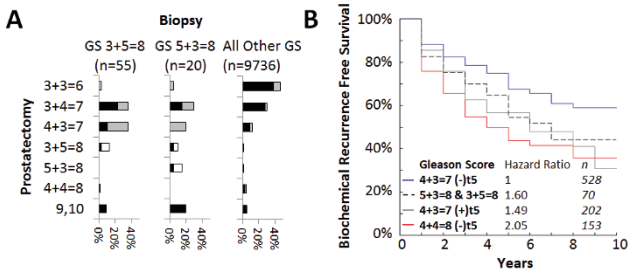

***Figure 1.** (A) GS at RP from 3+5=8 and 5+3=8 at biopsy exhibit a wide spectrum with an enrichment for tertiary Gleason pattern 5.* The composition of Gleason scores at prostatectomy are shown via a horizontal bar graph. The total bar length represents the proportion with the designated GS. The grey and white portions of the bar represent the fractions with a tertiary Gleason pattern 5 or 4, respectively. (B) *The BRFS for 3+5=8 and 5+3=8 at RP is in between 4+3=7 and 4+4=8 without tertiary Gleason pattern 5.*

Conclusions: There is a markedly wide spectrum of GS in RP from patients with GS 3+5=8 and 5+3=8 on bx. GS 3+5=8 on Bx often consists of a primary pattern 3 with secondary pattern 4 and then a tertiary pattern 5, which is graded as most common (3) + highest (5) Gleason grades = 8. It is therefore not surprising that at RP the most common GS are 3+4 or 4+3 (Table 1), raising the question of whether grading Bx by adding most common and highest grade patterns results in overgrading the Bx relative to the RP. However, as seen in the Figure, 3+5 on Bx with 3+4 or 4+3 at RP often has tertiary pattern 5 at RP which worsens the prognosis. 5+3 on Bx is less common and often has 3+4 and 4+3 with tertiary 5 at RP yet also has 20% of GS 9-10 at RP where the minor pattern 3 is not recorded in the GS.

820 Multi-Institutional Assessment of Prognostic Gleason Grade Groupings: Potential Basis for a New Prostate Cancer Grading System

Alexander Baras, Lars Egevad, Cristina Magi-Galluzzi, Victor Reuter, Samson Fine, Anil Parwani, Jonathan Epstein. Johns Hopkins, Baltimore, MD; University of Pittsburgh, Pittsburgh, PA; Memorial Sloan Kettering Cancer Center, New York, NY; Karolinska, Stockholm, Sweden; Cleveland Clinic, Cleveland, OH.

Background: There are several problems with the current Gleason system. Gleason scores (GS) effectively start at 6 out of a total of 10, suggesting an intermediate prognosis. All GS 7 is combined into "intermediate risk" by clinicians, yet it represents a heterogeneous group comprised of 3+4=7 and 4+3=7 which have been shown to exhibit significantly different biochemical recurrence free survival (BRFS). Clinicians combine GS 8-10 into a single high risk group, despite the worse prognosis of GS 9-10 as compared to GS 8. The current modified Gleason system also has many differences compared to the original Gleason system in terms of grading rules and assigning grades based on morphology.

Design: BRFS was examined in GS: 3+3=6, 3+4=7, 4+3=7, 4+4=8, 9/10 across five independent institutions totaling of 19,055 cases with a median follow-up time of 3.1 years and a median time to progression of 1.1 years.

Results: The pooled data from 5 separate institutions are consistent with the previously reported prognostic Gleason grade groupings of GS at RP. The hazard ratio approximately doubles with each increment in grade group, Figure 1. The 5 year BRFS in grade groups 1-5 were 0.97, 0.93, 0.78, 0.64, and 0.49 respectively.

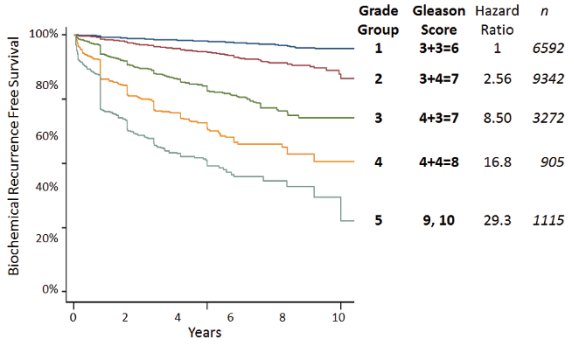

***Figure 1.** Biochemical recurrence free survival for Gleason score groupings across 5 separate institutions*
A fairly consistent doubling of the hazard ratio is observed with each increment in grade group.

All curves in Figure 1 were significantly separate from each other ($p<0.00001$).

Conclusions: A new grading system for prostate cancer should be considered based on: 1) More accurate prognostic stratification than the current system; 2) Lowest grade is 1 not 6, which has the potential to reduce over treatment of indolent cancer; 3) Simplified reporting of 1-5 versus 2-10; 4) The current grading system used for prostate cancer, although based on the original Gleason system, departs from the original system sufficiently to warrant a new name. Initially, the new grading system would be used in conjunction with Gleason score and eventually may replace it.

821 The Effect of Higher Tertiary Gleason Patterns at Radical Prostatectomy on Biochemical Recurrence Free Survival Is Most Prominent With Gleason Score 4+4=8, Intermediate With Gleason Score 7, and Only Marginal With Gleason Score 6

Alexander Baras, Anil Parwani, Jonathan Epstein. Johns Hopkins, Baltimore, MD; University of Pittsburgh, Pittsburgh, PA.

Background: The effect of higher tertiary Gleason pattern (T) at radical prostatectomy (RP) on biochemical recurrence free survival (BRFS) is not yet fully characterized. It is accepted that T has an overall adverse effect on prognosis but the magnitude of the effect for each RP Gleason score (GS) is not known.

Design: The effect of T on BRFS was examined in GS: 3+3=6, 3+4=7, 4+3=7, and 4+4=8 and compared to the same grades without T along with GS 9-10. The data from our institution encompassed 5,483 patients with a median follow-up time of 3 years. The data from an outside institution was also included, encompassing 2,123 patients with a median follow-up time of 3.89 years.

Results: The effect of T on BRFS is not uniform across GS (Table 1). GS 3+3=6 with T has only a marginal absolute effect on the BRFS (Table 1, Figure 1). The effect of higher tertiary Gleason pattern (T) is most significant with GS 4+4=8, wherein GS 4+4=8 with T exhibits BRFS equivalent to GS 9,10. GS 3+4=7 with T exhibits a BRFS in between GS 3+4=7 and GS 4+3=7, both without T. Similarly, GS 4+3=7 with T exhibits a BRFS in between GS 4+3=7 and GS 4+4=8, both without T.

Table 1. Effect of higher tertiary Gleason pattern (T) on BRFS stratified by Gleason scores.

			Gleason Score			
			3+3=6	3+4=7	4+3=7	4+4=8
Difference +/- T		n	3014	2811	1037	185
5yr BRFS	T	-	97%	91%	69%	45%
		+	95%	79%	57%	23%
		difference	***2%***	***11%***	***12%***	***23%***
		p-value	*0.040*	*<0.001*	*<0.001*	*0.018*
Overall BRFS		***p-value***	***0.081***	***<0.001***	***<0.001***	***0.003***

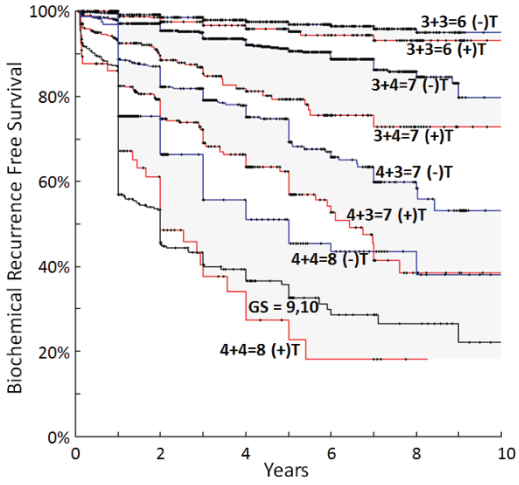

Figure 1. *Biochemical recurrence free survival for Gleason score groupings stratified by the presence of higher tertiary Gleason pattern.*

The effect of higher tertiary Gleason pattern (T) is most significant with GS 4+4=8, wherein GS 4+4=8 with T exhibits BRFS equivalent to GS 9,10. GS 3+4=7 with T exhibits a BRFS in between GS 3+4=7 and GS 4+3=7, both without T. Similarly, GS 4+3=7 with T exhibits a BRFS in between GS 4+3=7 and GS 4+4=8, both without T. The effect of T in GS 3+3=6 is marginal.

Conclusions: These data support the notion that the effect of T is not uniform across GS. Whereas omitting the T in GS 3+3=6 will not have a major affect in predicting a patient's prognosis after RP, doing so with higher GS at RP results in an false prediction of a better prognosis than is actually present. In GS 4+4=8, the presence of T worsens the prognosis to the next highest grade group of prostate cancer (GS 9,10). The effect of T in GS 3+4=7 and 4+3=7 does worsen the prognosis but to an intermediate degree as compared to what is seen is GS 4+4=8.

822 Immunohistochemical Characterization of Nephrogenic Metaplasia With HNF-1β, PSMA, PAX8, and GATA3

Eva Bashover, Gregory MacLennan, Robin Elliott. Case Western Reserve University, Cleveland, OH.

Background: Nephrogenic metaplasia (NM), alternately known as nephrogenic adenoma, is a rare, benign lesion of the urothelial tract. Proposed theories of its pathogenesis include true metaplasia akin to squamous and glandular urothelial metaplasia as a response to injury and proliferation of displaced renal tubular cells. It is vital to differentiate NM from histological mimics including low grade urothelial neoplasms, prostatic and urothelial adenocarcinoma, and clear cell carcinoma. Immunohistochemistry (IHC) may be useful in distinguishing NM from these entities in limited biopsy material. A potentially useful panel may include PAX8, a transcription factor (TF) expressed in renal tubular epithelium; GATA3, a TF expressed in urothelium; PSMA, a membrane glycoprotein specific for prostate adenocarcinoma; and HNF-1β, a TF expressed in clear cell carcinomas of the gynecologic and urinary tracts. We studied the expression of the aforementioned antigens in cases of NM.

Design: Eighteen patients with a diagnosis of NM were identified in our archives. A microarray of these patients' formalin-fixed, paraffin-embedded tissue samples was used to prepare 4μ-thick sections. IHC for HNF-1β (clone H-205; Santa Cruz Biotech, Santa Cruz, CA) and GATA3 (clone L50-823; Cell Marque, Rockland, CA) was performed using a BondMax Automated Immunostainer (Leica), and IHC for PAX8 (polyclonal, rabbit; Cell Marque) and PSMA (Clone 1D6; Santa Cruz Biotech) was performed using a BenchMark Ultra Immunostainer (Ventana Medical Systems) with standard protocols. The samples were scored as positive (+) and negative (-). Positives were divided into diffuse positive (>50% cells staining) and focally positive (<50% cells staining).

Results: Of the 18 samples tested, 4 were excluded from the analysis due to technical failure. Of the remaining 14 samples, 12 (86%) were (+) for PAX8, 6 (50%) for GATA3, and 12 (86%) for HNF-1β. None expressed PSMA. All PAX8+ samples were also HNF-1β+. Five samples were PAX8+/HNF-1β/GATA3+. Of the 6 GATA3+ samples, 3 were focally positive. PAX8 and HNF-1β showed strong, diffuse staining in all (+) cases.

Conclusions: Consistent with prior studies, we found that PAX8 is highly expressed in NM (86%).

GATA3, when used alone, is not useful in excluding NM as it is expressed in a significant proportion of NM (50%).

PSMA is not expressed in NM, and is thus useful in distinguishing NM from prostatic adenocarcinoma.

HNF-1β is highly expressed in NM , exposing a potential diagnostic pitfall in differentiating NM from clear cell carcinoma.

823 Clinicopathological Features of 15 Penile Squamous Cell Carcinoma in Circumcised Men

Dilek Baydar, Hampar Akkaya, Duygu Apa, Nebil Bal, Asli Demirsam, Berrin Gucluer, Nalan Nese, Aysegul Sari. Hacettepe University, Ankara, Turkey; Baskent University, Alanya, Turkey; Mersin University, Mersin, Turkey; Baskent University, Adana, Turkey; Bucak State Hospital, Burdur, Turkey; Medeniyet University, Istanbul, Turkey; Celal Bayar University, Manisa, Turkey; Ataturk Education and Research Hospital, Izmir, Turkey.

Background: Cancer of the penis is uncommon and more than 95% of cases of penile malignancy are squamous cell carcinoma. These have several histologic subtypes with different clinicopathologic, viral, and outcome characteristics. We present clinical and morphological features of 15 cases of invasive penile squamous cell carcinoma (SCC) in a circumcised male population.

Design: Retrospective data from eight different center databases were searched for penile malignancies in circumcised men that were undergone resection and diagnosed as invasive squamous carcinoma. Fifteen adult patients (median age, 65 years; range, 37 to 83 years) were determined. All surgical, pathologic, and oncologic outcome data were analyzed.

Results: Local excision (2 cases), penectomy (7 cases) or partial penectomy (6 cases) were preferred surgical choices. Most tumors (73%) were located in glans. Tumor size ranged from 1.8 to 6 cm. The morphological subtypes recognized were: (1) conventional keratinizing squamous type: 6 cases, (2) well-differentiated papillary type: 3 cases, (3) basaloid type: 2 case, (4) warty-basaloid type: 1 case, (5) verrucous type: 1 case, (6) pseudohyperplastic type: 1 case, (7) acantolytic type: 1 case. Invasion of penile erectile tissues and involvement of urethra were frequent (80% and 47% respectively). Inguinal nodal metastases were found in 4/8 patients with groin dissections. Four patients died because of disease (2 months to 2 years after surgery), one died from causes other than penile cancer.

Conclusions: Penile SCC in circumcised males is a disease of old age and majority occur in glans. Most common histologic variant is conventional non-verruciform keratinizing subtype. It is associated with high stage presentation and frequent lymph node metastasis. >25% die due to disease within 2 years.

824 Long Term Outcome in a Biopsy Cohort of 988 Conservatively Treated Prostate Cancers. Evidence for Revised Gleason Grading and Use of the Worst Scoring Core

Luis Beltran, Bernard North, Gabrielle Fisher, Henrik Moller, Peter Scardino, Jack Cuzick, Daniel Berney. Queen Mary University, London, United Kingdom; Memorial Sloan Kettering Cancer Center, New York, NY; Kings College, London, United Kingdom.

Background: It is suggested that Gleason scoring (GS) should be revised to into 5 prognostic grade groups (GS ≤ 6; 3 + 4; 4 + 3; 8; ≥9). However most studies are on patients treated radically or by using pathological surrogates for outcome. There is also debate as to whether an 'overall' or 'worst' Gleason score should be used.

Design: Men with clinically localized prostate cancer diagnosed by needle biopsy from 1990-2003 were included. The endpoint was prostate cancer death. Clinical variables included GS, PSA, age, clinical stage, and disease extent. Patients treated radically within 6 months, those with objective evidence of metastases or who had prior hormone therapy were excluded. Follow up was through cancer registries up until 2012. Deaths were divided into those from prostate cancer and those from other causes, according to WHO criteria. 988 biopsy cases were centrally reviewed by two uropathologists using the ISUP 2005 GS criteria. Cores were separately graded, as well as an 'overall' score given.

Results: 6506 cores were graded. The median number of cores per case was 6. Cases were divided into 5 prognostic grade groups (GS ≤ 6; 3 + 4; 4 + 3; 8; ≥9). Using both 'worst' and 'overall' GS yielded 5 prognostic groups. Both 'overall' and 'worst' score analysis yielded highly significant results on univariate analysis with worst GS slightly but insignificantly outperforming overall GS. It should be noted that GS 3+4=7 separated highly significantlly from GS 4+3=7.

Gleason score	No (Deaths)	Hazard ratio (CIs)	X2(1df)	p value
6	306(15)	1(ref)	102.2	5.0x10-24
3+4=7	246(31)	2.66(1.43-4.92)		
4+3=7	212(47)	5.28(2.95-9.47)		
8	109(28)	6.96(3.72-13.1)		
9 and above	115(48)	12.2(6.81-21.7)		

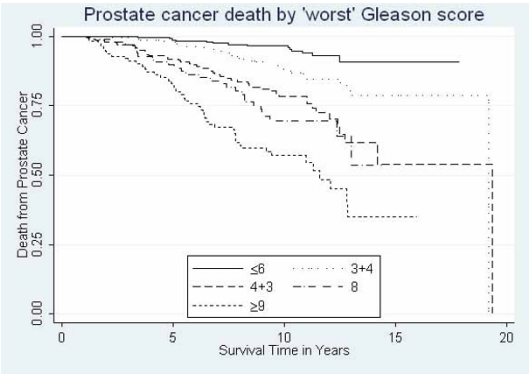

Conclusions: This is the largest conservatively treated biopsy cohort with long term follow up and contemporary assessment of GS. It validates the formation of 5 prognostic groups and suggests that 'worst' GS is a valid and possibly preferable method of GS assessment which could be adopted internationally to improve prognostic information and simplify GS for clinicians and patients.

825 A High Incidence of Malignancy in the Urinary Bladder Diverticula – Analysis of Pathology Findings in a Series of 41 Bladder Diverticula

John Biemer, Maria Picken. Loyola University Medical Center, Maywood, IL.

Background: Most bladder diverticula are small and asymptomatic, but they can be associated with infections and stones due to urine stasis, urinary retention and perforation. Malignancy has been reported to occur in 1-10% of bladder diverticula. All variants of urothelial cell carcinoma (UC) have been reported in bladder diverticula, with a relatively higher frequency of unusual subtypes compared to the general population. The goal of this study was to characterize the histopathology in surgical pathological cases involving bladder diverticula at a tertiary institution.

Design: Patients with bladder biopsies or cystectomies with pathological diagnoses made on a diverticulum were retrospectively identified during a 10-year period. Data were abstracted from their electronic charts and statistical analysis was performed.

Results: 41 patients were identified who had bladder diverticula within their specimens from June 2004 to June 2014. There were 12 cystectomies (29.3%) and 29 (70.7%) lesser procedures such as biopsies and excisions. The age ranged 4- to 86-years-old (mean: 66.1 years) and 92.7% of the patients (38/41) were male. The bladder diverticula were diagnosed with malignancy in 20 cases (48.8%), inflammation in 18 cases (43.9%) and were benign in the remaining three cases (7.3%). In 1 of the cases of inflammation and 1 of the benign diverticula cases there was a malignancy identified in another part of the bladder, making a total of 22 cases with malignancies (53.7%).

Of the 22 cases of malignancy, 20 were UC (90.9%), with 4 showing unusual features (such as sarcomatoid, neuroendocrine or squamous differentiation). There were 2 cases of non-UC bladder cancer (9.1%): both were squamous cell carcinoma. In 10/22 malignancy cases (45.5%), a tumor was identified only in the diverticulum. In 12/22 cases (54.5%), tumor was diagnosed outside the diverticulum (including the 2 cases where tumor was identified only outside the diverticulum). In 5/22 cases of malignancy (22.7%), a higher grade tumor was identified within another part of the bladder than was present in the diverticulum. In the 12 cystectomy cases examined, 1 was staged as Tis, 4 as T1, 1 as T2, 4 as T3 and 2 as T4.

Conclusions: In this study, close to 50% of bladder diverticula were diagnosed with malignancy, including malignancy limited to diverticula in 25% of cases and unusual and high grade malignancies. There was also a high rate of inflammation. Thus, a high index of suspicion is necessary when examining such specimens and direct diverticulum sampling should be considered.

826 Bladder Diverticulum Malignancy as a Diagnostic Pitfall

John Biemer, Guliz Barkan, Maria Picken. Loyola University Medical Center, Maywood, IL.

Background: Most bladder diverticula are small and asymptomatic, but malignancy has been reported to occur in 1-10% of cases. The goal of this study was to identify cases of malignancy in bladder diverticula, at a tertiary institution, and examine the efficacy of urine cytology for their diagnosis.

Design: The authors retrospectively identified patients, during a 10-year period, with bladder biopsies or cystectomies with pathological diagnoses made on a diverticulum. Data were abstracted from their electronic charts and statistical analysis was performed.

Results: 41 patients were identified who had bladder diverticula within their specimens, from 06/2004 to 06/2014. There were 12 cystectomies (29.3%) and 29 (70.7%) lesser procedures, such as biopsies and excisions. The age range was 4- to 86-years-old (mean: 66.1 years) and 92.7% of the patients (38/41) were male. Bladder diverticula were diagnosed with malignancy in 20 cases (48.8%), inflammation in 18 cases (43.9%), and were diagnosed as benign in the remaining three cases (7.3%). In 1 case of inflammation, and 1 of the benign diverticula cases, a malignancy was also identified in another part of the bladder, making a total of 22 cases with malignancies (53.7%).

In 10/22 malignancy cases (45.5%), a tumor was identified only in the diverticulum. In 12/22 cases (54.5%), tumor was diagnosed outside the diverticulum (including the two cases where tumor was identified only outside the diverticulum). In the 10 cases where the malignancy was present only in the diverticulum, eight were high-grade urothelial carcinoma (UC) (including two cases of in situ carcinoma), one was low-grade UC, and one was moderately differentiated squamous cell carcinoma.

In 7/10 cases with malignancy present only in the diverticulum, urine cytology had been done within the three months prior. Cytology was positive for UC in two of the seven cases (28.6%) and suspicious for UC in one case. In 3/7 cases, including 2 cases of high grade malignancy, urine cytology was negative for malignancy, and in 1/7 cases with high grade malignancy, on cytology, rare atypical urothelial cells were found.

Conclusions: In this study, close to 50% of bladder diverticula were diagnosed with malignancy. Cytology failed to detect malignancy limited to the diverticulum in 4/7 concurrently examined specimens, including 3/7 high grade UC. Isolated malignancies in bladder diverticula are more difficult to detect by urine cytology than tumors in the rest of the bladder. Thus, a high index of suspicion is necessary when examining such specimens, and direct targeting of the diverticulum with biopsy and/or cytology may be necessary.

827 Bowenoid Papulosis of the Male Genitalia: Morphologic Features of 15 Cases

Athanase Billis, Maria Cintra, Maria Guillen, Marcelo Mota, Kelson Carvalho, Camila de Angelis, Leandro Freitas, Larissa Costa. School of Medical Sciences, State University of Campinas (Unicamp), Campinas, SP, Brazil.

Background: The term bowenoid papulosis was first used in 1978 to describe lesions on the penile shaft and perineum in young men. Histologically, bowenoid papulosis closely resembles squamous cell carcinoma in situ. However, its clinical behavior significantly differs from that of Bowen's disease. The lesion is a HPV-related condition that affects young males and spontaneous regression has been reported in a number of cases. The aim of the study was to describe the histologic spectrum of the lesion.

Design: The study was based on the morphologic features of the lesions from 15 males with clinical diagnosis or suspicious for bowenoid papulosis of the penis or perineum. We evaluated the frequency and intensity of several histologic features: hyperkeratosis, parakeratosis, acanthosis, papillomatosis, dyskeratosis, cellular atypia, mitosis (atypical, in metaphase, or in anaphase), cytoplasmic clearing, koilocytotic atypia, melanin in dermis, and dermal inflammation. The morphology of the lesions was compared to carcinoma in situ of the male genitalia of 17 patients ≥ 60-year-old. We used the new nomenclature for intraepithelial neoplasia of the male genitalia proposed by Cubilla: 1. differentiated intraepithelial neoplasia; 2. undifferentiated condylomatous (warty) intraepithelial neoplasia; 3. undifferentiated basaloid intraepithelial neoplasia; 4. undifferentiated condylomatous/basaloid intraepithelial neoplasia; and, 5. mixed differentiated and undifferentiated intraepithelial neoplasia.

Results: The mean and median age (range) of the 15 patients with bowenoid papulosis was 27, and 27 (13-40) years. The histologic findings were indistinguishable from intraepithelial neoplasia of the male genitalia from the patients ≥ 60-year-old. According to the nomenclature proposed by Cubilla the distribution of the lesions was: 9/15 (60%) - differentiated intraepithelial neoplasia; 3/15 (20%) - undifferentiated mixed condylomatous/basaloid intraepithelial neoplasia; 2/15 (13%) undifferentiated condylomatous intraepithelial neoplasia; 1/15 (7%) undifferentiated basaloid intraepithelial neoplasia. No single histologic feature according to frequency or intensity differed significantly from the 17 patients ≥ 60-year-old with intraepithelial neoplasia.

Conclusions: Bowenoid papulosis is indistinguishable morphologically from all histologic subtypes of intraepithelial neoplasia of the male genitalia. No single histologic feature according to frequency and intensity is distinctive of the lesion. The diagnosis is based essentially on age and clinical findings of the patient.

828 Predictive Criteria on Biopsies of Insignificant Prostate Cancer: What Is the Correspondence in Linear Extent To Percentage of Cancer in a Single Core?

Athanase Billis, Maisa Quintal, Leandro Freitas, Larissa Costa, Ubirajara Ferreira, Marcelo Mota, Kelson Carvalho, Camila de Angelis. School of Medical Sciences, State University of Campinas (Unicamp), Campinas, SP, Brazil.

Background: Epstein's criteria on needle biopsies for prediction of clinically insignificant prostate cancer in surgical specimens are widely used. Epstein's criterion "no single core with >50% cancer" has no correspondence in linear extent. The aim of this study is to find this correspondence.

Design: From a total of 401 consecutive patients submitted to radical prostatectomy, 17 (4.2%) met criteria for insignificant cancer in the surgical specimen. We defined insignificant cancer in radical prostatectomy, patients with T1c clinical stage, organ-confined tumor (pT2), minimal tumor extent, negative surgical margins, and Gleason score ≤ 6. These 17 patients had no biochemical recurrence in a mean follow-up of 89 months (median 96, range 38-160). Pathologic density was evaluated as serum preoperative PSA/weight of the prostate in surgical specimen. Tumor extent was evaluated by a semiquantitative point-count method previously described. A total of ≤ 10 positive points correspond to ≤ 0,5 cm^3 tumor. The clinicopathologic findings in the correspondent biopsies were compared with Epstein's criteria for insignificant cancer. Cancer in a single core was evaluated in percentage as well as linear extent in mm. We also evaluated the length of cancer in all cores in mm.

Results: Mean, median (range) for pathologic PSA density was 0.19, 0.17 (0.11-0.27); for the number of cores with cancer 1.41, 1 (1-2); for the maximum percentage of length in a single core 13.69, 12 (4.5-25); for maximum length of cancer in a single core in mm 1.19, 1 (0.5-2.5); and, for the length of cancer in all cores in mm 1.47, 1.5 (0.5-3). Comparing the clinicopathologic findings with Epstein's criteria predictive of insignificant cancer, there was 100% concordance for clinical stage T1c, no Gleason pattern 4 or 5, ≤ 2 cores with cancer, and no single core with > 50% cancer. Only 23.53% patients had density ≤ 0.15. We found that Epstein's criterion of "no single core with >50% cancer" corresponds to 2.5 mm in linear extent. The extent of cancer in all cores in mm was 3 mm.

Conclusions: To pathologists that use Epstein's criteria on biopsies predictive of insignificant cancer and measure linear extent in mm, our study favors that "no single core > 50% cancer" may correspond to >2.5 mm in linear extent.

829 A 16 Gene Signature for Assessing Risk of Recurrence in Renal Cancer: Performance Beyond Conventional Pathologic Factors and Impact of Tumor Heterogeneity

Michael Bonham, Serge Koscielny, Margarita Lopatin, Christer Svedman, Virginie Verkarre, Camelia Radulescu, Yann Neuzillet, Isabelle Hemmerle, Timsit Marc Olivier, Jean Francois Martini, James Williams, Athanasios Tsiatis, Dejan Knezevic, Thierry Lebret, Audrey Goddard, Arnaud Mejean, Bernard Escudier. GHI, Redwood City, CA; IGR, Villejuif, France; Necker, Paris, France; Foch, Suresnes, France; Pfizer, San Diego, CA.

Background: The 16-gene Recurrence Score (RS) was developed in a cohort of 931 stage I-III ccRCC patients (pts) from Cleveland Clinic. A large prospectively-designed clinical validation study of the RS in stage I-III ccRCC pts from 1995 to 2007 at the French consortium was recently reported. The present analysis assesses the performance of the (RS) against conventional pathologic factors and tumor heterogeneity.

Design: The genes, algorithm, endpoints, methods, and analysis plan were pre-specified prior to merging clinical and molecular data. RT-PCR in fixed paraffin-embedded tissue was performed without knowledge of clinical data. Recurrence-free interval was analyzed using Cox regression stratified by stage with data censored at 5 years, and using Kaplan-Meier methods. To assess the impact of tumor heterogeneity, consistency of expression for the 16 genes and the RS was examined in a separate cohort of 8 patients with two blocks per patient and 3 different depth levels per block.

Results: RS was successfully generated in 626/645 pts (97%): 398 stage I, 54 stage II, 174 stage III. Most (71%) patients were male, 29% were ≥ 70 years, and 36% had a partial nephrectomy, 46% with tumors ≤4 cm, 65% with Fuhrman grade (FG) 3-4, and 27% with invasion. The continuous RS predicted recurrence risk (HR per 25 point increase in RS =3.9, 95% CI 2.6-5.8, p<0.001). RS continued to predict recurrence after adjustment for tumor size, FG, and Leibovich score (p<0.001). RS identified 39% of stage I pts with an average 5-yr recurrence risk of 2% (95% CI 0-7%) and 15% of pts with a 23% (95% CI 13-39%) risk. In stages II-III, RS identified 19% of pts with a 2% (95% CI 0-16%) and 44% of pts with a 39% (95% CI 29-50%) recurrence risk. The performance of RS was similar across age groups (<60, 60-70 or ≥70), gender, partial/radical nephrectomy, tumor size (≤4, 4-7 or >7cm), FG, and presence/absence of invasion (all interaction p>0.29). There was no substantial heterogeneity in single gene expression or RS (<1 SD) both within and between blocks in the separate 8-patient study.

Conclusions: The RS is validated as a predictor of clinical outcome in stage I-III ccRCC patients providing significant information beyond conventional pathologic measures. Gene expression variability within and between blocks for the 16 gene RS was low, indicating that the assay has a robust performance despite tumor heterogeneity.

830 The Methylation Landscape of the Mediator Complex in Prostate Cancer

Martin Braun, Mario Deng, Anne Offermann, Isabella Syring, Zaki Shaikhibrahim, Sven Perner. University Hospital of Bonn, Bonn, Germany.

Background: The Mediator is a multi-subunit protein complex that regulates gene transcription and serves as a hub for a variety of cell signalling pathways. Recently, we showed that the Mediator is implicated in prostate cancer (PCa), as the subunits MED12 and MED15 are overexpressed in lethal forms of the disease, and drive cancer by modulation of TGF-ß. However, few efforts have been made to unravel the underlying mechanism that lead to Mediator overexpression. We thus explored gene methylation of the Mediator in PCa, and studied its relationship to gene expression and clinical presentation.

Design: 369 PCa specimens for which genomic methylation data (HumanMethylation450 BeadChip) was available were obtained from The Cancer Genome Atlas. Where available, matched gene methylation of adjacent benign tissue was included in the analysis. For each Mediator subunit, methylation measure points distributed over promoters, gene bodies and transcriptional enhancer sites were selected. Further, expression data was extracted and normalized. For most cases, clinical data was accessible. Wilcoxon sum-rank test was used to identify differentially methylated regions. Unsupervised clustering was performed to determine methylation based subgroups of PCa. Statistical analysis was done using R and SPSS.

Results: Virtually all Mediator promoters are demethylated, while most gene bodies reveal high methylation levels. Enhancer regions, however, present with variable methylation. Substantial methylation differences with respect to normal tissues could only be observed for a few subunits. Most strikingly, MED20 gene body methylation is considerably reduced in 16% of PCa, and associated with higher Gleason Score and lower time to biochemical recurrence. Further, MED12 transcriptional enhancer hypermethylation predicts MED12 expression and correlates with Gleason Score, and tumor stage. In most other subunits, methylation changes in a given gene region do not impact its expression. Interestingly, unsupervised clustering of tumor methylation subdivided PCa into two clinically distinct subgroups, with MED20 body hypomethylation being the most important classifier.

Conclusions: Generally, methylation changes in promoters and other regions do not predict expression, and differences compared to matched benign tissue are low. However, MED20 gene body hypomethylation is very common and linked to an unfavourable phenotype, though the underlying mechanism remains unclear. Further, transcriptional enhancer site methylation of MED12 might be accounting for MED12 intertumor expression heterogeneity.

831 Whole Exome Sequencing of Matched Primary Prostate Cancer and Lymph Node Metastases

Martin Braun, Roopika Menon, Wenzel Vogel, Diana Boehm, Mario Deng, Sven Perner. University Hospital of Bonn, Bonn, Germany.

Background: Prostate cancer (PCa) usually disseminates to regional lymph nodes before giving seed to distant metastasis. The underlying genetic mechanisms leading to spreading of the tumor, however, are poorly understood. In particular, the genetic relationship between primary PCa and its lymph node metastases is only partially elucidated. Hence, we generated and compared whole exome sequencing data of paired primary PCa and lymph node metastases.

Design: Specimens of 5 PCa patients with matched primary tumor, lymph node metastasis and adjacent benign tissue have been subjected to SOLiD 4 whole exome sequencing, with 100x coverage. Raw reads were mapped using BFAST with default parameters. Reads with a PHRED-score under 30 and potential PCR duplicates were removed using SAM-Tools. Realignment around INDELs was performed using GATK. Somatic variant calling was accomplished using Somatic Sniper. For validation purposes, we used publicly available (The Cancer Genome Atlas, TCGA) gene sequencing and expression data of primary PCa.

Results: Overall, number of somatic variants in matched primary PCA and lymph node metastasis were within a comparable range, but mostly higher in lymph node metastases. Despite a similar number of mutations, overlapping alterations between the matched pairs were surprisingly low, ranging from 13 to 17%. Interestingly, cell cycle regulator CCNE2, NWD1 (function unknown) and kinesin KTN1 were mutated in all lymph node metastases, but none of the primary tumors. While CCNE2 is known to be amplified in approximately 5% of primary PCa, mutations have not been reported so far. Mutations in NWD1 or KTN1 in primary PCa have been noted, but are extensively rare (<1%, TCGA). Notably, zinc finger ZNF717 and microRNA MIR4273 were mutated in all analyzed primary PCa and lymph node metastases.

Conclusions: Our results demonstrate that lymph node metastases show a high genetic diversity in comparison to their seeding primary tumors. Moreover, the substantial amount of genetic heterogeneity found between different lymph node metastases reflects the variety of alterations that PCa evolve during the metastatic process. Results further indicate that mutations in CCNE2, NWD1 and KTN1 might be associated with metastasized PCa.

832 Cystic Clear Cell Tubulo-Papillary Renal Cell Carcinoma (CCTP-RCC): Is Multilocular Clear Cell Cystic Neoplasm of Low Malignant Potential (MCCN LMP) Related To CCTP-RCC?

Fadi Brimo, Chantal Atallah, Gangyong Li, John Srigley. McGill University Health Center, Montreal, QC, Canada; Trillium Health Partners, Mississauga, ON, Canada.

Background: This study reports the morphological spectrum of CCTP-RCC with a prominent cystic pattern, an entity which overlaps with other cystic renal lesions including MCCN LMP.

Design: Nine cases from two large academic centers were identified and detailed morphological and immunohistochemical findings were recorded.

Results: The mean age was 63 years and the mean tumor size was 2.1 cm (range= 1-4.4). The pathological T-category was T1a in all cases. The macroscopic description was simple cyst in three and multilocular cyst in six cases. The original diagnosis was MCCN LMP in five and CCTP-RCC in four cases. All cases were composed of variably sized cysts lined by one layer of clear cells. While two cases were exclusively cystic, seven showed tubular formation in the septae; two of which had very rare tubules and five in which the tubular growth was compact imparting a pseudo-solid appearance. In addition, two cases had foci of nests and single cells which along with the pseudo-solid areas showed similarities to the cellular areas present in the septae of the classically described MCCN LMP. The tubular/pseudo-solid/nested/ single cells foci formed microscopic nodules ranging in size from 1 to 5 mm (mean 1.8 mm). Three cases had focal intra-cystic micropapillary formation. The neoplastic cells had clear cytoplasm and were of ISUP nucleolar grade 1-2/4. In all cases, the neoplastic nuclei were aligned away from the basement membranes at least focally. All tumors were strongly and diffusely positive for PAX-8, CAIX (seven in a cup-shaped distribution), CK7, CK34BE12, and were negative for CD10.

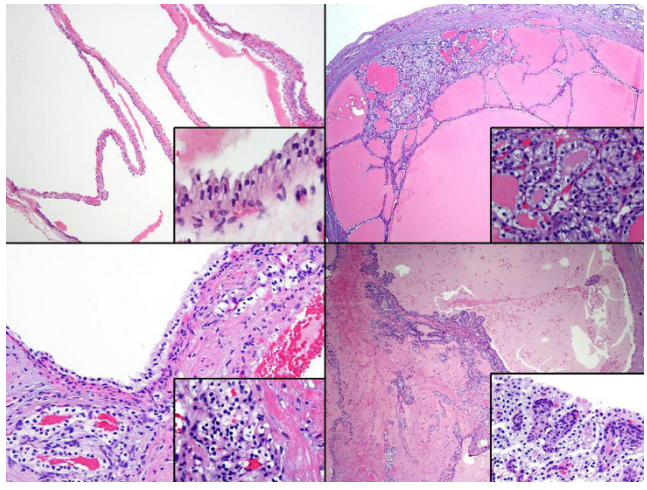

Conclusions: Cystic CCTP-RCC is a pattern that should be recognized as it shows overlapping morphological features with both multilocular cyst and MCCN LMP. The characteristic nuclear alignment and the presence of tubular and micropapillary architecture in addition to the distinctive immunohistochemical profile are helpful diagnostic clues. This report raises the question of whether some examples of MCCN LMP reported in the literature were in fact cystic CCTP-RCC, an observation which could explain the heterogeneous molecular findings reported in MCCN LMP.

833 Continuous Spatial Sequences of Lichen Sclerosus (LS), Penile Intraepithelial Neoplasia (PeIN) and Invasive Carcinomas

Sofia Canete, Diego Sanchez, Adriano Piris, Patricia Zarza, Sabrina Oneto, Cecilia Lezcano, Gustavo Ayala, Mai Hoang, Martin Mihm, Antonio Cubilla. Instituto de Patología e Investigación, Asunción, Paraguay; Facultad de Ciencias Médicas – UNA, Asunción, Paraguay; Massachusetts General Hospital and Harvard Medical School, Boston, MA; University of Pittsburgh, Medical Center, Pittsburgh, PA; University of Texas, Houston, TX.

Background: If sufficient number of sections are examined, LS is found in about two thirds of resection specimens with penile cancer. It has been hypothesized that LS represents a precancerous condition. To qualify as such, spatial correlation between LS and neoplastic lesions needs to be demonstrated, in addition to the presence of cytological atypia.

Design: Circumcision (28 cases) and penectomy (81 cases) specimens were evaluated. All cases had LS, PeIN and/or invasive carcinomas. We prepared a diagrammatic model of each case where LS, PeIN and invasive carcinomas were represented as rectangles, squares and triangles, respectively.

Results: All cases (109) were classified in 4 general patterns with frequency and confidence interval (CI) calculated as shown in Figure 1.

Pattern	Sequences	Total (%)	CI 95%
1		25 (33)	15-31%
2		46 (42)	33-52%
3		35 (32)	23-41%
4		3 (3)	-0.3-6%

Conclusions: In most cases, LS was sequentially and continuously located with this distribution: 1) next to PeIN, 2) next to and below PeIN, and 3) next to and below/within PeIN/invasive carcinoma. In a minority of cases, LS was separated or discontinous from the sequence LS-PeIN-Carcinoma. LS within the cancer was not previously described. The striking spatial relationship among LS, PeIN and invasive carcinoma as shown in this study is a necessary (but no sufficient) condition for the hypothesis postulating LS as a penile precancerous lesion.

834 International, Multicenter Study of FOXA1 Expression in Urothelial Carcinoma of the Upper Urinary Tract

Carla Caruso, Laura-Maria Krabbe, Payal Kapur, Linda Hynan, Jose Karam, Alon Weizer, Mesut Remzi, Nathalie Rioux-Leclerq, Andrea Haitel, Arthur Sagalowsky, Shahrokh Shariat, Yair Lotan, Richard Bruggeman, Catherine Abendroth, Zhaohai Yang, David DeGraff, Jay Raman. Penn State Hershey Medical Center, Hershey, PA; University of Texas Medical Center, Dallas, TX; University of Muenster Medical Center, Muenster, Germany; University of Texas MD Anderson Cancer Center, Houston, TX; University of Michigan Cancer Center, Ann Arbor, MI; Medical University of Vienna, Vienna, Austria; Centre Hospitalier Universitaire de Rennes, Rennes, France.

Background: Upper tract urothelial carcinoma (UTUC) accounts for 10% of urothelial tumors. Current studies implicate standard pathologic parameters which may not dictate the variable biologic behavior of UTUC. Forkhead Box A1 (FOXA1) expression maintains differentiation of bladder urothelium. Yet the role of FOXA1 in UTUC is unknown.

Design: An international consortium of 633 patients undergoing nephroureterectomy for UTUC was used to create a tissue microarray with annotated clinical data. FOXA1 immunohistochemistry was performed and assessed in a semi quantitative fashion and calculated by FOXA1 intensity multiplied by percentage involvement. Statistical analysis determined the association of FOXA1 expression with clinical parameters.

Results: Within this cohort, 53% of patients had muscle-invasive, 74% high grade, and 8% lymph node metastases. Three-quarters of tumors were located in the renal pelvis, 84% presented papillary architecture, and 13% had necrosis. FOXA1 expression was lost in 217 cases (34.6%). Additionally, 237 (37.86%), 118 (18.8%) and 54 (8.63%) cases expressed low, moderate and high levels of FOXA1 expression, respectively. FOXA1 loss was associated with papillary architecture (median, 14%, p=0.004), absence of tumor necrosis (median 15%, p=0.002), and renal pelvis location (median 7%, p <0.001). At last follow-up, 212 patients were dead, 154 patients experienced disease relapse, and 133 died of disease. Loss of FOXA1 is correlated with increased likelihood of death (p=0.065) and death from disease (p=0.09).

Conclusions: Loss of FOXA1 is associated with several pathologic features and may be associated with disease specific outcomes in UTUC. Further investigation regarding the role of FOXA1 in UTUC is warranted.

835 HAS3 Underexpression as a Poor Prognostic Factor in Patients With Urothelial Carcinomas of Upper Urinary Tracts and Urinary Bladders

I-Wei Chang, Chien-Feng Li. E-DA Hospital, Kaohsiung, Taiwan; Chi Mei Medical Center, Tainan, Taiwan.

Background: Urothelial carcinoma (UC) is the most common tumor type of urinary tract. Despite the less frequent prevalence and worse prognosis of upper tract urothelial carcinoma (UTUC) compared with urinary bladder urothelial carcinoma (UBUC), tumorigenesis of UC arising from both areas may share a similar pathway. Hyaluronan synthase activity is one of the most important events of carcinogenesis that has not been systemically investigated in UC. Through data mining from a published transcriptomic database of UBUCs (GSE31684), *hyaluronan synthase 3 (HAS3)* was identified as the most significant gene showing stepwise downregulation from early tumor development to progression among those associated with hyaluronan synthase activity (GO:0050501). The glycosaminoglycan hyaluronan and its synthases, hyaluronan synthases (HAS1-3), are increasingly implicated in cancer growth and progression. We therefore analyze *HAS3* transcript and protein expressions and their associations with clinicopathological factors and survivals in our well-characterized cohort of UC.

Design: Real time RT-PCR was used to detect *HAS3* messenger RNA (mRNA) level in 40 UTUCs and 35 UBUCs, respectively. Immunohistochemistry evaluated by using H-score was used to determine HAS3 protein expression in 295 UBUCs and 340 UTUCs, respectively. The mRNA and protein expression statuses were further correlated with clinicopathological features. The prognostic significance of HAS3 protein expression was further evaluated for disease-specific survival (DSS) and metastasis-free survival (MeFS).

Results: Lower *HAS3* transcript level was associated with higher pT status and nodal metastasis in both UTUC and UBUC (all p<0.05). HAS3 protein underexpression was also significantly associated with advanced pT status (both p<0.001), lymph node metastasis (both p£0.001), high histological grade (both p<0.001), vascular invasion (UTUC, p<0.001; UBUC, p=0.003), frequent mitoses (both p<0.001) in both groups of UC. HAS3 underexpression not only predicted worse DSS and MeFS at univariate analysis, but also implicated inferior DSS (both p£0.001) and MeFS (both p£0.001) in multivariate analysis.

Conclusions: HAS3 underexpression is associated with advanced tumor status and implicated adverse clinical outcome for both patients of UTUC and UBUC. Our study disclosed that HAS3 plays an important role in tumor progression in UC and may serve as a potential prognostic biomarker and a novel therapeutic target of UC.

836 Clinical Significance of Atypical Prostate Glands in Transurethral Resection of Prostate Specimens

Sonja Chen, Ali Amin, Andres Matoso. Rhode Island Hospital, Providence, RI.

Background: Prostate needle biopsies with foci of atypical glands suspicious, but not diagnostic of carcinoma are associated with an increased risk of prostate cancer diagnosis in subsequent biopsies. The characterization and clinical significance of similar findings in transurethral resections of the prostate (TURP) is largely unknown.

Design: A total of 1260 specimens without a diagnosis of cancer were retrieved from our surgical pathology files from 1994 through 2014. Specimens with a malignant diagnosis (prostate or urothelial carcinoma) and patients with prior history of adenocarcinoma of the prostate were excluded. Immunohistochemistry for p63, high molecular weight cytokeratin, and racemase (PIN4) was performed in all cases. To be considered atypical suspicious for carcinoma, cases must have been reported as such by the pathologist and must show glands that are negative for basal cell markers.

Results: 17 cases (1.4%) were identified with the diagnosis of suspicious for carcinoma. The average age was 72 years (range: 47-87) and the average specimen weight was 17 g (range: 3-57). Followup biopsies were noted with a median followup of 6.5 months (range: 0-156). The cases were grouped based on the main benign mimicker of cancer that could not be excluded from the differential diagnosis and prevented a definitive diagnosis of cancer. The results are summarized in Table 1.

Benign mimicker that could not be excluded	N	%
Cribriform clear cell hyperplasia	1	5.9
Adenosis	8	47.1
Basal cell hyperplasia with atypia	2	11.8
Crush/cautery artifact	6	35.3
TOTAL	17	100.0

2 patients (12%) had followup biopsies showing prostatic adenocarcinoma Gleason grade 3+3=6; both were treated and alive 3 years after initial diagnosis.

Conclusions: While the most frequent benign mimickers that prevent a definitive diagnosis of cancer in needle biopsies are the small size of the atypical foci, PIN and partial atrophy, in the TURP specimens, they are adenosis and crush/cautery artifact. The rate of cancer diagnosed in followup is 12%, which is similar or lower than in patients with prior benign prostate needle biopsies and significantly lower than in patients with a prior diagnosis of atypical glands suspicious for carcinoma in prostate needle biopsies of the periferal zone. A study with more patients would be necessary to safely conclude that a focus of atypical glands suspicious for carcinoma on TURPs, by itself, does not warrant further diagnostic work-up.

837 Predictive Value of Mitotic Count in Tumor Progression of Non-Invasive High Grade Papillary Urothelial Carcinoma of Urinary Bladder

Wei Wei Chen, Yuguang Liu, Norbert Sule, Bo Xu. Roswell Park Cancer Institute, Buffalo, NY.

Background: Urothelial carcinoma (UC) accounts for more than 90% bladder cancers. UC is separated clinically into superficial or muscle invasive tumors and majority of superficial UC presents as noninvasive. As 2004 WHO/ISUP removed the ambiguity diagnostic category of grade 2 UC and reclassified them into low and high grade, the population of non-invasive high grade papillary urothelial carcinoma has been expanded considerably. In this study, we investigate the relationship between mitotic activity and tumor progression in non-invasive high grade papillary UC of urinary bladder.

Design: 49 cases of non-invasive high grade papillary UC were retrieved from pathology archive between 2005 and 2014. All tumors presented on the initial biopsy specimen were graded based on 2004 WHO/ISUP criteria. Mitotic figures were counted in 10 high power filed (HPF) in double blinded fashion to avoid bias. Mean and standard error were calculated and subjected to statistical analyses. Slides from follow-up procedures, including repeat biopsies, transurethral resection or cystectomy were also reviewed. Five cases with no proper follow-up information were eliminated from the study. Invasion into lamina propria or beyond or distant metastases in follow up procedures are considered tumor progression.

Results: The mitotic count in 44 biopsy specimens ranges from 0 to 13/10 HPF with average count of 2.6 $\pm$ 0.5/10 HPF. Then cases were divided into two groups: >3 and $\leq$ 3 mitotic counts. Among 12 cases that contain more than 3 mitotic counts/HPF, 8 cases displayed tumor progression in follow up time of 19.5 $\pm$ 6.1 months, whereas in 32 cases that have equal or less 3 mitotic counts/10 HPF, only 2 showed tumor progression in follow up time of 29.2 $\pm$ 3.7 months. The relative risk (RR) for tumor progression is 10.7 with 95% confident interval (CI) 2.6-43 for biopsy specimens containing more than 3 mitotic figures. Among all cases, the male to female ratio is 4, and no age difference was found between two groups of patients.

Conclusions: We demonstrate that increased mitotic count (>3/10 HPF) in non-invasive high grade papillary UC is associated with higher risk for tumor progression into invasive tumor and/or distant metastases. Our data provide valuable information to further stratify risk factors for tumor progression among non-invasive high grade papillary UC, so patients with high mitotic count in their initial biopsies can be monitored and treated earlier in the course of disease.

838 Hereditary Leiomyomatosis and Renal Cell Carcinoma (HLRCC)-Associated Renal Cancer: A Comparison of Fumarate Hydratase (FH) and S-(2-Succino)-Cysteine (2SC) Immunohistochemistry as Ancillary Tools

Ying-Bei Chen, Max Kong, Ann Bialik, Rohit Mehra, Ajjai Alva, Norma Frizzell, Sahussapont Sirintrapun, Anuradha Gopalan, Hikmat Al-Ahmadie, Samson Fine, Arul Chinnaiyan, Satish Tickoo, Victor Reuter. Memorial Sloan Kettering Cancer Center, New York, NY; University of Michigan, Ann Arbor, MI; University of South Carolina, Columbia, SC.

Background: HLRCC-associated RCCs are highly aggressive and can exhibit a wide histologic spectrum. We have previously shown that a marker for aberrant succination of cellular proteins, 2SC, is useful for differentiating HLRCC renal cancers from high-grade sporadic RCC. As HLRCC tumors are characterized by a functional loss of FH, we sought to compare the utility of FH immunohistochemistry (IHC) to that of 2SC in this differential diagnosis.

Design: We performed FH (Santa Cruz Biotech, clone J-13) and 2SC IHC on multiple tissue microarrays and tissue sections representing 440 renal tumors, including 14 genetically confirmed HLRCC-associated RCCs, 204 clear cell, 65 papillary, 23 chromophobe, 109 high-grade unclassified RCCs, 19 oncocytoma, 2 clear cell papillary, 2 TFE3 translocation-associated and 2 renal medullary RCCs.

Results: We found that FH was ubiquitously expressed in normal kidney and all clear cell, clear cell papillary, chromophobe, oncocytoma, TFE3 translocation RCC and renal medullary carcinoma cases; although the expression levels varied. This finding was consistent with either negative or cytoplasmic-only 2SC staining in these cases. Conversely, all 14 genetically confirmed HLRCC showed strong nuclear and cytoplasmic 2SC staining, while loss of FH was observed in 12 (86%) of the 14 cases. The other two HLRCC cases had heterogeneous FH staining with some areas showing retained strong or weak FH expression. Molecularly, these 2 cases had germline/somatic missense or other in-frame *FH* mutations that may result in protein expression. The vast majority of papillary and unclassified RCC was negative or had cytoplasmic-only 2SC staining while showing retained FH. However, we found 6 cases, 1 (1.5%) of papillary and 5 (5%) of unclassified, which showed 2SC immunoreactivity identical to that of the confirmed HLRCC cases. Although genetic testing result is not available, FH loss was seen in 3 of these 6 cases, while the remaining 3 had heterogeneous FH staining.

Conclusions: Our study suggests that FH loss by IHC has a comparable specificity to 2SC staining for separating HLRCC from high-grade sporadic RCC, although its sensitivity may be lower due to retained FH expression seen with some *FH* mutations. While more readily available than 2SC, caution needs to be taken when using FH to screen for HLRCC-associated RCC. Further molecular study to investigate 2SC+/FH+ cases is warranted.

839 TSC1 or TSC2 Inactivation Is a Common Driving Event in Tuberous Sclerosis-Associated Renal Epithelial Neoplasms Exhibiting Diverse Histology

Ying-Bei Chen, Helen Won, Hikmat Al-Ahmadie, Anuradha Gopalan, Samson Fine, Pedram Argani, Lu Wang, Michael Berger, Satish Tickoo, Victor Reuter. Memorial Sloan Kettering Cancer Center, New York, NY; Johns Hopkins Hospital, Baltimore, MD.

Background: Renal cell carcinoma (RCC) is a rare presentation of tuberous sclerosis complex (TSC). The reported histology of TSC-associated renal epithelial tumors has been quite heterogeneous, with some tumors resembling clear cell (ccRCC), chromophobe (chRCC) or oncocytoma while others displaying unique or unclassified histology. The genetic makeup of these histologically diverse tumors remains unknown.

Design: We identified 45 renal epithelial tumors resected from 8 TSC patients. H&E slides of all cases were reviewed. DNA was extracted from representative tumors and matched normal controls and was analyzed by a targeted next-generation exome sequencing platform for mutations/copy number alterations (CNA) in 270 cancer-related genes and by a SNP array platform for copy-neutral loss of heterozygosity (CN-LOH).

Results: The 8 TSC patients were 5 men and 3 women. Mean age at first nephrectomy was 21.5 years (12-43), and the number of tumors excised in each patient ranged from 1 to 20, including 2 patients with bilateral nephrectomies. Among these 45 tumors, 21 (47%) were predominantly composed of clear cells, 18 with a papillary architecture, 2 with nests/alveoli (ccRCC-like), and 1 with a mixture of these patterns; 8 (18%) tumors had hybrid oncocytic/chromophobe features; and 16 (35%) tumors exhibited eosinophilic cells with tubular/papillary/sheet-like growth patterns and focal or diffuse high-grade nuclear features. Molecular study of 7 tumors from 3 patients representing the entire histologic spectrum showed that a second hit of the *TSC1*/*TSC2* gene through inactivating mutation (5 tumors), deletion (1) or CN-LOH (1) was the main molecular event driving the development of these tumors. Except for rare chromatin modifying gene mutations (*MLL* in 1), no other mutations (including *VHL*/*MET*/*FH*/*FLCN*/*SDHB*) were identified in these tumors. There was also no CNA detected in the 2 tumors with clear cells and a papillary architecture, 1 ccRCC-like and 1 chRCC-like tumor, whereas the tumors with high grade nuclear features (2) had variable copy number gains involving chromosomes 7, 11, 12, 13 or 16.

Conclusions: Our data strongly indicate that a complete loss of TSC1/TSC2 function via germline and somatic alterations is the common driving mechanism underlying the tumorigenesis of TSC-associated renal epithelial neoplasms. Although they are morphologically diverse and frequently mimic sporadic RCCs, all these tumors arise through a distinct oncogenic pathway.

840 Prognostic Value of Eosinophilic Cytoplasmic Components in Clear Cell Renal Cell Carcinoma

Jinrong Cheng, Weiwei Chen, Thomas Schwaab, Eric Kauffman, Bo Xu. University at Buffalo, Buffalo, NY; Roswell Park Cancer Institute, Buffalo, NY.

Background: Clear cell renal cell carcinoma (CCRCC) consists of more than two thirds of all renal cell carcinomas. Several clinical and pathological and clinical features of CCRCC have been established as prognostic factors, such as tumor stage, nuclear grade, sarcomatoid/rhabdoid differentiation and tumor necrosis. In this study, we evaluate possible predicting value of eosinophilic cytoplasmic components in CCRCC and correlate it with several known prognostic factors.

Design: After reviewing a cohort of patients with CCRCC who received nephrectomy at our institute, slides from 50 patients with 5-year survival and 26 patients died of CCRCC within 5 year of surgery were retrieved from pathology archive and reviewed by two independent pathologists. The percentage of eosinophilic components of each tumor was recorded. A Student's *t*-test was used to compare the average portion of eosinophilic components between patients with 5-year survival and those died of CCRCC. Regression analyses were used to evaluate the associations of the percentage of eosinophilic cells in each tumor with tumor stage and nuclear grade.

Results: The average portion of eosinophilic tumor cells was significantly lower in CCRCC from patients with 5-year survival than those died of CCRCC (15.8% vs. 47.4%, p=.0001). Pathological stages of CCRCC in the patients with 5-year survival vs. those died from cancer were as follows, 49% vs 15.4% (T1a), 27.5% vs 19.2% (T1b), 7.8% vs 11.5% (T2a), 3.9% vs 7.7% (T2b), 5.9% vs 26.9% (T3a) and 5.9% vs 19.2% (T3b). Tumor nuclear grade in patients with 5-year survival vs. those died from cancer were as follows, 14% vs 0% (grade 1), 42% vs 26.9% (grade 2), 36% vs 50% (grade 3) and 8% vs 23.1% (grade 4). The average percentage of eosinophilic component of CCRCC was not associated with tumor pathological stage (r^2=.1883) or nuclear grade (r^2 =.1633).

Conclusions: Our study showed that eosinophilic component in CCRCC can be used as a new independent prognostic factor for CCRCC. Patients with CCRCC containing 40% or more of eosinophilic component are likely to have adverse clinical outcome.

841 The Influence of Nodal Variant Histology in Bladder Cancer

Liang Cheng, Kevin Rice, Chia-Sui Kao, Jose Pedrosa, Hristos Kaimakliotis, Timothy Masterson, Michael Koch. Indiana University School of Medicine, Indianapolis, IN.

Background: The effect that the presence of urothelial histologic variants has on the behavior of urothelial carcinoma remains poorly defined. The goal of this study was to examine the relationship between different histologic variants and the presence and histology of lymph node metastases.

Design: We analyzed bladder cancer patients who demonstrated variant histology at cystectomy performed between 2001 and 2012. Overall, 292 patients demonstrated variant histology at cystectomy. After excluding patients with primary adenocarcinoma, sarcoma, and squamous variants, 141 patients remained, of which 65 demonstrated node-positive disease. Fifty-seven of these node-positive patients had slides available for review.

Results: Node positivity was most common in the micropapillary (MP), clear cell urothelial carcinoma (CC), and plasmacytoid (PC) variants. The remaining variants

demonstrated node-positive rates ranging from 11–38%. When nodes were positive, the variants found in the nodal metastases most commonly were MP, CC, glandular, nested, and lymphoepithelioma-like variants. Median lymph node density was highest in PC (33%) and CC (35%) variants, although these differences were not statistically significant. Variant histology predominated the nodal metastases regardless of predominance in bladder for the MP (84%) and CC (100%) variants. The PC variant exhibited the high incidence of positive surgical margins.
Conclusions: Lymph node metastases were most common in the MP, CC, and PC variants. Variant histology was present and predominated nodal histology in the majority of MP and CC cases. These results suggest that the variant histology itself may be driving lymphatic spread in MP and CC cases. Conversely, the PC variant may be a marker for locally-advanced and aggressive disease rather than specifically influencing lymphatic spread.

842 Three-Tiered Nodal Classification System for Bladder Cancer: A New Proposal

Liang Cheng, Jose Pedrosa, Hristos Kaimakliotis, M Francesca Monn, Timothy Masterson, Michael Koch. Indiana University School of Medicine, Indianapolis, IN.
Background: Evaluations on the current TNM staging system do not show prognostic differentiation between the three N groups in bladder cancer patients with metastatic lymph nodes (LNs). We evaluated the prognostic power of the number of positive LNs and how this indicator performs across different pelvic LN dissection (PLND) templates and adjuvant chemotherapy status.
Design: We evaluated 244 patients with positive LN urothelial cancer who underwent radical cystectomy and PLND between 2000 and 2011. Survival analyses utilizing the Kaplan–Meier method and log rank test were performed. Median followup was 55.3 months (range, 0.4–141). Multivariable Cox proportional hazards models were built to evaluate the prognostic stratification.
Results: Extended PLND template was performed on 152 (62.3%) patients and standard on 92 (37.7%). The median number of LNs resected was 14 in the standard group vs 22 in the extended group (P<0.01) and positive LNs was 2 vs 3 (P=0.09), respectively. Stratification in patients with: 1 positive LN, 2–5 positive LNs, or >5 positive LNs led to 5-year recurrence-free survival of: 48.6%, 34.5%, and 15.9% for each group, while the 5-year overall survival was: 43.0%, 22.1%, and 11.3%, respectively. Stratification in the three groups was also verified irrespective of PLND template and adjuvant chemotherapy. Two multivariable models confirmed the findings when controlling for demographic features and known pathologic risk factors.
Conclusions: Three-tiered nodal classification system using the number of metastatic LNs (1, 2–5, and >5) stratified patients with lymphatic disease into distinct prognostic groups.

843 Men With Prior Benign, High-Grade Prostatic Intraepithelial Neoplasia or Atypical Small Acinar Proliferation on Biopsy Have Lower Rates of Biochemical Recurrence After Radical Prostatectomy

Bonnie Choy, Blake Anderson, Gladell Paner. University of Chicago Medicine, Chicago, IL.
Background: High-grade prostatic intraepithelial neoplasia (PIN) is generally considered a precursor lesion of prostate cancer. Atypical small acinar proliferation (ASAP), unlike PIN, may represent an under-sampled cancer. Previous studies have shown PIN does not confer a greater risk of subsequent cancer on follow-up biopsies. Few studies have described the findings at radical prostatectomy (RP) from men with prior isolated PIN, revealing mostly favorable cancer characteristics on RP; however, rates of biochemical recurrence (BCR) are limited.
Design: A search in the University of Chicago surgical pathology database of 3674 RPs for patients with an initial negative biopsy for cancer and subsequent RP revealed 46 total cases: 24 were benign, 11 were isolated PIN, and 11 had ASAP. A control group of 40 cases was randomly selected with an initial positive biopsy for cancer and subsequent RP.
Results: The median age at cancer diagnosis for benign, PIN, ASAP, and control groups was 62, 61, 61, and 63, respectively. The characteristics of RP for benign, PIN, ASAP, and control groups were: Gleason score (GS) 6: 9/24 (38%), 5/11 (45%), 6/11 (55%), and 24/40 (60%); GS 3+4=7: 11/24 (46%), 6/11 (55%), 4/11 (36%), and 11/40 (28%); GS 4+3=7 in 3/24 (13%), 0/11, 1/11 (9%), and 2/40 (5%); GS 8 or higher in 1/24 (4%), 0/11, 0/11, and 3/40 (8%) of the control group. Involvement of the seminal vesicle was seen only in 1/24 (4%) of the prior benign group. Extraprostatic extension was seen in 2/24 (8%), 0/11, 0/11, and 6/40 (15%) of the benign, PIN, ASAP, and control groups, respectively. Positive margin was seen in 2/24 (8%), 2/11 (18%), 2/11 (18%), and 11/40 (28%) of the benign, PIN, ASAP, and control groups, respectively. Median length of follow-up was 13 months, 13 months, 19 months, and 87 months for benign, PIN, ASAP, and control groups, respectively. Median time to BCR in the control group was 13 months. BCR occurred in 1/24 (4%), 0/11, 0/11, 8/40 (20%) of benign, PIN, ASAP and control groups, respectively.
Conclusions: Our retrospective study demonstrates a lower frequency of BCR in patients with a prior benign, isolated PIN or ASAP diagnosis on prostate biopsy on men with cancer, compared to those with an initial positive biopsy for cancer. This study also supports the favorable RP cancer characteristics in patients with prior PIN on biopsy.

844 The Utility of SALL4, CDX2 and CK 20 in the Diagnosis of Somatic Malignant Transformation of Testicular Germ Cell Tumors: An Immunohistochemical and Cytogenetic Study

Maurizio Colecchia, Alessia Bertolotti, Elena De Paoli, Maria Grazia Facciorusso, Maria Adele Testi, Biagio Paolini. Fondazione IRCCS Istituto Nazionale dei Tumori, Milan, Italy.
Background: The somatic-type (or "non-germ cell") malignancies (SMs) occurring in testicular tumors are attributed to "malignant transformation" of a preexisting teratomatous element or evolving from totipotent malignant germ cell precursors. The SMs were recently reported as ephitelioid or sarcomatoid neoplasms , the former presenting more commonly the histopathologic features of adenocarcinoma. Germ cell origin of SMs occurring as adenocarcinoma with features overlapping with other somatic malignancies is difficult to recognize in metastatic sites (i.e. retroperitoneum, liver, lung) .
Design: We retrieved 16 metastatic SMs occurred in the period of 1995-2014 in patients with history of germ-cell testis tumors from the archives of the Fondazione IRCCS Istituto Nazionale dei Tumori di Milano .These tumors showed gastrointestinal features with mucinous differentiation in five cases, enteric-type adenocarcinomas resembling colonic or small intestinal adenocarcinomas in the remaining eleven cases. Additionally five metastatic cases of enteric-type somatic adenocarcinomas from large-bowel primaries were also analyzed. Immunohistochemical staining for CDX2, SALL4, CK20, OCT3/4 and MUC2 were performed and the distribution, percentage and intensity were assessed. All the 21 cases were studied to evaluate 12p overexpression by FISH, that is a common finding in germ-cell tumors.
Results: SALL4 was strongly positive in 11/16 SMs with a variable expression (20% to 100% positive tumor cells). All the five SALL4 – SMs showed 12p overexpression. OCT3/4 was negative in all the 16 cases. Five SMs showed SALL4 + CDX2 + CK20 + immunoprofile. Six cases were SALL4 + CDX2 + CK20 -, while all the five SALL4 negative tumors showed CDX2 positive stains. MUC 2 was focally present in 5/16 SMs. Metastatic intestinal somatic adenocarcinomas had the following immunostainings: CDX2 + MUC2 + CK20 + SALL4 – OCT3/4 -. The FISH analysis was formed in paraffin embedded tissues of these five tumors showing absence of 12p overexpression.
Conclusions: Combined use of FISH and IHC performed for 12p overexpression and SALL4 allows to recognize germ cell origin of metastatic epithelioid SMs with adenocarcinomatous features. Due to the high sensitivity the combination of FISH analysis and immunohistochemistry is recommended in the SMs occurring in metastatic sites.

845 Analysis of Pediatric Pure Mature Testicular Teratomas (PMTT) for Chromosome 12p Abnormalities and IMP3 Expression

Kristine Cornejo, Liang Cheng, Alanna Church, Zhong Jiang. University of Massachusetts Medical School, Worcester, MA; Indiana University School of Medicine, Indianapolis, IN; Boston Children's Medical Center, Boston, MA.
Background: Although the histologic appearance of pure mature testicular teratomas (PMTTs) is similar in children and adults, the prognosis is dramatically different. Pediatric PMTTs are rare, with a benign clinical course, while the adult cases typically have malignant outcomes. Chromosome 12p abnormalities are seen in the majority of adult testicular germ cell tumors (TGCTs), but have not been described in pediatric TGCTs, suggesting that pediatric cases are genetically distinct. IMP3 (U3 small nucleolar ribonucleoprotein, chr 15) is an oncofetal protein that is highly expressed in many malignant neoplasms. Our previous study has demonstrated that IMP3 is expressed in adult mature testicular teratomas, but not in mature ovarian teratomas. Expression of IMP3 in pediatric PMTTs has not been reported. The aim of this study was to assess chromosome 12p abnormalities and to investigate the expression of IMP3 in pediatric PMTTs.
Design: A total of 7 cases (excision, n=1; orchiectomy, n=6), were obtained from the surgical pathology files of two large Medical Centers between 1957-2013. All 7 cases were investigated for isochromosome 12p [i(12p)] and 12p copy number gain using interphase fluorescence in situ hybridization (FISH) analysis and were examined by immunohistochemistry for IMP3 expression.
Results: Patients ranged in age from 0.9-3.9 (mean 2.3) years. A positive immunohistochemical stain for IMP3 (cytoplasmic staining) was identified in 2 of 7 cases (29%). i(12p) was detected in 1 case (14%) which also expressed IMP3. Somatic copy number alterations of 12p were not observed (0%).
Conclusions: We are the first to describe a 12p abnormality and IMP3 expression in pediatric PMTTs. Our data indicates a small subset of PMTTs harbor typical molecular alterations observed in adult TGCTs. The vast majority of pediatric PMTTs do not develop in the background of 12p abnormalities, but via an alternate genetic pathway. IMP3 overexpression, which has now been described in cases with and without i(12)p, may be associated with a novel pathway for oncogenesis in both pediatric and adult TGCTs.

846 Testicular Biopsy: Qualitative Morphologic Findings in Male Infertility

Larissa Costa, Athanase Billis, Leandro Freitas, Ruana Rocha, Gabriel Oliveira, Lucas Bastos, Maria Guillen, Marcelo Mota. School of Medical Sciences, State University of Campinas (Unicamp), Campinas, SP, Brazil.
Background: Male infertility is a common clinical condition. In infertile couples, male infertility is the primary cause in 40% of cases. Testicular biopsy is only performed in a minority of cases, mostly in men with azoospermia, and one of the main purposes is to distinguish obstructive versus nonobstructive etiology. Due to the fact that testicular biopsy is not a common procedure, the pathologist must be familiar with the histology of the seminiferous epithelium for a proper diagnosis.

Design: We studied the qualitative morphology of 41 testicular biopsies from infertile males all fixed in Bouin. The morphologic findings were classified into: 1) normal spermatogenesis (the diameter of the tubules and the thickness of the epithelium are normal, and all seminiferous cells are present including spermatogonia, Sertoli cells, primary and secondary spermatocytes, spermatids, and spermatozoa); it is also important to be aware that cellular associations in humans occur in quadrants and not along all extent of a transverse section of the seminiferous tubule; 2) maturation arrest (either in spermatocytes or spermatids and no spermatozoa present); 3) germ cell aplasia (only Sertoli cells present); 4) hypospermatogenesis (all cells of the seminiferous epithelium are present but reduced in number; the latter is characterized morphologically by thinning of the germinal epithelium and vacuolation of the cytoplasm of Sertoli cells due to germ cell loss); and, 5) peritubular fibrosis (the *tunica propria* may range from slight to severe thickening and the germinal epithelium may show any one of the previous lesions and at an end stage the tubules may be completely hyalinized).
Results: From the 41 testicular biopsies, normal spermatogenesis was present in 5 (12.2%), germ cell aplasia in 6 (14.6%), maturation arrest in 6 (14.6%), peritubular fibrosis in 7 (17.1%), and hypospermatogenesis in 17 (41.5%). All males with normal spermatogenesis, germ cell aplasia, and maturation arrest were azoospermic. Patients with hypospermatogenesis were oligospermic and patients with peritubular fibrosis were either azoospermic or oligospermic according to the lesion of the epithelium.
Conclusions: The pathologist must be familiar with the histology of the seminiferous epithelium for a proper diagnosis. Fixation in Bouin is essential for the identification of germ cells. Formaldehyde fixation is contraindicated due to the strong artifacts preventing a proper diagnosis. Testicular biopsy is essential for the proper management of infertility in cases of azoospermia.

847 Chromophobe Renal Cell Carcinoma – A Simplified and Reproducible Two Tier Approach to Tumor Grading

Hannah Coulson, Paola Dal Cin, Toni Choueiri, Michelle Hirsch. Brigham & Women's Hospital, Boston, MA; Dana-Farber Cancer Institute, Boston, MA.
Background: Grading of Chromophobe renal cell carcinoma (ChRCC) is controversial, and currently an accepted grading scheme has not been established. In fact, the most recent recommendation by the International Society of Urologic Pathology was to not grade ChRCC at all. Nevertheless, it is clear that some ChRCCs are high grade and more aggressive, so there is need to distinguish such tumors from the more typical indolent ChRCC. The goal of this study was to validate a simple and reproducible grading scheme for ChRCC that correlates well with clinical outcome.
Design: 63 ChRCCs were re-reviewed for morphological confirmation. All cases were scored by 2 pathologists using the following systems: Fuhrman nuclear grade (FNG), nucleolar grade, chromophobe tumor grade (CTG), and the new method proposed in this study which simply categorizes tumors as low (LG) versus high grade (HG). HG is applied to tumors with increased nuclear atypia, hyperchromasia, the presence of necrosis, and increased mitotic activity; tumors without these findings are classified as LG. Final grade was based on the worst area. Findings were correlated with vascular invasion, stage, and clinical follow-up including recurrence and death of disease.
Results: With the newly proposed grading scheme, 48 cases (76%) were LG and 15 cases (24%) were HG. HG lesions accounted for 60% of T3/4 tumors. Metastases occurred in 4 patients with 1 dying from disease; the primary ChRCCs in these patients were all HG. In contrast, FNG 3-4, nucleolar grading 2-3, and CTG 2-3 predicted 75%, 75%, 100% of the metastatic cases, respectively. Nevertheless, sensitivity for predicting adverse disease and the negative predictive value for the absence of adverse disease are more compromised in the previously described grading methods when compared to the LG-HG method.

Grading Method	Sensitivity	Specificity	PPV	NPV
Furhman Nuclear Grade (1-2 vs 3-4)	28%	83%	60%	57%
Nucleolar Grade (1 vs 2-3)	27%	93%	70%	64%
Chromophobe Tumor Grade (1 vs 2-3)	21%	95%	90%	37%
Low vs High Grade	40%	92%	60%	83%

Conclusions: Most ChRCCs are biologically indolent; however, there is a subset that are more aggressive. In the absence of a grading system for ChRCC there may not be a clear understanding as to which cases should be followed or treated more aggressively. The use of a LG-HG system based on atypia, necrosis and mitotic activity is a reproducible and reliable method that correlates well with adverse outcome.

848 Targeted Next Generation Sequencing of Testicular Germ Cell Tumors

Hannah Coulson, Massimo Loda, Elizabeth O'Donnell, Christopher Sweeney, Michelle Hirsch. Brigham & Women's Hospital, Boston, MA; Dana-Farber Cancer Institute, Boston, MA.
Background: Germ cell tumors (GCTs) are a heterogenous group of testicular tumors that can be subclassified into pure and mixed subtypes based on distinct morphologic and immunohistochemical findings. Previous studies have demonstrated commonly encountered DNA mutations, including NRAS, KIT, MET, KRAS, and TP53, in GCTs. Further genetic profiling in the form of targeted next generation sequencing (NGSeq) is a platform that can be used to identify additional mutations and DNA alterations in solid tumors, and the goal of this study was to evaluate such findings in a cohort of testicular GCTs.
Design: Genotyping (NGSeq or 'profiling') was performed on 32 testicular GCTs, including 19 pure seminomas, 1 pure embryonal carcinoma (EC), 2 pure teratomas, and 10 malignant mixed GCTs. The oncopanel assay surveys exonic DNA sequences from 300 cancer genes and 113 introns across 35 genes for rearrangement detection. DNA is isolated from tissue and analyzed by massively parallel sequencing using a solution-phase Agilent SureSelect hybrid capture kit and an Illumina HiSeq 2500 sequencer.
Results: Approximately 60 different gene mutations in the 32 tumors were observed. The total number of mutations per subtype of GCT ranged from 1 to 11 in this targeted analysis. The 1 pure EC had 3 mutations, the pure seminomas ranged from 1 to 7 mutations (average 3 mutations), the 2 teratomas had 1 and 11 mutations, respectively, and the MGCTs varied from 1 to 7 mutations per case (average 3 mutations). Beyond the typical gene mutations already described (KIT, KRAS, etc), mutations were most frequently seen in oncogenes, transcription factors, and those associated with tyrosine kinases/tyrosine kinase receptors, such as CREBBP, FGFR, FLT1/3, JAK3, NFKB, and PDGFR. Fewer mutations were seen in DNA repair genes, but some examples include ARID1, BRCA and ERCC3/4. 8 cases in this cohort, including 3 seminomas, 3 mixed GCTs and 2 teratomas, were associated with subsequent metastasis, and the number of mutations in the primary tumor ranged from 1 to 11. Overall, there was no clear association with gene mutation combinations and tumor subtype and/or metastatic disease.
Conclusions: Targeted NGSeq has identified ~60 gene mutation in both pure and malignant mixed GCTs, the majority of which were associated with signal transduction genes. Further evaluation of these findings may lead to a better understanding of the pathophysiology of testicular tumors and the use of targetable therapies if needed in the setting of recurrence or resistance to more traditional therapies.

849 Low Immunoexpression of phosAKT Correlates With Upregulation of mTOR Pathway and HIF1a Gene Expression

Claudia Coutinho-Camillo, Luciana Schultz, Isac Castro, Gilcy Damm, Isabela Cunha, Luiz Onuchic, Fernando Soares. A.C.Camargo Cancer Center, São Paulo, Brazil; Universidade de São Paulo, São Paulo, Brazil; Instituto de Anatomia Patologica, Santa Barbara d'Oeste, Brazil.
Background: Drugs that target the PIK3/AKT/mTOR pathway are been considered for advanced or post-cysplatin bladder cancer. Clinical trials have shown long term response in some patients but resistance is not infrequent and is may relate to pathway interactions or deregulation. Accessible biomarkers of tumor response are needed for better patient selection.
Design: Samples from 72 bladder tumors resected by cystectomy and adjacent histologically-benign urothelium (paired control) were collected. Immunohistochemistry (IHC) for phosAKT (Ser473) was performed and scored as percent of positive cells. Cluster analysis identified 2 groups and a cut-off of 3.3 was reached by ROC curve. Gene expression of mTOR pathway members (PTEN, AKT3, MTOR, EIF4EBP1 and RPS6), HIF1α and cell cycle (TP53, RB1 and MIK67) were analyzed by RT-PCR. Categorized phosAKT expression was then compared to mRNA levels by Kruskall-Wallis test with Muller-Dunn post-test.
Results: Mean (median) phosAKT expression was 18.8 (10.0) in malignant samples and 61.8 (70.0) in controls. Tumors in the cluster with lower levels of phosAKT (n=7) significantly associated with higher mRNA expression of all genes related with mTOR pathway and HIF1α ($p<0.001$), but not with those related to cell cycle (p=NS). Mean mRNA expression in this subset compared to the remaining samples were 3.45 vs. 0.44 for PTEN, 2.87 vs. 0.08 for AKT3, 19.53 vs. 0.09 for MTOR, 15.70 vs. 0.18 for EIF4EBP1, 6.12 vs. 0.24 for RPS6 and 14.17 vs. 0.12 for HIF1a.
Conclusions: Bladder tumors showed lower levels of phosAKT compared to adjacent histologically-benign urothelium, suggesting that phosAKT loss is implicated in bladder oncogenesis. Furthermore, the subset with more intense loss showed significant upregulation of mTOR pathway and HIF1a gene expression.

850 Epithelial-Mesenchymal Transition (EMT) Phenotype at Invasion Front Is a Prognostic Discriminator in Usual Squamous Cell Carcinoma of the Penis

Isabela Cunha, Maria Leonardi, Marcos Leal, Stenio Zequi, Ademar Lopes, Antonio Cubilla, Rafael Rocha, Walter Costa, Jose Vassallo, Gustavo Guimaraes, Fernando Soares. A.C.Camargo Cancer Center, São Paulo, Brazil; Hospital Aristides Maltez, Salvador, Brazil; Instituto de Patologia, Asunción, Paraguay.
Background: Epithelial-mesenchymal transition (EMT) is a phenomenon associated with local invasion and metastasis. In this study, we investigate the significance of EMT phenotype (EMTp) as a prognostic factor in penile carcinoma (PC).
Design: Consecutive 149 usual squamous cell PC and 14 normal mucosa were selected. The following variables were analyzed: histologic grade, staging, pattern of invasion, LN involvement, perineural/vascular invasion. Loss of expression of ECAD and expression of VIM as prototype of EMTp were analyzed in 2 areas of the tumor (central/invasion front). Since the downregulation of ECAD was more prominent in invasion front, we used this data to establish EMT phenotype. Cases were classified into EMT normal-like (ECAD+/VIM), partial EMTp (ECAD-/VIM-) and complete EMTp (ECAD-/VIM+).
Results: The main results of the study are presented in Table 1. EMTp correlates with histological grade, pattern of invasion, LN mets, perineural and vascular.

	Normal-like N (%)	PartialEMT N (%)	CompleteEMT N (%)	p
Histologic grade WD MDPD	40 (27)51 (34)58 (39)	12 (30)14 (28)11 (19)	1 (3) 17 (33)32 (55)	
Pattern of Invasion InfiltrativePushing	116 (78)33 (22)	29 (25)8 (24)	48 (41)2 (6)	
LN mets NoYes	109 (73)40 (27)	33 (30)4 (10)	21 (19)29 (73)	
Perineural invasion NoYes	114 (77)35 (24)	28 (25)9 (26)	32 (28)18 (51)	0,0160
Vascularinvasion NoYes	53 (48)62(42)	30 (27)7(18)	28 (25)22(58)	0,0010

Patients in the complete EMTp-group had a higher probability of death from cancer (HR 7.6, P < 0.001) and overall death (HR 3.0, P < 0.001).

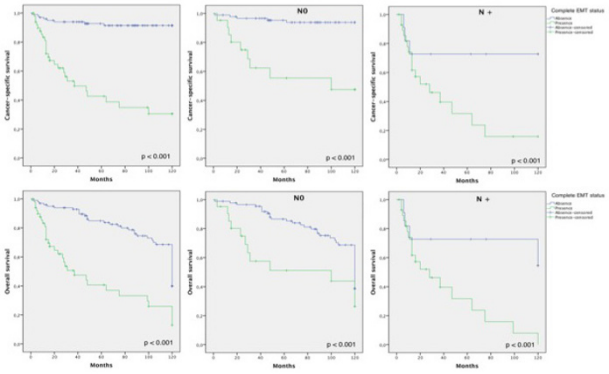

Figure 1. Survival analysis based on complete EMT status. A) Cancer-specific survival (CSS) based on EMT status. B) CSS in cases without lymph node involvement. C) CSS in cases with lymph node involvement. D) Overall survival (OS) based on EMT status. E) OS in cases without lymph node involvement. F) OS in cases with lymph node involvement

Conclusions: In conclusion, EMT phenotype is a strong prognostic predictor for penile cancer and should be evaluated at the invasive edge of the tumor.

851 Comparative Histological and Molecular Profiles of Clear Cell Renal Cell Carcinomas and Their Corresponding Metastases

Julien Dagher, Solene-Florence Kammerer-Jacquet, Angelique Brunot, Alexandra Lespagnol, Florence Jouan, Lorrie Lepage, Laurence Cornevin, Frederic Dugay, Gregory Verhoest, Karim Bensalah, Marc-Antoine Belaud-Rotureau, Nathalie Rioux-Leclercq. Rennes University Hospital, Rennes, France; Rennes Faculty of Medicine, Rennes, France; Centre Eugène Marquis, Rennes, France.

Background: Clear cell renal cell carcinoma (ccRCC) is the most frequent histological subtype of renal cancers. Patients with metastatic ccRCC are eligible to targeted therapies by antiangiogenic agents. However if the disease worsens or if patients resist to treatment, metastases are rarely biopsied, and little is known about the different profiles they could have regarding their corresponding primary tumors.

Design: Three patients with operated ccRCCs and their corresponding metastases for which frozen sections were available were retrospectively included. These metastases were either synchronous (nodal and hepatic) or metachronous (pulmonary). The tumor specimens were analyzed at different levels: histological, immunohistochemical (VEGF-A, CD31-SMA, Ki67, p53 and PAR-3), molecular by the study of the complete *VHL* gene status (deletion, mutation or promoter hypermethylation by Fluorescent in situ Hybridization FISH, New Generation Sequencing NGS and Methylation-Specific-Multiplex Ligation-Dependent Probe Amplification MS-MLPA), and finally by Array Comparative Genomic Hybridization CGH.

Results: Histological and immunohistochemical aspects of the metastases were similar to that of the high grade zones of the corresponding primary tumors. *VHL* gene was constantly inactivated in each couple by two frequent events: a deletion and a mutation. The same mutation was observed in each corresponding couple. No promoter hypermethylation was detected. CGH-array superposed DNA of metastases to that of primary tumors and showed different profiles. In particular, an arm level gain of the locus 3q22 present in metastases of all patients but not in their primary tumors. This region contains five genes (*PPP2R3A*, *STAG1*, *MSL2*, *NCK1*, and *TMEM22*) that could potentially play a role in tumor proliferation or metastatic dissemination. The overexpression of the TMEM22 protein has been described only once as being associated to increased growth of ccRCC cells.

Conclusions: This study shows that the chromosomal profile of metastases differs from that of their corresponding primary tumors. Further studies are ongoing to detail if genes on the 3q22 locus could have any metastatic potential.

852 Distinct Clinical and Histological Features in Clear Cell Renal Cell Carcinomas Harboring Wild Type VHL Genes

Julien Dagher, Solene-Florence Kammerer-Jacquet, Angelique Brunot, Christophe Perrin, Gregory Verhoest, Yannick Arlot-Bonnemains, Cecile Vigneau, Jean-Jacques Patard, Florence Jouan, Karim Bensalah, Nathalie Rioux-Leclercq. Rennes University Hospital, Rennes, France; Rennes Faculty of Medicine, Rennes, France; Centre Eugène Marquis, Rennes, France; Kremlin Bicêtre University Hospital, Le Kremlin-Bicêtre, France.

Background: Clear cell renal cell carcinoma (ccRCC) is an aggressive tumor with a 50% risk of metastases at initial diagnosis or at follow-up. It is characterized by an inactivation of the tumor suppressor gene *VHL* in more than 70% of sporadic cases by a double combination of three different mechanisms: locus deletion, gene mutation or promoter hypermethylation.

Design: In this study we correlated the complete status of the *VHL* gene in a series of 98 ccRCC tumors with pathological criteria, intra-tumoral expression of VEGF and CAIX, and a 10-year clinical follow-up of patients. ccRCCs operated between 2002 and 2005 were retrospectively included. From frozen tumor sections, *VHL* gene deletions (72.4%), mutations (69.4%) and promoter hypermethylations (13.5%) were screened by gene copy analysis (Multiplex Ligation-dependent Probe Amplification, MLPA), gene sequencing and Methylation Specific-MLPA respectively.

Results: Mutations and promoter hypermethylations were mutually exclusive. 33.6% of ccRCCs had 0 or 1 alteration (non inactivated *VHL*) *vs*. 66.3% with 2 inactivating events (inactivated *VHL*). The first group of tumors was associated with a higher Fuhrman grade 4 (p=0.02), metastases (p=0.04), sarcomatoid component (p=0.01), dense lymphocyte infiltrate (p=0.013) and to VEGF overexpression (>30%) (p=0.003). VEGF overexpression was also an independent factor associated to non inactivated *VHL* tumors after multivariate analysis. Furthermore, wild type *VHL* tumors (no alteration of the gene, 11.2%) were associated to nodal involvement (p=0.019). This subgroup of patients had a specific survival of 33 months compared to patients with ccRCCs having 1 or 2 *VHL* inactivating events (107 months) (p =0.016).

Conclusions: In this long term study, we confirm that ccRCCs with wild type *VHL* genes are highly aggressive tumors with a particular histological aspect, that need to be formerly identified.

853 Expanding Genetic and Molecular Findings in Mucinous Tubular and Spindle Cell Carcinoma

Paola Dal Cin, Bianca Espinet, Marta Galeote, Nuria Juanpere, Juan Luis Garcia, Jesus Hernandez, Patricia Antunez, Michelle Hirsch. Brigham & Women's Hospital, Boston, MA; Hospital del Mar, Barcelona, Spain; IESCYL, IBMCC, Salamanca, Spain; Hospital Universitario, Salamanca, Spain.

Background: Mucinous tubular and spindle cell carcinoma (MTSCC) is a less common renal cell carcinoma (RCC) with morphologic and immunophenotypic similarities to other RCCs, especially papillary RCC (PRCC). A few previously reported karyotypes for MTSCC have described multiple chromosomal (ch) loss; however, in fewer chromosomes than typically seen in chromophobe RCC (ChRCC). Additinally, the molecular features of MTSCC are not entirely understood. The goal of this study was to better characterize the genetic and molecular features of MTSCCs in comparison to other renal epithelial neoplasms (RENs).

Design: 10 MTSCCs were obtained and re-reviewed for morphologic confirmation. Available karyotypes were reviewed and FISH analysis with tricolored centromeric probes for ch1, ch7, ch17 was performed on 9 RCCs with known but blinded karyotypes to attempt to distinguish MTSCC, PRCC and ChRCC. Array CGH was also performed in 8 MTSCCs. Gene expression profiling was performed on 19 RENs: 3 genetically characterized MTSCCs, 4 clear cell RCCs (CCRCC), 4 PRCCs, 4 ChRCCs, and 4 renal oncocytomas (RO). Supervised analysis was applied to identify a discriminatory gene signature, as well as differentially expressed genes.

Results: Conventional cytogenetics demonstrated multiple chromosome loss in 6 MTSCCs, and chromosomes 1, 6, 14, 15 and 22 were most frequently affected. Similar results were found in all 8 MTSCC evaluated by array CGH. Correct classification of RCC was possible with FISH in 8/9 cases (89%), based on loss of ch1 only in 3/3 MTSCCs, loss of ch1 and ch17 in 3/4 ChRCCs, and gain of ch7 and ch17 in 2/2 PRCCs; the 1 non-diagnostic case was a ChRCC with loss of ch1 and normal ch17. Supervised algorithms showed that expression profiles for MTSCC were distinct from other RENs, and included 530 coding genes: 26 genes were down regulated and 504 genes were overexpressed. Pathway analysis demonstrated an enrichment of genes involved in signaling and regulation of RhoA, RCA1, CDC42, Wnt and GnRH pathways. 4 less well understood genes, ALPK2, PLEKHH2, FIGN, and DOCK11, and CDHR1 (cadherin superfamily) were also overexpressed in MTSCC compared to the other RENs.

Conclusions: This study confirms by karyotype and/or aCGH that multiple chromosomal loss (esp. chs 1, 6, 14, 15, and 22) is a frequent finding in MTSCC. When necessary, FISH analysis can be used to distinguish MTSCC from PRCC. Additionally, gene expression profiling demonstrates distinct differences between MTSCC and other RENs.

854 Biomarkers for the Detection of Prostate Cancer in Patients With High-Grade Prostatic Intraepithelial Neoplasia (HGPIN)

Ines De Torres, Tamara Sequeiros, Stefania Landolfi, Juan Maria Bastaros, Marina Rigau, Jacques Planas, Mireia Olivan, Santiago Ramon y Cajal, Juan Morote, Andreas Doll. Hospital Universitari Vall d'Hebrón and Universitat Autònoma de Barcelona (UAB), Barcelona, Catalunya, Spain; Research Institute Vall d'Hebron University Hospital (VHIR), Barcelona, Catalunya, Spain.

Background: The patients with diagnosis of HGPIN in the first transrectal ultrasound-guided prostate biopsy, often face several years of active surveillance including repeat biopsies. Finding new biomarkers that could differentiate between indolent HGPIN cases and those with prostatic cancer (PCa) associated would be of great value for clinical practice.

Design: We studied a cohort of 114 patients, with initial diagnosis of HGPIN in the first prostatic biopsy who underwent at least two repeat biopsies and a posterior follow up of at least two years. Urine sediment samples (30-50mL) after prostatic massage, two days before repeat biopsy, were collected in each patient. For the initial sample cohort studied, 90 out of the 114 urine samples yielded sufficient prostate derived cells or overall amount of RNA for the analysis in benign pathology (78.9%) and prostatic carcinoma (21.1%). The expression of 21 putative PCa biomarkers (*ABCA5, AGR2, AURKA, CDH1, CHKA, EN2, GOLM1, KLK3, PCA3, PSGR, PSMA (4 isoforms types) PTPRC, S100A9, SLC12A1, SPINK1, TIMP4, UPK2)* using quantitative PCR were measured in all urine samples.

Results: PSMA, PCA3, PSGR, GOLM, KLK3 and CDH1 selected by univariate statistical analysis of the obtained data, were significant predictors of PCa. All of them appeared overexpressed in PCa urine samples with compared to urine from patients presenting isolated HGPIN. Through multivariate analysis we established three multiplex models comprising different combinations of KLK3, PSMA, PSGR, GOLM1 and CDH1. Each one of these models greatly outperformed PCA3 score (multiplex models AUC=0.81-0.86 vs. PCA3 AUC=0.70). With a fixed sensitivity of 95%, the specificity of the three pannels was of 41-58%, compared to the 30% of PCA3. It is worth noting that our multiplex models would allow to save more than a third (33-47%) of repeating prostatic biopsies in those patients with a first diagnosis of HGPIN without cancer.

Conclusions: The results lay the foundations for the development of improved sediment urine biomarker tests for a more accurate diagnosis of prostatic carcinoma in prostatic biopsy with isolated HGPIN and thus avoid repeat prostatic biopsy in these patients.

855 Renal Cell Carcinomas With Mixed Histologic Patterns Resembling Both Clear Cell RCC (CCRCC) and Clear Cell Papillary RCC (CCPRCC): Analysis of 39 Cases

Hari Dhakal, Jesse McKenney, Jordan Reynolds, Cristina Magi-Galluzzi, Christopher Przybycin. Cleveland Clinic, Cleveland, OH.

Background: CCPRCC is considered distinct from CCRCC and papillary RCC. Proper diagnosis is crucial, as CCPRCC has not been associated with aggressive behavior.

Design: We reviewed 843 consecutive RCCs diagnosed as CCRCC to find cases resembling both CCRCC and CCPRCC; we added 4 recent cases. As solid areas have been reported in CCPRCC, we restricted cases to those with areas of larger nests with more irregular and haphazard nuclei indistinguishable from typical CCRCC. We recorded ISUP nucleolar grade, stage, and necrosis, performed CK7 immunostains (avoiding cystic areas), and obtained follow up.

Results: We found 39 such tumors and identified 2 patterns: Pattern 1 had nests of cells with clear to granular cytoplasm and a delicate vascular network, otherwise diagnosable as CCRCC, mixed with nests having a linear array of nuclei away from the basement membrane as in CCPRCC, but no discrete areas fully diagnostic of CCPRCC. Pattern 2 had discrete areas fully characteristic of CCPRCC and other areas characteristic of CCRCC.

Pattern 1 (N=20): CCPRCC-like areas were grade £2 in all cases; CCRCC-like areas were grade 2 in 16 (80%) and 3 in 4 (20%). 14 cases were £pT1b, 1 pT2a, 1 pT2b, 4 pT3a. None had necrosis. In CCPRCC-like areas, CK7 was positive in all 15 stained cases (diffuse/strong in 8 (53%)). In CCRCC-like areas, 3 (15%) cases were negative and 9 (45%) weakly or focally positive. 20 patients had follow up (median 75 mo): 4 (20%) had metastases, 1 (5%) died of unknown cause, and 1 (5%) died of disease (CCRCC-like areas in this patient were grade 3).

Pattern 2 (N=19): CCPRCC-like areas were grade £2 in 18 (95%) cases, grade 3 in 1 case; CCRCC-like areas were grade ³3 in 15 (79%) cases. 5 cases were £pT1b, 3 pT2b, 11 pT3a. 7 (37%) cases had necrosis; 4 (21%) had rhabdoid features (1 also sarcomatoid). CCPRCC-like areas were CK7 positive in all 17 cases stained (strong/diffuse in 8 (47%) cases). In CCRCC-like areas, CK7 was negative in 11 (65%) cases, focal/weak in 2 (12%). Follow up (N=17, median 61 mo) showed: 6 (35%) had metastases, 3 (18%) died of unknown cause, 3 (18%) died of disease. All who died of disease had pT3a tumors with CCRCC-like areas of grade³3 and necrosis.

Conclusions: RCCs with mixtures of histologic patterns/immunophenotypes closely resembling both CCRCC and CCPRCC occur. Some can have high grade/high stage aggressive components. Given this malignant potential, we would presently diagnose such cases as CCRCC. These cases underscore the need for caution in diagnosing CCPRCC on limited sampling.

856 GATA3 as a marker in Primary and Metastatic Extramammary Paget's Disease

Jasreman Dhillon, Marino Leon, Philippe Spiess, Ardeshir Hakam. Moffitt Cancer Center, Tampa, FL.

Background: Extramammary Paget's disease (EMPD) is a rare, slow-growing intraepithelial neoplasm arising in areas rich in apocrine sweat glands that in rare instances can be invasive and metastasize. In this study, we investigated the GATA3 staining pattern of EMPD including their metastases to explore its potential diagnostic role.

Design: We searched the database from 2009-2013 from our tertiary care cancer center for cases of penoscrotal, vulvar and anal EMPD including metastases and performed GATA3 immunohistochemical staining on some of the cases. Whole slide sections of 10 cases were immunohistochemically stained with mouse monoclonal GATA3 (dilution 1:100, Cell Marque, Rocklin, CA) using the Benchmark Ultra automated stainer (Ventana Medical Systems, Tucsan, AZ).

Results: There were 22 cases of EMPD including anal (4), vulvar (9) and penoscrotal (9) sites. Nine primary sites and one metastatic site were stained for GATA3. All the cases stained showed strong nuclear positivity in the tumor cells. The details including the clinicopathological features and GATA3 reactivity are listed in Table 1.

Site (# of cases)	Age (range in years)	Duration of symptoms (months)	Invasive (# of cases)	Metastases (sites)	Associated second malignancy	Follow up (months)	GATA3 Positivity (positive cases/ Total cases stained)
Anal (4)	56-80	12-16	1 (25%)	0	Breast ca = 1Skin ca = 1	36-120	3/3
Penoscrotal (9)	65-88	6-240	3 (33%)	1 (Bone)	Skin ca = 3Prostatic ca = 3Melanoma = 1Colon ca = 1	1-25	3/3
Vulva (9)	63-86	16-192	3 (33%)	1 (inguinal LN)	Skin ca = 2Breast ca = 1Colon ca = 1	1-204	4/4 including 1 metastatic LN

Conclusions: 1. EMPD is usually a slow-growing indolent tumor but can be invasive, especially in long standing cases, and may metastasize.

2. GATA3 is expressed in EMPD including anal, vulvar and penoscrotal sites.

3. Rare metastatic cases of EMPD may express GATA3, although further studies are warranted to verify these findings. This differential must be considered when working up a GATA3 positive carcinoma from unknown primary site.

857 Alpha-Enolase Is a Potential Prognostic Marker in Clear Cell Renal Cell Carcinoma

Ashley Di Meo, Nicole White, Andreas Scorilas, Fabio Rotondo, Olena Masui, Annetta Seivwright, Manal Gabril, Andrew Girgis, Michael Jewett, George Yousef. The Keenan Research Centre for Biomedical Science at the Li KaShing Knowledge Institute, Toronto, ON, Canada; University of Toronto, Toronto, ON, Canada; University of Athens, Athens, Greece; York University, Toronto, ON, Canada; London Health Sciences Centre and Western University, London, ON, Canada; Princess Margaret Hospital, Toronto, ON, Canada.

Background: Clear cell renal cell carcinoma (ccRCC) is an aggressive disease with unpredictable behaviour. Clinical parameters are not adequate for prognosis prediction. The integration of molecular markers to prognostic models can significantly improve prognostic assessment and consequently patient management.

Design: We assessed the expression of alpha-enolase (ENO1) protein by immunohistochemistry in 360 patients with primary ccRCC and correlated its expression with multiple clinicopathological parameters including stage, grade, tumor size, disease-free and overall survival. Cox proportional hazard regression models, adjusted for clinicopathological factors, were used to test for a link between alpha-enolase expression and both disease-free and overall survival. We correlated alpha-enolase mRNA expression with overall survival in an independent set of 428 ccRCC cases from The Cancer Genome Atlas.

Results: There is statistically significant negative correlation between alpha-enolase expression, tumor stage, and grade. Alpha-enolaseexpression also shows a statistically significant direct correlation with disease-free survival ($p = 0.011$) and overall survival ($p = 0.030$) in ccRCC. These findings were validated at the mRNA level in an independent set of 428 ccRCC cases which also showed that low alpha-enolase expression is associated with significantly shorter overall survival. Copy number alterations analysis showed that the ENO1 locus is deleted in a subset of ccRCC cases.

Conclusions: Our data suggests that the down-regulation of alpha-enolase can be a predictor of poor prognosis in ccRCC. Alpha-enolase represents a potential prognostic marker for ccRCC.

858 Implementing Multiparametric MRI and MRI/Ultrasound Fusion-Guided Biopsy To Detect Clinically Significant Prostate Cancer

Melissa Dillard, Win Shun Lai, John Thomas, Jeffrey Nix, Soroush Rais-Bahrami, Jennifer Gordetsky. University of Alabama, Birmingham, AL.

Background: Multiparametric MRI incorporates high resolution anatomic imaging and functional imaging of tissue density and vascularity to aid in the detection of intraprostatic lesions suspicious for prostate cancer (PCA). We aim to identify the association between imaging findings on multiparametric prostate MRI (MP-MRI) and pathologic findings on MRI/Ultrasound (US) fusion-guided prostate biopsies.

Design: We retrospectively reviewed men who underwent MP-MRI and MRI/US fusion-guided prostate biopsy between January and July 2014. Clinicopathologic and MP-MRI findings were reviewed. All MRI studies were assigned a modified NIH suspicion score to all suspicious lesions visualized based upon identification on each of three imaging paramaters (T2-weighted MRI, diffusion-weighted MRI, and dynamic contrast-enhanced MRI). Patients underwent standard 12-core extended-sextant TRUS-guided biopsy and fusion-guided biopsies of MRI-identified lesions using the UroNav biopsy platform. All pathology was reviewed by a single pathologist.

Results: We identified 28 patients for analysis. The median age was 61 years and the median PSA was 5.6 ng/mL. 17 cases had PCA, 7 were benign, and 2 had atypical small acinar proliferation (ASAP). The two cases of ASAP were identified by targeted biopsy alone. Of the 17 men with PCA, 3 were identified by targeted biopsy alone, 6 by standard biopsy alone, and 8 were identified by both techniques. Clinically significant PCA was missed on targeted biopsy in 2 cases and on standard biopsy in 3 cases. Six patients with prior negative biopsies had PCA. In this subset, targeted biopsy identified all clinically significant PCA, whereas standard biopsy missed 2 high-grade tumors (Gleason Score 4+5=9). Six cases had perineural invasion, 5 of which were identified only on targeted biopsy. The only finding of extraprostatic extension was identified on targeted biopsy. Overall, stepwise increase in MRI suspicion level was associated with an increased PCA detection rate (OR 5.55, p=0.019) on logistic regression modeling and increased risk stratification (no cancer vs Gleason 6 vs Gleason ≥ 7), p=0.027 by Fisher Exact probability testing. Furthermore, all patients with high-risk disease (Gleason ≥ 8) had pre-biopsy MP-MRI with assignment of the highest level suspicion score.

Conclusions: The findings suggest MP-MRI improves detection of prostate cancer and may target more clinically significant prostate cancers than those found by standard-of-care 12-core biopsies. However, definitive conclusions cannot be drawn without evaluating the outcomes of a larger sample size.

859 Long-Term Follow-Up Study of Clear Cell Papillary Renal Cell Carcinoma (CCPRCC): Should These Lesions Be Renamed To Reflect Their Low Malignant Potential?

Mairo Diolombi, Jonathan Epstein. Johns Hopkins Medical Institutions, Baltimore, MD.

Background: There have been no recurrences or metastases of CCPRCC in ~280 reported cases in the literature.

Design: We identified all our cases of CCPRCC (1990-2013), reviewing all cases that preceded the formal designation of the entity. IHC stains were done on 28 cases during their initial work-up, with stains for CAIX and CK7 done at the time of this study on 2 more cases to support the diagnosis. In classic cases, IHC was not performed. 51 patients with follow-up data were included in our study; 32 cases from our consult service.

Results: Patients' ages ranged from 36 to 83 yrs. 29 patients had cystic lesions; 4 tumors were multifocal. The majority (49 patients; 96%) presented with stage pT1 disease and the remaining 2 with pT2 disease (range 0.2 to 10.3 cm). Treatment consisted of 26 partials, 23 radicals, 1 cryoablation, and 1 cyst ablation. Margins were negative in all but 1 case, with this case disease free at 26 mos. 2 patients had intraoperative tumor disruption and were disease free at 9 and 34 mos. 3 patients had ipsilateral metachronous non-CCPRCC. Median follow-up time was 21 mos. with all but 2 patients having no evidence of disease. Metastatic disease to the lung was present in 1 patient with a cystic pT1b tumor at diagnosis, and the other case 8 mos. after resection of pT1b sarcomatoid CCPRCC. Both patients had radical nephrectomy with adjuvant Sutent and Avastin respectively. The patient with sarcomatoid RCC died of disease 13 mos. after resection (Figure 1).

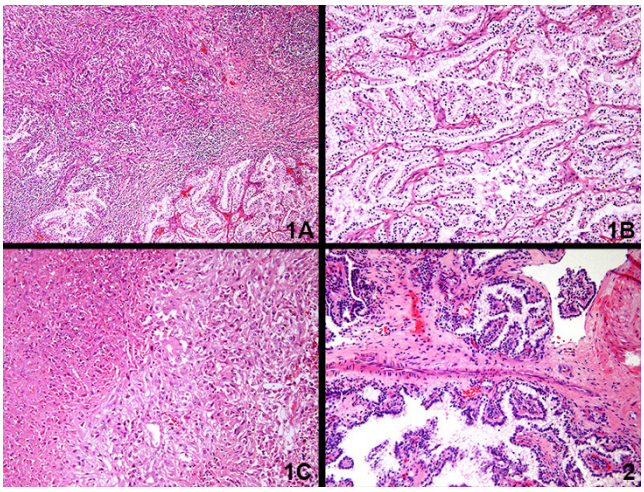

CCPRCC adjacent to sarcomatoid RCC (1A); High power of CCPRCC focus in sarcomatoid RCC (1B); High power of sarcomatoid RCC with adjacent necrosis (1C); Cystic CCPRCC with reported metastasis (2).

Conclusions: Our study, the largest to date with follow-up, along with others suggest that CCPRCC is a benign tumor. One patient in our series had metastases but a higher grade lesion may have been missed during sampling of the predominantly cystic lesion and tissue confirmation of the metastases was not obtained. We are in the process of doing FISH for 3p loss in our 2 atypical cases to rule out CCPRCC-like tumor associated with VHL.

860 Diagnostic Utility of a Comprehensive Immunohistochemical (IHC) Panel for Testicular Sex Cord Stromal Tumors (TSCST): A Study of 76 Cases

Mukul Divatia, Steven Smith, Maurizio Colecchia, Manju Aron, Mitual Amin, Steven Shen, Donna Hansel, Pheroze Tamboli, Gladell Paner, Mariza de Peralta-Venturina, Loren Herrera Hernandez, Allen Gown, Mahul Amin. Cedars-Sinai Medical Center, Los Angeles, CA; Virginia Commonwealth University, Richmond, VA; Fondazione IRCCS Istituto Nazionale dei Tumori, Milan, Italy; University of Southern California, Los Angeles, CA; William Beaumont Hospital, Royal Oak, MI; Methodist Hospital, Houston, TX; University of California, San Diego, CA; University of Texas MD Anderson Cancer Center, Houston, TX; University of Chicago, Chicago, IL; Mayo Clinic, Rochester, MN; Phenopath Laboratories, Seattle, WA.

Background: TSCSTs exhibit a wide range of morphologic patterns which may be simulated by overlap with germ cell tumors, paratesticular neoplasms, and metastatic tumors. Several novel markers, including transcription factors involved in adrenal and gonadal development, Forkhead Box L2 (FOXL2), steroidogenic factor-1 (SF-1) and beta-catenin protein have been evaluated in ovarian SCSTs. These promising markers have not been studied in a large cohort of TSCSTs and in conjunction with traditionally used markers.

Design: 76 SCSTs were evaluated by SF-1, Beta-catenin, FOXL2, inhibin, calretinin, cytokeratin (OSCAR), WT-1, synaptophysin, S-100, CD99 and Melan-A.

Results: IHC profiles (%) are summarized in Table 1.

Type	LCT (Pure 36; Mixed 2)	SCT (Pure 13; Mixed 5)	USCST (8)	GCT (Pure 6; Mixed 3)	LCCST (4)	TTAG (2)
SF-1	92	75	57	50	50	100
FOXL2	21	83	67	100	-	-
Beta-catenin	50	83	60	43	50	100
Inhibin	97	67	38	67	75	100
Melan A	94	67	75	50	50	100
Calretinin	97	56	75	44	75	100
WT-1	0	82	57	50	75	50
CD99	74	56	25	86	0	0
Synaptopyhsin	65	24	29	0	0	50
CK	22	78	17	43	67	-
S100	28	28	43	38	75	0

LCT- Leydig Cell Tumor, SCT-Sertoli Cell Tumor, MSCT- Mixed SCST, UCST- Unclassified SCST, GCT- GranulosaCell Tumor, LCCSCT- Large Cell Calcifying SCT, TTAG- Testicular Tumor ofAdrenogenital Syndrome

Conclusions: SF-1 is the most sensitive marker amongst the common types of TSCSTs. Among traditional markers, inhibin, calretinin and Melan A offer overall similar sensitivity, although calretinin lacks specificity considering the tumors in the differential diagnosis at this site. A combination of SF-1, inhibin and Melan A or calretinin as a first line IHC panel provides maximum sensitivity identifying > 80% of TSCSTs.

861 Refining the Diagnostic Criteria and Immunophenotype of Collecting Duct Carcinoma (CDC) in Light of Emerging Entities

Mukul Divatia, Steven Smith, Ondrej Hes, Jonathan Epstein, Jesse McKenney, Paulo Guilherme Salles, Priya Rao, L Priya Kunju, Isabela Werneck da Cunha, Luciana Schultz, Maurizio Colecchia, Michelle Hirsch, Eva Comperat, Claudia Zampini, Mariza de Peralta-Venturina, Mitual Amin, Ping Zhang, Jonathan McHugh, Rohit Mehra, Scott Tomlins, Mahul Amin. Cedars-Sinai Medical Center, Los Angeles, CA; Virginia Commonwealth University, Richmond, VA; Charles University Hospital, Plzen, Czech Republic; Johns Hopkins Hospital, Baltimore, MD; Cleveland Clinic, Cleveland, OH; Associacao Mario Penna, Hospital Luxemburgo, Belo Horizonte, MG, Brazil; University of Texas MD Anderson Cancer Center, Houston, TX; University of Michigan, Ann Arbor, MI; A.C.Camargo Cancer Center, São Paulo, Brazil; Instituto de Anatomia Patológica, Piracicaba, Brazil; Fondazione IRCCS Istituto Nazionale dei Tumori, Milan, Italy; Brigham & Women's Hospital, Boston, MA; Groupe Hospitalier Pitié-Salpétrière, Paris, France; William Beaumont Hospital, Royal Oak, MI.

Background: The recent ISUP classification for Renal Cell Carcinoma (RCC) requires a CDC to involve the collecting system; show predominant glandular formation with a desmoplastic stromal reaction; exhibit high-grade cytologic features; and show an infiltrative growth pattern. It is essential to rule out urothelial carcinoma, metastatic carcinoma, and other RCC subtypes simulating CDC, specifically renal medullary carcinoma (RMC) and tubulocystic carcinomas with dedifferentiated foci resembling CDC (TC-D). Additionally, recent studies suggest that fumarate hydratase (FH)-deficient RCCs are often classified as CDC.

Design: 36 CDCs, 24 RMCs and 14 TC-Ds were analyzed by a panel of IHC markers.
Results: Greater than 90% of all 3 tumor types were PAX8 and S100A1 (+). IHC profiles are summarized as (%) in Table 1.

Tumor	RCCma	CA IX	hKim-1	Oct 3/4	INI1 (-)	FH (-)
CDC	36	61	42	0	0	14
TC-D	21	79	30	0	0	29
RMC	0	8	6	42	100	0

hKim1: human kidney injury molecule, RCC ma: RCC monoclonalantibody

RMC was easily excluded by loss of INI1 or induction of OCT3/4, while TC-D subsets shared RCC, CAIX, and hKim1 with CDC. Intriguingly, similar to TC-D, 5 of 36 cases otherwise designated as CDC showed FH loss, prompting workup for HLRCC or FH-deficient carcinoma.
Conclusions: 1. The vast majority of high-grade distal nephron-related adenocarcinomas express PAX8/S100A1, and are frequently RCC (-). 2. In the light of expanding morphologic spectrum of these tumors and promising new IHC markers, we suggest that the ISUP CDC diagnostic approach should be revised to recommend, in the appropriate clinical and morphologic contexts, exclusion of RMC [INI1 (-)/Oct 3/4 (+)] and FH deficient RCC [FH (-)] before definitive diagnosis of CDC.

862 Renal Cell Carcinoma, Unclassified – Medullary Phenotype (RCCU-MP): Findings Supporting a Close Relationship With Renal Medullary Carcinoma (RMC)

Mukul Divatia, Steven Smith, L Priya Kunju, Michelle Hirsch, Maurizio Colecchia, Ondrej Hes, Jonathan Epstein, Jesse McKenney, Paulo Guilherme Salles, Priya Rao, Isabela Werneck da Cunha, Luciana Schultz, Eva Comperat, Claudia Zampini, Mariza de Peralta-Venturina, Rohit Mehra, Scott Tomlins, Mahul Amin. Cedars-Sinai Medical Center, Los Angeles, CA; Virginia Commonwealth University, Richmond, VA; University of Michigan, Ann Arbor, MI; Brigham & Women's Hospital, Boston, MA; Fondazione IRCCS Istituto Nazionale dei Tumori, Milan, Italy; Charles University Hospital, Plzen, Czech Republic; Johns Hopkins Hospital, Baltimore, MD; Cleveland Clinic, Cleveland, OH; Associacao Mario Penna, Hospital Luxemburgo, Belo Horizonte, MG, Brazil; University of Texas MD Anderson Cancer Center, Houston, TX; A.C.Camargo Cancer Center, São Paulo, Brazil; Instituto de Anatomia Patológica, Piracicaba, Brazil; Groupe Hospitalier Pitié-Salpétrière, Paris, France.
Background: RCCU-MP has been recently proposed for high grade renal adenocarcinomas with morphologic, immunohistochemical (IHC) or molecular features characteristic of RMC arising in a patient without evidence of hemoglobinopathy (Hbpathy). The aim was to provide a diagnostic term, distinct from collecting duct carcinoma (CDC) & RMC with their known clinical implications, to designate such cases for prospective study.
Design: Clinicopathologic features of 5 cases were analyzed. IHC profile was compared with a control cohort of 36 CDC & 24 RMC.
Results: Five RCCU-MPs were identified in 4 Caucasians & 1 West Asian, F:M=3:2, with no positive test for any Hbpathy (3), no history (2) or drepanocytes in tumor sections (5). Ages ranged from 24-63y (median 37y). Tumor size ranged from 3.4-6.5 cm (median 4.5 cm), 2 right & 3 left sided, presenting with hematuria (5). Tumors had an epicenter in the renal medulla & showed RMC-like histology with reticular, cribriform & yolk sac tumor-like growth patterns; one tumor showed notably rhabdoid morphology. Necrosis (60%), renal sinus invasion (80%) & nodal metastasis at presentation (60%) were noted. All patients received adjuvant chemo- or targeted therapy. Short term follow up (< 1yr) in 4 cases showed distant metastasis in one case & no disease progression in 3 cases. IHC profiles summarized as (%) in Table 1.

Tumor	INI Loss	Oct 3/4	RCC	CA IX
RCCU-MP	100	100	0	0
RMC	100	43	0	4
CDC	0	0	37	67

Conclusions: The RCCU-MP designation allows diagnosis of cases with features of RMC despite lack of Hbpathy. This first reported series of RCCU-MP suggests a close IHC similarity to RMC, prompting testable hypotheses on their alternative pathway to oncogenesis, beyond Hbpathy, in these SMARCB1/INI1 deficient renal neoplasms.

863 Significance of Mucosal Margin Status at Radical Cystectomy for Urothelial Carcinoma (UC) in a Cohort of Patients Undergoing Routine Follow-Up

Kathryn Dyhdalo, Christopher Przybycin, Jesse McKenney, Cristina Magi-Galluzzi, Holly Harper, Jordan Reynolds. Cleveland Clinic, Cleveland, OH; Case Western Reserve University, Cleveland, OH.
Background: Radical cystectomy (RC) patients are at risk for upper tract (UT) and urethral recurrence. Correlation of initial mucosal margin status assessed at frozen section (FS) with subsequent local recurrence (LR) in the form of urothelial carcinoma in situ (CIS) or invasive UC is controversial. Pursuit of re-resection of mucosal surfaces to obtain a negative margin is also controversial.
Design: All radical cystectomy specimens with routine follow up were retrieved from 1/2000-10/2013 (all patients minimum follow up 1 year). Margin status of ureteral and urethral mucosa (both initial and final margin) was recorded and correlated with patient follow up data. LR was defined as biopsy confirmed CIS or invasive UC. Statistics were performed using JMP Pro 10 (SAS, Cary, IN).
Results: 414 RC with routine follow up were found during the 13 year study period (332 male, 82 female 4:1 ratio, mean age 65, range 26-93). Median follow-up was 84 months (range 13 – 216 months). On initial FS evaluation, 55/414 patients (13.3%) had a positive margin which included CIS (52/55, 95%), 2 invasive high grade papillary carcinomas (2/55, 3.6%), and 1 non-invasive papillary TCC. 46/55 (83.6%) involved the UT and 9/55 (16.3%) involved the urethra. 19 of these patients had additional FS to pursue a final negative margin (18 UT, 1 urethra). On follow-up, 3/19 (15.8%) patients had cancer specific death of which one patient had biopsy confirmed LR (CIS of UT). 36 patients remained margin positive on final diagnosis (27 UT, 8 urethra). On follow-up, 10/36 (27.7%) had cancer specific death, of which 4 had biopsy confirmed LR (2 UT, 2 urethra). Of the 26 remaining patients, 4 had biopsy confirmed LR (3 UT, 1 urethra). Of 359/414 (86.7%) patients who never had a positive margin, 58/359 (16.2%) had cancer specific death of which 8/58 (13.7%) patients had biopsy confirmed LR (7 UT, 1 urethra). 301/359 (83.8%) did not have cancer specific death. 10/301 (3.3%) of these had LR (5 UT, 5 urethra). Risk of developing LR after having any positive vs negative margin was significant (9/55,16.3% v 18/359,5.0% respectively, p=.004). Patients with persistent positive margins had higher risk of LR than those with margin re-excision to achieve negative margins (8/36 22.2% v 19/378 5.0% respectively, p=.001).
Conclusions: Patients with positive UT/urethral margins are significantly at risk for local recurrence.

864 Microscopic Bladder Neck Invasion in pT3a Prostate Cancer Staging: Can Bladder Detrusor Muscle Be Differentiated From Prostatic Fibromuscular Stroma in the Bladder Neck Based on Size?

Joshua Ebel, Meredith Morse, Megan Merrill, Debra Zynger. Ohio State University, Columbus, OH.
Background: Microscopic bladder neck invasion is defined as pT3a. Within the bladder neck, there are no specific criteria to distinguish bladder detrusor muscle from prostatic fibromuscular stroma. We histologically assessed the bladder neck to identify size criteria for the differentiation of these organs in order to improve the diagnosis of microscopic bladder neck invasion.
Design: Sagittally sampled bladder neck slides from cystoprostatectomies from 2009-2011 were reviewed (n=158). On the slide, optimal anatomical orientation was verified via the presence of prostatic glands inferiorly, urothelium anteriorly, and transverse intervening adipose (n=52). The largest muscle bundle was measured within 0.0-0.2 cm, 0.2-0.5 cm, and 0.5-1.0 cm increments from the intervening adipose towards the bladder (superior) and the prostate (inferior). Distance from the adipose to the superiormost non-neoplastic prostatic gland was measured. Bladder neck slides from prostatectomies with reported bladder neck invasion and a subset of cases without reported invasion from 2011-2013 were reviewed. The largest muscle bundle diameter on each bladder neck slide was measured. Pearson's chi-squared and Wilcoxon signed-rank exact test were used to compare groups.
Results: Near the junction of the bladder and prostate (0.0-0.2 cm superior vs inferior), there was no difference in size of the largest muscle bundle (mean for both=0.05 cm, p=0.68). Further from the junction, there was a significant difference in size (0.2-0.5 cm: mean superior=0.06 cm vs inferior=0.03 cm, p<0.001; 0.5-1.0 cm: mean superior=0.07 cm vs inferior=0.01 cm, p<0.001). Muscle bundle size ³0.05 cm was 70% sensitive for bladder detrusor. The junction of the organs was <1.0 cm from the superiormost non-neoplastic prostatic gland in 95% of cases. In prostatectomies, the incidence of bladder neck invasion was 5.4% (59/1094). Prostatectomies with reported bladder neck invasion displayed no difference in size of the largest bladder neck smooth muscle bundle compared to cases without reported invasion (mean for both=0.08 cm, p=0.24).
Conclusions: Muscle bundle size ³0.05 cm in the bladder neck is likely to represent detrusor muscle. In a well oriented specimen, distance from the superiormost non-neoplastic prostatic gland may be helpful to differentiate prostate fibromuscular stroma from bladder detrusor muscle. In prostatectomy specimens, there was no relationship between bladder neck muscle bundle size and reported bladder neck invasion.

865 Correlation of Gleason Score in Biopsy and Radical Prostatectomy Specimens 2000-2012 – A Registry Study of 15598 Men

Lars Egevad, Daniela Danneman, Par Stattin, Linda Drevin. Karolinska Institutet, Stockholm, Sweden; Uppsala University Hospital, Uppsala, Sweden; Memorial Sloan Kettering Cancer Center, New York, NY.
Background: Over the past decades there has been a considerable inflation of Gleason grading of prostate cancer. In a recent registry study we found that Gleason scores 7-10 increased from 16.3% 1998 to 39.9% 2011 among men with stage T1c cancers and serum PSA (S-PSA) 4-10 ng/ml. The International Society of Urological Pathology (ISUP) revision of Gleason grading in 2005 may have contributed to this trend. One of the purposes of the ISUP revision was to improve biopsy prediction of prostatectomy grade. We aimed to investigate this correlation and its change over time, using a national registry of prostate cancer.
Design: All newly diagnosed prostate cancers in Sweden are reported to the National Prostate Cancer Registry (NPCR). We retrieved grade data from biopsy and prostatectomy specimens of 15598 men with a primary diagnosis of prostate cancer on needle biopsy with clinical stage T1-2, M0 or MX, age at diagnosis ≤70 years, S-PSA <20 ng/ml and treated with radical prostatectomy within 180 days 2000-2012.
Results: Correct prediction of prostatectomy Gleason score improved from 55.2% to 68.2% from 2000 to 2012. From 2000 to 2005 the improvement was 8.4% and from 2005 to 2012 it was 4.6%. Undergrading decreased from 32.3% to 21.8% and overgrading decreased from 12.4% to 10.1% from 2000 to 2012. Undergrading of 2 or more Gleason score units decreased from 11.1% to 2.4%. Logistic regression showed fewer grading errors over time (OR 0.97, p<0.001) but when GS distribution was accounted for the grading precision decreased (OR 1.02, p<0.001).

Conclusions: Over the past 13 years there has been an improved correlation of biopsy and prostatectomy Gleason score. Most of this improvement occurred before the ISUP 2005 revision of the Gleason system. There are several possible explanations of the improved results: greater number of biopsy cores are taken in each biopsy, the lowest Gleason scores (2-5) are not used, educational efforts have improved the grading skills among pathologists and selection criteria for prostatectomy have changed. Furthermore, a changed distribution of Gleason scores with concentration to fewer grades may have given a false impression of improved grading precision.

866 Clinico-Pathologic Comparison of Neoadjuvant Therapy Responders Versus Failures Following Radical Cystectomy/ Cystoprostatectomy for Urothelial Carcinoma of the Bladder: A Five Year Retrospective Review

Carla Ellis, Adeboye Osunkoya. Emory University Hospital and School of Medicine, Atlanta, GA.

Background: There is limited data in the pathology literature regarding the long term natural history of urothelial carcinoma following neoadjuvant therapy and subsequent radical cystectomy or cystoprostatectomy. No prior study has specifically looked at the pathologic features associated with neoadjuvant failures (as compared to successes) in these types of radical resection specimens.

Design: A search of our pathology data system was performed. All radical cystectomy and cystoprostatectomy specimens in patients who received neoadjuvant therapy (chemotherapy and/or radiation) were reviewed in the 5 year period between 2009 and 2014, and analyzed in terms of demographic information (age, sex and race) pathological stage and grade, aggressive pathological features (carcinoma in situ, angiolymphatic invasion, positive margins), type of neoadjuvant therapy and clinical follow up data. Successes were defined as no evidence of residual carcinoma (ypT0) and failures as evidence of residual carcinoma at the time of surgery.

Results: A total of 53 cases (27 successes, 51% and 26 failures, 49%) were reviewed. All patients had chemotherapy (>90%) or radiation. The mean patient age at the time of surgery was 68 years (range: 51-88 years). Thirty-seven of 53 (70%) patients were male and sixteen of 53 (30%) patients were female. The mean duration of follow up for successes and failures were 26.3 months (range: 0-60 months) and 20.1 months (range: 1-54 months) respectively. Twenty of 26 (77%) failures showed evidence of one or more aggressive pathologic features. Five of the 26 (19%) failures were upstaged to M1 (distant metastasis) after review of clinical follow up data. Eleven of the 26 (42%) failures were either alive with disease, dead of disease or status post resection of a metastasis, as compared to 4/27 (15%) successes (p=0.0352).

Conclusions: In our 5 year cohort with representative cases from a single institution, it appears that failure of neoadjuvant therapy is associated with aggressive pathologic features and a poor clinical outcome. Further studies with longer follow up and molecular analysis of tumors that failed therapy are required for a better understanding of the biologic nature of these tumors.

867 Pathologic Characteristics of Stage pT2b Prostate Cancer and Its Value in Staging

Mark Ettel, Fang-Ming Deng, Ming Zhou, Jonathan Melamed. New York University Langone Medical Center, New York, NY.

Background: Organ-confined prostate cancer is subclassified under current staging protocols (TNM 2010) into pT2a (unilateral tumors <1/2 of lobe), pT2b (unilateral tumors ≥ 1/2 of lobe) and pT2c (bilateral tumors). There is a low incidence of pT2b stage in most studies and behavior and characteristics of these tumors is controversial. We analyzed pathologic characteristics and biochemical recurrence-free survival (BFS) of these tumors compared to other pT2 tumors.

Design: Patients with pT2 tumors were selected among patients who underwent RP from 1991 to 2008 in a single institution. Pathologic characteristics were assessed for all tumors (chi-squared, *t*-test and ANOVA). For cases with sufficient follow-up, Kaplan-Meier analysis was used to evaluate BFS and multivariate Cox proportional hazards regression was used to evaluate predictors of survival.

Results: 1588 stage pT2 tumors included 294 pT2a (18.5%), pT2b (1.9%) and pT2 c (79.6%). Pathological characteristics of pT2b tumors were similar to those of pT2c tumors, with no difference in dominant nodule size (DNS) (p=0.656), positive surgical margins (PSM) (p=0.247), and Gleason score (GS) (p=0.054). Characteristics were different from those of pT2a tumors, with significant differences observed in DNS (p<0.001), PSM (p=0.023) and GS (p=0.008). PSA follow-up was available for 1035 patients (17.7% pT2a, 2.0% pT2b and 80.3% pT2c). BFS was significantly lower in pT2b disease than in pT2a disease (p=0.023) in univariate analysis, while there was no difference compared to pT2c disease (p=0.067). On multivariate analysis, there was no significant difference compared to stage pT2a disease (p=0.089) or pT2c disease (p=0.121).

Stage	No.	No. with PSM	Mean DNS (cm)
pT2a	294	18 (6.1%)	0.78
pT2b	30	5 (16.7%)	1.19
pT2c	1264	178 (14.1%)	1.15

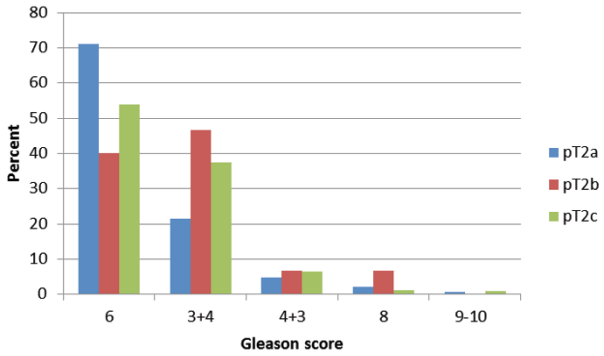

Conclusions: Prostate cancer staged as pT2b is a rare entity with qualities similar to those of pT2c tumors and different from those of pT2a tumors. BFS in pT2b tumors is lower than that of pT2a tumors in univariate analysis, but this difference loses significance on multivariate analysis. These results confirm pT2b prostate cancer as a limited group without specific characteristics or prognostic value to justify pT2b subclassification.

868 Percentage Gleason 4/5 as Predictor of Biochemical Recurrence in Prostate Cancer in and Before the Contemporary Era of Radical Prostatectomy

Mark Ettel, Fang-Ming Deng, Ming Zhou, Jonathan Melamed. New York University Langone Medical Center, New York, NY.

Background: The risk for biochemical recurrence (BCR) in prostate cancer following radical prostatectomy (RP) has been shown by us and others to vary by percentage of Gleason 4/5 component. Many of the studies used to assess its impact draw on cohorts from different eras of PSA screening. Additionally, sampling strategies earlier were partial compared to our current practice of entire submission. Our objective is to determine whether percentage of Gleason 4/5 provides a better predictor of BCR in the contemporary era (CE) of RP compared to the early era (EE) of RP.

Design: Patients with pT2 and pT3 tumors and pN0/Nx were selected among patients who underwent RP at a single institution from 1991 to 2008. EE in which radical prostatectomy specimens were partially submitted was defined as 1991-97 and CE during which the entire radical prostatectomy was submitted was defined as 1998-2008. Kaplan-Meier analysis was used to evaluate BCR-free survival (BFS). Separate multivariate Cox proportional hazard regression models were fitted for both the EE and CE cohorts.

Results: Of 1468 patients included, 442 were in the EE cohort and 1026 in the CE cohort. BFS was significantly lower (p<0.001) for the EE cohort than for the CE cohort in multivariate analysis, and predictive accuracy of the CE model was greater than that of the EE model. Significance of percentage of Gleason 4/5 differed in separate multivariate regression models for the EE and CE cohorts. Percentage of Gleason 4/5 was predictive of BFS in univariate analysis in both EE and CE cohorts (p<0.001). Multivarate analysis was then performed. Percentage Gleason 4/5 was not independently significant in the EE model. In the CE model, percentage of Gleason 4/5 (p=0.003) was an independent predictor of BFS and outperformed traditional Gleason score.

Conclusions: Percentage of Gleason 4/5 component is a stronger predictor of BFS in the CE as compared to the EE of RP. Percentage of Gleason 4/5 is not independently significant in older cohorts after adjusting for traditional Gleason score, but outperforms traditional Gleason score in a predictive model for the CE of RP. Changes in patient selection as well as more comprehensive tissue sampling may contribute to the enhanced performance of Gleason 4/5 in the current era compared to previously.

869 Refining pT2 Substaging of Prostate Cancer

Mark Ettel, Fang-Ming Deng, Ming Zhou, Jonathan Melamed. New York University Langone Medical Center, New York, NY.

Background: The current subclassification of pT2 prostate cancer into pT2a (unilateral tumors <1/2 of lobe), pT2b (unilateral tumors ≥ 1/2 of lobe) and pT2c (bilateral tumors) is of questionable relevance. Many studies show no difference in prognosis between substages, and incidence of pT2b prostate cancer is low. Other classification systems have been proposed based on tumor volume, measured by dominant nodule size (DNS) or tumor percentage (TP). We assessed the utility of the current pT2 substaging in prediction of biochemical recurrence-free survival (BRFS) in the modern era of radical prostatectomy and compared with other methods based on tumor volume.

Design: Patients with pT2 tumors were selected among patients who underwent RP from 1998 to 2008 in a single institution with subsequent standardized review of all cases by single pathologist. Dominant nodule size was analyzed based on ≥1.6 cm vs. <1.6 cm. TP was visually estimated within 4 groups: 0-5%, 5-25%, 25-50% and 50-100%. Kaplan-Meier analysis was used to estimate BRFS and multivariate Cox proportional hazard regression models were used to evaluate predictors of BRFS.

Results: 787 patients met the criteria, of which 145 (18.4%) were pT2a, 15 (2.1%) were pT2b and 627 (79.7%) were pT2c. Compared to substage pT2a on univariate analysis, BRFS for substage pT2c was barely significantly different (p=0.0488) and pT2b was not significantly different (p=0.105). The pT2 substages were no longer significant predictors of BRFS on multivariate analysis which also included Gleason score (GS) and margin status (MS). In a multivariate model including both DNS and TP, TP (p=0.033) was a significant predictor while DNS (p=0.344) was not significant.

Conclusions: In patients with stage pT2 prostate cancer, the current substaging method lacks predictive value for BRFS after accounting for other pathologic and clinical predictors. A substaging method using TP as an estimate of tumor volume is a promising approach with predictive value that remains on multivariate analysis.

870 Gleason Grading of Prostate Cancer By Canadian Pathologists: A Survey of Members of the Canadian Network of Uropathology (CNUP)

Andrew Evans, John Srigley, Jennifer Merrimen, Lars Egevad. University Health Network, Toronto, ON, Canada; McMaster University, Hamilton, ON, Canada; Dalhousie University, Halifax, NS, Canada; Karolinska Institutet, Stockholm, Sweden.

Background: CNUP is a communication network for Canadian pathologists interested in uropathology (UP). It provides a mechanism for conducting studies aimed at standardizing diagnostic criteria in areas such as grading prostatic adenocarcinoma (PC) in needle biopsies. CNUP members were invited to review photomicrographs and provide Gleason scores (GS) for a series of prostate biopsies containing GS 6-7 PC assigned using the 2005 International Society of Urological Pathology modification of Gleason grading (ISUP 2005).

Design: In a previous effort to collect consensus cases for standardizing Gleason pattern 3 and 4 PC using ISUP 2005, 15 UP experts reviewed 25 biopsies with GS 6-7 PC. Fifteen were selected where two-thirds consensus was reached. Eighty-five photomicrographs were obtained from these biopsies at low and intermediate magnification and were attached to a SurveyMonkey link emailed to CNUP members. Members were asked to indicate their preferred GS for each biopsy from a fixed list of choices. The same image set was previously reviewed by 337 members of the European Network of Uropathology (ENUP) in 2011, creating an opportunity to compare the opinions of CNUP and ENUP members in relation to the expert UP panel.

Results: Complete surveys were received from 47 CNUP members across Canada, 57% based in academic centers and 43% in community practice. The most commonly assigned GS for each biopsy by CNUP members was identical the experts in 14 of 15 biopsies (93%). The lone discordant biopsy had a GS of 4+3 as determined by the experts, while 56% of CNUP members assigned GS 4+4 and 43% 4+3. In the 2011 survey of ENUP members (representing 19 different countries with 39% based in academic centers), the most commonly selected GS agreed with the experts in 12 of 15 biopsies (80%). The ENUP members selected higher GS than the expert UP panel in the discordant biopsies.

Conclusions: We observed outstanding agreement between CNUP members and an expert UP panel when assigning GS to biopsies with GS 6-7 PC. The higher agreement observed with CNUP over ENUP members (93% vs 80%) is likely multifactorial. CNUP members represent one country and had a higher proportion of its members based in academic centers (57% vs 39%). The CNUP survey was also conducted 3 years after the ENUP study, suggesting that CNUP members may have become more standardized as a result of 3 extra years of educational activity on the ISUP 2005 system.

871 Renal Cell Carcinoma Occurring in Patients With Prior Neuroblastoma: A Distinct Morphologic Entity?

Sara Moscovita Falzarano, Jesse McKenney, Rodolfo Montironi, John Eble, Adeboye Osunkoya, Juan Guo, Shengmei Zhou, Cristina Magi-Galluzzi. Cleveland Clinic, Cleveland, OH; University of Ancona, Ancona, Italy; Indiana University, Indianapolis, IN; Emory University School of Medicine, Atlanta, GA; Kaiser Permanente Panorama City Medical Center, Panorama City, CA; Children's Hospital Los Angeles, Los Angeles, CA.

Background: Renal cell carcinoma (RCC) associated with neuroblastoma (NB) was included as a distinct entity in the 2004 WHO classification of kidney tumors and has been reported in both patients with and without prior therapy. We describe a series of RCCs in patients with history of NB, with emphasis on their morphologic and immunophenotypic heterogeneity.

Design: 8 RCCs diagnosed in 7 patients with history of NB were reviewed. Clinical and pathologic characteristics were collected. Microscopic features and PAX8, Cathepsin K and SDHB immunohistochemical expression were evaluated in all tumors; EMA was evaluated in a subset.

Results: Median age at NB and RCC diagnosis was 2 and 8 years (range 0.1-6, and 0.9-40), respectively. Median interval from NB to RCC diagnosis was 6.8 years (range 0.8-38). 4 patients were male and 3 female. NB stage was IV in 2, III in 1, and unknown in 4. 3 patients received chemotherapy for NB, 1 radiation, and 1 both (treatment unknown in 2). 4 patients underwent partial and 3 radical nephrectomy for RCC. 5 RCCs involved the right kidney, including the case with two separate foci. RCC median largest dimension was 4 cm (range 1-15). 5 tumors were confined to kidney; 3 extended into perinephric fat. Pathology review revealed 4 distinct morphologic RCC subtypes: 1) 3 tumors (including two from same patient) displayed a tubular and solid architecture with cyst formation, and were characterized by cells with abundant eosinophilic (oncocytoid) cytoplasm and irregular nuclei with prominent nucleoli; 2) 3 tumors showed features of translocation-associated RCC (MiT-RCC); 3) 1 had features of a hybrid oncocytic-chromophobe tumor (HOCT); and 4) 1 tumor had classic papillary type 1 RCC histology. All RCCs expressed PAX8 and retained SDHB. Cathepsin K was positive in 2 of 3 tumors with MiT-RCC morphology and all 3 were EMA negative. A lymph node metastasis was present in 1 MiT-RCC case.

Conclusions: While some RCCs associated with NB have the classically described morphology characterized by prominent oncocytoid cytoplasm, MiT-RCC (possibly therapy related), HOCT, and otherwise typical sporadic subtypes may also occur. In this series, SDHB deficiency was not present. RCCs occurring in patients with history of NB do not represent a single entity, but a heterogeneous group of renal neoplasms.

872 Is Dominant Tumor Nodule Size a Significant Predictor of Adverse Outcome in Prostate Cancer? A Study of 283 Whole Mount Radical Prostatectomy Cases

Laura Favazza, Alpa Shah, Mireya Diaz-Insua, Sean Williamson, Hans Stricker, Craig Rogers, James Peabody, Mani Menon, Nilesh Gupta. Henry Ford Hospital, Detroit, MI.

Background: Multiple studies have evaluated maximum tumor diameter (MTD) of prostatic adenocarcinoma (PCA) as a predictor of biochemical recurrence (BCR) in PCA with confounding results regarding its significance. The aim of our study is to better characterize the relationship of MTD with multiple pre-operative clinical parameters and pathologic variables and to analyze if MTD is a significant predictor of BCR.

Design: 283 radical prostatectomy (RP) specimens were evaluated by whole mount (WM) processing of entire prostate. Tumor dimensions were measured on WM sections. The following variables were noted in all cases. Age, pre-operative PSA (PSA), body mass index (BMI), Gleason score (GS), tumor volume percentage (TV%), organ confined disease (OCD), extraprostatic extension (EPE), seminal vesicle invasion (SVI), surgical margin status (R0=negative margins, R1F=focal margin positive, R1=non-focal margin positive), lymph node status (pNx=lymph nodes not submitted or found, pN0=lymph nodes negative, pN1=positive lymph nodes).

Results: Median follow-up among 283 men was 21.2 months (range 1 to 51.5 months). Mean MTD in study population was 2.5 (0.5, 5.5) cm compared to 3.0 (1.2, 4.5) cm in the 41 cases with BCR.

Relation of MTD ≥2.5cm with other pathologic variables:

1. With GS 8 or >: 33/41=80.5% vs. 137/242=56.6%, p-value = 0.003 (Fisher exact test),
2. Stage: OCD 49/119=41.2%, EPE 88/127=69.3%, SVI 33/37=89.2%, p-value<0.001 (Chi-square test)
3. Positive margins: p-value=0.009 (Chi-square test)
4. Positive nodes: 22/24=91.7%, pNx 26/50=52%, pN0 122/209=58.4%, p-value=0.003 (Chi-square test)
5. Preop PSA: It was significant (p-value<0.001) but weakly associated (Pearson rho=0.26).

Rate of BCR was significantly different for MTD of 2.5 or > compared to BCR when MTD was < 2.5cm 10/113 = 8.9% vs. ≥ 2.5cm 31/170 = 18.2% (p-v=0.038, fisher exact test). In univariate analysis increased tumor%, maximum dimension 2.5 cm or greater, GS 8 or >, pN1, SVI and R1 were predictive of earlier BCR. In multivariable analysis, only pN1, GS 8 or >, and R1 remain independent predictors of earlier recurrence.

Table. Hazard ratio and 95% confidence interval (p-value) from Cox proportional hazards model estimating biochemical recurrence

Variable	Univariate	Multivariable
Tumor (%)	1.04 (1.02, 1.06), p-v<0.001	0.98 (0.96, 1.01), p-v=0.232
Max dim ≥2.5cm	2.08 (1.02, 4.24), p-v=0.044	1.21 (0.50, 2.92), p-v=0.680
Age (years)	1.03 (0.99, 1.08), p-v=0.184	1.00 (0.95, 1.04), p-v=0.835
BMI	0.98 (0.91, 1.05), p-v=0.564	0.93 (0.86, 1.00), p-v=0.058
Preop PSA (ng/ml)	1.01 (0.98, 1.03), p-v=0.610	1.00 (0.96, 1.04), p-v=1.000
Gleason 8-10	6.56 (3.55, 12.12), p-v<0.001	3.66 (1.66, 8.06), p-v=0.001
pN0 vs pNx	1.57 (0.47, 5.27), p-v=0.464	1.12 (0.32, 3.85), p-v=0.863
pN1 vs pNx	18.91 (5.52, 64.76), p-v<0.001	12.75 (2.89, 56.28), p-v<0.001
OCD vs SVI	0.19 (0.10, 0.37), p-v<0.001	0.53 (0.15, 1.89), p-v=0.327
EPE vs SVI	0.10 (0.04, 0.24), p-v<0.001	0.78 (0.27, 2.20), p-v=0.634
R1F vs R0	2.18 (0.92, 5.13), p-v=0.076	2.10 (0.82, 5.35), p-v=0.121
R1 vs R0	3.22 (1.61, 6.45), p-v<0.001	3.79 (1.76, 8.13), p-v<0.001

Conclusions: MTD is not an independent prognostic factor for BCR in patients treated with RP, irrespective of the risk profile. Additional studies are needed to evaluate the role of MTD in OCD with R0 and pN0.

873 Detection of HPV Genotypes According To Subtypes of Penile Intraepithelial Neoplasia (PeIN) – A Study of 126 Lesions in 43 Patients Using Laser Capture Microdissection (LCM)-PCR

Maria Jose Fernandez-Nestosa, Nuria Guimera, Diego Sanchez, Sofia Canete, Elsa Velazquez, David Jenkins, Wim Quint, Antonio Cubilla. Facultad Politécnica – UNA, San Lorenzo, Paraguay; DDL Diagnostic Laboratory, Rijswijk, Netherlands; Instituto de Patología e Investigación, Asunción, Paraguay; Facultad de Ciencias Médicas – UNA, Asunción, Paraguay; Miraca Life Sciences and Tufts University, Boston, MA.

Background: A sub classification of PeIN has been recently proposed. We found no studies of HPV genotypes by LCM-PCR in these lesions.

Design: Paraffin blocks with unifocal and multifocal precancerous lesions from Paraguay were submitted to the DDL laboratory. Sections were stained and placed on the Aperio® imaging system where lesions were marked. Analyses on whole tissue sections (WTS) and laser capture microdissected (LCM) regions were performed by SPF_{10}-DEIA-$LiPA_{25}$ (version 1). DNA quality of negative cases was confirmed by RNaseP/PhHV qPCR.

Results: WTS-PCR detected 46/126 (37%) lesions with multiple HPV genotypes of which 41/46 (89%) lesions had only one HPV genotype by LCM-PCR.

PeIN	Number of Cases	HPV+ LCM (%)	HPV 16 (%)
Differentiated	44	3 (7)	2 (5)
Basaloid	25	23 (92)	15 (60)
Warty-basaloid	33	32 (97)	18 (55)
Warty	24	24 (100)	4 (17)
Total	126	82	39

PeIN	HPV genotypes other than 16
Differentiated	74*
Basaloid	18, 35, 44* (3 lesions), 52, 56, 58
Warty-basaloid**	18, 30 (2 lesions), 33, 35, 52, 56 (7 lesions), 44, 51, 59
Warty***	11* (2 lesions), 18 (3 lesions), 30, 33 (2 lesions), 39 (3 lesions), 56 (5 lesions), 66, 73, 84*, 87*

*Low risk HPV. ** Lesion with multiple HPV genotypes (44/51/59) in the same lesion. *** 2 lesions with 2 HPVgenotypes (30/33 and 56/16).

Conclusions: LCM-PCR was found to be a more appropriate and accurate method to detect HPV types in specific lesions than WTS-PCR. HPV was rare in differentiated and common in warty/basaloid PeIN. High risk HPVs predominated (90%) but low risk types were also noted. HPV 16 was prevalent in basaloid and warty-basaloid PeINs but not in warty PeIN. Higher variation of HPV genotypes was present in warty PeIN some of which were exclusive (39, 66, 84 and 87). Warty PeIN, morphologically and molecularly distinctive, should be distinguished from other PeINs. There is more variety of HPV genotypes in PeIN than in invasive cancers. This finding may be important to guide strategies in male vaccination programs.

874 TMPRSS2-ERG Gene Fusion Is Rare But PTEN Deletions Are More Commonly Observed in Stage T1a Prostate Cancer

Kurt Fisher, Shaobo Zhang, Mingsheng Wang, Rodolfo Montironi, Lisha Wang, Antonio Lopez-Beltran, Liang Cheng. Indiana University, Indianapolis, IN; Polytechnic University of the Marche Region, United Hospitals, Ancona, Italy; Fudan University Shanghai Cancer Center, Shanghai, China; Cordoba University, Cordoba, Andalusia, Spain.

Background: T1a prostate cancers are indolent tumors that are derived from the transition zone. The overexpression of ERG and the inactivation of PTEN have been shown to be important drivers of carcinogenesis in large series of prostate cancer, but the genetics of transitional zone tumors have not been well characterized.

Design: We evaluated the status of ERG and PTEN in formalin-fixed paraffin-embedded tissue using immunohistochemical and FISH analysis in 47 pT1a tumors that arose within the transition zone. The protein expression of ERG was determined using a rabbit monoclonal antibody (clone EPR 3864, Epitomics Inc) and nuclear staining was scored as positive or negative. The genomic status of ERG was determined using 3 colored FISH using an ERG-TMPRSS2 tri-color probe set (5' ERG green, 3' ERG gold, TMPRSS2 Aqua). The protein expression of PTEN was determined using a rabbit monoclonal antibody (D4.3, Cell signaling technology) and cytoplasmic and nuclear staining was scored as positive or negative. The genomic status of PTEN was determined using dual color FISH with a PTEN probe and a CEP10 probe.

Results: We found ERG rearrangement and coordinate protein overexpression in 1 of 47 tumors (2.1%). No adjacent benign tissue showed ERG overexpression or rearrangement. We found PTEN inactivation in 8 of 47 tumors (17.1%). Seven of the 8 PTEN alleles were inactivated by deletion. No homozygous PTEN deletion was observed. PTEN deletion and ERG rearrangement were mutually exclusive.

Conclusions: ERG rearrangement and PTEN loss are both underrepresented in pT1a transition zone tumors, however, PTEN loss is relatively common in pT1a prostate cancers.

875 Predictors of Tumor Upgrading or Upstaging After Radical Prostatectomy in Patients With Gleason Score 3+4=7 Prostate Cancer (PCa) at Transrectal Ultrasound (TRUS) Guided Needle Biopsy

Trevor Flood, Soufiane El Hallani, Kien Mai, Eric Belanger, Nicola Schieda. Ottawa Hospital, Ottawa, ON, Canada; University of Ottawa, Ottawa, ON, Canada.

Background: Select patients with TRUS guided biopsies containing Gleason Score 3+4=7 PCa may be considered candidates for active surveillance. The purpose of this study was to determine if there are features that predict PCa upstaging and/or upgrading after radical prostatectomy (RP) in patients with 3+4=7 PCa diagnosed on TRUS guided biopsies.

Design: We searched our institution's database for patients with Gleason Score 3+4=7 PCa diagnosed on TRUS guided biopsy and who underwent RP between January 2012 and May 2014. Forty-nine patients were identified. Two blinded genitourinary pathologists independently reviewed the biopsies and assessed: a) nuclear size, nucleolar size, and distribution of macronucleoli of PCa which were subjectively graded using a semiquantitative scale from 1 to 3, b) extent of Gleason Pattern 4, and c) PCa with cribriform morphology. Patient age and serum PSA were also recorded. The Gleason Score and stage (presence or absence of organ confined disease [OCD]) was retrieved from RP reports. Comparisons were performed between groups using the chi-square test and Spearman correlation.

Results: The mean age and PSA at diagnosis was 64 years (±5.77) and 8.34 ng/mL (±5.14), respectively. Gleason Scores were upgraded in 17 patients (34.7%) and 26 patients (53.1%) did not have OCD after RP. PSA correlated with tumor upgrading (r=0.43, p=0.002) but not with absence of OCD (p=0.28). The median extent of Pattern 4 was 20% (10-30 IQR) and this was associated with tumor upgrading after RP (r=0.32, p=0.03). Ten patients had cribriform morphology on core biopsy of which 70% were upgraded after RP (p=0.009). Eighty percent of tumors with cribiform morphology did not have OCD and this difference was not significant (p=0.06). There was no association between age, nuclear size, nucleolar size, and/or distribution of macronucleoli with upgrading and/or absence of OCD (p>0.05).

Conclusions: A proportion of patients with Gleason Score 3+4=7 PCa at needle biopsy do not have OCD or are upgraded to higher Gleason Scores after RP. Features on needle biopsy that are associated with Gleason Score upgrading after RP include PSA, extent of Pattern 4, and the presence of cribriform morphology. Gleason Score 3+4=7 biopsies with cribriform morphology are associated with tumor upgrading after RP and may be considered a contraindication to active surveillance.

876 Correlation of Urinary T2:ERG Fusion Detection and Tissue ERG Expression: Comprehensive Evaluation of Prostatectomy Specimens From the EDRN Study

Jacqueline Fontugne, Martin Sanda, Scott Tomlins, John Wei, Dattatraya Patil, Huihui Ye, Kyung Park, Jonathan Chipman, Meredith Regan, Douglas Scherr, Javed Siddiqui, Arul Chinnaiyan, Mark Rubin, Juan Miguel Mosquera. Weill Cornell Medical College, New York, NY; Emory University School of Medicine, Atlanta, GA; University of Michigan Medical School, Ann Arbor, MI; Beth Israel Deaconess Medical Center, Boston, MA; Dana-Farber Cancer Institute, Boston, MA.

Background: Studies have shown that detecting urinary *T2:ERG* fusion transcript combined with other biomarkers is a useful, non-invasive method to predict prostate cancer (PCA) at biopsy. Importantly, PCA is multifocal and ERG status in biopsies may not reflect ERG status of all tumor foci, due to sampling. We sought to interrogate how urinary *T2:ERG* fusion detection predicts IHC ERG positivity in radical prostatectomies (RP) and to determine an optimal urinary cut-point to predict ERG presence in overall cancer tissue.

Design: Pre-surgery post-DRE urine and matching RP specimens were prospectively collected from 269 patients enrolled in the well-characterized, multi-institutional EDRN trial. Each tumor focus was identified, measured and interrogated for ERG status by IHC in each RP. Gleason scores were noted for each focus. A RP was considered ERG+ when it harbored at least one ERG+ tumor focus. In each corresponding urine, amounts of *T2:ERG* fusion transcript was determined by TMA assay. Logistic regression provided the ROC curve for prediction of tissue ERG status by urinary *T2:ERG* score. Bootstrap sampling helped estimate the performance measures such as sensitivity, specificity, PPV, and NPV at urinary thresholds. Cut-point for prediction of tissue presence of ERG+ PCA by urinary *T2:ERG* score was determined where sensitivity and specificity were about equal.

Results: The number of foci per RP ranged from 1 to 18 and measured 0.09 to 2.7 cm, with Gleason scores from 6 to 10. Overall ERG expression frequency in the RP specimens was 62% (167/269). Mean urinary *T2:ERG* score was 90.5 (SD ±423.3, min:0, max:6325.88). The association of urinary *T2:ERG* score with ERG IHC expression was determined with an AUC of 0.6954. We established a *T2:ERG* score of 10 for predicting RP tissue presence of ERG+ cancer, corresponding to about 0.63 sensitivity and specificity.

Conclusions: RP specimens frequently harbor multiple tumor foci. Since every tumor focus was interrogated by IHC, our study may represent the gold standard of *T2:ERG* fusion status assessment in RP specimens. Our model shows that urinary *T2:ERG* predicts the presence of ERG in RP tissue with an AUC of 0.69. Further efforts to optimize specific cut-points and to determine a potential transition towards clinical application are needed.

877 DNA Damage Response Genes in Prostate Cancer: Development of a Novel Targeted Sequencing Platform

Jacqueline Fontugne, Sinan Ramazanoglu, Karen Knudsen, Johann De Bono, Felix Feng, Andrea Sboner, Mark Rubin. Weill Medical College of Cornell University, New York, NY; Thomas Jefferson University, Philadelphia, PA; The Institute of Cancer Research/The Royal Marsden, Sutton, Surrey, United Kingdom; Universtity of Michigan, Ann Arbor, MI.

Background: Recent studies suggest that DNA damage response (DDR) gene alterations increase as a function of prostate cancer (PCA) progression. Importantly, next-generation sequencing from FFPE material is challenging yet critical when identifying genomic alterations associated with disease progression, in order to interrogate archival primary tumors matched with metastatic tissue. We sought to develop a targeted sequencing assay, suitable for FFPE material, in order to assess DDR gene alterations and their relation to disease progression.

Design: FFPE material was obtained from 69 tumors from 51 patients with a spectrum of localized and advanced PCA. At least 1ug DNA was extracted. After hybridization capture, sequencing was performed (Illumina HiSeq 2500). Raw sequences were aligned to the human genome reference sequence. An in-house tool identified the somatic single nucleotide variants (SNVs) by comparing the tumor to its matching normal. A total of 523 genes, including 112 genes related to DDR pathways, 334 recurrently mutated genes in PCA and 77 other cancer-related genes, were assessed for somatic alterations.

Results: We obtained an average sequencing depth of >265X. Advanced cases harbored significantly more alterations than localized PCA (figure). No recurrent alterations were identified in DDR genes in the localized PCA cases. However, in advanced disease, we detected recurrent alterations in DDR-related genes such as *TP53* (SNVs and indels: 47%; deletions: 100%), *BRCA2* (SNVs and indels: 6%; deletions: 94%), *GML* (amplifications: 94%), *NBN* (amplifications: 65%), *TP53BP1* (deletions: 29%), *RAD23B* (amplifications: 18%), *TOP2A* (SNVs: 12%), and *MDB4* (amplifications: 12%).

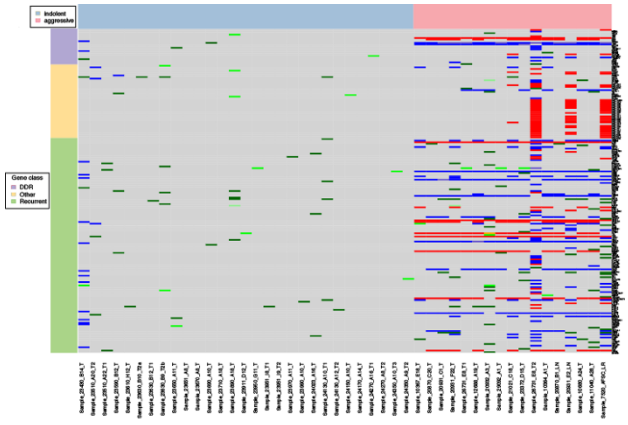

Figure 1: Heat map representing the alterations found in the panel of genes on the current cohort of indolent and aggressive PCA cases. Samples are ordered by their agressiveness on the columns; genes are ordered by there type in the rows. Blue, red and green represent deletions, amplifications and mutations, respectively.

Conclusions: We successfully developed a sequencing assay -suitable for FFPE material- targeting a PCA-specific panel of genes, including DDR genes. This panel is crucial for molecular subtyping and identifying mutations defining therapeutic response. Advanced disease harbored significantly more genomics alterations overall, and in DDR genes in particular. Further analysis is ongoing.

878 Intraoperative Depletion of Ureteral Frozen Section Margins

Jessica Forcucci, Stephen Savage, M Timothy Smith. Medical University of South Carolina, Charleston, SC.

Background: At our institution, ureteral frozen section margins are completely exhausted or depleted at the time of frozen section. Generally, four levels are obtained to completely sample submitted tissue; however, larger specimens may require additional levels. This practice allows for accurate determination of margin status intraoperatively, and eliminates the possibility of a more malignant diagnosis on permanent section control due to sampling error.

Design: A retrospective review of exhausted ureteral frozen sections between 2011 and 2013 was performed. The resection specimen diagnosis and margin status was recorded. When margin status was not benign (atypical, carcinoma in situ, or carcinoma), the number of slides where abnormality was present was also recorded.

Results: 204 exhausted ureteral frozen section margins from 94 patients were identified. Resection specimen diagnoses included urothelial carcinoma, urothelial carcinoma in situ, adenocarcinoma, squamous cell carcinoma, squamous cell carcinoma in situ, angiomyxoma, poorly differentiated carcinoma, and no residual tumor. Of the ureteral margins, 173 were benign or reactive (85%), 5 were atypical (3%), 13 demonstrated carcinoma in situ (6%), and 13 contained invasive carcinoma (6%).

With regards to abnormal margins, lesional tissue was present on all levels examined in 21 frozen section margins (68%). Of the remaining margins, tumor was present on greater than half of the levels in 5 margins (16%). Tumor was present on less than half of the levels in 5 margins (16%), which may not be identified due to sampling error using the traditional frozen section protocol of two frozen section levels, and one permanent frozen section control.

Eight ureters were unable to be converted to negative margins despite additional resection. Tumor was present within the adventitia or lymphovascular spaces in five ureters. In the remaining three ureters, carcinoma in situ was consistently present on newly submitted margins leading to unilateral nephrectomy in one case.

Conclusions: Intraoperative depletion of ureteral frozen section margins allows for the detection of focal disease, although rare, which may be missed using standard frozen section procedure due to sampling error. The availability of this information in the intraoperative setting facilitated the conversion of positive margins in more than half of patients with an abnormality at frozen section, which has been previously reported to be associated with upper tract recurrence.

879 Plasmacytoid Variant of Urothelial Carcinoma: A Clinicopathological Study of 49 Cases

Melanie Fox, Li Xiao, Bogdan Czerniak, Charles Guo. University of Texas MD Anderson Cancer Center, Houston, TX.

Background: Plasmacytoid urothelial carcinoma (PUC) is a rare variant of urothelial carcinoma (UC). There have been limited studies regarding this disease. Herein we report the largest case series of PUC from a single institution, providing detailed clinicopathological features of the disease, including treatment and follow-up.

Design: We identified 49 cases of PUC from our surgical pathology files between 1992 and 2014. Slides from each case were reviewed for pathological analysis. The patient's demographic and clinical information was obtained from electronic medical records.

Results: Of the 49 patients, 44 were male and 5 were female. The patient's mean age was 62 years (range, 45 to 86 years). Gross hematuria was the most common presenting symptom (61%). Other common symptoms included dysuria, urinary frequency and lower abdominal pain. PUC showed a diffusely infiltrative growth pattern, and the tumor cells were characterized by eccentric nuclei and abundant eosinophilic cytoplasm, closely resembling plasmocytes. Conventional UC was identified in all cases, and other UC variants, including sarcomatoid (n=5), micropapillary (n=3), nested (n=2), small cell carcinoma (n=1) and lipoid (n=1) variants, were also present. PUC accounted for an average of 68% (range, 5 to 95%) of the tumor. Signet ring cells were found in 12 cases, and lymphovascular invasion was identified in 21 cases. All PUCs were invasive, including pT1 (n= 4), pT2 (n=16), pT3 (n=17) and pT4 (n=12). Metastasis was present in 47% (15/32) of cases in which lymph nodes were sampled. Immunohistochemical analysis showed PUCs were positive for CK7 (89%, 17/19), CK20 (76%, 13/17), uroplakin II (69%, 11/16) and GATA-3 (50%, 9/18). Patients received chemotherapy (n=39), radical cystectomy (n=31) and radiation treatment (n=6). Among the 41 patients who had followup information (with a mean follow-up time of 23 months), 25 patients died of disease, and 16 were alive.

Conclusions: PUC is a highly aggressive disease which often presents at an advanced stage with metastasis. PUC is usually associated with conventional UC and other UC variants. UC immunohistochemical markers, particularly GATA-3 and uroplakin II, are useful in differentiating PUC from other plasmacytoid carcinomas. Despite multimodality treatment, the prognosis for this disease remains poor.

880 Do Histopathologic Variables Impact the Reporting of Lymphovascular Invasion in Testicular Germ Cell Tumors?

Bryce French, Debra Zynger. Ohio State University, Columbus, OH.

Background: The identification of true lymphovascular invasion (LVI) in testicular germ cell tumors (GCT) is a challenging, yet important aspect of cancer reporting. LVI may be difficult to differentiate from pseudo-lymphovascular invasion, including displaced tumor and retraction artifact. Accurately diagnosing LVI is essential because its presence changes tumor stage and can alter therapeutic management. Our study aimed to identify pathologic features which impact the reporting of LVI.

Design: A retrospective search was performed to identify pathology reports from all patients who had an orchiectomy with GCT performed at our tertiary care institution between January 2007 and March 2013. Reports were analyzed for prospector type (resident or pathology assistant), tumor size, tumor type, and documented LVI. Pathology slides were reviewed by a blinded genitourinary pathologist, reassessing LVI, histological features of the tumor emboli, and presence of tissue butter artifact. Statistical analysis was performed using chi-square test, student-t test, and Fisher's exact test.

Results: 158 orchiectomies were identified (69 pure seminomas, 89 mixed GCT). Seminomas grossed by residents had a higher rate of reported LVI compared to specimens grossed by pathology assistants (46% vs 15%, p=0.04). Tissue butter artifact was frequent, with 60% of seminomas having butter artifact compared to 38% of mixed GCT (p=0.05). Seminomas with tissue butter were larger (4.4 cm) then those without artifact (2.8 cm) (p=0.02). Concordance for diagnosing LVI was high upon blind review (k=0.77), with all cases in disagreement having tissue butter artifact (p<0.01). Tumor emboli from cases reported to have LVI had a higher frequency of tumor cohesiveness (79% vs 14%, p<0.01), smooth contours (70% vs 21%, p<0.01), and adherence to vessel walls (70% vs 14%, p<0.01) compared to tumor emboli that were considered pseudo-lymphovascular invasion. Presence of fibrin (79% vs 71%, p=0.44) and admixed red blood cells (92% vs 100%, p=0.63) were features found at a similar frequency in tumor emboli that were reported as LVI compared to emboli that were deemed artifactual.

Conclusions: In GCT, tumor type, tumor size, prospector, and tissue butter artifact may impact the reporting of LVI. Tumor cohesiveness, smooth contours, and adherence to vessel walls were features of tumor emboli predictive of diagnosing LVI while presence of fibrin and admixed red blood cells were not.

881 Evaluation of the Concordance of Histologic Subtype and Prognostic Indicators Between Renal Cell Carcinoma Biopsies and Their Subsequent Resections

Paul Friedman, Maryam Sayah, Adesuwa Egharevba, Kyle Molberg, Jeff Cadeddu, Dinesh Rakheja, Payal Kapur. University of Texas Southwestern Medical Center, Dallas, TX.

Background: In recent years, due to an increased use of cross-sectional imaging, there is a rise in the incidence of renal masses being detected. With the advent of targeted therapies, pathologists are increasingly asked to subtype renal tumors on limited biopsy material.

Design: We retrospectively evaluated 326 patients that underwent needle biopsies of renal masses from January 2008 to May 2014. The masses were treated with radiofrequency ablation in 110 (34%) and 96 (29%) patients had subsequent nephrectomies. A definitive histologic renal tumor subtype or differential diagnosis was rendered in 85 (89%) of the biopsies. The remainder was either non-neoplastic (8%), diagnosed RCC without a specific subtype (1%), or were metastatic carcinomas involving kidney (2%). Tumor subtype and other prognostic indicators were retrospectively evaluated for concordance between biopsies and subsequent resections.

Results: The 85 studied renal masses included 57 clear cell, 16 papillary, 6 chromophobe, 3 unclassified, 1 hereditary leiomyomatosis and renal cell carcinoma (HLRCC), 1 clear cell papillary, and 1 hybrid renal oncocytoma/chromophobe. IHC was performed to assist with definitive diagnoses on 54% (46/85) of biopsies and 33% (28/85) of resections. In 80 cases the histologic subtype diagnosed on the biopsy material was confirmed on the subsequent nephrectomy specimen, giving an overall concordance rate of 94% (80/85). The concordance rate for clear cell, papillary, chromophobe, and unclassified were 100% (57/57), 94% (15/16), 100% (6/6), and 75% (3/4). In five cases (6%) a definitive histologic subtype could not be rendered. There were no discordant diagnoses. Fuhrman nuclear grade was concordant in 49% (33/67) of cases (46% [28/61] for low grade (G1-2) and 83% [5/6] for high grade (G3-4)). The concordance rate for coagulative necrosis and sarcomatoid dedifferentiation was 66% (56/85) and 97% (82/85).

Conclusions: Our data shows a high accuracy of the diagnosis of subtype rendered on biopsies of malignant renal masses. Other prognostic indicators, including Furhman nuclear grade, necrosis, and sarcomatoid changes, are less reliable. This may be due to various factors, including tumor heterogeneity, and the avoidance of necrotic areas based on imaging.

882 Dual Staining of p16/Ki67 Is Highly Specific in High Grade Urothelial Carcinoma

Chen Gao, Yousef Soofi, Noreen Ersing, Jordan Almonte, Lourdes Ylagan. Roswell Park Cancer Institute, Buffalo, NY.

Background: p16 is an important cell cycle control regulator and its expression has been shown in urothelial carcinoma to be related to tumor progression. However, most authors believe its expression is not related to HPV infection as in cervical cancer. A few studies have shown p16/Ki67 dual labeling as a marker for high-grade urothelial cells in urine cytology. In the current study we investigated p16/Ki67 dual staining in urothelial carcinomas from resected and biopsy specimens.

Design: Dual immunostains for $p16^{(INK4a)}$ /Ki67 were performed and compared in 29 cases of low grade urothelial carcinomas (LGUC) along with 29 cases of high grade urothelilal carcinomas(HGUC). The intensity for p16 and Ki67 staining were graded as 0(no staining), 1+(mild), 2+(moderate) and 3+(high). The extent of staining for p16 and Ki67 were graded as 1+ (<10%), 2+(10-50%) and 3+(>50%). The intensity and extent of p16 and Ki67 staining were scored individually. Dual staining for p16/Ki67 was also evaluated and defined as positive when >10% of Ki67 staining was present in p16 positive cells.

Results: p16 is positive in 48% of LGUC and 62% of HGUC. Both the intensity and extent of p16 staining are statistically higher in HGUC compared with LGUC (Table1). As expected, the scores for the extent of Ki67 staining are higher in HGUC (2.65±0.23) than LGUC (1.13±0.12), p<0.01. The intensity for Ki67 is strong (3+) in both groups. Significantly, among p16 positive cases, most HGUC (16 out of 18) are positive for dual p16/Ki67 staining while none of the LGUC (0 out of 14) is dual stained (Table2).

Table1

	LGUC	HGUC
p16 Positive	14/29(48%)	18/29(62%)
p16 Intensity		
1+	12/14(86%)	7/18(39%)
2+	2/14(14%)	7/18(39%)
3+	0/14(0%)	4/18(22%)
Mean±SD	1.1±0.1	1.8±0.6 (p
p16 Extent		
1+	4/14(29%)	5/18(28%)
2+	10/14(71%)	3/18(16%)
3+	0/14(0%)	10/18(56%)
Mean±SD	1.7±0.2	2.2±0.8 (p

Table2

	LGUC	HGUC
p16/Ki67 Dual Stain Positive	0/14 (0%)	16/18(89%)
Percentage p16/Ki67 Positive Cells	2±0.05%	38±6% (p

Conclusions: P16 stain alone is neither sensitive nor specific for HGUC. However, our data shows that dual staining for p16/Ki67 is highly specific for HGUC. The results from this study would support the usage of p16/Ki67 to confirm presence of HGUC in difficult cases in urine cytology.

883 Pathologic Findings in Patients on Active Surveillance for Prostate Cancer: Utility of Targeted Magnetic Resonance Imaging-Guided Biopsies

Rachel Geller, Sherif Nour, Adeboye Osunkoya. Emory University School of Medicine, Atlanta, GA.

Background: Some patients (PTs) with a Gleason score of 3+3=6 are eligible for active surveillance. Targeted magnetic resonance imaging-guided biopsies (TMRI-GB) target regions of the prostate suspicious for prostate cancer (PCa), based on findings on multiparametric MRI. There is a dearth of literature examining the pathologic findings identified by TMRI-GB in PTs undergoing active surveillance.

Design: A search was made through our Urologic Pathology files for prostate needle core biopsies that were obtained via TMRI-GB from 2012-2014. Only patients on active surveillance were included in the study.

Results: Fifteen cases were identified. Mean PT age was 59 yrs (range: 50-74 yrs). All PTs had a Gleason score of 3+3=6. All PTs had at least one prior transrectal ultrasound-guided biopsy (TRUS-GB). Fourteen PTs had cancer identified on TRUS-GB, and 1 PT had a benign TRUS-GB followed by a malignant TMRI-GB. Eighty percent (12/15) of PTs on active surveillance had a prostate specific antigen > 4ng/ml. All PTs were described as having at least one focal abnormality suspicious for PCa on preliminary diagnostic MRI. A total of 78 lesions were sampled. An average of 4.5 lesions were identified per patient, and an average of 2.3 cores were removed from each lesion. A total of 177 cores were sampled, with an average of 11.8 cores sampled per patient (range 7-20 cores). Nine of 15 (60%) PTs had malignant TMRI-GB biopsies, and the remaining 6 had benign biopsies. Of the 9 PTs with malignant TMRI-GBs, 5 PTs had 3+3=6, 3 PTs had 3+4=7, and 1 PT had 4+5=9. Fourteen of 78 (18%) lesions biopsied were malignant. A total of 41 cores were removed from these malignant lesions, and cancerous glands were identified in 30/41 (73%) cores.

Conclusions: TMRI-GB may have a critical role in PTs on active surveillance, which will likely evolve as ability to identify malignant lesions improves. In this cohort of men on active surveillance, 18% of lesions sampled by TMRI-GB were found to be malignant. This may be due to inclusive radiologic criteria designed to increase sensitivity and identify all malignant lesions in men with a prior PCa diagnosis. In addition, 73% of cores from malignant lesions revealed cancerous glands, which indicates a high degree of precision via TMRI-GB.

884 Targeted MRI Guided Prostate Needle Core Biopsies: Ready for Prime Time?

Rachel Geller, Sherif Nour, Adeboye Osunkoya. Emory University School of Medicine, Atlanta, GA.

Background: In contrast to the systematic (non-targeted) sampling approach of transrectal ultrasound-guided biopsies (TRUS-GB), targeted magnetic resonance imaging-guided biopsies (TMRI-GB) target regions of the prostate suspicious for prostate cancer (PCa), based on findings on multiparametric MRI. There are limited studies in the literature examining the pathologic findings identified following TMRI-GB.

Design: A search was made through our Urologic Pathology files for prostate needle core biopsies that were obtained via TMRI-GB from 2012-2014.

Results: Forty-six cases were identified. Mean patient (PT) age was 62 yrs (range: 50-78 yrs). Twenty-one of 46 (46%) had a history of PCa, 10/46 (22%) PTs had a history of negative TRUS-GB, and the remaining 15/46 (32%) had never undergone biopsy. Of the 31 PTs with a prior biopsy, 3/31 (10%) had a TMRI-GB and 28/31 (90%) had a TRUS-GB. Of the 21 PTs with previous PCa diagnosis, 15 PTs had a Gleason score of 3+3=6. Four had a Gleason score of 7 (3+4 or 4+3), 1 PT had ductal PCa (4+4=8), and 1 PT had a Gleason score identified only as 9; all of whom were considering focal therapy. All PTs were described as having at least 1 focal abnormality suspicious for PCa on diagnostic MRI. An average of 4.6 lesions were identified per PT, and an average of 12.9 cores (range: 3-23) were collected per TMRI-GB procedure. TMRI-GB results were malignant in 27/46 (59%) and benign in 19/46 (41%) PTs. The highest Gleason score documented for each of the 27 PTs with PCa is as follows: 10 had 3+3=6, 10 had 3+4=7, 2 had 4+3=7, 2 had 4+4=8, 2 had 4+5=9, and 1 had 5+4=9. Five of 10 (50%) PTs with a history of benign biopsy had PCa identified by TMRI-GB. Ten of 15 PTs (67%) with no prior biopsy had a malignant TMRI-GB. Twelve of 21 (57%) PTs with a prior diagnosis of PCa had PCa identified by TMRI-GB. A total 212 lesions were identified; 50 were malignant and 162 were benign. Non-cancerous findings included: inflammation (24%), atypical small acinar proliferation (2%), high grade prostatic intraepithelial neoplasia (6%), benign prostatic hyperplasia (1%), treatment effect (5%), no prostatic tissue identified (3%), and otherwise unremarkable benign prostatic tissue in the remaining 95 lesions (59%).

Conclusions: TMRI-GB may be ready for prime time as a tool for active surveillance, tumor mapping, and primary detection of PCa.

885 Mutation Profile of Tumor-Associated High Grade Prostatic Intraepithelial Neoplasia

Sean Gerrin, Adam Sowalsky, Steven Balk, Huihui Ye. Beth Israel Deaconess Medical Center, Boston, MA.

Background: High grade Prostatic Intraepithelial Neoplasia (HGPIN) is the putative precursor lesion to prostatic adenocarcinoma (PCa). Approximately 20% of HGPINs harbor *ERG* fusion. Genetic alterations that drive HGPIN to invasive PCa are not clear. Recent studies pioneered by our laboratory demonstrated a clonal relationship between adjacent Gleason pattern 3 (Gp3) and Gleason pattern 4 (Gp4) tumors in Gleason score 7 (GS7) PCa. In addition, we have identified many shared and unique mutations in the clonally related Gp3 and Gp4 tumors. In this study, we investigated relationship of tumor-associated HGPINs to adjacent Gp3 and Gp4 tumors through examining tumor-specific mutations in HGPIN.

Design: We evaluated 12 radical prostatectomy cases of GS7 PCa that had been previously mapped for genetic alterations in the adjacent Gp3 and Gp4 tumors using whole exome sequencing. We selected one case that had prostatic tissue entirely submitted and identified a total of six tumor-associated HGPIN foci showing concordant *ERG* expression with the invasive tumor. We laser capture microdissected HGPIN epithelium, extracted genomic DNA (gDNA), and examined gDNA for the mutations detected in the invasive tumors through deep sequencing. A total of 51 tumor-specific genetic targets were examined, including 39 Gp3/Gp4 shared, 6 Gp3-specific, and 6 Gp4-specific mutations.

Results: All six HGPIN foci shared the same tumor-specific *TMPRSS2:ERG* fusion breakpoints, indicating that they were all precursors of the adjacent invasive tumor. Among 51 gene targets mutated in invasive tumor, only one genetic lesion, a missense mutation of the *OR2AP1* gene, was found in a single focus of HGPIN. *OR2AP1* mutation was a trunk mutation shared by both Gp3 and Gp4 tumors. The remaining gene targets were successfully sequenced and proven to be wild-type in all six HGPIN foci.

Conclusions: *ERG* fusion in this patient was a very early event in PCa development and the HGPIN lesions with this fusion appear to be otherwise genetically stable as the majority of trunk mutations in the invasive tumors were not present in HGPIN. Our findings suggest a punctated evolution model for PCa development in this patient. First, an early precursor cell develops *ERG* fusion and proliferates into HGPIN. A second hit in a subclone then triggers genomic instability, which is followed by a burst of multiple mutations that result in rapid evolution into an invasive tumor.

886 MicroRNA Profiling of Morphologically Heterogeneous Clear Renal Cell Carcinoma

Alessio Giubellino, Ang Li, Karlena Lara-Otero, Marston Linehan, Maria Merino. National Institutes of Health – National Cancer Institute, Bethesda, MD.

Background: Intratumoral heterogeneity (IH) has been recently described as an important contributor to tumor growth through a branched rather than a linear pattern of tumor evolution for renal cell carcinoma. Whether the miRNA profiling of the heterogeneous areas is the same or different it is not known. We studied differences and similarities of this profiling, since it may have great implications for the development of predictive biomarkers and the identification of druggable targets with improvement of combinatorial therapeutic approaches for the effective treatment of kidney cancer.

Design: Five cases of Clear cell RCC showing diffuse tumor heterogeneity were evaluated. Tissue was procured from different regions representing different morphological areas and miRNA extracted for PCR array profiling. The miRNA expression of these samples was compared with the normal renal parenchyma.

Results: Six different morphological patterns, including four different pattern of clear cell (large, solid small, dense eosinophilic nodule, and diffuse), sarcomatoid and high grade patterns were identified in the tumors. Distinct miRNA expression signatures for each morphological subtype were recognized. When compared to normal, the sarcomatoid type had a significant increase in miR-1283, miR-210, among others, and down-regulation of miR-143-3p, miR-200c-3p, mir-204-5p. The other morphological patterns showed a distinct pattern of up- and down-regulated miRNA which could uniquely identify different regions of the tumor.

Conclusions: The recognition that different morphological patterns (IH) inside the same tumor are associated with distinct miRNA signature, is of particular interest as novel selective therapies could be implemented in a combined fashion when appropriate. As miRNA become interesting molecular targets, our results also suggest novel therapeutic options for renal cell carcinoma for personalized medicine strategies.

887 MAGI2 Is a Novel Biomarker for Prostatic Neoplasia

Jeffery Goldstein, Rajen Goyal, Omar Hameed, Lan Gellert, Chaochen You, Peter Clark, Giovanna Giannico. Vanderbilt University Medical Center, Nashville, TN.

Background: MAGI2 (Membrane-associated guanylate kinase, WW and PDZ domain-containing protein 2) is a multidomain scaffolding protein that interacts with PTEN via the PDZ-2 domains of MAGI2 and the PDZ-binding motif of PTEN. We examined MAGI2 expression by immunohistochemistry (IHC) to test the hypothesis that MAGI2 expression is a marker for prostate cancer.

Design: Material from 78 patients with invasive prostate carcinoma was used to construct a tissue microarray (TMA) consisting of 408 1mm cores to include normal histology, benign prostatic hyperplasia (BPH, grouped as 'benign'), high grade prostatic intraepithelial neoplasia (HGPIN), and carcinoma. IHC was performed for MAGI2 (HPA013650). Digital images were acquired using the Leica SCN400 scanner. Regions of interest were manually outlined and MAGI2 cytoplasmic expression was analyzed using the Ariol SL-50 system. We report two results: %Area [area stained divided by area analyzed (μm2/μm2)]; and Area*ODS (mean optical density multiplied by %Area). Statistical analysis was done with the Kruskal-Wallis test and post-hoc Dunn's tests.

Results:

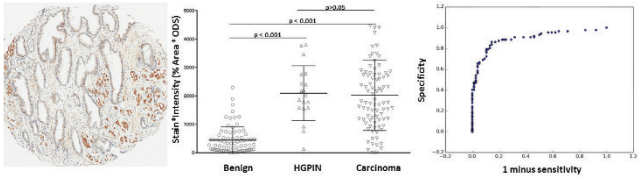

MAGI2 was strongly expressed in carcinoma and HGPIN, with lower expression in benign. The median Area*ODS was 310.5 (95% CI 165 - 457 %*ODS) in benign, compared to 1763 (95% CI 1544 - 2311 %*ODS) for carcinoma. The median %Area was 2.00% (95% CI 1.14-3.02%) in benign compared to 12.95% (95% CI 10.56-17.06) in carcinoma. Area*ODS and %Area were significantly different overall ($p<1e-10$), between benign and HGPIN ($p<0.001$) and between benign and carcinoma ($p<0.001$), while HGPIN and carcinoma were not significantly different ($p>0.05$). Using a receiver/operator curve to distinguish benign and carcinoma, the area under the curve is 0.902. A threshold of 1470 %*ODS gives a sensitivity of 0.66 and specificity of 0.96.

Conclusions: To our knowledge, this is the first report of MAGI-2 expression in prostate cancer. MAGI2 immunoreactivity is elevated in prostate cancer and HGPIN. Additional study will determine if MAGI2 IHC is useful in prostate needle biopsies.

888 Utility of TERT Promoter Mutations in Urine Specimen for Diagnosis of Urothelial Carcinoma

Michael Goltzman, Jian Zhuge, Fei Ye, David Zhang, John Fallon, John Phillips, Minghao Zhong. New York Medical College, Valhalla, NY; Westchester Medical Center, Valhalla, NY; Icahn School of Medicine at Mount Sinai, New York, NY.

Background: Urothelial carcinoma (UC) is the 5th most common solid organ malignancy in men and is associated with high recurrence rates and costs of surveillance. Currently, the gold standard for UC diagnosis and surveillance is cystoscopy, an invasive and expensive option. Urine cytology is a non-invasive method but is limited by a low sensitivity, especially for low grade UC. Recent studies have demonstrated that ~70% (low or high grade) UC carried *TERT* promoter mutations and suggested that these mutations are a biomarker for UC. We hypothesized that *TERT* promoter mutations in urine samples may detect bladder cancers with an improved sensitivity than cytology.

Design: After IRB approval, urine samples were collected from patients with and without a known history of UC. Cell pellets were generated by centrifugation and subjected to standard cytologic assessment. Concurrent pathologic tumor specimens were also collected, ensured that tumor components exceeded 20% of all tissue, and, where feasible, performed macro-dissection. Whole DNA was extracted from those cell pellets and tissue using standard techniques and *TERT* promoter mutations were detected by PCR-sequencing. Statistical considerations included Fisher's exact test with an alpha set at 0.05.

Results: A total of 100 cases of urine samples were collected, 40 cases from patients without a history of UC. Sixty cases were derived from patients undergoing a work up for UC, 10 of which were positive for UC including 8 cases of low grade UC and 2 cases of high grade UC. *TERT* promoter mutations were identified in 8 out of 10 positive cases (7 low grade and 1 high grade UC). Among those 7 low grade UC, only 2 cases were reported as suspicious for UC by urine cytology. In all 90 cases that were negative for UC, no *TERT* promoter mutations were identified ($p<0.01$). Sensitivity and specificity of this test was 80% and 100%, respectively.

Conclusions: Testing for *TERT* promoter mutations in urine is a sensitive and non-invasive method for diagnosis of UC. In our pilot study this test has 80% sensitivity and 100% specificity. Especially for low grade UC, the sensitivity of this test is much higher than that of urine cytology, which is limited by low sensitivity, ranging from 28 to 100% with a median of 48%. The clinical utility of this test warrants larger, multicenter studies.

889 Postchemotherapy Cystic Trophoblastic Tumor: Expanding the Morphologic Spectrum

Dibson Gondim, Thomas Ulbright, Liang Cheng, Muhammad Idrees. Indiana University, Indianapolis, IN.

Background: Cystic trophoblastic tumor (CTT) has been described in postchemotherapy retroperitoneal lymph node dissections (PC-RPLND) of patients with testicular germ cell tumors (GCT). Prognostically, this lesion is similar to teratoma and no further treatment is required after surgery in the absence of other components. However, the experience is limited to only one prior publication. We documented additional CTTs from RPLNDs and other sites to assess the morphologic spectrum and provide clinical correlation.

Design: An electronic search was performed for postchemotherapy CTT from 2000-2013 from departmental files. Diagnosis was confirmed by reviewing H&E stained slides by all the authors. Immunohistochemical stains for inhibin, hCG and p63 were performed when possible to confirm the diagnosis. Pertinent clinical and followup data were obtained.

Results: A total of 35 cases of CTT were found; 26 in RPLNDs, 3 in lung, 2 in liver, 1 in spermatic cord, 1 neck mass,1 pelvic mass and 1 primary mediastinal. Most of the CTT cases had known primary testicular GCTs (32/35) and occurred in metastatic sites (34/35). One metastatic CTT in liver had a prior diagnosis of esophageal adenocarcinoma with elevated hCG without a testicular primary. Morphologically, CTT displayed predominantly cystic architecture, but more solid foci, clusters and single infiltrating trophoblastic cells also occurred. The CTTs lacked exaggerated pleomorphism; mitotic activity was inconspicuous. A few cases showed multinucleated cells but no syncytiotrophoblasts. Teratoma was associated with 33/35 CTTs and the remaining two were pure. Other associated components were YST (2), Wilms-like tumor (1), embryonal carcinoma (1), and rhabdomyomatous tumor (1). The most common component in the testicular primary was teratoma (22/32). Although elevated serum hCG was noted in 19/35 cases prior to primary tumor resection, choriocarcinoma was present in only four cases. At followup (2 mo-13 yr) no case showed subsequent metastatic CTT.

Conclusions: CTT is mostly found as a minor component in postchemotherapy resections of metastatic GCTs arising in the testis. Although most are cystic, solid foci and single cells can be seen. It is usually associated with teratoma. We propose that CTT represents the end stage of regression of choriocarcinoma without capability of further metastasis, and, therefore, its prognosis is similar to teratoma.

890 PD-L1 Expression By Immunohistochemistry in Clear Cell Renal Cell Carcinoma Is Associated With High Tumor Stage and Nuclear Grade

Steven Goodman, Pheroze Tamboli, Jaime Rodriguez-Canales, Edwin Parra, Jose Karam, Christopher Wood, Priya Rao. University of Texas MD Anderson Cancer Center, Houston, TX.

Background: High expression of programmed death ligand (PD-L1) is associated with poor outcome in renal tumors, and is being exploited for targeted therapy in solid tumors. The focus of our study was to assess PD-L1 expression in stage specific renal cell carcinoma (RCC) and identify clinical and pathologic correlates associated with overexpression of this marker.

Design: Stage specific tissue microarrays (TMA) were prepared from formalin fixed paraffin embedded tissue from CCRCCs diagnosed between 1990-2010 at a single institute. 3 separate cores were obtained from each tumor. TMA slides were stained with the anti-PD-L1 antibody using routine immunohistochemistry protocols. PD-L1 expression was scored as positive if at least 5% tumor cells showed membranous staining. Antibody expression was correlated with clinicopathologic data from all the cases.

Results: Due to drop-out of the TMA cores, data was generated on 354 tumors, with a minimum of 2 cores present which included: 78 stage I, 93 stage II, 95 stage III, & 88 stage IV CCRCCs. The results are summarized in [table1].

	Stage 1	Stage 2	Stage 3	Stage 4	Total
Grade 1	0%	0%	0%	0%	0%
Grade 2	11%	0%	0%	6%	11%
Grade 3	6%	6%	16%	16%	44%
Grade 4	0%	6%	0%	33%	39%
Total	17%	12%	16%	55% (p=0.004)	100%

Statistically significant correlates of increased PD-L1 expression included high tumor stage (stage IV tumors showed significantly greater expression when compared with all other stages combined; p = .004, Fischer's exact test) and high nuclear grade; Fuhrman nuclear grade 3-4 tumors showed significant increase in expression when compared with Fuhrman nuclear grade 1-2 tumors (p = .04, Fischer's exact test). There was no statistically significant correlation between PD-L1 expression and overall survival (OS).
Conclusions: In our patient cohort of 354 CCRCC, PD-L1 expression was shown to be associated with high tumor stage and high Fuhrman nuclear grade. A total of 55% of tumors with PD-L1 expression were stage IV, and 83% were high nuclear grade. In contrast to previously published studies, our series did not show correlation with overall survival. Our study further demonstrates the high grade and high stage nature of PD-L1 expressing tumors in which PD-L1 expression may be considered a potential target for personalized therapy.

891 ERG and PTEN Protein Expression in High Risk (High Volume, High Gleason Grade, High pT Stage) Primary Prostate Cancer and Corresponding Regional Lymph Node Metastases

Anuradha Gopalan, Ann Bialik, Sahussapont Sirintrapun, Yingbei Chen, Hikmat Al-Ahmadie, Samson Fine, Howard Scher, Satish Tickoo, Victor Reuter. Memorial Sloan Kettering Cancer Center, New York, NY.
Background: PTEN loss at the genomic and protein levels occurs in about 30-70% of localized prostatic adenocarcinoma (PC) and this loss is significantly associated with TMPRSS2-ERG gene rearrangement (incidence ~50%) in human PC. Data in mouse models has shown that ERG cooperates with PTEN haplo-insufficiency to promote PC progression. However these genetic alterations have not been well described in the specific clinical setting of high grade, high stage and high volume PC with lymph node metastases (LNM).
Design: Study cohort consisted of 29 cases of Gleason 8-10, high volume, >=pT3 PC with LNM in 22/29 (76%), which did not fulfill criteria for castrate resistant prostate cancer and were treated by radical prostatectomy. 14/29 (48%) patients received neoadjuvant therapy including androgen deprivation/ immune checkpoint blockade. Immunohistochemistry for ERG and PTEN was performed on sections from the dominant primary tumor and the corresponding LNM, when available. Sequencing data were available in 4 cases.
Results: 29 primary PC and 17 LNM samples were evaluable. ERG protein was overexpressed (ERG+) in 12 of 29 (40%) primary tumors and 9 of 17 (53%) LNM. PTEN loss was seen in 17/29 (59%) primary tumors and 10/17 (59%) LNM. Concomitant ERG (+) and PTEN loss was present in 10/29 (34%). ERG protein status of the dominant primary tumor and the LNM were 100% concordant. PTEN protein expression was discrepant in one case, where PTEN was retained in the primary tumor and lost in the LNM. Sequencing data for PTEN (in 4 cases) correlated with PTEN protein status. Intratumoral heterogeneity (positive and negative foci within the same tumor) for PTEN was seen in 7/29 (24%) and for ERG in 1/29 (3%) primary tumors. Of the 7 patients who received neoadjuvant therapy and had ERG (+) tumors, 4 (57%) showed heterogeneous intensity of ERG expression (faint, weak, moderate, strong) in different areas of the dominant tumor. This heterogeneous expression was not present in untreated tumors.
Conclusions: Concomitant ERG overexpression and PTEN loss was present in about a third of this biologically aggressive cohort of primary prostate cancer.
Intratumoral heterogeneity was higher with PTEN (24%) as compared to ERG (3%). Heterogeneous intensity of ERG expression was present in over half of tumors from patients with neoadjuvant treatment but not in treatment naïve tumors, which may suggest effects of decreased/ dysregulated androgen signaling.
Except for a single case with discordant PTEN, the ERG/ PTEN status of the LN mets mirrored the primary dominant tumor.

892 Intestinal Metaplasia of the Bladder With Dysplasia: A Risk Factor for Carcinoma?

Jennifer Gordetsky, Jonathan Epstein. University of Alabama, Birmingham, AL; Johns Hopkins Hospital, Baltimore, MD.
Background: Intestinal metaplasia (IM) of bladder is a benign glandular proliferation where the urothelium becomes lined by mucin producing cells that resemble goblet cells of the intestinal tract. IM has been documented both in normal bladders and in association with adenocarcinoma of the bladder. Long-term follow-up studies have shown no association between IM and an increased risk for the development of adenocarcinoma. In rare cases, IM shows dysplastic changes like those seen in the gastrointestinal tract. These changes range from adenomatous low-grade dysplasia to high-grade dysplasia. Although IM has been well studied, the significance of IM with dysplasia is unknown.
Design: Consult cases between 2000 and 2014 which contained IM were prospectively selected for dysplastic features. Cases included bladder biopsies and resection specimens with and without concurrent carcinoma.
Results: We identified 20 cases of IM of the bladder with dysplasia, which included 17 males and 3 females, ages 31 to 85 years (mean 60). Five (25%) patients had chronic cystitis, 2 (10%) had neurogenic bladder, and one (5%) had a bladder diverticulum. Nine (45%) patients had a history of smoking. Twelve (60%) patients had low-grade dysplasia, characterized by elongated pseudostratified nuclei, mild nuclear atypia, and maintained cell polarity. Eight (40%) patients had high-grade dysplasia, which showed enlarged, hyperchromatic nuclei, prominent nucleoli, increased mitoses, and loss of polarity. Focal dysplastic changes were found in 8 (40%) patients and non-focal dysplasia was seen in 12 (60%) patients. IM with dysplasia was found with concurrent adenocarcinoma in 8 (40%) cases. Five of these patients (63%) had disease recurrence and 3 (38%) patients died from their disease. IM with dysplasia was found with concurrent urothelial carcinoma in one case. Eleven patients had IM with dysplasia without any evidence of malignancy on initial biopsy. Of these, ten had clinical follow-up. Of the patients who presented with IM with dysplasia without any evidence of malignancy on initial biopsy, one went on to develop noninvasive, high-grade papillary urothelial carcinoma. In no cases was persistent/recurrent dysplasia or progression to adenocarcinoma identified.
Conclusions: IM with dysplasia is associated with concurrent carcinoma of the bladder. There might be an increased risk for the development of subsequent carcinoma, especially in cases of non-focal, high grade dysplasia. Patients who are diagnosed with glandular dysplasia require a repeat biopsy and follow-up.

893 The Cost and Utility of Frozen Section During Partial Nephrectomy

Jennifer Gordetsky, Michael Gorin, Joe Canner, Mark Ball, Phillip Pierorazio, Mohamad Allaf, Jonathan Epstein. University of Alabama, Birmingham, AL; Johns Hopkins Hospital, Baltimore, MD.
Background: Current guidelines recommend partial nephrectomy (PN) as the treatment of choice for patients diagnosed with a small renal mass. Intraoperative frozen section (FS) of the resection bed margin is commonly performed during PN. We investigated the utility and cost of FS analysis performed during PN as well as its influence on intraoperative management.
Design: We performed a retrospective analysis of consecutive PN cases performed at the Johns Hopkins Hospital from 2010-2013. Frozen section margins were obtained by intraoperative biopsy of the nephrectomy bed. In some cases, the mass was sent for a FS to determine the type of tumor present. We evaluated the concordance between "FS diagnosis" and "FS control" and between "FS diagnosis" and the final specimen margin. Operative reports were reviewed for change in intraoperative management for cases with a positive FS diagnosis, or if the mass was sent for FS. The FS cost analysis utilized professional and technical component charge data provided by our institutional billing office. Cost was calculated from the average cost-to-charge ratio at Johns Hopkins Hospital, which is 0.798 of the billing fees.
Results: 576 intraoperative FS were performed in 351 cases to assess the tumor bed margin, 19 (5.4%) of which also had a mass sent for FS to assess the tumor type. The concordance rate between our "FS diagnosis" and the "FS control" was 98.3%. There were 30 (8.5%) final positive specimen margins, 17 (4.8%) of which were RCC. Of the 30 cases with a final positive specimen margin, 9 (30%) were called positive, 4 (13.3%) "atypical" and 17 (56.7%) negative on FS diagnosis. Intraoperative management was influenced in 6 of 9 cases with a positive FS diagnosis and in 1 of 9 cases with a FS diagnosis of "atypia". 4 of 9 (44.4%) cases with "atypia" on FS diagnosis had a final positive specimen margin. The total cost for FS over three years was $110,089.
Conclusions: In summary, the FS diagnosis is extremely accurate in PN cases. "Atypia" on FS diagnosis should not be considered the same as "benign" as 44% of these cases had a final positive margin. Although FS diagnosis is highly accurate, up to 5% of final specimen margins may be falsely considered negative based on intraoperative biopsy. Although the cost of a FS is low, the relatively high false negative rate and inconsistency in influencing intraoperative management, argues against the routine use of FS in PN cases.

894 Initial Prostate Biopsy Diagnosis of HGPIN Versus ASAP: Implications for Repeat Biopsy Findings

Kashika Goyal, Joshua Ebel, Soud Sediqe, Debra Zynger. Ohio State University, Columbus, OH.
Background: A follow-up needle core prostate biopsy may be indicated following an initial prostate biopsy. As extended prostate biopsies are routine and immunohistochemistry is frequently employed, the current diagnostic implications of an initial biopsy on the findings in repeat biopsies need to be evaluated. The purpose of our study was to correlate diagnoses identified in initial extended prostate biopsies with diagnoses in subsequent extended biopsies in the setting of a single institution.
Design: 1,489 men who underwent transrectal ultrasound-guided prostate needle core biopsies from 2008-2013 were retrospectively evaluated to identify individuals with at least two biopsies during this time period. Procedures were performed at our tertiary care institution with subspecialized genitourinary pathology sign-out. Initial and repeat biopsies were classified based on the most aggressive diagnosis in the case: 1) carcinoma, 2) HGPIN+ASAP, 3) HGPIN, 4) ASAP, or 5) negative. Clinically insignificant cancer was defined as Gleason score ≤6, £2 cores with carcinoma, ≤50% tumor in each core, and unilateral cancer. Statistical analysis was performed using the Fisher Exact test.
Results: 189 men underwent 1 or more follow-up prostate biopsies during the study period. Diagnoses of HGPIN+ASAP, HGPIN, ASAP, and negative had similar rates of cancer in repeat biopsies (p=1). An initial diagnosis of HGPIN and HGPIN+ASAP had a less frequent negative follow-up biopsy than ASAP, although the difference was not statistically significant (p=0.16). Immunostains (AMACR/HMWK/p63) were used in 87.0% cases with an initial diagnosis of ASAP and HGPIN+ASAP, higher than the other diagnostic categories (p<0.001, p=0.008 respectively). Patients initially diagnosed with carcinoma did not have cancer in 27.9% of follow-up biopsies. Of the 54 men with initially insignificant cancer, 35.2% did not have tumor in the repeat biopsy, 37.0% remained insignificant, and 27.8% transitioned to significant carcinoma.

	Follow-up Diagnosis		
Initial Diagnosis	Carcinoma	HGPIN, ASAP or HGPIN+ASAP	Negative
Carcinoma	72.1%	9.3%	18.6%
HGPIN+ASAP	37.5%	25.0%	37.5%
HGPIN	33.3%	50.0%	16.7%
ASAP	33.3%	13.3%	53.3%
Negative	36.8%	10.3%	52.9%

Conclusions: In our investigation, a prostate biopsy diagnosis of HGPIN or ASAP had a similar rate of cancer upon follow-up. Our data does not support utilizing a less stringent follow-up protocol for an initial diagnosis of HGPIN versus an initial diagnosis of ASAP.

895 Urologist's Impact on Extended Needle Core Prostate Biopsy Histopathologic Variables Within a Single Institution

Kashika Goyal, Joshua Ebel, Soud Sediqe, David Sharp, Debra Zynger. Ohio State University, Columbus, OH.

Background: Prostate needle core biopsy is a critical procedure to diagnose and manage prostatic adenocarcinoma. However, there is a lack of understanding of how the submitting urologist impacts histopathologic metrics. Our study aimed to elucidate the relationship between submitting urologist, number of containers in which cores are submitted, longest core length, total core length, and individual core length threshold values on cancer detection rate per case within extended core biopsies.

Design: A retrospective search was performed to identify pathology reports from patients who had an extended transrectal ultrasound guided prostate needle core biopsy at our institution between 2008-2013. Reports were analyzed for submitting urologist, number of containers submitted, total number of cores, individual core lengths, and diagnosis of cancer within a case. Within the time period of the study, 1 urologist decreased the number of submitted containers from 12-14 to 6-9 for the sole purpose of reducing patient expenditures, with no other changes to his biopsy strategy. Results from these 2 subgroups were compared. Statistical analyses were performed using the Kruskal-Wallis test, Wilcoxon rank sum test, and logistic regression.

Results: 1,262 prostate biopsies included in this 5 year study were submitted by 13 urologists. Total core length (mean 12.8-23.1 cm, $p<0.001$) and longest core length (mean 1.7-2.2 cm, $p<0.001$) significantly varied by submitting urologist but these variables did not impact cancer detection rate per case ($p=0.97$, $p=0.26$, respectively). The number of individual cores that met threshold values of 0.5 cm ($p<0.001$), 1.0 cm ($p<0.001$), and 1.5 cm ($p<0.001$) significantly varied between urologist, although there was no correlation between these threshold values and cancer detection ($p=0.75$, $p=1.0$, $p=0.47$, respectively). Container number differed significantly between urologists ($p<0.001$) but did not correlate with cancer detection ($p=0.13$). For the single urologist with a change in his submission protocol during the study period, the cancer detection rate was no different comparing 12-14 containers versus 6-9 containers ($p=0.64$).

Conclusions: Submitting urologist significantly impacts variables including number of containers in which cores are submitted, total core length, longest core length, and number of cores meeting threshold values. However, these variables did not impact overall cancer detection per case. Reduction of the number of containers utilized in prostate biopsy submission may be an opportunity for cost control.

896 Characterization of Renal Epithelial Neoplasms Arising in Non-Functioning Kidneys – A Study of 259 Cases

Rajen Goyal, Xiaoqi Lin, Ximing Yang. Northwestern University, Feinberg School of Medicine, Chicago, IL.

Background: Non-functional kidneys due to various causes show different histopathologic features. Studies on renal cell cancer (RCC) incidence and types using current classification in various types of non-functioning kidneys are limited. Our study documents tertiary hospital experience on tumor incidence, risk and subtype in various types of non-functioning kidneys such as acquired cystic disease (ACD), end stage renal disease (ESRD), adult polycystic kidney disease (APKD), transplant nephrectomies (TN; failed transplants) and obstructive/inflammatory conditions (OBS; stones, pyelonephritis, hydronephrosis) over 5 years.

Design: Over 2009-2014, 259 of 886 nephrectomies were grouped into 5 types of non-functional kidneys based on clinicopathologic features: 40 ACD, 50 ESRD, 36 APKD, 95 TN and 38 OBS. Medical records, gross and histologic features were reviewed. Dialysis history was documented. Tumor incidence and risk were calculated and statistical analyses were performed.

Results:

Disease	ACD (40)	ESRD(50)	APKD (36)	TN (95)	OBS (38)
Cancer incidence	70%	44%	3%	0	5%
Dialysishistory	65% (26)	44% (22)	36% (13)	NS	NS
Mean dialysis duration (months)	82.5	22.6	24.3	NS	NS
Clearcell RCC (CCRCC)	8	9	0	0	1
PRCC	10	9	1	0	0
Clearcell PRCC (CCPRCC)	10	1	0	0	0
ACD-RCC	6	0	0	0	0

*NS: Not significant

ACD and ESRD combined had the highest cancer incidence and comprised almost all of the cancers seen (53/55 cancers, 96%; Chi^2 is 117; $P<0.001$). The risk of cancer development in ACD and ESRD together is 110 times that of the other groups combined ($P<0.0001$). PRCC and CCRCC were two common RCC types in ACD and ESRD. ACD-RCC and CCPRCC were seen mainly in ACD and this likely explains why ACD had a greater cancer incidence than ESRD ($P=0.018$). ACD had a stronger association with dialysis ($P=0.028$) and had a significantly longer mean dialysis duration than ESRD and APKD ($P=0.001$).

Conclusions: 1) ACD and ESRD had the highest cancer incidence and risk. **2)** PRCC and CCRCC were the most frequent tumors in ACD and ESRD combined. **3)** ACD had the strongest association with dialysis and longest mean dialysis duration. ACD-RCC was only seen in ACD as expected. Dialysis may be related to formation of cysts, tumor precursor lesions and subsequent cancers such as ACD-RCC. **4)** CCPRCC was more frequent in ACD. This may be related to dialysis and cysts, but CCPRCC also arises in normal kidneys.

897 The Utility of STAT6 Expression in the Differential Diagnosis of SFT Vs Stromal Prostatic Neoplasms

Gunes Guner, Justin Bishop, Stephania Bezerra, David Zahavi, Maria Angelica Mendoza Rodriguez, Rajni Sharma, Jonathan Epstein, George Netto. Johns Hopkins Hospital, Baltimore, MD.

Background: The diagnosis of solitary fibrous tumor (SFT) in the prostate can be challenging on a small biopsies. Prostatic stromal tumors of unknown malignant potential (STUMP) and SFT may share some overlapping morphologic features and both express CD34. *NAB2-STAT6* gene fusions have recently been identified in SFT of various sites, the fusion leads to nuclear translocalization of the STAT6 protein. Immunohistochemical nuclear staining of the STAT6 antibody is now considered an adjunct for the diagnosis. We evaluated the utility of STAT6 immunostain in the differential diagnosis of SFT vs stromal lesions of the prostate.

Design: A total of 31 cases (11 needle biopsies, 13 RRP and 7 TURP) were retrieved from our surgical pathology and consultation archives (1995-2014). They included 15 STUMP, 11 SFT, 4 low grade prostatic stromal sarcomas. Sections were stained with polyclonal STAT6 antibody (Santa Cruz, S20, 1:100). Only unequivocal nuclear staining (with or without cytoplasmic staining) was considered positive. Cases with "background" nuclear staining in glandular epithelium or lymphocytes were excluded from the analysis.

Results: All 9 evaluable SFT cases demonstrated nuclear STAT6 positivity. None of 10 evaluable STUMP cases had nuclear staining (see Table 1). All of the four low grade stromal sarcomas of the prostate were STAT6 negative.

STAT6 status	SFT	STUMP	Stromal sarcoma
Positive	9	0	0
Negative	0	10	4

Conclusions: STAT6 is a useful marker in the differential diagnosis of SFT vs stromal prostatic tumors that will complement existing morphologic and immunohistochemical criteria for the diagnosis of mesenchymal lesions of prostate.

898 Gene Expression Profile of Micropapillary Bladder Cancer

Charles Guo, Tadeusz Majewski, Vipulkumar Dadhania, Daniel Willis, Maciej Sykulski, Weronika Wronowska, Ashish Kamat, Woonyoung Choi, David McConkey, Colin Dinney, Anna Gambin, Bogdan Czerniak. University of Texas MD Anderson Cancer Center, Houston, TX; University of Warsaw, Warsaw, Poland.

Background: Micropapillary urothelial carcinoma (MPUC) is a distinct variant of bladder cancer characterized by unique microscopic features and aggressive clinical behavior. Our recent whole genome analyses have identified two major molecular phenotypes of conventional invasive bladder urothelial carcinoma (UC) defined as basal and luminal subtypes. To better understand the biology of MPUC, we analyzed its gene expression profile in the context of molecular subtypes of UC.

Design: UC tissue samples, including conventional UC (n=110) and MPUC (n=41), were microdissected from formalin fixed paraffin embedded tissue blocks. All UCs were high grade and invasive. RNA was extracted and analyzed by direct hybridization on Illumina HT-12v4 DASL chips. Array data was subject to a supervised hierarchical cluster analysis. Luminal and basal subtypes were determined using previously reported analytical algorithms.

Results: Patients' demographic and pathologic features were summarized in [table1].

Table 1. Demographic and pathologic features of patients with bladder urothelial carcinomas

UC	Mean age (range)	Sex (M:F)	pT1	pT2	pT3	pT4	Total
Conventional	68 (32-90)	83:27	2	23	63	17	110
MPUC	70 (46-89)	36:5	2	12	20	7	41

Gene expression analysis demonstrated that a large number of genes were differentially expressed between MPUC and conventional UC. The differentially expressed genes were most commonly involved in the p53, ERK, and mTOR signaling pathways. A panel of top 20 differentially expressed genes, including HIST1H2BM, EFNB1, TRIM14 among others, distinguished MPUC from conventional UC with a positive predictive value of 95.1%. Conventional UC could be separated into luminal subtype (52%) (57/110) and basal subtype (48%) (53/110). In contrast, 93% (38/41) of MPUC were of luminal phenotype, which was significantly higher than that in conventional UC ($p<0.0001$), and only 7% (3/41) were basal subtype.

Conclusions: MPUC demonstrates a unique gene expression pattern that differs from conventional UC. A number of genes in key oncogenic pathways are differentially

expressed in MPUC and conventional UC. Furthermore, MPUC exhibits a significantly higher frequency of luminal genomic subtype than conventional UC. The distinct gene expression of MPUC may contribute to its aggressive clinical behavior.

899 Histopathologic Characterization of High Grade Neuroendocrine Carcinoma of the Bladder Treated By Cystectomy: A Comparison To Typical Urothelial Carcinoma

Sounak Gupta, Prabin Thapa, Loren Herrera Hernandez, Rafael Jimenez, Robert Thompson, Igor Frank, Stephen Boorjian, Brian Costello, John Cheville. Mayo Clinic, Rochester, MN.

Background: In our referrel practice, 45% of small cell carcinomas are diagnosed as typical urothelial carcinoma (UC) prior to secondary review. The appropriate diagnosis is critical as patients with small cell carcinoma have a significantly improved outcome with adjuvant chemotherapy in combination with cystectomy. The objective of this study was to characterize the histopathologic features of a large series of small cell carcinomas (high grade neuroendocrine carcinomas- HGNE Ca) treated by cystectomy matched to patients with UC.

Design: 79 patients with HGNE Ca were matched with 123 patients with UC treated by radical cystectomy between 1987 and 2014. Morphometric analysis was performed using the cellSens software (Olympus). Tissue microarrays were constructed using 4, 1.0mm cores each. These were immunostained for neuroendocrine markers (chromogranin, synaptophysin, CD56, NSE, TTF1), cell-cycle regulators (p16, p53, p63, c-Myc, CyclinD1) as well as CK20 and targeted therapy-related markers (CD117, HER2). Ki67 assessed proliferation rates. Cancer specific survival (CSS) was estimated by the Kaplan-Meier method and compared with the log rank test.

Results: The mean nuclear size (3443 relative pixel units (rpu), range, 1844 to 6405 rpu) in HGNE Ca was significantly smaller than UC (4031 rpu, range, 1828 to 8965) (p<0.001). HGNE Ca originally diagnosed as UC had a significantly larger mean cell size (3687 rpu, range, 1934 to 6405 rpu) than tumors originally classified as small cell carcinoma (3217 rpu, range, 1844 to 4474 rpu) (p<0.05). The sensitivity and specificity for the neuroendocrine markers were as follows: chromogranin-76%, 100%; synaptophysin-92%, 98%; CD56-92%, 96%; NSE-100%, 22% and TTF1-54%, 97%. HGNE showed significantly higher expression compared to UC of p16 and CD117 and lower expression of CK20, p63, c-Myc, cyclin D1 and HER2 (all p values < 0.001). Ki67 proliferative index was significantly higher in HGNE Ca compared to UC (p<0.0001).

Conclusions: Morphometric studies indicated nuclear size variation of HGNE Ca overlapping with UC supporting the terminology of high-grade neuorendocrine carcinoma rather than small cell carcinoma. Immunostains can be helpful in the separation of HGNE Ca and UC particularly in HGNE Ca with larger cell size.

900 Primary Renal Leiomyoma and Leiomyosarcoma: An Analysis of 61 Cases

Sounak Gupta, Rafael Jimenez, Andrew Folpe, John Cheville. Mayo Clinic, Rochester, MN.

Background: Primary renal leiomyomas (RLM) and renal leiomyosarcomas (RLMS) are rare and poorly characterized, in particular RLM. We studied the clinicopathological features of a series of RLM and RLMS.

Design: Available slides and blocks from 61 renal smooth muscle tumors (23 RLM, 38 RLMS) were retrieved. Criteria were: RLM- circumscribed, no atypia, few if any mitotic figures, no necrosis; RLMS- some combination of these features. Tissue blocks from 19 RLM and 24 RLMS were used to construct a tissue microarray with 5 representative 2.0mm cores from each case. TMAs were stained for smooth muscle actin (SMA), desmin, h-caldesmon, calponin, myogenin,HMB45, Melan A, cytokeratin (OSCAR), CD117, Ki67, estrogen receptor (ER) and progesterone receptor (PR). The French Federation of Cancer Centers (FNCLCC) grading system was used. Follow up was available for 14 RLM (mean: 71 months, range 11 to 226 months) and 20 RLMS (mean: 45 months, range 2 to 138 months).

Results: RLM occurred in 22F (96%) and in 1 M (4%) with a mean age of 57 years (range 28-75 years). RLMS occurred in 22F (58%) and 16M (42%) with a mean age of 61 years (range 24-81 years). The majority of RLM and RLMS arose from the renal capsule (RLM: 20/23 cases, 88%; RLMS: 22/38 cases, 58%) with only a small fraction arising from the renal parenchyma (RLM: 0 cases; RLMS: 6 cases, 15%). RLM were small (mean size, 3.9cm, range, 0.3 to 20cm). In contrast, RLMS were large (mean size, 9.8cm, range, 2 to 25.5cm), exhibited necrosis in 30 (79%) cases, showed increased cellularity, and had a mean mitotic count of 7/10 hpf (range 0 to 36/10 hpf). RLMS were grade 1 in 7 cases (18%), grade 2 in 27 cases (71%), and grade 3 in 4 cases (11%). All RLM uniformly expressed all smooth muscle markers. RLMS, in contrast, were more variable with expression of these markers (SMA: 23/24, 96%; desmin: 20/24, 83%; h-caldesmon: 19/24, 79%; calponin: 24/24, 100%). RLM were estrogen and progesterone receptor positive in 17/19 (90%) of cases in contrast to RLMS (8/24, 33% ER positive; 9/24, 38% PR positive). In addition RLMS showed a significantly higher Ki67 proliferative rate than RLM(p<0.0001). Follow-up (14 RLM, 20RLMS): RLM- no recurrences or metastases; RLMS- metastases in 14 (70%) and death from disease in 7 (35%).

Conclusions: The criteria listed above reliably separate RLM from RLMS. RLM typically in occur in women, express hormone receptors and have benign outcomes. In contrast, RLMS show equal gender distribution, lack hormone receptor expression, and have significant potential for adverse patient outcome, with death from disease in 35% of patients.

901 The Role of TXNDC5 in Castration Resistant Prostate Cancer – Involvement of Androgen Receptor Signaling Pathway

Bo Han, Lin Wang, Guanhua Song, Weiwei Tan, Mei Qi, Zhiyan Liu. Shandong University Medical School, Jinan, Shandong, China; Shandong Academy of Medicinal Sciences, Jinan, Shandong, China; Institute of Basic Medicine, Jinan, Shandong, China.

Background: Castration-resistant prostate cancer (CRPC) continues to be a major clinical problem and the mechanisms behind it remain unclear. Thioredoxin domain containing protein 5 (TXNDC5) is involved in protein folding and chaperone activity and its overexpression has been reported in multiple malignancies. However, the exact role of TXNDC5 in CRPC has not yet been investigated so far.

Design: TXNDC5 expression was validated in PCa tissues by immunohistochemistry. Gain- and off- functional experiments were designed to characterize the biological activities of TXDNC5 in PCa *in vitro* and *in vivo*, especially in CRPC. Co-IP and mass spectrometry were utilized to identify TXNDC5-interacting proteins. Real time PCR, western blot, and luciferase reporter gene assay were applied to evaluate the effects of TXDNC5 on androgen receptor signaling.

Results: TXNDC5 is up-regulated following long-term androgen-deprivation treatment (ADT) and highly overexpressed in CRPC tumors compared to hormone-naive PCa cases. Functionally, *in vitro* and *in vivo* studies demonstrated that TXNDC5 overexpression promotes the growth of both androgen-dependent and castration-resistant PCa xenografts.

Figure 1

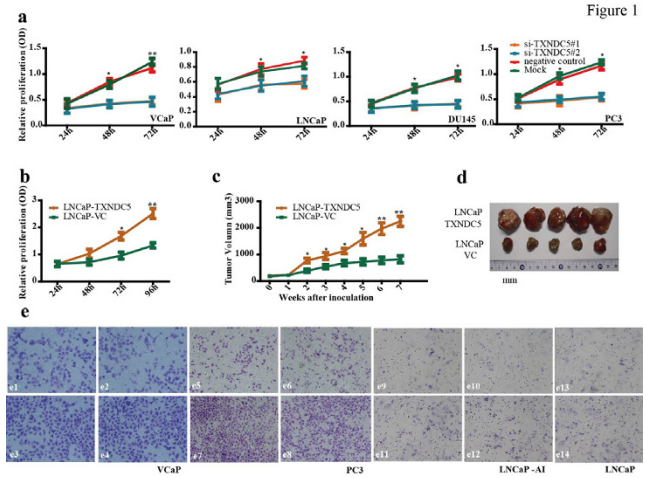

Mechanistically, TXNDC5 directly interacts with the AR protein to increase its stability and thus enhances its transcriptional activity. TXDNC5-mediated CRPC growth can be fully abolished by AR inhibition, suggesting TXDNC5 up-regulation as an escape pathway for aberrant AR re-activation.

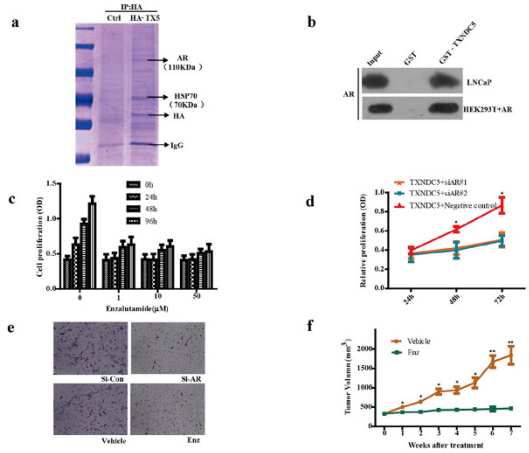

Further, TXNDC5 expression is induced by ADT-induced hypoxia through HIF-1α in a miR-200b dependent manner.

Conclusions: Overall, we defined an important role of TXNDC5 in CRPC development. Further investigations are needed to screen TXNDC5 antagonists as novel therapeutic approaches to treat CRPC patients.

902 Primary Mucinous Adenocarcinoma of the Female Urethra

Saul Harari, Liang Cheng, Adeboye Osunkoya. Emory University School of Medicine, Atlanta, GA; Indiana University School of Medicine, Indianapolis, IN.

Background: Primary adenocarcinoma of the female urethra is rare and may lead to both diagnostic and nosologic challenges. The confluence of multiple adjacent organ systems in this region, including the bladder, genital tract and colorectum, makes it imperative to rule out metastasis or direct extension of adenocarcinomas from other sites. Although primary mucinous adenocarcinoma of the prostatic urethra has been well characterized in men, this is the largest study to date of primary mucinous adenocarcinoma of the female urethra.

Design: A search was made through the surgical pathology and expert consultation files of two academic institutions for cases of confirmed primary mucinous adenocarcinoma arising from the female urethra. Only cases with available tissue blocks were selected. Tumors arising from adjacent organs were excluded both clinically and pathologically in all cases. Clinicopathologic data was obtained. Immunohistochemical stains for GATA3, p63, CK7, CK20 and CDX2 were performed on all cases.
Results: Five cases were identified. The mean patient age was 67 years (range: 54-74 years). Three of the patients presented with urinary retention/incomplete voiding and one of the patients presented with a mass prolapsing through the meatus. All of the tumors were comprised of adenocarcinomas with associated dissecting pools of mucin. Associated signet ring cells were present in 1/5 (20%) cases. Adjacent/overlying urethritis cystica et glandularis, intestinal type, was present in all cases. Pathologic stages were as follows; pT4 3/5 (60%) cases; pT3 1/5 (20%) cases and pT2 1/5 (20%) cases. Immunohistochemical stains were positive in the tumor cells for CDX2 in 4/5 (80%) cases; focally positive for CK20 in 4/5 (80%) cases; focally positive for CK7 in 4/5 cases (80%) and negative for p63 and GATA3 in all cases. In patients with available follow up data, mean follow up was 25 months (range: 4 - 54 months).
Conclusions: We present the largest series to date of primary mucinous adenocarcinoma of the female urethra. These rare tumors are aggressive and present at a locally advanced stage. The majority of tumors had overlapping immunohistochemical profile with enteric tumors which may be a potential diagnostic pitfall, in view of the fact that these tumors are negative for GATA3 and p63. It is critical for pathologists to be aware of this entity in light of potential prognostic and therapeutic implications of misdiagnosis.

903 Intraductal Carcinoma of the Prostate: Interobserver Reproducibility Survey of 39 Urologic Pathologists

Nicholas Harding-Jackson, Lars Egevad, Jun Ma, David Bostwick, Kenneth Iczkowski. The Medical College of Wisconsin, Milwaukee, WI; Karolinska Institutet, Stockholm, Sweden; Bostwick Laboratories, Orlando, FL.

Background: The diagnosis of intraductal carcinoma of the prostate (IDC) remains subjective, as 3 sets of diagnostic criteria are in use. Given the uncertainty of the histologic features and its clinical importance, we assessed the interobserver reproducibility of an IDC diagnosis, and correlated IDC consensus with histologic findings.
Design: An internet survey was compiled from 38 photomicrographs showing duct proliferations: 14 signed out as high-grade prostatic intraepithelial neoplasia (HGPIN), 17 IDC, and 7 invasive cribriform/ductal carcinoma. Presence of 9 histologic criteria ascribed to IDC was assessed for each image, and 39 urologic pathologists rendered their diagnoses: benign, HGPIN, borderline between HGPIN and IDC, IDC, or invasive carcinoma.
Results: Agreement with original diagnoses was 70% for HGPIN, 73% for invasive carcinoma, but 43% for IDC ($p<0.001$, chi-square). Respondents considered 19 of 38 (50%) cases as IDC candidates, of which 5 (26%) had a two-thirds consensus for IDC; two-thirds consensus for either borderline or IDC was reached in 9 (47%). The remaining 19 of 38 cases attained consensus for HGPIN or invasive carcinoma. Across all diagnoses, findings differing significantly included lumen-spanning neoplastic cells, 2x benign duct diameters, duct space contours, papillary growth, dense cribriform or solid growth, and comedonecrosis. Features that most often precluded an IDC consensus included: only loose cribriform growth (5/19), central nuclear maturation—shrinkage of central nuclei (5/19), or comedonecrosis (3/19). By multivariate analysis, only one of the nine histologic criteria retained significant correlation with a consensus diagnosis of IDC: the presence of solid areas ($p=0.038$). Rare exceptions to the rule of 2x duct enlargement were noted. 20.5% of respondents agreed that an isolated diagnosis of IDC on needle biopsy warrants definitive therapy, 20.5% disagreed, and 59.0% considered the decision to depend upon clinicopathologic variables.
Conclusions: Reproducibility of IDC diagnosis is not strong. We propose the following criteria: a lumen-spanning proliferation of neoplastic cells in pre-existing ducts, with a dense cribriform or partial solid growth pattern. Solid growth, in any part of the duct space, emerges as the most reproducible finding to rule in a diagnosis of IDC. Comedonecrosis is rarer, but in the absence of solid/dense cribriform growth, should also rule in IDC.

904 PAX8 and GATA3 Immunophenotypes in Upper Tract Urothelial Carcinoma (UC): Emphasis on Variation By Anatomic Site and in Histologic Variants

Holly Harper, Cristina Magi-Galluzzi, Jesse McKenney. Cleveland Clinic, Cleveland, OH.

Background: Immunohistochemistry is often utilized to evaluate renal based neoplasms that undergo needle biopsy sampling, particularly for the distinction of renal cell carcinoma from other carcinomas, such as UC. Only limited data regarding the immunohistochemical profile of upper tract UC is available, especially in histologic variants at this site.
Design: We evaluated 59 UTUC from 58 patients (one with synchronous bilateral tumors). The tumor morphology of these 59 cases was reviewed and each was analyzed for expression of PAX8 (Protein Tech Group; polyclonal) and GATA3 (BioCare; L50-823) by immunohistochemistry. Results were considered positive if the intensity of nuclear staining matched that of the internal control in any focus. Typical and variant UC morphology was scored separately for each case.
Results: Patients had a mean age of 68.6 years (range of 41 to 94). 37 patients were male, while 21 were female. GATA3 expression was identified in all tumors, but PAX-8 expression by site was: renal pelvis: 15/30 (50%), ureter: 8/20 (40%), and involving both: 2/9 (22%). Eight histologic variants were identified: glandular (1), chordoid/myxoid (1), plasmacytoid (1), sarcomatoid (2), undifferentiated (1), squamous (1), and micropapillary (1). GATA-3 expression was retained in all variant patterns, but was only focal in 1 sarcomatoid and 1 glandular UC. PAX-8 staining was present in only 3 (38%) of the variant patterns: 1 chordoid/myxoid and 2 sarcomatoid.
Conclusions: GATA3 shows strong and diffuse staining in the majority of upper tract UC, including both invasive and non-invasive components, but may be more focal in histologic variants. PAX8 showed immunoreactivity in 42% of cases and was more common in the renal pelvis (50%). Although PAX-8 expression was often lost in variant patterns of UC, it was maintained in both sarcomatoid UCs, underscoring the need for caution in the distinction from sarcomatoid renal cell carcinoma.

905 Upper Tract Urothelial Carcinomas (UTUC): Frequency of Association With Microsatellite Instability and Lynch Syndrome

Holly Harper, Jesse McKenney, Thomas Plesec, Cristina Magi-Galluzzi. Cleveland Clinic, Cleveland, OH.

Background: Increased risk for UTUC is described in patients with Lynch syndrome (LS), caused by mutations in mismatch repair (MMR) genes. We aimed to identify the frequency of MMR protein loss in UTUC and its potential for identifying an association with LS.
Design: We queried our institution database to identify UTUC excised between 1995 and 2014. Cases were then cross-referenced for patients with history of colorectal adenocarcinoma (CRC) to enrich for potential LS. Tumor histopathologic characteristics were reviewed and each case was analyzed for loss of MMR proteins (MMRP), MLH-1, MSH-2, MSH-6 and PMS-2 by immunohistochemistry (IHC).
Results: Of the total 482 patients with UTUC, a subset of 58 (encompassing 8 patients with UTUC and CRC) were included in this study. Of the 8 patients with UTUC and CRC, 3 had documented LS, 1 had uterine cancer, 1 had ampullary adenocarcinoma and 4 had bladder carcinoma. Patients mean age was 69 years (range 41-94); 37 were male and 21 female. One patient had synchronous bilateral UTUC. Twenty (34%) UTUC involved ureter (UUC), 30 (51%) renal pelvis (RPUC), and 9 (15%) both (U+RPUC). Loss of MMRP expression or high-level microsatellite instability (MSI-H) was identified in 6/59 (10%) tumors in 58 patients: 3 UUC and 3 RPUC. Patients with MSI-H had age range from 45 to 90 years (mean: 75). MSI-H cases demonstrated loss of MSH-2 and MSH-6, but retained MLH-1 and PMS-2 expression. All MSI-H cases were high-grade with no pleomorphism or variant histology and showed pushing borders without destructive infiltrative edges; 2 were stage Ta, 4 T1-T3. Intratumoral lymphocytes (ITL) were often identified in 2 (33%) MSI-H UTUC, but in none of the cases with retained MMRP expression. Four MSI-H tumors occurred in patients with CRC, including all 3 with LS and one with CRC and ampullary cancer. Neither of the other 2 MSI-H cases had Lynch-associated neoplasms.
Conclusions: MSI-H was identified in 4% of the consecutive UTUC series and in 50% of the selected group with CRC (including 3 confirmed LS) suggesting a potential role in identifying syndromic association. Lack of nuclear pleomorphism, presence of pushing borders without destructive infiltrative edges and ITL may help identify potential MSI-H UTUC cases.

906 Mapping of Urothelial Carcinoma in Radical Cystectomy Specimens

Muhannad Hassan, Eric Belanger, Kien Mai. Ottawa Hospital and Ottawa University, Ottawa, ON, Canada.

Background: Urothelial carcinoma (UC) is commonly a multifocal disease with superficial spread of the disease by tumor soil-seeding mechanism and field effect. Topographic study of urothelial neoplastic lesion may elucidate the histopathogenesis of multifocality, tumor spread into prostate, urethra, ureters, tumor recurrence and progression.
Design: Consecutive specimens of radical cystectomy for UC without extensive squamous or glandular differentiation and without pre-operative treatment with radiotherapy. The specimens were bisected in horizontal plane at the middle portion of the urinary bladder (UB). The specimens were fixed without tissue stretching in 10% buffered formalin for at least 24 hours. The UB (still attached to prostate or uterus) were serially sectioned in the same horizontal plane from the UB neck to the dome into rings of 5-10 mm thickness. The sections were orderly arranged and photographed. Four to six rings of tissue with at least two rings through the main lesion, and one ring each below and above the lesion of interest were entirely submitted. Additional sections of areas of interest or representative areas, ureters and entire prostate were also submitted. Clinical charts and microscopic slides were reviewed.
Results: Fifty UC specimens were comprised of 39 from men and 11 from women (9 for superficial UC and 41 for muscle invasive UC). UC were associated with satellite urothelial neoplastic lesions in 72%, ipsilateral ureteral, controlateral ureteral, and prostatic involvement in 16, 4 and 10% of cases respectively. Within the urinary bladder, satellite urothelial neoplastic lesions in areas of less than 3 cm, and more than 3 cm were identified in 16, and 7% of cases. In 84% of cases, satellite neoplastic lesions tend to decrease in size as they become more distant from the main lesion.
Conclusions: The topographic distribution of neoplastic urothelial lesions appears to be random as seen in field effect in a small number of cases. In a majority of cases, satellite multiple neoplastic lesions were in the vicinity of the main lesion, suggestive of soil-seeding phenomenon.

907 Prostate Cancer Grade Is Associated With TMPRSS2-ERG and ERG mRNA Overexpression Assessed By qRT-PCR

Silvia Hernandez, Alba Font, Silvia de Muga, Nuria Juanpere, Marta Lorenzo, Sergio Serrano, Josep Lloreta. Universitat Pompeu Fabra, Barcelona, Spain; Hospital del Mar – Parc de Salut Mar – IMIM, Barcelona, Spain; Autonomous University of Barcelona, Barcelona, Spain.

Background: There are limited studies on the effects of the different expression levels of both the *TMPRSS2-ERG* fusion and *ERG* gene. In addition, the differential effects of the many different types of *TMPRSS2-ERG* fusion transcript variants have received little attention in the literature. *ERG* rearrangements and *PTEN* loss are frequent and associated events in prostate cancer progression. The aim of the present study has been to investigate the effect of the quantitative differences in *TMPRSS2-ERG* and *ERG* expression, as well as their association with *PTEN* loss, in prostate cancer.

Design: RNA was extracted in 83 PrCa and 3 normal prostate samples (Parc de Salut MAR Biobank, Barcelona, Spain). Quantitative mRNA levels of *TMPRSS2-ERG*, *ERG,* and *PTEN* were analyzed by qRT-PCR (Applied Biosystems, Foster City, CA, USA). The cDNA from the *TMPRSS2-ERG* cases was, in addition, amplified by RT-PCR and sequenced (Big Dye Terminator Kit v.3.1) to identify the rearrangement variants. The intensity of ERG immunostaining was assessed in a series of matched FFPE (n = 57) prostate tumors.

Results: There were no statistical differences in the prevalence of the different rearrangement variants with regard to tumor grade. *TMPRSS2-ERG* and *ERG* mRNA overexpression were found in 57 and 54 tumors, respectively. Among the *TMPRSS2-ERG* positive cases, high rearrangement levels (2+) were found in 37.2% of GS ≤ 7 and in 71.4% of GS ≥ 8 tumors (p= 0.025). *ERG* mRNA overexpression was found in 36.5% of GS ≤ 7 and in 60% of GS ≥ 8 prostate tumors (p= 0.047). High levels of *ERG* overexpression (2+) were found in 56% of GS ≤ 7, and in 92.3% of GS ≥ 8 (p= 0.02) prostate tumors. Decreased *PTEN* expression was detected in 28 tumors (39%) and was more frequent in cases with *TMPRSS2-ERG* rearrangement (p= 0.01) and with *ERG* mRNA overexpression (p= 0.003). Loss of *PTEN* expression was associated with GS ³ 7 prostate tumors (p= 0.041). Concurrent *TMPRSS2-ERG*and *PTEN* loss (p= 0.04), and *ERG* overexpression and *PTEN* loss (p= 0.04) were also associated with GS ³ 7.

Conclusions: Rather than the mere detection of the fusion and its ERG product, it is the expression levels of *TMPRSS2-ERG* and *ERG* mRNA, as well as the concurrent loss of *PTEN* expression, what is related with adverse histology in prostate cancer. Quantitative assessment of *TMPRSS2-ERG* rearrangement or *ERG* mRNA constitute potential molecular markers of prostate cancer progression.

908 Biphasic Squamoid Alveolar Renal Cell Carcinoma Is Probably Part of the Spectrum of Papillary Renal Cell Carcinoma: Clinicopathologic, Immunohistochemical and Molecular Genetic Analysis of 22 Cases

Ondrej Hes, Enric Condom-Mundo, Jose Lopez, Kvetoslava Peckova, Petr Martinek, Pavla Rotterova, Giovanni Falconieri, Abbas Agaimy, Stela Bulimbasic, Ivan Damjanov, Milan Hora, Michal Michal. Charles University and Charles University Hospital, Plzen, Czech Republic; Bellvitge University Hospital, Barcelona, Spain; Cruces University Hospital, Barakaldo, Spain; Policlinico di Cattinara, Trieste, Italy; University Hospital of Erlangen, Erlangen, Germany; University Hospital Dubrava, Zagreb, Croatia; Kansas University, Kansas City, KS.

Background: Biphasic squamoid alveolar renal cell carcinoma (BSARCC) has been described recently. We collected 22 cases from 11 institutions and further examined this unusual entity.

Design: Tumors were examined using routine histology, immunohistochemistry, arrayCGH and confirmatory FISH.

Results: Patients were 13 males, 9 females, age range 41-79 years (mean 59.9, median 58.5 years). Size of tumors ranged from 1.5 to 16 cm (mean 4.84, median 2.8 cm). Follow up was available for 15 patients, range 0.6-8 years, metastatic spreading was confirmed in 4 cases (26%).

13 tumors were arranged in solid and alveolar patterns. The tumors were composed of a dual cell population: small low-grade neoplastic cells with clear to eosinophilic cytoplasm and large, high-grade squamoid cells forming round solid islands. In 9 tumors a transition was seen from papillary areas containing groups of large squamoid cells to a fully developed solid-alveolar pattern. Necrosis was noted in 3/22 and emperipolesis in 20/22. Immunohistochemically 22/22 tumors were positive for cytokeratins (AE1-AE3, CK 7), EMA, racemase, and vimentin.

ArrayCGH in 7 analyzable cases revealed multiple numerical changes, gains of chromosomes 7,17 were present in 7/7 tumors.

Conclusions: 1, BSARCC showed a in a morphologic spectrum ranging from RCC with papillary architecture and large squamoid cells to fully developed BSARCC with extensive squamoid areas. 2, Emperipolesis was frequent finding within squamoid areas. 3, All cases expressed AE1-AE3, CK 7, EMA, vimentin, and racemase. 4, Multiple chromosomal aberrations were identified, all analyzable cases showed gains of chromosomes 7 and 17. 5, BSARCCs may behave aggressively. 5, Cases with available follow up had a favorable outcome (11/15) but some (4/15) behaved as aggressive tumors and metastasized. 6, According to the morphological, immunohistochemical and molecular genetic evidence, BSARCC appears to be a peculiar variant of papillary renal cell carcinoma.

909 Oncocytic Renal Neoplasms With Unique Cytogenetic Profiles

Cigdem Himmetoglu Ussakli, Yajuan Liu, Tatjana Antic, Lawrence True, Maria Tretiakova. University of Washington, Seattle, WA; University of Chicago, Chicago, IL.

Background: Morphology and genomic profiles of renal oncocytoma (RO) and its malignant counterpart chromophobe renal cell carcinoma (CHRCC) are distinctly different. However, there is a substantial group of sporadic oncocytic tumors with peculiar phenotype as well as perplexing morphologic and immunohistochemical overlap between classic RO and CHRCC with eosinophilic cytoplasm (CHRCC-EOS). Our aim is to cytogenetically profile such borderline oncocytic tumors in comparison with classic ROs.

Design: Oncocytic neoplasms with unusual morphologic features (N=15), classic RO (N=17) and CHRCC-EOS (N=3) were selected from the archives of 2 institutions and reviewed by 4 pathologists. Histological type was determined according to the WHO 2004 classification. Unusual oncocytic tumors (OT-NOS) were defined as tumors with architectural atypia (compact solid growth pattern, lack of classic archipelago-like nests and edematous/scarred stroma, presence of necrosis), cytological atypia (perinuclear halos and nuclear irregularities) or a combination of both. The tumors were immunostained for CK7 and S100A1. DNA from the FFPE tissues was extracted and analyzed using Cytogenome Microarray Analysis. Data analysis was performed using Cytogenomics 2.7 (Agilent Technologies Inc. CA) with global ADM2 algorithm to identify copy number alterations (CNA).

Results: Cases were categorized into 4 cytogenetic groups.

			Cytogenetic Diagnosis		
Morphologic Diagnosis	N	RO	CHRCC	Unique 1	Unique 2
RO	17	12 (70%)	1 (6%)	2 (12%)	2 (12%)
OT-NOS	15	8 (53%)	0	3 (20%)	4 (27%)
CHRCC-EOS	3	1 (33%)	1 (33%)	1 (33%)	0

Twelve cases had unique cytogenetic profiles. These were further categorized as unique 1 (no Chromosome 1 abnormalities but having other recurrent CNA with multiple gains) and unique 2 (1p deletion or monosomy 1 with additional non-recurrent CNA). Unique cytogenetic features were identified in 4 of 17 classical ROs, 7 of 15 OT-NOS, and 1 of 3 CHRCC-EOS. Presence of unique cytogenetic profile is NOT significantly associated with group morphology (p=0.27, Fisher Exact test).

Conclusions: We report two distinct cytogenetic profiles not previously described in oncocytic tumors. One of these profiles substantially overlaps with cytogenetic data from several TCGA CHRCC cases, and could represent a new entity of oncocytic tumors. Another molecular profile shares some similarities with RO and most likely represents tumors related to classic RO. No apparent histomorphologic features were predictive of unique cytogenetic profile.

910 S100P and Uroplakin II Expression in Matched Paired Primary and Metastatic Urothelial Carcinomas

Cigdem Himmetoglu Ussakli, Lei Zhao, Tatjana Antic, Maria Tretiakova. University of Washington, Seattle, WA; University of Chicago, Chicago, IL.

Background: The morphologic and immunohistochemical identification of metastatic carcinomas of urothelial origin is problematic in part due to lack of specific markers. The existing markers thrombomodulin and uroplakin III are diagnostically suboptimal because of their low sensitivity. In contrast, the more commonly used urothelial carcinoma (UC) associated antigens p63, CK7 and GATA3 lack specificity. Two novel urothelium specific markers, placental S100 (S100P) and uroplakin II (UPII), have recently been reported to be more specific than GATA3 for UC. Expression of UPII and S100P has not been studied in primary UC compared to their paired regional and distant metastases.

Design: Tissue microarrays including 68 matched primary and metastatic UCs were constructed. Each case was represented by five 1 mm cores: 2 duplicate cores from the primary UC and 2-3 cores from lymph node metastases. Immunohistochemical stains for polyclonal S100P(Cell Marque) and UPII(clone BC21, Biocare Medical) were performed with appropriate controls; results were scored as negative (0), weak (1+) or strong (2+).

Results: In primary UC, S100P and UPII showed positive staining in 49/68(72.5%) and 48/66(72.7%) cases, respectively. No cases demonstrated loss of S100P or UPII expression at the metastatic sites. S100P was gained in 9 and UPII was gained in 1 metastatic UCs, thus increasing sensitivity to 85% and 74%, respectively. UPII exhibited significantly higher staining intensity than S100P (2+ in 64% vs 44% of primary UC cases, and 71% vs 48% in metastatic UC), and less background staining.

Marker		Primary UC			Metastatic UC		
	N	0	1+	2+	0	1+	2+
S100P	68	19 (28%)	19 (28%)	30 (44%)	10 (15%)	25 (37%)	33 (48%)
UPII	66	18 (27%)	6 (9%)	42 (64%)	17 (26%)	2 (3%)	47 (71%)

Conclusions: S100P and UPII show similar high sensitivity for UC. Matched primary-metastatic UC study demonstrates that S100P and UPII expression is not only maintained but increased at the metastatic sites, thus making both markers suitable for detecting metastatic carcinomas of urothelial origin. Comparison of staining intensities revealed superior quality of UPII with majority of positive cases showing strong diffuse reactivity without non-specific labeling.

911 Renal Cell Carcinoma With Monosomy 8 and CAIX Expression: A Distinct Entity or Another Member or the Clear Cell Tubulopapillary RCC/RAT Family?

Michelle Hirsch, Justine Barletta, Melissa Gorman, Paola Dal Cin. Brigham & Women's Hospital, Boston, MA.

Background: Morphologic, immunophenotypic, and genetic findings in kidney tumors have led to the identification of multiple renal cell carcinoma (RCC) subtypes. Tumors in the clear cell tubulopapillary (CCTPRCC)/renal angiomyoadenomatous tumor (RAT) family have been recognized as distinct on the basis of morphologic and immunophenotypic findings. However, unlike other subtypes of RCC, no specific chromosomal abnormalities have been found to be associated with these tumors. We have identified monosomy 8 in a subset of RCCs (m8RCC) that have overlapping features with clear cell RCC (CCRCC), CCTPRCC and RAT. The goal of this study was to further characterize these cases.

Design: 13 cases were studied: 6 cases of m8RCC identified by karyotype were compared to 3 CCRCCs (2 with known loss of 3p by karyotype) and 4 CCTPRCCs (2 with known normal karyotype) by H&E, immunohistochemistry (IHC), and fluorescence in situ hybridization (FISH) using probes for chromosomes 8 (experimental), 21 (control), and 3p. FISH analysis was performed on tumor and normal parenchyma in each case, and was scored blind to all other results.

Results: All m8RCCs demonstrated morphologic features that raised the possibility of CCRCC, CCTPRCC, and RAT, but also had distinct features including a prominent 1-2 mm thick tumor capsule with associated thick fibrous bands that separated the mass into smaller nodules, tubulopapillary and nested architecture, voluminous cytoplasm, and basally located nuclei with slightly more atypia than typically seen in CCTPRCC/RAT (i.e., Fuhrman nuclear grade 2-3). IHC in m8RCC was typically positive for CK7, AMACR (weak/focal), CD10 (focal), and CAIX, a profile distinct from that seen in the CCRCCs and CCTPRCCs/RATs. FISH analysis was performed successfully in 12 cases, and confirmed monosomy 8 in the 5/5 examined m8RCCs; normal ch8 was present in all CCRCCs and CCTPRCCs. In contrast, 3p loss by FISH was seen in the CCRCCs, and normal 3p was present in the m8RCCs and CCTPRCCs. Clinically, all m8RCCs were small (pT1) and none have recurred (median f/u 62 months, range 7-133 months).

Conclusions: m8RCC appears to be a distinct tumor type that has overlapping morphologic features of both CCRCC and CCTPRCC/RAT. In difficult cases, IHC and/or FISH can be used to more definitively distinguish m8RCC from CCRCC and CCTPRCC/RAT. Clinically, these tumors appear to be biologically low grade/indolent, and the presence of CAIX in the absence of 3p loss suggests changes in the HIF pathway downstream of VHL.

912 FOXA1 and GATA3 Immunohistochemical (IHC) Expression: Role in Differentiating Prostatic and Urothelial Carcinoma

Anne Hoffa, Cynthia Cohen, Momin Siddiqui. Emory University School of Medicine, Atlanta, GA.

Background: FOXA1 and GATA3 are transcription factors that are considered to aid in cell development and regulation. Both bind to consensus DNA sequences and with loss of function, a known factor in the pathogenesis of various cancers. GATA3 is a well-recognized IHC marker for urothelial carcinoma. The role of FOXA1 in genitourinary tumors is not well studied. This study reviews the potential role for these two IHC stains in prostatic and urothelial carcinoma, with other tumors for comparison.

Design: Tissue microarrays (TMAs) of two 1 mm cores each of 600 tumors were immunostained for GATA3 and FOXA1. Table 1 indicates the site and numbers of the carcinomas included. Twenty-seven malignant melanomas were negative controls.

Results: The patterns of GATA3 and FOXA1 staining were intensely nuclear. None of our cases had cytoplasmic staining. Table 1 indicates FOXA1 and GATA3 expression in the carcinomas examined. Table 2 shows the statistical analysis of the two antibodies in prostate and urothelial carcinoma.

Table 1: FOXA1 and GATA3 IHC Profile.				
Carcinoma (number)	FOXA1(+)	FOXA1(-)	GATA3(+)	GATA3(-)
Prostatic (48)	42 (88%)	6 (12%)	0	48 (100%)
Urothelial (79)	4 (5%)	75 (95%)	56 (71%)	23 (29%)
Breast (77)	33 (43%)	44 (57%)	35 (45%)	42 (55%)
Hepatocellular (100)	0	100	0	100
Colonic (81)	0	81	0	81
Pancreatic (28)	0	28	0	28
Gastric (31)	0	31	0	31
Endometrial (27)	0	27	0	27
Ovarian Serous (27)	0	27	0	27
Lung adenocarcinoma (27)	0	27	0	27
Renal Cell (48)	0	48	0	48
Melanoma (27)	0	27	0	27

Table 2: Statistical analysis for FOXA1 and GATA3 IHC expression	FOXA1 (Prostate Carcinoma)	FOXA1 (Urothelial Carcinoma)	GATA3 (Prostate Carcinoma)	GATA3 (Urothelial Carcinoma)
Sensitivity	88%	0%	0%	71%
Specificity	99%	99%	100%	100%
PPV	91%	0%	0%	100%
NPV	99%	99%	100%	95%

Conclusions: FOXA1 and GATA3 are sensitive and specific markers for prostate and urothelial carcinoma respectively, when excluding breast carcinoma. This is one of the first studies that highlights FOXA1 immunoreactivity in prostate carcinoma, which may have potenital diagnostic value in excluding other malignancies, including urothelial carcinoma (except breast carcinoma).

913 Sarcomatoid Carcinoma of the Urinary Bladder: A Clinicopathological Analysis of 73 Cases

He Huang, Li Xiao, Miao Zhang, Bogdan Czerniak, Charles Guo. University of Texas MD Anderson Cancer Center, Houston, TX.

Background: Sarcomatoid carcinoma (SC) is a rare variant of bladder cancer composed of both carcinomatous and sarcomatous components. Because of its rarity, there have been limited studies of SC and most studies have been either case reports or small series. Here we reported a large series of SC of the bladder from a single institution.

Design: We identified 73 cases of bladder SC from our surgical pathology files between 1987- 2014. Slides were reviewed for pathologic analysis, including sarcomatous and carcinomatous components, stage, metastasis and immunohistochemistry. Demographic and clinical information were collected from patients' medical records.

Results: The patients included 48 men and 25 women with a mean age of 68 years old (range 36-89 years). Hematuria was the most common presenting symptom (81%). Other common symptoms included dysuria, lower abdominal pain, and recurrent urinary infection. All sarcomatous components were characterized by poorly differentiated spindle or polymorphic tumor cells except for one case, which contained heterologous chondroid and osseous elements. The majority of carcinomatous components are high-grade urothelial carcinoma or urothelial carcinoma in situ (n=64). Other carcinomatous components included squamous cell carcinoma (n=14), adenocarcinoma (n=7), and small cell neuroendocrine carcinoma (n=2). All SCs were invasive, including pT1 (n=6), pT2 (n=31), pT3 (n=28), and pT4 (n=8). 12 of the 36 patients who received lymph node dissection had local metastasis. In addition, 26 patients developed distant metastasis, most commonly to the lungs (n=10). Immunohistochemical stains showed that a subset of SCs were positive for uroplakin II (23%, 10/43), GATA-3 (18%, 8/45), and uroplakin III (7%, 3/44). Most patients underwent radical cystectomy (n=52) and chemotherapy (n=39). Followup information was available for 71 patients with a mean follow up of 29 months (range 3- 257 months). 52 patients died of disease in a mean time of 32 months, and 19 patients were alive in a mean time of 25 months.

Conclusions: SC of the bladder is a highly aggressive disease. While the sarcomatous components are most commonly characterized by high-grade spindle and polymorphic cells, the carcinomatous components are predominantly high-grade urothelial carcinoma. The overwhelming majority of SCs are presented at an advanced stage. Despite multimodality therapy, the prognosis for this disease remains poor.

914 Secondary Malignancies in Kidney Biopsies: A Clinical and Pathological Study of 73 Cases

He Huang, Jose Karam, Raghu Vikram, Pheroze Tamboli, Miao Zhang. University of Texas MD Anderson Cancer Center, Houston, TX.

Background: Secondary involvement of the kidney by tumor is uncommon. Differentiating secondary malignancies from primary kidney/urothelial tumors can be challenging, especially on limited biopsy material.

Design: We identified 73 cases of non-primary kidney/urothelial tumors diagnosed on kidney biopsies between 2002-2014. Clinical information and pathological reports were reviewed. Follow-up was obtained from medical records and/or provided by referring physicians.

Results: Over 1400 cases of CT-guided kidney biopsies were identified, of which 73 (5.1%) revealed secondary malignancies. There were 38 male and 35 female patients with the mean age of 59.5 yrs (range 21-83 yrs). Majority of the secondary malignancies were from solid tumors (72.6%, 53/73), with lung being the most common primary site (30.1%, 22/73), followed by thyroid (7/73), head and neck (5/73), soft tissue (5/73), gastrointestinal tract (4/73), uterus and cervix (3/73), breast (3/73), prostate (1/73), testis (1/73), thymus (1/73), and adrenal (1/73). Diffuse large B cell lymphoma was the most common hematological malignancy (6/73) secondarily involves the kidney. Radiographically, 82.1% (60/73) of the cases presented as solitary kidney masses, within which, 51 also had lesions in other organs and 9 had no other site of disease. Primary malignancy was known prior to the kidney biopsy in 80.8% (59/73), and the mean interval between diagnoses of primary and secondary malignancy was 4.5 years (range 1 month-39 years). Hematologic malignancy (5) and lung cancer (5) were the two most common primaries, in which the kidney mass was biopsied concurrently. Immunohistochemical stains were performed in 86.3% (63/73) of the cases. Depending on the differential diagnosis, TTF-1(18/66), CK7 (14/66), CD20 (14/66), CD10 (13/66), and CD3 (13/66) were the most common stains utilized.

Conclusions: Secondary malignancy in the kidney often presents radiographically as a solitary mass, which may be clinically indistinguishable from a primary kidney tumor. In some case, primary diagnosis was established concurrently, while in others, the interval was as long as 39 years (adenoid cystic carcinoma). When reviewing

kidney biopsies pathologist should be aware of the possibility of secondary malignancy. Accurate diagnoses can be rendered by correlating the pathological features with clinical, radiographic findings, and judicious use of ancillary studies.

915 SPINK1 Overexpression Is Rare Event in Association With ERG Expression and Is Exclusive of PTEN Homozygous Deletion in Localized Prostate Cancer

Kuo-Cheng Huang, Andrew Evans, Michael Dolph, Tarek Bismar. University of Calgary and Calgary Laboratory Services, Calgary, AB, Canada; University Health Network, Toronto, ON, Canada.

Background: SPINK1 has been proposed as a prognostic marker for several types of human cancer and its over-expression in prostate cancer (PCA) has recently been described. However, data is conflicting as to its relation to other genetics aberration of ERG and PTEN, as well as its prognostic value.

Design: We assessed SPINK1 expression in relation to ERG and PTEN genetic aberration and its potential prognostic value in localized PCA.The study consists of two cohorts (Calgary, n= 218 and UHN, n=168) of men who were treated by radical prostatectomy for localized prostate cancer. SPINK1, ERG and *PTEN* deletions were evaluated by immunestochemistry and fluorescence in situ hybridization assays and inter correlated. In addition, the prognostic value of SPINK1 overexpression was also assessed.

Results: SPINK1 protein overexpression was detected in 15.3% and 10% of PCA cases of the two cohorts. There was an inverse association between SPINK1 expression and ERG-fusion/protein expression. Specifically, SPINK1 expression was detected in 48/779 (6.2%) of ERG negative and 3/779 (0.39%) of ERG positive PCA cores ($p<0.0001$). Those three cores belonged to two patients, who exhibited both SPINK1 and ERG expression within the same core. A subset (14.2%) of PCA also showed interfocal heterogeneity in SPINK1 expression, but not intrafocal heterogeneity. There was predominance of SPINK1 positive cores in PCA cores with no PTEN deletion (74.0%; $p=0.079$). The remaining 26.0% of SPINK1 positive PCA cores were exclusively noted in PCA tumors with hemizygous PTEN deletion. None of the 56 (8.4%) PCA-cores with homozygous PTEN-deletion exhibited SPINK1 expression. This relation was validated on the cohort from UHN with all SPINK1 positive cases occurring in non *PTEN* deleted cores. Rarely, few patinets with SPINK1 positive cores had different cancer foci (typically on the opposite side of the gland) with hemizygous *PTEN* deletions (3 cases) or *TMPRSS2-ERG* rearrangements (3 cases). Despite slight association of SPINK1 expression with high GS (>7), SPINK1 expression was not significantly associated with stage or biochemical recurrence.

Conclusions: SPINK1 is not an independent predictor of biochemical recurrence in patinets with localized PCA. We show for the first time the that SPINK1 expression is mainly restricted to cases with intact PETN or hemizygous deletions and does not occur in the presence of homozygous PTEN genomic deletion.

916 A Clinicopathological Study of Renal Oncocytoma and Related Unclassified Oncocytic Neoplasms: Should the Morphological Spectrum of Renal Oncocytoma Be Expanded?

Ying Huang, Sana Jadallah, Nitin Sharma, Abraham Hakimi, Mariam Imnadze, Ying-Bei Chen, Anuradha Gopalan, Hikmat Al-Ahmadie, Sahussapont Sirintrapun, Samson Fine, Paul Russo, Victor Reuter, Satish Tickoo. Memorial Sloan Kettering Cancer Center, New York, NY; New York Hospital Medical Center Queens, New York, NY.

Background: Oncocytic renal cortical tumors with the typical architectural & cytological features as defined by WHO are easily classifiable as renal oncocytoma. However, classification of some tumors with oncocytoma like appearance, but with atypical cytological or architectural features is often problematic. We investigated classical oncocytomas & oncocytic neoplasms with atypical pathologic features, with the longest clinical follow-up to date, to determine the association of the pathologic atypia with clinical behavior.

Design: We reviewed pathologic features & clinical outcome of 183 patients with oncocytic neoplasms resected at our institution from 2000-2010. Based on consensus of 2 experienced genitourinary pathologists, this cohort was divided into 3 groups. Group 1-definite oncocytoma; Group 2-no agreement for a definitive diagnosis (oncocytoma vs not oncocytoma); and Group 3-unclassified oncocytic neoplasm. Tumors regarded as eosinophilic variants of chromophobe RCC were excluded from this study. The pathological features in group 2 tumors were evaluated in greater detail.

Results: 10/183 patients had multifocal or bilateral tumors. The distribution of the 193 tumors was as follows: Group 1-102(53%); Group 2-56 (29%); Group 3-35 (18%). The morphologic features that contributed to Group 2 included: nuclear atypia, 42/56 tumors (nuclear enlargement & irregularities in 29, nuclear enlargement with coarse chromatin in 12, and macronucleoli in 1), and/or unusual growth patterns in 14 (focal desmoplastic stroma in 10, solid growth characterized by sheets of cells in 3, and tubular growth pattern in 1). Over a median follow-up of 5 years (range, 5 days to 13 years), neither metastasis nor disease-related deaths occurred in any of the 3 groups. To put in perspective, in comparison, our previously published data shows disease specific adverse event rate of 5% in EChRCC over a median follow-up of 6.2 years.

Conclusions: Renal oncocytoma or oncocytoma-like tumors all have excellent long-term prognosis. Nuclear atypia & focal solid/tubular/sheet-like architectural patterns in a tumor that otherwise resembles renal oncocytoma did not alter the long-term clinical outcome in this series; these features are likely unduly overemphasized in excluding the diagnosis of renal oncocytoma. Further investigations, possibly multi-institutional, are warranted to establish whether the acceptable morphological spectrum of renal oncocytoma needs to be expanded.

917 Multiplex TSA-Plus Fluorescence IHC Combined With Spectral Image Analysis for PI3K Pathway Dysregulation in Prostate Cancer

Ying Huang, Michaela Bowden, Massimo Loda. Dana-Farber Cancer Institute, Boston, MA.

Background: Dysregulation of the PI3K pathway is frequently activated in aggressive prostate cancers (PCa), which plays a major role in progression. Targeting the PI3K pathway may be an effective strategy for advanced PCa. The current study involves developmenting of multiplexed fluorescence IHC (FIHC) assay to assess co-expression of PI3K activation markers, incorporating the use of AMACR and p63, as tumor and benign cells molecular masks of epithelial glands.

Design: We constructed a control TMA, including 16 PCa cases, each represented tumor in triplicate and benign in duplicate. We initially optimized single staining FIHC on 5 paraffin-embedded cell pellet sections derived from 3 prostate (DU145, PC3 and LNCap), breast (BT549) and lung (A549) cell lines. Multiplex tyramide signal amplification (TSA)-plus FIHC staining via sequential tyramide labeling was implemented on this TMA for PI3K pathway markers, PTEN, pS6 and stathmin (STMN1). Multispectral image analysis was performed, and classified cells into categories based on the AMACR and p63 masking efficiency.

Results: We successfully worked up TSA-plus FIHC for each marker in three prostate control cell lines, utilizing the breast and lung controls to confirm marker specificity, antibody dilutions and background thresholds for subsequent image analysis. Six fluorescent-based sequential stains for PI3K activation markers were applied to the PCa TMA. Tumor and stroma compartments were identified and generated the readout of each cell's co-expression level for all markers. PTEN was significantly decreased in PCa compared to benign cells ($F=4281$, $P<0.001$); While STMN1 and pS6 were significantly increased in PCa tissues ($F=1729$ and $F=2482$ respectively, $P<0.001$). We also found significant correlations among protein levels of PTEN, pS6 and STMN1 in PCa ($P<0.001$).

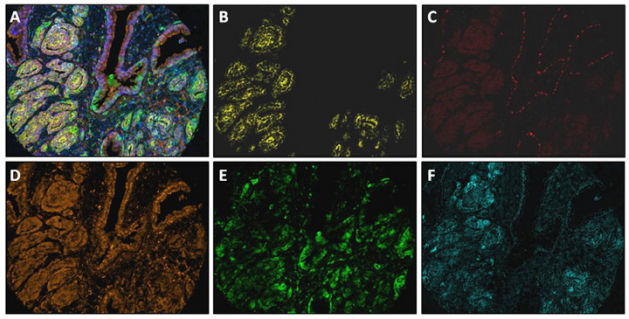

Figure1. Multiplex FIHC staining for PI3K pathway markers in a representative PCa tissue. A, multiplex FIHC for PTEN, pS6, STMN1, AMACR and P63. Classified cells into tumor and benign categories base on AMACR (B) , P63 (C) masking. D, E ,F indicating single staining of PTEN, pS6 and STMN1, respectively.

Conclusions: We developed a novel method for semi-quantitative analysis of PI3K activation markers co-expression in PCa. Expression of PTEN, pS6 and STMN1 were significantly different between tumor and benign prostate tissues, and there were significant correlation between these PI3K activation markers. We now aim to validate this multiplexed assay in the context of a large clinical cohort of PCa TMAs.

918 Inactivation of PTPRD and p16INK4A Are Prognostic Markers in Clear Cell Renal Cell Carcinoma

Rania Ibrahim, Samantha Wala, Andrew Girgis, Jason Karamchandani, Fabio Rotondo, Andreas Scorilas, Dina Boles, Hala Girgis, Ghassan Allo, Jason Lee, Kenneth Pace, Michael Ordon, George Yousef. St. Michael's Hospital, Toronto, ON, Canada; University of Toronto, Toronto, ON, Canada; University of Athens, Athens, Greece.

Background: Clear cell renal cell carcinoma (ccRCC) is the most common adult kidney cancer and can exhibit varying degrees of aggressiveness. There are currently no molecular-based prognostic markers routinely used in the clinic to identify patients with an aggressive form of ccRCC. Accurate assessment of prognosis is key towards personalized medicine.

Design: Chromosomal aberrations were assessed on 435 cases of ccRCC from The Cancer Genome Atlas (TCGA). The prognostic significance of protein tyrosine phosphatase receptor type D (*PTPRD*) and *p16INK4A*, which are encoded on 9p, was evaluated at the gene expression and methylation level. bioinformatic findings were validated by immunohistochemistry on 294 independent primary ccRCC cases. We further investigated the prognostic significance of *PTPRD* and *p16INK4A* by analyzing the correlation of their downstream targets with overall survival (OS).

Results: Lower expression of *P16INK4A* was significantly associated with worse OS ($p= 0.047$). Decreased expression of *PTPRD* correlated with a worse prognosis ($p= 0.044$). Hypermethylation of the chromosome 9p region encompassing *p16INK4A* and *PTPRD* was significantly associated with a worse prognosis ($p= 0.038$). Univariate and multivariate analyses were performed for immunohistochemistry on p16Ink4a and Ptprd. Down-expression of p16Ink4a was found to be a marker of poor prognosis. It retained its prognostic value independent of other variables for disease-free survival (DFS) ($p= 0.005$, HR: 0.44). Ptprd was prognostically significant for both DFS ($p< 0.001$, HR: 0.10, 95% CI: 0.04-0.26) and OS ($p= 0.025$, HR: 0.31). Kaplan-Meier analyses showed that patients with lower expression of p16Ink4a had a significantly shorter DFS ($p= 0.007$), and patients with lower Ptprd expression had a decreased DFS ($p< 0.001$) and OS ($p= 0.004$). Overexpression of downstream targets of Ptprd, namely signal transducer and activator of transcription 3 and aurora kinase A, demonstrated a

significant (p= 2.3e-05 and 3.4e-05) correlation with decreased OS. High expression of p16Ink4a gene targets, such as cyclin-dependent kinase 4 and 6, was significantly (p= 2.7e-05 and 0.00047) associated with a worse prognosis.
Conclusions: Expression of *PTPRD* and *p16INK4a* may serve as strong candidates for ccRCC prognostication.

919 MiR-210 Is a Prognostic Marker in Clear Cell Renal Cell Carcinoma

Rania Ibrahim, Sara Samaan, Heba Khella, Qiang Ding, Andrew Evans, Evi Lianidou, Manal Gabril, Sergey Krylov, Michael Jewett, Georg Bjarnason, George Yousef. St. Michael's Hospital, Toronto, ON, Canada; Princess Margaret Hospital, Toronto, ON, Canada; London Health Sciences Centre and Western University, London, ON, Canada; York University, Toronto, ON, Canada; Sunnybrook Odette Cancer Center, Toronto, ON, Canada.
Background: miRNAs are short non-coding RNA molecules that control the expression of their target genes, and are implicated in cancer. We explored the role of miR-210 as a prognostic marker in clear cell renal cell carcinoma (ccRCC).
Design: We analyzed the expression of miR-210 by qRT-PCR in 276 cases of primary ccRCC. We also compared its expression in 40 pairs of adjacent normal and cancerous tissues, as well as in primary and metastatic tumors, common RCC subtypes and the benign oncocytoma. Finally, we validated our results with an independent dataset of 481 cases from The Cancer Genome Atlas.
Results: miR-210 was significantly overexpressed in ccRCC compared to normal kidney, and its expression was higher in metastatic than in primary tumors. miR-210-positive patients had a statistically higher chance of disease-recurrence and shorter overall survival relative to miR-210-negative patients. Kaplan-Meier survival curves indicate that miR-210-positive patients had significantly lower disease-free survival (p = 0.015) and overall survival (p = 0.011). Papillary RCC showed comparable miR-210 overexpression, while much less upregulation was seen in chromophobe RCC and oncocytoma. Our in-silicoanalysis showed a negative correlation between miR-210 expression and a number of its predicted gene targets which aredownregulated in ccRCC tissues relative to normal kidney.
Conclusions: Our results demonstrate the role of miR-210 as a potential independent marker of poor prognosis in ccRCC and a potential therapeutic target.

920 Exploring Multiphoton Microscopy as a Novel Tool To Differentiate Chromophobe RCC From Oncocytoma in Fixed Tissue Sections

Manu Jain, Brian Robinson, Binlin Wu, Sushmita Mukherjee. Weill Cornell Medical College, New York, NY.
Background: Distinguishing chromophobe RCC from oncocytoma on H&E can be difficult, and may require time consuming procedures such as special stains, IHC and electron microscopy (EM). Multiphoton microscopy (MPM) relies on intrinsic tissue emissions to rapidly generate sub-cellular, histological resolution images from tissues and warrants exploration as an alternative rapid diagnostic tool.
Design: Tumor areas in unstained deparaffinized sections of chromophobe RCCs (n=10) and oncocytomas (n=10) were imaged at 150x total magnification and 2x digital zoom. Signals were collected from second harmonic generation and autofluorescence (AF); both short and long wavelengths, and color coded.
Results: Chromophobe RCC had sheet-like or trabecular growth composed of large cells with distinct cell borders, wispy cytoplasm and pleomorphic nuclei (AF) with peri-nuclear halos. Oncocytomas had nested/acinar pattern with uniform population of small cells having abundant cytoplasm and central nucleus (low or no signal). The cytoplasm fluoresced in short wavelength channel in both tumors. Intra-cytoplasmic granules (AF short and long wavelength), were the most prominent and unique features in both the tumors. In chromophobe RCC, the granules were sparse, small with mainly diffuse cytoplasmic distribution. In contrast, the granules of oncocytoma were abundant, brighter and bigger with apical, luminal, and/or perinuclear distribution. Based on the size and distribution of these granules and prior EM studies, we hypothesize their origin from micro-vesicles in RCC and mitochondria in oncocytoma. The single oncocytic variant of chromophobe RCC included in the study was correctly diagnosed by the presence of a peri-nuclear halo and small, dispersed cytoplasmic granules seen in the other chromophobe RCCs.

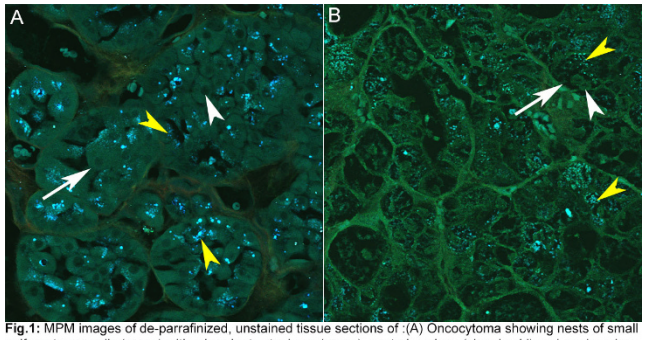

Fig.1: MPM images of de-parrafinized, unstained tissue sections of :(A) Oncocytoma showing nests of small uniform tumor cells (arrow) with abundant cytoplasm (green), central nucleus (signal void) and peri-nuclear or apical granules (bright blue; yellow arrowheads).(B) Chromophobe RCC showing sheets of large pleomorphic cells (arrows) with wispy cytoplasm, nucleus (green; arrowhead) and diffusely scattered granules (greenish blue; yellow arrowheads). Total magnifications A,B= 300x

Conclusions: For the first time, we characterized signatures of chromphobe RCC and oncocytoma on MPM. However, our study was limited by small sample size and only 1 oncocytic variant of chromophobe RCC, which often poses the biggest diagnostic challenge. Studies are ongoing that include diagnostically challenging cases and that use morphometric analysis to improve diagnostic accuracy. If successful, MPM can be used as an additional tool for differentiating oncocytic tumors.

921 Loss of Expression of SWI/SNF Chromatin Remodeling Complex Components and SetD2 Are Heterogeneous, Widespread, and Co-Occur in Clear Cell Renal Cell Carcinoma

Wei Jiang, Essel Dulaimi, Theodore Parsons, Qiong Wang, Karthik Devarajan, Raymond O'Neill, Charalambos Solomides, Stephen Peiper, Joseph Testa, Robert Uzzo, Haifeng Yang. Thomas Jefferson University, Philadelphia, PA; Fox Chase Cancer Center and Temple University, Philadelphia, PA.
Background: Polybromo-1 (Pbrm1), a subunit of the SWI/SNF chromatin remodeling complex, is the second most mutated gene (40%) in clear cell Renal Cell Carcinoma (ccRCC). Arid1A, another subunit that competes with Pbrm1 for binding to the complex, was infrequently mutated. The protein expressions of Brg1 and Brm (two catalytic subunits of the complex), and SetD2, a histone modifier (10-15% mutation rate), are not known in ccRCC. In this study we examined their protein expressions by immunohistochemistry (IHC) in TMAs, and investigated the prevalence of loss of expression, heterogeneity, and the potential co-loss patterns of these proteins.
Design: 160 ccRCC tumors were used to generate tissue microarray (TMA), with 40 tumors from each pathologic stage (1-4). For each tumor, 4 different foci representative of morphologic heterogeneity were selected. IHC studies using Pbrm1, Arid1A, SetD2, Brg1, and Brm antibodies were performed, and two surgical pathologists reviewed the slides. Loss of expression was defined as 0-5% staining within tumor nuclei in each focus.
Results: 15% (24/160) of ccRCC showed loss of Brg1 expression, and 38% (61/160) lost Brm expression, which have not been reported. 31% (49/160), 51% (81/160), and 14% (23/160) of tumors showed loss of Pbrm1, Arid1A, and SetD2 expression, respectively. Very high percentage of tumors displays heterogeneity in loss of expression, since frequently <4 foci from the same tumor had loss of a certain protein. Strikingly, novel co-loss patterns were identified among these proteins - Arid1A loss almost always accompanied Pbrm1 loss, Brm loss almost always accompanied Brg1 loss, Pbrm1 loss or Arid1A loss, and SetD2 loss almost always co-occurred with the loss of one or more of the other four proteins. The 2-sided p values for these associations (Fisher's exact tests) were all <0.0001, and the strong positive associations were true when tumor foci or tumors were compared.
Conclusions: The loss of protein expression of Brg1 and especially Brm in ccRCC were novel findings. As mutational analysis is expensive and rarely covers hundreds of samples, routine IHC provides a quick, reliable, and inexpensive method to assess tumor heterogeneity in large number of cases. It is also striking to find the co-losses of SWI/SNF components in ccRCC. As genetic interactions play powerful roles in cancer biology, these findings will provide insights and guidance to basic research and therapeutic development.

922 Phylogenetic Tree Construction and "Truncal Loss" Analysis Reveal Hidden Associations Between Loss of Protein Expression in SWI/SNF Complex Components and Tumor Stage in Clear Cell Renal Cell Carcinoma (ccRCC)

Wei Jiang, Essel Dulaimi, Theodore Parsons, Qiong Wang, Raymond O'Neill, Charalambos Solomides, Stephen Peiper, Joseph Testa, Robert Uzzo, Karthik Devarajan, Haifeng Yang. Thomas Jefferson University, Philadelphia, PA; Fox Chase Cancer Center and Temple University, Philadelphia, PA.
Background: Polybromo-1 (Pbrm1), a subunit of the SWI/SNF chromatin remodeling complex, is mutated in ~40% of ccRCC. Whether its mutation is correlated with tumor stage is controversial. We examined the protein expressions of four components of the complex, and SetD2, a histone modifier, in ccRCC, and investigated their correlations with tumor stage.
Design: ccRCC TMAS were generated using 160 tumors (40 per stage, 4 foci per tumor). IHCs were performed, and scored by two pathologists. Loss of expression was defined as 0-5% of tumor nuclear staining in individual focus.
Results: 49/160 (31%), 81/160 (51%), 23/160 (14%), 24/160 (15%), and 61/160 (38%) ccRCC showed loss of Pbrm1, Arid1A, SetD2, Brg1, and Brm expression, respectively. Heterogeneity was evidenced by loss of expression of individual protein in only a fraction of the 4 foci. "Truncal Loss" for individual protein was defined as the most ubiquitous loss of expression in the foci from the same tumor, and "The Only Truncal Loss" if there was no co-loss with other proteins. "Truncal Loss" was most likely an early event in tumorigenesis, and phylogenetic tree of protein expression was constructed for individual tumors. Through this analysis, otherwise hidden associations between protein expression and tumor stage were uncovered (Table 1), and both positive and negative associations were identified. For example, for Arid1A, the association was only significant in "The Only Truncal Loss" category. For SetD2, the association was only significant in "Truncal Loss" category (Table 1).

Stage	Pbrm1		
	The Only Truncal Loss	Truncal Loss	Any Loss in Tumor
1 (n=40)	3	5	10
2 (n=40)	2	4	12
3 (n=40)	2	4	7
4 (n=40)	12	18	20
p	*0.0002*	*<0.0001*	*0.003*

Stage	Brm		
	The Only Truncal Loss	Truncal Loss	Any Loss in Tumor
1 (n=40)	8	14	19
2 (n=40)	5	15	18
3 (n=40)	1	6	10
4 (n=40)	0	8	14
p	*0.001*	*0.012*	*0.05*

Stage	Arid1A		
	The Only Truncal loss	Truncal Loss	Any Loss in Tumor
1 (n=40)	6	12	16
2 (n=40)	8	19	20
3 (n=40)	14	21	22
4 (n=40)	10	19	23
p	*0.028*	0.2	0.21

Stage	SetD2		
	The Only Truncal loss	Truncal Loss	Any Loss in Tumor
1 (n=40)	0	1	2
2 (n=40)	0	1	5
3 (n=40)	2	4	6
4 (n=40)	3	6	10
p	0.06	*0.032*	0.07

Stage	Brg1		
	The Only Truncal Loss	Truncal Loss	Any Loss in Tumor
1 (n=40)	0	1	6
2 (n=40)	1	2	10
3 (n=40)	0	0	3
4 (n=40)	1	2	5
p	1	1	0.12

Conclusions: Using phylogenetic tree and "truncal loss" analysis, we identified statistically significant associations between loss of protein expression in SWI/SNF complex components and tumor stage in ccRCC, while the commonly used "Loss in Tumor" analysis either failed to do so or did so weakly, making these analyses very useful tools in uncovering such hidden connections, which may be important events in tumorigenesis and potential tharapeutic targets.

923 Clinical Outcome and Pathological Features in Synchronous and Metachronous Metastatic Clear Cell Renal Carcinoma VersusNon Metastatic Clear Cell Renal Carcinoma: A Ten Year Follow-Up

Solene-Florence Kammerer-Jacquet, Adelaide Pladys, Angelique Brunot, Julien Dagher, Alexandra Lespagnol, Gregory Verhoest, Florence Jouan, Brigitte Laguerre, Karim Bensalah, Jean Mosser, Marc-Antoine Belaud-Rotureau, Nathalie Rioux-Leclercq. Centre Hospitalier Universitaire de Rennes, Rennes, France; IGDR, Rennes, France; EHESP, Rennes, France; CRLCC, Rennes, France.

Background: Forty to 50% of patients with clear cell renal carcinoma (CCRC) develop metastases that are either synchronous or metachronous. Clarifying whether there is a biological difference between the two groups of metastases could have important clinical implications. Moreover pathological characteristics of synchronous and metachronous metastatic CCRC (mCCRC) are scarce. We compared clinicopathological features of synchronous and metachronous primary CCRC to non-metastatic primary CCRC.

Design: We retrospectively included 98 cases of CCRC diagnosed in 2002-2005. With a median follow-up of 10 years, 49 patients were non metastatic and 49 patients were metastatic (26 synchronous and 23 metachronous metastases). For each primary tumor, pathological prognostic criteria, intra-tumoral expression of VEGFA in immunohistochemistry, complete *VHL* status were analysed. Univariate analysis was performed and survival using Kaplan Meier curves and log rank test was studied.

Results: Patients with synchronous metastases had a worse cancer specific survival (CSS) than patients with metachronous metastases (p<0,004) with a median survival of 12 months and 54 months respectively. Their primary tumors were different as synchronous mCCRC compared to metachronous mCCRC were significantly associated with non-inactivated *VHL* gene (p=0,026), higher Fuhrman grade (p=0,010) and sarcomatoid component (p=0,002). Patients with metachronous metastases had a worse CSS than non-metastatic patients (p<0,001). Their primary tumors were different as metachronous mCCRC compared to non mCCRC were significantly associated with granular component (p<0,001), microvascular invasion (p=0,001), sarcomatoid component (p=0,037), necrosis (p=0,001), overexpression of VEGFA (>30%) (p=0,005), higher grade (p=0,007), size (p<0,001) and pT status (p<0,001).

Conclusions: We observed that metachronous mCCRC were different from synchronous mCCRC in terms of survival, pathological features and *VHL* gene status underlying different oncogenic pathways that may be involved in mCCRC. Moreover the group of CCRC at risk of metachronous metastases should be individualised from non mCCRC at the time of diagnosis as they could benefit from adjuvant therapy trial.

924 Overexpression of Both PD-1 and PDL-1 in Clear Cell Renal Carcinoma Indicates Poor Prognosis in Metastatic Patients With Sunitinib First-Line Treatment

Solene-Florence Kammerer-Jacquet, Angelique Brunot, Julien Dagher, Adelaide Pladys, Alexandra Lespagnol, Gregory Verhoest, Florence Jouan, Brigitte Laguerre, Karim Bensalah, Jean Mosser, Marc-Antoine Belaud-Rotureau, Nathalie Rioux-Leclercq. Centre Hospitalier Universitaire de Rennes, Rennes, France; IGDR, Rennes, France; CRLCC, Rennes, France; EHESP, Rennes, France.

Background: Programmed death-1 (PD-1) receptor negatively regulates T cell-mediated responses. PD-1 ligand (PD-L1) is aberrantly expressed in clear cell renal carcinoma (CCRC) and is associated with worse prognosis. Clinical trials evaluating anti-PD-1 and anti-PD-L1 antibodies in CCRC have shown promising efficacy in a subset of metastatic patients. We assessed the PD-1 and PD-L1 expression in primary CCRC of metastatic patients with sunitinib first-line treatment.

Design: Formalin-fixed paraffin-embedded specimens were obtained from primary CCRC of 47 metastatic patients with sunitinib first-line treatment and baseline characteristics including prognostic pathological criteria and clinical outcome data collected with a median follow up of 2 years after introduction of sunitinib. PD-1 and PD-L1 expression was evaluated by immunohistochemistry on the most inflammatory territory and the highest Fuhrman nuclear grade area respectively. For PD-1 expression, density of positive immune cells were evaluated as absent, focal, moderate or marked. For PDL-1 expression, percentage and intensity (mild to strong) of membranous stained tumor cells were reported. PD-1 was overexpressed when at least a moderate or marked density of positive immune cells was observed. PDL1 was overexpressed when at least 30% of tumor cells were positive with a moderate to strong membranous staining intensity. Univariate analysis was performed and survival using Kaplan Meier curves and log rank test was studied.

Results: Overexpression of both PD-1 and PD-L1 was observed in a subgroup of 17/47 primary CCRC (36%). This subgroup was not associated with prognostic pathological criteria. Metastatic patients with overexpression of both PD-1 and PD-L1 compared to other metastatic patients had a worse progression free survival (p<0,003) with a median survival of 10 months and 19 months respectively.

Conclusions: This is the first study to assess the PD-1 and PD-L1 expressions in primary CCRC of metastatic patients with sunitinib first-line treatment. The subgroup of primary CCRC with both PD-1 and PD-L1 overexpression should be individualized as corresponding metastatic patients were associated with poor prognosis when treated by sunitinib and could benefit from anti-PD-1 or anti-PD-L1 immunotherapies.

925 Juvenile Granulosa Cell Tumors (JGCT) of the Testis: A Clinicopathologic Study of 68 Cases With Emphasis on Its Wide Morphologic Spectrum

Chia-Sui Kao, Kristine Cornejo, Thomas Ulbright, Robert Young. Massachusetts General Hospital and Harvard Medical School, Boston, MA; Indiana University School of Medicine, Indianapolis, IN.

Background: We reviewed the clinicopathologic features of testicular JGCT, a rare neoplasm, about which information is limited.

Design: 68 JGCTs were identified from both institutions; most were consultation cases. Available clinical histories, gross descriptions, histologic and immunohistochemical (IHC) features and followup information were recorded.

Results: Patients were 30-weeks gestational age to 10 years old; 58/65 (89%) were ≤6 months. 52 underwent gonadectomy, 5 had wedge excision, and 2 biopsy only. 6 occurred in undescended testis and 2 in dysgenetic gonads. 6 patients had elevated serum AFP (likely physiologically) and 1 had gynecomastia. The tumors measured 0.5 to 5 cm (mean, 1.8) and were commonly well-circumscribed; 26 (59%) were grossly cystic, while 30% were solid and typically yellow-tan. Histology showed that all had a lobular appearance. 65 were punctuated by variably sized follicles containing basophilic or eosinophilic material, or both, while 3 were purely solid. In nonfollicular areas, the tumor cells were typically diffuse, but occasionally had a trabecular arrangement or reticular appearance. The stroma varied from fibrous to fibromyxoid. The tumor cells were mostly small with round to nuclei containing inconspicuous nucleoli and moderate to abundant, but occasionally scant, pale to lightly eosinophilic, sometimes vacuolated, cytoplasm; nuclear grooves were infrequent (6%). Mitoses were easily appreciable in 35% and apoptosis was prominent in 46%. Intratubular JGCT was seen in 43%. Rare patterns/features included: basaloid, spindle cell predominant, pseudopapillary, microcystic, and adult granulosa cell-like patterns as well as regressed tumor foci, and hyaline globules. Vascular invasion was seen in 2 cases, rete testis invasion in 4, and necrosis in 1. Inhibin, calretinin, FOXL2, and SF1 were almost always positive, while SALL4 and AFP were negative. All 16 patients with followup had no evidence of disease (2-124 months; mean, 45.4).

Conclusions: Testicular JGCT has a wide morphologic spectrum and also occurs in undescended testes and dysgenetic gonads. The solid and reticular patterns may pose diagnostic challenges but the lobular appearance, follicular differentiation, and fibromyxoid stroma are characteristic; IHC stains may aid in its distinction from other neoplasms of young males. These tumors appear to be benign, despite often brisk mitoses and apoptosis, supporting testis sparing surgery.

926 The Utility of SOX9, FOXL2, and SF1 Immunohistochemical (IHC) Stains in the Diagnosis of Testicular Sex Cord-Stromal Tumors (SCST) Compared To Other Commonly Used Markers

Chia-Sui Kao, Liang Cheng, Thomas Ulbright, Muhammad Idrees. Massachusetts General Hospital and Harvard Medical School, Boston, MA; Indiana University School of Medicine, Indianapolis, IN.

Background: Testicular SCSTs often show overlapping morphology. We investigated the ability of 3 markers important in gonadal development, SOX9, FOXL2, and SF1, to differentiate sex cord/stromal lineage of testicular SCSTs compared to other traditional sex cord markers.

Design: 120 testicular SCSTs were identified, and IHC stains for SOX9, FOXL2, SF1, inhibin, calretinin, and WT1 were performed. Positivity was defined as ≥10% of sex cord and/or stromal tumor cells showing at least moderately intense reactivity.

Results: SF1 was overall a more sensitive (87%) testicular SCST marker compared to inhibin (70%) and calretinin (55%); FOXL2 (44%) and SOX9 (41%) were slightly more sensitive than WT1 (34%). SOX9 was 57% sensitive and 70% specific for all Sertoli cell tumors. FOXL2 was 100% sensitive and 64% specific for granulosa cell tumors. FOXL2 was also positive in all stromal-derived tumors/components. Sertoli cell tumors with and without malignant features showed no significant difference in staining patterns or frequencies for all three novel stains; the same held true for Leydig cell tumors.

Tumor (# of cases)	SOX9 (% pos)	FOXL2 (% pos)	SF1 (% pos)	Inhibin (% pos)	Calretinin (% pos)	WT1 (% pos)
SCT, NOS (11)†	73	73	100	36	50	50
SCT with malignant features (17)	59	29	75	53	63	33
Sclerosing SCT (10)	56	33	70	33	13	40
Large cell calcifying SCT (7)	29	0	86	100	50	17
LCT, NOS (23)‡	17	0	100	95	94	6
LCT with malignant features (13)	23	15	92	100	55	9
Adult granulosa (4)	25	100	100	100	50	100
Juvenile granulosa (9)	63	100	88	100	83	83
Sertoli-stromal (4)	sex cord: 100; stromal: 0	50; 100	100; 0	100; 0	0	100; 50
Granulosa-stromal (1)	sex cord: 100; stromal: 0	100; 100	100; 0	100; 100	0	100; 100
Unclassified SCST (13)	38	77	92	25	25	33
Fibrothecoma (5)	60	100	80	80	20	50
Myoid gonadal stroma tumor (3)	0	100	100	66	0	33

†SCT, Sertoli cell tumor; ‡LCT, Leydig cell tumor

Conclusions: SOX9, FOXL2, and SF1 expression are not lineage specific in testicular SCSTs and therefore do not aid in their subclassification. SF1 is the most sensitive of all six markers. SOX9 and SF1 are better markers for sex cord elements whereas FOXL2 is best for stromal components.

927 Multiplex Real-Time PCR Assay for HPV detection Is a Useful Tool To Help Distinguish Primary Bladder Cancer From Secondary Involvement With Invasive Cervical Cancer in the Urinary Bladder

Hualin Kao. Taipei Veterans General Hospital, Taipei, Taiwan.

Background: This study investigated the prevalence of high-risk human papillomavirus (HR-HPV) in uterine cervical squamous cell carcinoma (CSCC) with secondary involvement of the urinary bladder and primary bladder cancer (PBC) and explore whether the detection of HR-HPV could help to differentiate between the two.

Design: A total of 33 patients who were diagnosed of CSCC with bladder involvement, 4 patients with PBC with uterine involvement, 2 patients with both CSCC and PBC and 185 patients with PBC were retrospectively studied. Multiplex PCR assay for the detection of seven most common HR-HPVs were performed.

Results: All 33 cases of CSCC with bladder involvement showed concordant HR-HPV-positive pattern in the paired cervical and bladder specimens. The 4 cases of PBC with uterine involvement were negative for HR-HPV. HR-HPV was detected in CSCC but not in the PBC of the two patients with both CSCC and PBC. HR-HPV could not be detected in the 185 PBCs.

Conclusions: Our findings demonstrate multiplex real-time PCR assay for HR-HPV detection as a useful tool to distinguish PBC from secondary involvement of CSCC in the bladder.

928 The Pathologic Features in Radical Cystectomy Specimens of Patients Receiving Neoadjuvant Chemotherapy for Bladder Cancer: Is Tumor Regression Important?

Nooshin Karamzadeh Dashti, Rafael Jimenez, Frank Igor, Stephen Boorjian, R Houston Thompson, Brian Costello, R Jeffrey Karnes, John Cheville. Mayo Clinic, Rochester, MN.

Background: There is limited data regarding the prognostic significance of pathologic changes in cystectomy specimens following neoadjuvant chemotherapy (NAC). A recent study proposed a three-tier tumor regression grade (TRG) associated with outcome in patients receiving NAC prior to cystectomy. The objective of this study was to examine the pathologic features of cystectomy specimens following NAC, and the association of TRG and cancer-specific (CS) survival.

Design: The study consisted of 75 patients that received NAC for bladder cancer prior to cystectomy (cases) matched to 132 patients who met eligibility criteria for but did not receive NAC prior to cystectomy (controls). TRG was determined as previously described: TRG1- complete response with no residual tumor; TRG2- strong response with predominantly fibrosis with cancer occupying less than 50% of the original tumor bed, and TRG3- weak or no response with tumor predominating in the original tumor bed (>50% of tumor cells in bed). Similar TRG was defined for the control group to determine if effects such as prior treatment, initial tumor volume and stromal reaction influenced the TRG. Survival analysis was performed using Kaplan-Meier method and compared with the log rank test.

Results: There was no difference in pTNM distribution or TRG between cases and controls. TRG was predictive of CS survival in both cases and controls but had greater significance in the case group. The 5-year CS survival for cases was as follows: TRG1 (26 patients) 64%, TRG2 (16 patients) 46%, and TRG3 (33 patients) 16% ($p<0.0001$).

Conclusions: In patients receiving NAC, pathologic assessment of tumor by TRG provides important prognostic information.

929 Immunohistochemical Expression of ARID1a in Upper Tract Urothelial Carcinomas: A Tissue Microarray Study of 99 Cases

Sarah Karram, Sheila Faraj, Kazutoshi Fujita, Enrico Munari, Ie-Ming Shih, Alcides Chaux, George Netto. Johns Hopkins Medical Institutions, Baltimore, MD; Osaka University, Osaka, Japan; Norte University School of Medicine, Asunción, Paraguay.

Background: AT-rich interactive domain 1A (ARID1A) is tumor suppressor gene that interacts with BRG1 ATPase to form a SWI/SNF chromatin remodeling protein complex. Inactivation of ARID1A has been described in several neoplasms, including epithelial ovarian and endometrial carcinomas, and has been correlated with prognosis. We have previously demonstrated that low ARID1A expression was associated with a lower rate of tumor progression and better disease-specific survival (DSS) in urothelial carcinoma patients undergoing cystectomy. Given known biologic differences among upper and lower urinary tract urothelial carcinoma, in the current study we assess the expression status and prognostic significance of ARID1A in upper tract urothelial carcinoma (UTUC).

Design: Two tissue microarrays (TMAs) were constructed from 99 Japanese patients with nonmetastatic UTUC who underwent radical nephroureterectomy with curative intent between 1997 and 2011 at one of the authors' institution. TMAs were constructed with triplicate tumor and paired benign urothelium. Nuclear ARID1A staining was evaluated using immunohistochemistry (HPA005456, Sigma-Aldrich, St Louis, MO). An H-score was calculated as the sum of the products of intensity (0-3) multiplied by extent of expression (0 to 100%). Average H-score per case was used for statistical analysis. High ARID1A expression was defined as H-score above the upper tertile.

Results: There was no difference in ARID1A expression between normal and UTUC tissue (P=0.77). ARID1A expression did not correlate with any clinicopathologic parameter evaluated. UTUC progression and disease-specific survival (DSS) rates were 38% and 70% respectively. We found no association between high/low ARID1A expression and UTUC progression [HR: 0.70 (0.37-1.3), p=0.27] or DSS [HR: 0.78 (0.37-1.62), p=0.50].

Conclusions: Our findings demonstrate that unlike in their bladder counterpart, ARID1A expression in UTUC does not appear to correlate with outcome. This further highlights that despite the many shared features between UTUC and bladder urothelial carcinoma, key clinical and molecular genetic differences exist. This distinction is critical clinically particularly in decisions involving the utilization of targeted therapy.

930 Immunohistochemical Analysis of the AMPK Pathway in Prostate Cancer in the Context of the Metabolic Syndrome

Elizabeth Kehr, Julie Batista, Giorgia Zadra, Rhonda Arthur, Birgitta Grundmark, Bjorn Zethelius, Mieke Van Hemelrijck, Lars Holmberg, Massimo Loda. Brigham & Women's Hospital and Harvard Medical School, Boston, MA; Harvard School of Public Health, Boston, MA; King's College London, School of Medicine, London, United Kingdom; Uppsala University, Uppsala, Sweden.

Background: 5' adenosine monophosphate-activated protein kinase (AMPK) and acetyl co-A carboxylase (ACC) are enzymes dysregulated in metabolic syndrome (MSx) and prostate cancer (PCa). We investigate AMPK pathway activation by evaluating the expression of phosphorylated AMPK (p-AMPK) and ACC (p-ACC) in men with PCa and MSx.

Design: The study subjects were from the Uppsala Longitudinal Study of Adult Men (ULSAM). 114 men (25 with MSx) had diagnostic tissue stained with antibodies against p-AMPK and p-ACC in tumor and in adjacent normal tissue. Biomarker expression was scored from 0 to 3; and as an additive score (range 0-6). Cross sectional associations between biomarker expression, the MSx, and pathologic features were assessed using unconditional logistic regression to estimate odds ratios (ORs) and 95% confidence

intervals (CIs); associations between biomarker expression and mortality were assessed using Cox proportional hazard regression to estimate hazard ratios (HRs) and 95% CIs. Models were adjusted for age, Gleason score, and stage.
Results: The additive score of p-AMPK and p-ACC expression was positively associated with MSx; multivariable-adjusted ORs (95% CIs) were 1.72 (1.14, 2.59) and 1.57 (1.02,2.43) for each 1-increment increase in the score when evaluated in tumor tissue and adjacent normal tissue . The p-AMPK/p-ACC additive score and the p-ACC individual score in tumor tissue were associated with obesity (OR=2.19; 95% CI: 1.18,4.07 and OR=2.28; 95%CI: 1.05,4.94). The p-AMPK score in tumor tissue was positively associated with fasting blood glucose (OR=2.44; 95% CI: 1.05-5.70). In multivariable-adjusted survival analyses, the p-AMPK/p-ACC additive score (HR=1.26; 95% CI: 1.05,1.51) and p-ACC score (HR=1.34; 95% CI: 1.05, 1.73) in tumor tissue were significantly associated with all-cause mortality. No associations were found for biomarker expression and PCa-specific mortality.
Conclusions: Our data show the activation of AMPK/ACC pathway in PCa tissue in the context of MSx, and this activation may indicate poorer prognosis. Larger studies are warranted to further explore the interaction of MSx, AMPK activation, and PCa outcomes.

931 Targeted Next Generation Sequencing of Renal Epithelial Tumors

Elizabeth Kehr, Massimo Loda, Ronny Drapkin, Paola Dal Cin, Toni Choueiri, Michelle Hirsch. Brigham & Women's Hospital, Boston, MA; Dana-Farber Cancer Institute, Boston, MA.
Background: Renal epithelial neoplasms (RENs) are a heterogenous group of sporadic kidney tumors that can be subclassified based on distinct morphologic, immunohistochemical and genetic findings. Recent finidngs based on the TCGA have identified somatic mutations in clear cell (CCRCC) and chromophobe RCCs (ChRCCs); but mutations in other RCC subtypes are less understood. Genetic profiling in the form of targeted next generation sequencing (NGSeq) is a platform that can be used to identify specific mutations and other DNA alterations in solid tumors, and the goal of this study was to evaluate such findings in a cohort of renal tumors in a tertiary care hospital.
Design: Genotyping (NGSeq or 'profiling') was performed on 147 RENs: 46 CCRCCs, 15 papillary RCCs, 6 ChRCCs, 2 Xp11.2 RCCs, 2 clear cell tubulopapillary RCCs (CCTPRCCs), 2 collecting duct carcinomas, 4 unclassfied RCCs, 9 metastatic RCCs, and 7 oncocytomas. The oncopanel assay surveys exonic DNA sequences from 300 cancer genes and 113 introns across 35 genes for rearrangement detection. DNA is isolated from tissue and analyzed by massively parallel sequencing using a solution-phase Agilent SureSelect hybrid capture kit and an Illumina HiSeq 2500 sequencer.
Results: The average number of somatic mutations per REN subtype ranged from 3 to 5 in this targeted analysis, with CCTPRCCs having the fewest number of mutations and CCRCCs having the greatest. In general, a significant number of mutations were observed in genes associated with DNA damage, chromatin remodeling, and cell cycle regulation, including ARID1A/B, ATM, CDK, CHEK2, ERCCC, FANCA, KDM6, MTOR, PRKC1/PRKDC, and SETD2. The latter was the most common observed mutation after VHL, and was found in 20 cases. Mutations in tyrosine kinases/TK receptors were also noted. Gene mutations known to occur in familial syndromes, such as mismatch repair genes, fumarate hydratase, succinate dehydrogenase, folliculin, and BRCA were found in ~15% of cases. There was no clear association for gene mutation combinations and tumor subtype.
Conclusions: Targeted NGSeq has identified >100 gene mutations in a variety of RENs. Interestingly, a good proportion of these mutations were related to DNA repair and chromatin remodeling; however other mutations were also identified in genes associated with apoptosis, transcription, oncogenes, and tumor suppressors. Further evaluation of these findings may lead to a better understanding in the pathophysiology of renal tumors and the use of targetable therapies for patients with aggressive forms of RCC.

932 Carcinoma of the Uterine Cervix (CX) Involving the Genitourinary Tract: A Potential Diagnostic Dilemma

Francesca Khani, Lauren Schwartz, Jonathan Epstein. Johns Hopkins Medical Institutions, Baltimore, MD.
Background: Uterine CX carcinoma secondarily involving the GU tract is rarely documented histologically. These tumors present a unique diagnostic challenge as they can appear morphologically similar to urothelial carcinoma as well as primary squamous cell carcinoma and primary adenocarcinoma of the bladder. In contrast to carcinomas involving the uterine CX, prior studies have shown that carcinoma of the urinary bladder is not HPV related.
Design: Consult cases at our hospital from 1984 to the present were searched for cases in which the differential diagnosis was primary bladder carcinoma versus secondary involvement by CX carcinoma. We identified 10 cases that met these criteria and evaluated 7 of them with immunohistochemical (IHC) stains for p16 and GATA3 and in situ hybridization (ISH) for HPV. IHC and ISH on 2 cases are forthcoming. In the 10th case, the lesional tissue was no longer present on the IHC and ISH slides, but the patient had a known primary cervical carcinoma with peritoneal spread.
Results: 4 cases were received with a gynecologic history and three were originally misdiagnosed as bladder carcinoma. Morphologically, the majority showed basaloid nests of tumor cells infiltrating muscle bundles, with several having foci that mimicked urothelial carcinoma in situ. Five tumors were found to be diffusely positive with p16, one patchy, and one negative. GATA3 staining was negative in three cases with four showing weak to strong positivity. Six cases were positive for high risk HPV (five for HPV 16, one for HPV 18).Case 7, which was equivocal for HPV clinically was an extrinsic mass between the vagina and the bladder, pushing into the bladder.

Case	p16	GATA3	HPV HR	HPV16	HPV18
1	Diffusely +	Negative	+	+	-
2	Patchy +	Moderate to Strong (30%)	+	+	-
3	Negative	Moderate to Strong (90%)	+	+	-
4	Diffusely +	Negative to Weak	+	-	+
5	Diffusely +	Negative	+	-	+
6	Diffusely +	Negative	+	+	-
7	Diffusely +	Weak	Equivocal	-	-

Conclusions: Based on our findings, we advocate a multifaceted approach, combining morphologic evaluation with ancillary studies including IHC and ISH in evaluation of GU specimens for secondary involvement by CX carcinoma. p16 IHC may be misleading, as urothelial carcinoma is p16 positive, thus requiring ISH for HPV to document high risk virus. Furthermore, gynecologic clinical history is critical to the evaluation and diagnosis of these specimens.

933 Gleason 3+3=6 and Intraductal Carcinoma (IDC-P) on Prostate Biopsy Specimens

Francesca Khani, Jonathan Epstein. Johns Hopkins Medical Institutions, Baltimore, MD.
Background: While IDC-P is typically present on biopsies where there is also invasive prostate carcinoma of Gleason pattern 4 or 5 and an associated unfavorable outcome, there are limited studies on IDC-P in needle core biopsies with a concomitant low-grade invasive component. There are differing opinions on whether IDC-P should be incorporated into the Gleason grade in such cases. Our study is the first to investigate clinical outcomes and radical prostatectomy (RP) findings in patients with Gleason 3+3=6 and IDC-P on biopsy.
Design: 73 patients in our consult files (2001-2014) who had IDC-P and associated Gleason 3+3=6 invasive carcinoma were identified. Cases with higher Gleason grades in any of the biopsy parts were excluded. Clinical follow up was available in 55 patients. 13 patients underwent RP, of which 10 were available for review.
Results: Treatment was RP in 11 men, radiation therapy (RT) in 28 men of which 12 also received androgen deprivation therapy (ADT), cryotherapy plus ADT in 2, and ADT alone in 1. 4 men had metastatic disease at the time of initial diagnosis. 8 men were placed on active surveillance, of which 2 underwent RP and 1 underwent ADT for progressive disease, and 1 developed metastatic disease after undergoing cryotherapy. Of the 13 total RP specimens, 7 were stage pT2, 4 were stage pT3a, and 2 were stage pT3b. In the RPs available for review, 2 had Gleason 3+3=6, 2 had Gleason 3+4=7, 3 had Gleason 4+3=7, 2 had Gleason 4+4=8, and 1 had Gleason 4+5=9. All cases had extensive IDC-P (>50%). 1 case had a component of sarcomatoid carcinoma and 1 case had ductal features in addition to IDC-P. At 3 years, there was a 27.3% progression rate (biochemical failure) in men who underwent either RP or RT, and 5 men (9.4%) died of metastatic disease. The median progression-free follow-up was 46 months and median time to progression 22 months.
Conclusions: Many men with IDC-P on biopsy have aggressive tumors even when the invasive tumor on biopsy is Gleason grade 6, as evidenced by the relatively high rate of progression observed in these patients. We recommend that IDC-P on biopsy is not graded as Gleason pattern 4 or 5 since a minority of men with IDC-P and Gleason 6 on biopsy have only Gleason 6 invasive cancer at RP and a favorable prognosis. Also, our prior study showed that only IDC-P on biopsy may uncommonly be associated with only IDC-P at RP. A note should be added to the biposy report with IDC-P stating that typically there is higher unsampled grade tumor in the prostate warranting definitive therapy.

934 The Prognostic Utility of miR-126 in Clear Cell Renal Cell Carcinoma

Heba Khella, Andreas Scorilas, Roy Nofech-Mozes, Lorna Mirham, Evi Lianidou, Sergey Krylov, Jason Lee, Michael Ordon, Robert Stewart, Michael Jewett, George Yousef. Keenan Research Centre in the Li Ka Shing Knowledge Institute St. Michael's Hospital, Toronto, ON, Canada; University of Athens, Athens, Greece; University of Toronto, Toronto, ON, Canada; York University, Toronto, ON, Canada; St. Michael's Hospital, Toronto, ON, Canada; Princess Margaret Hospital, University Health Network, Toronto, ON, Canada.
Background: Clear cell renal cell carcinoma (ccRCC) is an aggressive tumor with unpredictable behavior. Clinical parameters are not always accurate for predicting prognosis. miR-126 is differentially expressed in many cancers including RCC and was shown to be downregulated in metastatic compared to primary ccRCC.
Design: We assessed the prognostic significance of miR-126 in 264 Primary ccRCCs. We also compared its expression between normal kidney, primary and metastatic ccRCC, and among RCC subtypes. We validated our results on an independent set of 481 ccRCC cases.
Results: miR-126 was downregulated in metastatic compared to primary tumors. It was significantly downregulated in higher stage (p=0.005) and higher grade tumors (p=0.002)**.** miR-126 upregulation was associated with significantly prolonged disease-free ($p < 0.001$) and overall survival($p = 0.015$). In tumors > 4 cm, patients with higher miR-126 have significantly longer survival. Restoration of miR-126 expression decreases cellular migration and proliferation in RCC cell lines. The clear cell subtype showed the highest expression of miR-126 while the lowest expression was seen in papillary renal cell carcinoma. We identified a number of miR-126 targets and pathways that are involved in carcinogenesis, including the apoptosis signaling pathway.

Conclusions: miR-126 is a promising prognostic marker in ccRCC and can distinguish between the clear cell and papillary subtypes. In addition, miR-126 has potential therapeutic applications.

935 Molecular Subgrouping and Prognosis Prediction Using Immunoprofile of Urothelial Carcinoma

Jiyoon Kim, YM Cho, Jae Ro. Asan Medical Center, Seoul, Republic of Korea; Houston Methodist Hospital, Weill Medical College of Cornell University, Houston, TX.

Background: One of the major challenges in bladder cancer management is distinguishing aggressive tumors from indolent ones with similar clinicopathologic factors, especially those of high-grade stage T1 tumors.

Design: To define a set of prognostic factors that can be assessed easily in clinical practice with a high cost-effectiveness, expression of 11 proteins were examined immunohistochemically in 403 cases of transurethrally resected bladder tumor and correlated to clinical outcomes.

Results: Based on the protein immunoprofile, the urothelial carcinoma was divided into four intrinsic molecular subgroups with different clinical outcomes: subgroups 1 and 4 with the worst survivals, subgroup 2 with the best survival, and subgroup 3 in intermediate survival. The protein expression patterns of 4 subgroups were mutually exclusive: overexpression of p53, EZH2, E2F1, and IMP3 and high Ki-67 proliferation index in subgroup 1; overexpression of cytoplasmic survivin in subgroup 4; overexpression of membranous TSP1 and cytoplasmic p27 in subgroup 2; and no representative protein in subgroup 3. Predictive models using protein immunoprofile generated three risk groups, which well predicted disease-specific survival not only in total cases with a predictive accuracy of 0.737 but also in high grade stage T1 tumors with a predictive accuracy of 0.658.

Conclusions: These results showed that urothelial carcinoma were composed of four clinically relevant molecular subgroups based on protein expression and that overall survival of those patients could be predicted using a set of small number of protein expressions not only in total cases but also in high grade stage T1 tumors.

936 Transcriptome-Wide Analysis of Matching Tumor and Non-Neoplastic Biopsy and Radical Prostatectomy Specimens: Implications for Prostate Cancer Biomarker Signatures

Beatrice Knudsen, Hyung Kim, Nicholas Erho, Lucia Lam, Elai Davicioni, Imelda Tenggara, Theo Van Der Kwast, Neil Fleshner, Peter Carroll, June Chan, Matthew Cooperberg, Jeffrey Simko. Cedars-Sinai Medical Center, Los Angeles, CA, Cayman Islands; GenomeDx Biosciences, Vancouver, BC, Canada; University of California, San Francisco, CA; University Health Network, Toronto, ON, Canada.

Background: Molecular tests are becoming more prevalent in the management of prostate cancer, often guiding treatment decisions such as enrollment into active surveillance programs. We explore some of the challenges in utilizing molecular tests for this purpose including limited material in biopsy (Bx) specimens, tumor and specimen heterogeneity and fragmentation of RNA.

Design: 152 samples from 33 patients with matched FFPE Bx and radical prostatectomy (RP) specimens were identified at UHN, UCSF and Cedars Sinai. For most patients matching samples were taken from tumor and non-neoplastic tissue. RNA was extracted and 100ng was used for cDNA amplification, which was then hybridized to the 1.4 million feature Affymetrix Human Exon 1.0 ST array to measure RNA expression. Gene expression profiles of four published prognostic signatures were evaluated using Pearson correlation between Bx and RP (CCP, Decipher, GPS and Penney). Outlier analysis of ERG, other ETS family members and SPINK1 were used to classify tumor specimens as one of the following mutually exclusive categories: ERG+, ETS+, SPINK1+ or Triple Negative subtypes.

Results: From 1 mm cylindrical cores punched from FFPE blocks, 68/75 (91%) of the Bx specimens and 76/77 (97%) of the RP specimens had sufficient RNA and cDNA to generate expression data that passed quality control. Quality of RNA, cDNA and microarray data were comparable between Bx and RP specimens. Unsupervised principle components analysis showed the largest source of variation in expression between Bx and RP, followed by tumor and non-neoplastic tissue. Molecular subtyping revealed that 36% of Bx-RP matched pairs were discordant (e.g. Bx ERG+ but RP Triple Neg) and overall tumor Bx-RP correlations for Decipher (0.64) and the imputed CCP (0.19), GPS (0.58) and Penney (0.66) signatures were low. When discordant pairs were removed these correlations changed: CCP (0.52), Decipher (0.82), GPS (0.35), and Penney (0.86).

Conclusions: High quality transcriptome-wide expression data was generated from FFPE Bx specimens containing biologically relevant signal. After discordant cases (i.e., clonally distinct Bx and RP) were removed, prognostic signatures were found to be well correlated between Bx and RP tumor samples from the same patient. These results suggest that tumor clonality may be a potential source of variance for molecular signatures.

937 Comparison of Magnetic Resonance Imaging Targeted and Standard Prostate Biopsies in Cancer Detection, Gleason Grading and Tumor Volume Estimation

Max Kong, Fang-Ming Deng, Jonathan Melamed, Andrew Rosenkrantz, Samir Taneja, Ming Zhou. New York University Langone Medical Center, New York, NY.

Background: Magnetic resonance imaging (MRI) targeted prostate biopsy has been increasingly used for diagnosis and management of prostate cancer (PCa) , although this emerging biopsy technique awaits validation. In addition to its ability to detect clinically significant PCa, surgical pathologists are also concerned about how well MRI targeted biopsies correlate with radical prostatectomy (RP) in Gleason grade (GG) and tumor volume (TV). We compared MRI targeted and standard biopsies for PCa detection rate, GG and TV estimation.

Design: Patients enrolled in an IRB approved trial underwent standard 12-core sextant biopsy and simultaneous targeted biopsy of MRI suspicious lesions. 102 of such patients found to have PCa on biopsy and subsequently underwent RP were included in this study. GG and TV estimation using greatest length and % of PCa involvement in any single core were recorded for both standard and targeted biopsies. For RP, all cancer foci were traced on glass slides, then recorded on a "prostate map" with pathological data including GG, tumor dimension and TV of each cancer focus. GG and TV were correlated between biopsy and RP.

Results: Standard biopsy alone detected 84/102 (82.4%) and missed 18 (17.6%) of PCa. Similarly, MRI targeted biopsy alone detected 84/102 (82.4%) and missed 18 (17.6%) of PCa. PCa missed by MRI targeted biopsy had significantly lower GG and TV than PCa missed by the standard biopsy. The pT stage of PCa missed by MRI targeted biopsy was also marginally lower. GG and TV concordance between biopsy and RP was not statistically different between standard and MRI targeted biopsies.

		PCa missed by standard biopsy (n=18)	PCa missed by MRI targeted biopsy (n=18)	p value
Gleason score	6	5	7	0.025
	3+4	4	10	
	4+3	8	1	
	8	1	0	
pT stage	2a	1	5	0.057
	2b	4	0	
	2c	8	10	
	3a	5	2	
	3b	0	1	
TV (mean +/- S.D.) (mm3)		1.12 +/- 1.37	0.54 +/- 0.52	

Conclusions: Standard and MRI targeted biopsies have the same PCa detection rate and similar biopsy/RP concordance in terms of GG and TV estimation. They miss the same % of PCa. However, PCas missed by MRI targeted biopsy are less aggressive and of lower GG, pT stage and TV. Therefore, MRI targeted biopsy may be a better technique to detect clinically significant PCa.

938 Prostate Carcinoma in Magnetic Resonance Imaging and Biopsy Negative Prostate Lobes: Implication for Focal Therapy

Max Kong, Fang-Ming Deng, Jonathan Melamed, Andrew Rosenkrantz, Herbert Lepor, Samir Taneja, Ming Zhou. New York University Langone Medical Center, New York, NY.

Background: Focal therapy has been increasingly used for treatment of prostate carcinoma (PCa). It is in general indicated for patients with unilateral PCa confirmed on magnetic resonance imaging (MRI) and prostate biopsies (PBx). The efficacy of focal therapy depends in part on whether there is significant PCa on the contralateral side of the prostate gland. This study investigated the pathology of the prostate lobes contralateral to MRI and PBx detected PCa.

Design: Patients underwent prostate MRI and standard 12-core sextant biopsy and simultaneous targeted biopsy of MRI suspicious lesions. Prostate MRI was reviewed by a single radiologist and the location and degree of suspicion for cancer (1[negative] to 5 [almost certain for PCa]) were recorded. These patients subsequently underwent radical prostatectomy (RP). All cancer foci in RP were traced on the glass slides and then recorded on a "prostate map" with pathological data including GG, tumor dimension and TV of each traced cancer focus.

Results: On MRI and prostate biopsy (MRI/PBx), 43 patients had unilateral PCa. In RP, 10 of these cases had unilateral PCa on the same side of the prostate gland. No cases had unilateral PCa on the contralateral side. However, 33 (76.7%) cases had bilateral PCa. Of these 33 cases, 30 had dominant tumor nodules (DN) on the same side of MRI/PBx detected PCa; 3 had DN on the contralateral side. In 30 cases with DN on the same side of MRI/PBx detected PCa, 11 cases had significant PCa on the contralateral side (defined as tumor nodules with GG≥7 or extraprostatic extension). Therefore, 14 (3+11) of 43 (32.6%) unilateral PCa determined by MRI/PBx had significant PCa component on the contralateral side and were considered "misclassified" by MRI/PBx. Comparing the misclassified cases with the correctly classified ones regarding PCa laterality, the greatest length of PCa involvement in any single core in PBx, and MRI PCa suspicion levels were significantly greater in misclassified cases (p=0.014 and 0.010, respectively).

Conclusions: Although classified as unilateral disease based on MRI and biopsy, 1/3 of such cases bear significant bilateral disease. These patients tend to have larger tumor burden as demonstrated by higher greatest length of PCa involvement in any single PBx core and greater MRI PCa suspicion levels. Focal therapy may not be the best option for these patients.

939 Rethinking the T2 Substaging of Prostate Cancer

Max Kong, Fang-Ming Deng, Weisheng Xu, Jonathan Melamed, Ming Zhou. New York University Langone Medical Center, New York, NY.

Background: AJCC staging categorizes organ-confined prostate carcinoma (PCa) into 3 substages, T2a, T2b and T2c, based on the extent of tumor involvement of the prostate gland. T2 substaging is highly controversial leading to calls for its abolition. This study examines the pathological features of T2 PCa in radical prostatectomy (RP) specimens to provide anatomical basis for T2 substaging.

Design: 283 RP specimens which harbored organ-confined PCa were examined. Tumor foci were considered separate if they were >3 mm from each other. All cancer foci were traced on the glass slides and then recorded on a "prostate map" with pathological data including Gleason score (GS), dimension and volume (TV) of each traced cancer focus.
Results: T2c could be further divided into 3 categories: T2c1 (discrete small tumor foci with any individual TV≤0.5 cc or size ≤10 mm in the lobe contralateral to the dominant tumor nodule (DN)), T2c2 (discrete tumor foci with any individual TV>0.5 cc or size >10 mm in the lobe contralateral to DN) and T2c3 (contiguous tumor nodule crossed the midline to involve bilateral lobes).T2c1 and T2c2 tumors, both staged as T2c based on the current AJCC criteria, had significantly different pathological features. T2c2 tumors had greater TV and higher GS than T2c1 tumors. GS was 6 and ≥7 in 73.9% (105/142) and 37 (26.1%) of T2c1 tumors and 44.8% (13/29) and 55.2 (16/29) of T2c2 tumors (p=0.017). TV of T2a PCa was significantly less than PCa in other subcategories. T2b and T2c1 had similar TV but were significantly smaller than T2c2 and T2c3 tumors. The latter two had similar TV.

T2 subcategory	T2a	T2b	T2c1	T2c2	T2c3
n	42	15	143	29	54
Mean TV (mm3)	0.23	0.51	0.59	1.02	1.15
P value	0.016				
		0.493			
			0.001		
				0.676	

Conclusions: Bilateral tumors currently staged as T2c could be divided into 2 groups: tumors with discrete small tumor foci with any individual TV≤0.5 cc and size ≤10 mm in the lobe contralateral to DN should be staged as T2b, while tumors with discrete tumor foci with any individual TV>0.5 cc or size >10 mm in the lobe contralateral to DN and contiguous tumor nodule crossing the midline be staged as T2c.

940 Quantitative Insulin-Like Growth Factor-1 (IGF-1) and Insulin Receptor (IR) RNA Expression in Prostate Cancer (PCA): Novel In Situ Assay and Clinical Implications

Myriam Kossai, Kenneth Hennrick, Theresa MacDonald, Lily Wang, David Nanus, Lewis Cantley, Mark Rubin, Juan Miguel Mosquera. Weill Medical College of Cornell University, New York, NY; Weill Medical College of Cornell University and New York Presbytarian hospital, New York, NY; The Sandra and Edward Meyer Cancer Center of Weill Medical College of Cornell University and New York Presbyterian Hospital, New York, NY.

Background: Genetic aberrations in PTEN, the negative regulator of PI3K signaling, are common in PCA with high Gleason Score and correlate with adverse outcome. Clinical trials with PI3K pathway inhibitors (PI3Ki) are currently in progress. PI3Ki patients develop drug-induced hyperinsulinemia in response to hyperglycemia. In contrast to metformin, insulin could reactivate PI3K signaling in the tumor; therefore offsetting the therapeutic effect of PI3Ki. We optimized chromogenic RNA ISH (Affymetrix) and evaluated IR and IGF1 RNA expression in localized vs. metastatic PCA.
Design: In this pilot study, RNA ISH was optimized in tissue microarrays (n=39 cases) and validated in corresponding biopsies. PC3 cells knockdown for IR or IGF1 (confirmed by Western blot) were used as controls. Quantitative image analysis was performed (RNAStudioScope).
Results: A subset of each localized and advanced PCA showed IR and IGF1 RNA overexpression. When compared, higher IR and IGF1 RNA expression was observed in advanced PCA (Figure).

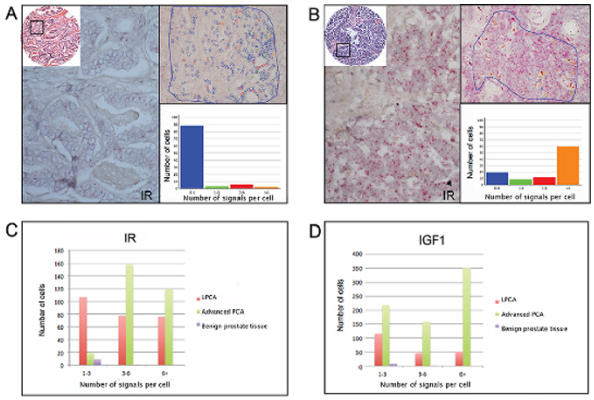

IR and IGF1 RNA ISH in prostate cancer. A) Localized prostatic adenocarcinoma, Gleason score 6. Quantitative image analysis for IR demonstrates that most cells have 0-1 signals (blue bar in histogram). B) Metastatic castrate resistant prostate cancer. Quantitative image analysis for IR demonstrates that most cells have >6 signals (orange bar in histogram). C) Histogram showing increased signals in advanced PCA compared to localized PCA corresponding to a higher IR mRNA expression. D) Histogram showing higher signals in advanced PCA compared to localized PCA corresponding to a higher IGF1 mRNA expression.

Conclusions: Chromogenic IR and IGF1 RNA ISH is a robust assay to quantify their expression in archival material. Comparison with protein expression by IHC is ongoing. IR and IGF1 RNA ISH will help in clinical trials investigating treatment of PI3Ki-induced hyperglycemia in PCA patients.

941 A Multiparametric Molecular Classifier for Improved Prediction of Prostate Cancer Prognosis

Stefan Kraft, Martina Kluth, Thorsten Schlomm, Ronald Simon, Guido Sauter. University Medical Center of Hamburg-Eppendorf, Hamburg, Germany; Martini Clinic, Hamburg, Germany.

Background: Better prognostic markers are urgently needed to distinguish between indolent and aggressive forms of prostate cancer from early on. While single markers are not sufficiently powerful for routine application, first generation commercial multiparametric test assays show promising results. We hypothesized that such test can be further optimized.
Design: A tissue microarray (TMA) containing 0.6 mm tissue cores from over 12,000 prostate cancer patients with long-term follow-up data was analyzed with more than 80 different antibodies and DNA probes by immunohistochemistry and FISH. Markers with strong and independent prognostic value in uni- and multivariate analyses were combined to obtain panels of markers that yield additional prognostic information beyond the standard parameters (including pre-operative PSA, Gleason grade, tumor stage, nodal stage) in a ROC analysis. For this purpose, a simple score (0-10 points) was determined based on the number and type of adverse features per tumor.
Results: Markers with strong independent prognostic relevance included deletions of 5q21 and PTEN, overexpression of RBM3, TUBB3, as well as nuclear accumulation of p53, indicating dominant-negative TP53 gene mutation. A total of 4,159 cancers harbored none of these alterations (score 0) and showed the best prognosis in a Kaplan-Meier plot using biochemical recurrence as the study endpoint. The worst prognosis was found for 570 tumors harboring ≥8 (score 8-10) of these alterations, while an intermediate prognosis with decreasing time to recurrence was found for cancers with scores 1-2 (n=2,365), 3-4 (n=1,499) and 5-7 ((n=1,111). The differences between the groups were highly significant (p<0.0001). The 5-gene classifier provided prognostic information independent from PSA, Gleason grade, stage, and nodal stage (p<0.0001).
Conclusions: Multiparametric classifiers have a high potential to improve the predictive accuracy of current established clinico-pathologic models. Analyses of very large sets of patient tissues are instrumental to identify the best candidates for such molecular marker panels. It is likely that continued analysis of our TMA will identify even better marker panels than the current 10-gene classifier.

942 Inverse Relation of Myc and p27 in Cribriform Pattern Prostate Cancer

Ibrahim Kulac, Jessica Hicks, Qizhi Zheng, Helen Fedor, Toby Cornish, Angelo De Marzo. Johns Hopkins University, Baltimore, MD.

Background: Prostate cancers composed exclusively of Gleason pattern 3 have an excellent prognosis, while those containing Gleason pattern 4 or higher are more aggressive. Gleason pattern 4 is composed of either fused glands, poorly formed glands or cribriform structures with cribriform structures being most readily recognized and shown to be of independent prognostic significance (PMIDS: 24145642; 25189638). However, the biological properties of these cribriform structures have not been studied. There is a spectrum of nuclear features in cribriform glands with cells towards the perimeter containing enlarged nucleoli, and open chromatin as compared to cells towards the center. Since MYC overexpression drives nucleolar enlargement we examined the pattern of expression of MYC protein in these structures. Also, we examined p27 staining since it has been reported to be more intense in the nuclei in the center of these structures (PMID:9731735).
Design: Cases with cribriform Gleason score 7 were used for IHC for MYC, p27 and Ki67 as well as double label immunofluorescence staining for p27 and MYC. Slides were scanned and regions were selected containing cribriform glands (N=18 total regions) and analyzed using image analysis software by Aperio Inc. We quantified the level of nuclear staining for MYC and p27 in relation to the outside/perimeter regions versus the inner aspect of the glands. Chromogenic in-situ hybridization for MYC mRNA was also performed.
Results: The increase in MYC staining in the perimeter aspects of the cribriform structures was highly significant as compared to the inner regions (P<0.0001, rank sum). Conversely, p27 staining showed an increase in the central region as compared to the perimeter aspect (P=0.0024). There was also a marked increase in staining for Ki67 (p<0.0001) as well as MYC mRNA in the perimeter cells. Double label fluorescent staining showed a tight inverse correlation between MYC and nuclear p27 staining.
Conclusions: Two distinct populations of cancer cells comprise cribriform carcinomas of the prostate; the central aspect is composed of cells with relatively small nucleoli that are non-proliferating with high levels of nuclear p27, and an outer layer that is composed of metabolically more active cells with increased MYC, nucleolar size and proliferative fraction. These findings provide new biological insights into the unique structure of cribriform prostate cancer lesions and suggest a complex interplay between the two cell types. Future studies are needed to determine how and whether these findings relate to disease aggresssiveness.

943 Concordance of ETS Fusion Status of Matched Metastatic Castration-Resistant Prostate Cancer and Primary Prostate Cancer: Data From NCI 9012, a Randomized ETS Fusion-Stratified Phase II Trial

L Priya Kunju, Nallasivam Palanisamy, Stephanie Daignault, Rohit Mehra, Javed Siddiqui, Shannon Carskadon, Przemyslaw Twardowski, Costantine Albany, Mark Stein, Walter Stadler, Jon Jacobson, Matthew Davenport, Scott Tomlins, Arul Chinnaiyan, Felix Feng, Maha Hussain. University of Michigan, Ann Arbor, MI; City of Hope Cancer Center, Duarte, CA; Rutgers Cancer Institute of New Jersey, New Brunswick, NJ; Indiana University, Bloomington, IN; University of Chicago, Chicago, IL.

Background: Fusions of androgen-regulated genes with ETS transcription family members have been reported in about 50% of localized prostate cancer (PCa) patients (pts), with *TMPRSS2-ERG* fusions being the most common. Preclinical models suggest that inhibition of Poly (ADP-ribose) polymerase 1 (PARP1) is preferentially cytotoxic to ETS translocation positive disease. A clinical trial of abiraterone +/- the PARP inhibitor veliparib, stratified by ETS translocation status is in process. An important secondary end point includes assessment of ETS status concordance between primary Pca and metastatic site.

Design: Eligible metastatic castrate resistant PCa (mCRPC) pts undergo a metastatic site biopsy to determine ETS fusion status by immunohistochemistry (ERG), fluorescent in-situ hybridization and/or RNA in-situ hybridization (ETV1) and next-generation sequencing (ETV4). Soft tissue biopsies are performed using 18-gauge needle: 1-cm core (≥ 6 specimens), 2-cm core (≥4 specimens) and CT guided bone biopsies using 11-15 gauge needle : 2-8 cores. We report interim results on rates of positive biopsy, ETS status/type and concordance between primary PCa and metastasis as well as SPINK1 protein expression in primary PCa.

Results: To date, 140 pts (Caucasians: 81%, African Americans 11%, Other 8%) with a median age of 70 years and a median PSA of 27.9 ng/ml have been enrolled. Of these, 60 pts had soft tissue and 76 had bone biopsies. All soft tissue and 55 (72%) bone biopsies were evaluable for analysis (21/136, 15% had no tumor). ETS fusion status was positive in 41/115 (36%) pts including ERG (30%), ETV1 (5%) and ETV4 (1%). Concordance of ETS status between primary PCa and metastatic site was noted in 55/61 pts (90 % [95% CI: 80-96%]. SPINK 1 expression was noted in 22% of primary PCa and was present exclusively in ETS negative pts.

Conclusions: Real time biopsies with adequate tumor yield and biomarker determination in mCRPC are feasible but more challenging in bone biopsies. ETS positivity rate (36%) including ERG and ETV1 protein expression in this mCRPC cohort analyzed to date is comparable to similar published cohorts. We demonstrate significant concordance of ETS status between primary PCa and metastasis in the subset analyzed to date.

944 Identifying TFE3 Related Translocation RCC By TCGA Pathology Reports and RNA-Seq Data

Boaz Kurtis, Yong Mao, Weihua Huang, Sitharthan Kamalakaran, Minghao Zhong, Nevenka Dimitrova, John Fallon. New York Medical College at Westchester Medical Center, Valhalla, NY; Philips Research North America, Briarcliff Manor, NY.

Background: *TFE3* translocation Renal Cell Carcinoma (RCC) is a distinct subtype of RCC with unique pathological- morphological features and clinical behavior. TFE3 IHC stain and *TFE3* break apart FISH can be useful accessory tools for the diagnosis. However, due to the limitation of these methods and overlapping morphological features with other subtypes RCC, it is not uncommon to misdiagnose *TFE3* translocation RCC to other common subtype RCC, such as clear cell renal cell carcinoma RCC (CCRCC) or papillary renal cell carcinoma (PRCC).

Design: *TFE3* translocation Renal Cell Carcinoma (RCC) is a distinct subtype of RCC with unique pathological- morphological features and clinical behavior. TFE3 IHC stain and *TFE3* break apart FISH can be useful accessory tools for the diagnosis. However, due to the limitation of these methods and overlapping morphological features with other subtypes RCC, it is not uncommon to misdiagnose *TFE3* translocation RCC to other common subtype RCC, such as clear cell renal cell carcinoma RCC (CCRCC) or papillary renal cell carcinoma (PRCC).

Results: We confirmed previously published 4 cases TCGA CCRCC with *SFPQ-TFE3* translocation. We also have identified additional 3 cases with *TFE3* related translocations in those 26 TCGA cases of PRCC: TCGA-G7-7501 with *SFPQ-TFE3* translocation; TCGA-BQ-5882 with *PRCC-TFE3* translocation; TCGA-BQ-7048 with *COL21A1-TFEB* translocation.

Conclusions: In this study, we demonstrate that it is feasible to identify *TFE3* related translocation RCC by combination of morphology and analyzing RNA-seq data. This result suggests that RNA-seq in the right clinical context can potentially be used clinically to identify chromosomal translocations with detailed information that routine IHC and FISH cannot provide: exact break point, partner gene or even novel translocation, such as *COL21A1-TFEB* translocation in current study.

945 Evaluation of Prox-1 Expression in Germ Cell Tumors and Its Utility as a Diagnostic Adjunct

Thanh Lan, Tatjana Antic. University of Chicago, Chicago, IL.

Background: Prox-1, prospero-related homeobox-1, is a transcription factor critical for lymphangiogenesis. Positive Prox-1 expression is described in lymphatic endothelium as well as a number of vascular neoplasms. Of note, Prox-1 staining has been observed in the normal developing yolk sac epithelium. However, it is not known whether Prox-1 is expressed in yolk sac tumor (YST) or other germ cell neoplasms. The aim of this project is to evaluate the expression of Prox-1 and its diagnostic utility in the setting of germ cell neoplasms, specifically YST, as compared to other established markers for YST such as AFP and CDX2.

Design: Formalin-fixed, paraffin-embedded sections from germ cell tumors identified from our institution's pathology archive (2005-2012) were cut at 4 µm-thick sections and immunolabed with Prox-1 (1:200), AFP (1:200), and CDX2 (1:200). Hemotoxylin and eosin sections for all cases were reviewed by two pathologists to confirm diagnosis and composition of mixed germ cell tumors. The percentage of germ cell tumor volume with nuclear immunoexpression was scored as negative, weak, moderate, or strong.

Results: Except for lymphatic endothelia and spermatids, which displayed a peri-nuclear pattern, other constituents of the seminiferous tubules, rete testes, epididymis, and stroma were negative for Prox-1 (n=11). 17 mixed germ cell tumor, 5 classic seminoma, 1 pure embryonal carcinoma, 2 choriocarcinoma, and 2 pure YST were studied (n=25). A component of YST was present in 15 cases, constituting <5% to 100% of tumor volume by H&E morphologic assessment. Prox-1 immunolabeling was absent in all seminoma, embryonal carcinoma, and teratoma. Rare multinucleated syncytiotrophoblasts in choriocarcinoma showed weak immunolabeling. Of the germ cell tumors with YST, 10 cases (67%) showed Prox-1 expression with variable intensity and distribution. 4 of these cases showed strong staining in at least 30% of the YST component. Interestingly, in these same 4 cases, CDX2 and AFP expression were markedly decreased in intensity, distribution, or both. In 4 of the 5 YST where Prox-1 is entirely absent, CDX2 and AFP were strongly expressed (30%-100% of tumor volume).

Conclusions: Prox-1 is a reliable marker for lymphatic endothelial cells. Little is known about expression of Prox-1 in germ cell tumors. Prox-1 does not appear to be a sensitive marker for YST compared to AFP and CDX2, but its strong expression in difficult cases where these stains are unequivocal or difficult to interpret suggests that it may be a useful adjunct tool in the diagnostic workup of germ cell neoplasms.

946 Progression-Free Survival Depends on Type and Extent of Invasion in pT1 Papillary Cancers of the Bladder

Margaret Lawless, Roman Gulati, Maria Tretiakova. University of Washington, Seattle, WA.

Background: Pathologic stage T1 (pT1) bladder cancers are a clinically heterogeneous group, although current guidelines for superficially invasive cancers do not discriminate between different levels of lamina propria invasion. Several substaging systems were proposed but showed either high inter-observer variation or no improvement in predicting recurrence or progression. Here we employed a novel approach to papillary pT1 substaging with respect to type and extent of invasion of the lamina propria and evaluated outcomes over long-term follow-up.

Design: Stage pT1 urothelial neoplasms from the years 1999-2009 were retrospectively reviewed and characterized as focal invasion confined to papillary stalk, focal invasion of tumor base, or extensive (multifocal) invasion of tumor base. Cases with high-grade or low-grade papillary lesions were included; cases with concurrent flat carcinoma in-situ, angiolymphatic space invasion, absent muscularis propria, or clinically advanced disease were excluded. We examined progression-free survival (PFS), defined by time to stage or grade progression or recurrence with death censored, using Kaplan-Meier estimation stratified by type and extent of invasion.

Results: Among 54 patients (n=50 high-grade and n=4 low-grade) satisfying inclusion criteria, 22 of 28 patients with base extensive invasion progressed while 1 of 11 with base focal and 0 of 15 with stalk only invasion progressed over a median of 2.5 years of follow-up. There is strong evidence that base extensive patients had worse PFS compared with base focal or stalk only counterparts ($p < 0.0001$ from log-rank test). Median PFS in this group was 4.8 (95% confidence interval 3.7 to 22.8) months.

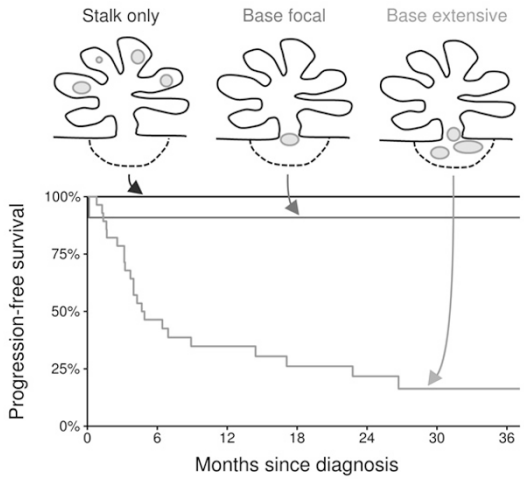

Stalk only	15 100%	15 100%	15 100%	13 100%	9 100%	9 100%	9 100%
Base focal	11 100%	10 91%	9 91%	9 91%	9 91%	8 91%	8 91%
Base extensive	28 100%	13 46%	10 35%	7 26%	6 22%	4 16%	4 16%

Conclusions: Our results suggest that site and extent of lamina propria invasion in patients with pT1 papillary urothelial cancers are significantly associated with risks of progression and prognosis. Our novel pT1 substaging system, if supported by a larger cohort, may be useful for improved prediction of recurrent or progressive disease.

947 Renal Angiomyoadenomatous Tumor (RAT): A Separate Entity or a Spectrum of Clear Cell Papillary Renal Cell Carcinoma (ccpRCC)

Jeong Hyeon Lee, Bryce Portier, Mi-sung Kim, Haijun Zhou, Kosuke Miyai, Mukul Divatia, Steven Shen, Alberto Ayala, Jae Ro. Houston Methodist Hospital, Houston, TX; Korea University Anam Hospital, Seoul, Korea; Asan Medical Center, Ulsan, Korea.

Background: RAT is a recently described candidate entity, characterized by clear cells, leiomyomatous stroma, and adenomatous structures. ccpRCC is one of newly proposed epithelial tumor entity, characterized by clear cells of low nuclear grade, and variable papillary, tubular, acinar, and cystic architectures. ccpRCCs may show smooth muscle bundles within the intratumoral stroma and share morphologic features of RATs. Therefore, it is currently unclear whether the RAT and ccpRCC are related, and criteria for diagnosing of RATs are still lacking.

Design: In this report, we present 4 RAT and 9 ccpRCC cases and describe their clinicopathologic and immunohistochemical (IHC) characteristics.

Results: 7 patients were male and 6 were female (M:F ratio of 2:2 in RAT, 5:4 in ccpRCC). The age ranged from 36 to 80 year (average 64.5 in RAT, 62.3 in ccpRCC). Tumor sizes averaged 2.1cm in RAT (range 0.9-3.5) and 2.43cm in ccpRCC (range 1.2-6). One patient had bilateral tumors: RAT on the left, and ccpRCC on the right kidney. All tumors were stage I and had a Fuhrman grade of 2, except for 1 ccpRCC of nuclear grade 1.

The leiomyomatous stroma in RATs formed abortive vascular structures and its amount averaged 50% (range 30-80), whereas the smooth muscle stroma in ccpRCCs was focal (<10%). The RAT muscular stroma could be divided into capsular and intratumoral stroma. 2 RATs had more intratumoral than capsular stroma, but the other 2 RATs were reversed. RAT and ccpRCC exhibited unique epithelial components: RATs were characterized by the monomorphic cells with basally located basophilic nuclei lacking linear polarization, and by the apical clear snouts ("shark smile"). In contrast, epithelial cells present in the ccpRCCs displayed a characteristic linear arrangement of nuclei away from the basal aspect of cells.

Immunohistochemically, RAT and ccpRCC expressed CK7, but did not express AMACR and RCC marker. CD10 immunostaining was faintly positive in focal patches of RATs, but not ccpRCCs.

Conclusions: In summary, this study compared the histologic and IHC features of RAT and ccpRCC. We found that in addition to leiomyomatous stroma, there are also some cytologic differences between the two, although both have similar clinical manifestation and IHC profile. Additional molecular studies including next generation sequencing are underway to further elucidate their histogenesis.

948 Micro RNas and Androgen Receptor in Prostate Cancer

Katia Leite, Denis Morais, Manuel Florez, Sabrina Reis, Nayara Viana, Miguel Srougi. University of São Paulo School of Medicine, São Paulo, Brazil.

Background: Molecular mechanisms involved in the androgen receptor (AR) activity in prostate cancer (PC) are not completely understood. Autocrine/paracrine phenomenon, mutations and alternative splicing of AR and even post-transcriptional control of AR expression have been studied. Micro RNAs are a class of small no coding RNAs responsible for the control of at least 30% of genes. Our aim is to study miRNAs related to the control of AR in localized PC.

Design: Based on the literature and Targetscan we studied the expression levels of miRNAs 9, 34a, 34c, 130a, 185, 299-3p, 371, 421 and 541 that have as target AR in 83 patients that underwent radical prostatectomy. Using lipid based assay we performed transfection of miR-371 in LNCaP and PC3 PC cell lines. Also, LNCaP cells were treated with Dyhydrotestosterone (DHT) and Flutamide followed by determination of miRNAs expression. The levels of AR and miRNAs were studied using qRT-PCR.

Results: AR was overexpressed in 89.2% of the cases. 5 from 9 miRNAs were underexpressed in the majority of cases: miRNAs 9 (73.5%), 34c (69.9%), 185 (80.7%), 371 (85.5%) and 541 (75.9%). Underexpression of miR-371 was related to non-organ confined disease (pT3)(p=0.009). miR-371 was not expressed by metastatic PC cell lines (LNCaP and PC3). AR expression was reduced in 22% to 28% in LNCaP and PC3 cells respectively after miR-371 transfection and KLK3 was also reduced in 51%. LNCaP treatment with DHT (100 nM) resulted in reduction in the expression of miR34a, 34c, 185, 21. Flutamide promoted a reduction in the expression of miRNAs 9, 34a, 34c, 21, 185. This effect was abolished when cells were treated with both flutamide and DHT 10nM.

Conclusions: miR-371 could influence PC behavior since its underexpression is related to non-organ confined disease probably failing to control AR. Also, treating LNCaP cells with DHT and Flutamide we showed change in the expression levels of many miRNAs involved in the control of important genes related to essential cell processes.

949 Uroplakin II Expression Is Maintained in Primary and Corresponding Metastatic Invasive Urothelial Carcinomas, and Is a Useful Marker, Particularly in Combination With GATA-3, for Identification of Carcinomas of Unknown Origin

Mariah Leivo, David Tacha, Donna Hansel. University of California San Diego, La Jolla, CA; Biocare Medical, Concord, CA.

Background: Uroplakin II (UPII) is an inherent protein of urothelial plaques, which are unique structures of urothelial differentiation. Our study aims to develop a panel containing innovating biomarkers UPII, GATA-3 and p40 for the diagnosis of invasive UCs. We compared the expression of those biomarkers on tissue microarrays (TMA) containing normal urothelium, high-grade invasive UCs and metastatic UCs. These markers are all promising in diagnosing challenging cases of UC, and have not been tested together.

Design: In this cohort study, each case was represented by four distinct punches on the TMA and a total of 64 cases were assembled and included: 8 primary invasive UCs; 46 metastatic invasive UCs and their respective metastases; and 10 normal urothelium specimens. Immunohistochemistry was performed using UPII, GATA3, and p40 antibodies. The positive cases were scored on staining intensity and proportion. Statistical differences of the immunostains scores were tested by the Wilcoxon matched-pairs test.

Results: UPII showed diffused membranous and cytoplasmic expression, and GATA3 and p40 showed nuclear staining. The overall positivity rates for UCs were: GATA-3 (100%), p40 (63%) and UPII (93%). The expression of GATA-3 and p40 was lower in metastatic tumors than in primary UCs (p=0.044 and p=0.003, respectively). On the other hand, UPII expression was higher in high-grade UCs than in normal urothelium (p=0.0015). An additional observation was the fact that UPII expression was highly maintained when moving from primary tumors to the related metastatic lesions in the lymph nodes. UPII expression was maintained in 88% of the metastatic lesions, where GATA-3 only corresponded in 37% and p40 in 50% of the cases.

Conclusions: The idea of constructing a panel of new biomarkers to confidently identify UCs drove our study. GATA-3 was positive in 100% of the UCs, while UPII was positive in 93%. UPII's high likelihood to maintain the same intensity and proportion of its expression in both primary UCs as well as their corresponding metastatic lesions is an advantage over other biomarkers in identifying carcinomas of unknown origin. Moreover, the difference in the sub-cellular staining patterns for GATA3, with its high sensitivity, and UPII, with its high specificity, means that these two markers may be used together as a urothelial panel to more accurately identify challenging cases of UC.

950 Urothelial Cysts of the Foreskin: Morphological and Immunohistochemical Characterization

Cecilia Lezcano, Alcides Chaux, Elsa Velazquez, Nilda Gonzalez-Roibon, Enrique Ayala, Ingrid Rodriguez, George Netto, Antonio Cubilla. University of Pittsburgh Medical Center, Pittsburgh, PA; Norte University, Asunción, Paraguay; Tufts University Medical Center, Miraca Life Center, Boston, MA; Johns Hopkins University, Baltimore, MD; Instituto de Prevision Social, Asunción, Paraguay; Instituto de Pathologia e Investigacion, Asunción, Paraguay.

Background: The majority of penile cysts are diagnosed as median raphe cysts due to their location on the ventral midline region. Their histogenesis is controversial. We present cysts exclusive of the foreskin, two of which arose in the dorsal aspect of the penis.

Design: Ten cysts of the foreskin were retrieved from the archives of the Instituto de Patología e Investigación in Asunción, Paraguay for evaluation of clinical, morphological and immunophenotypical features.

Results:

Patient	Age*	Site	Epithelial lining	CK7†	p63‡	Throm‡	GATA-3
1	8m	D	Cuboidal	+	+	Focal	-
2	19	D	Pseudostratified columnar	+	+	-	+
3	68	V	Pseudostratified columnar/Squamoid	+	+	-	+
4	ND	V	Pseudostratified columnar/Squamoid	+	+	-	+
5	ND	V	Pseudostratified columnar/Squamoid	+	+	+	+
6	44	V	Pseudostratified columnar/Squamoid	+	+	+	+
7	19	V	Pseudostratified columnar	+	+	-	+
8	36	V	Pseudostratified columnar	ND	ND	-	+
9	ND	V	Pseudostratified columnar	ND	ND	-	+
10	17	V	Cuboidal	ND	ND	ND	ND

*** years, m= months; ND= no data; D= dorsal; V= ventral; Thrombo= thrombomodulin; †mainly in superficial layers; ‡mainly in basal layers.**

Conclusions: The majority of cysts arose in the ventral penis and presented pseudostratified and columnar lining with mucinous glands often with areas of squamous epithelium. These features, and the positivity for CK7, p63 and GATA-3 found in the majority of the cases, are similar to those of distal urethral epithelia indicating that most foreskin cysts are urothelial.

951 Fibroblast Growth Factor 7 Overexpression Is an Independent Prognosticator for Patients With Urothelial Carcinoma of the Upper Urinary Tract and Urinary Bladder

Chien-Feng Li. Chi Mei Medical Center, Tainan, Taiwan.

Background: Urothelial carcinoma (UC) of urinary bladder (UBUC) and upper tract (UTUC) is the most common type of tumor occurring in the urinary tract, while its molecular pathogenesis and survival determinants remain obscure. By data mining a published transcriptomic database of UBUCs (GSE31684), we identified *fibroblast growth factor 7 (FGF7)* as the most significant gene upregulated during UC progression. We therefore used our well-characterized cohort of UC to analyze *FGF7* transcript and protein expression and its clinicopathological significance.

Design: We used real-time RT-PCR assay to detect *FGF7* transcript level in 20 UTUC and 20 UBUC fresh samples. Immunohistochemistry evaluated by H-score was used to determine FGF7 protein expression in 340 UTUCs and 295 UBUCs. The transcript and protein expression were correlated with clinicopathological features. We then further evaluated the prognostic significance of FGF7 protein expression for disease-specific survival (DSS) and metastasis-free survival (MeFS).
Results: Increased *FGF7* transcript level was associated with higher pT in UTUCs and UBUCs (P=0.041 and 0.008, respectively). In both groups of UCs, FGF7 protein overexpression was also significantly associated with advanced pT status (both P<0.001), lymph node metastasis (UTUC, P=<0.002; UBUC, P<0.004), high histological grade (UTUC, p=0.019; UBUC, P<0.001), vascular invasion (both P<0.001), perineurial invasion (UTUC, P=0.002; UBUC, P=0.021) and frequent mitoses (UTUC, P=0.002; UBUC, P=0.042). FGF7 overexpression predicted dismal DDS and MeFS in both univariate and multivariate analysis.
Conclusions: Our study shows that FGF7 overexpression is associated with advanced clinical features for both UTUC and UBUC patients, justifying its potential prognostic value in UC.

952 Immunohistochemical Distinction of Primary Adrenal Nodules, Including Oncocytic Tumor, From Metastases of Renal Cell Carcinoma To the Adrenal

Hongmei Li, Ondrej Hes, Gregory MacLennan, Kenneth Iczkowski. Medical College of Wisconsin, Milwaukee, WI; Charles University Hospital, Plzen, Czech Republic; Case Western Reserve University, Cleveland, OH.
Background: Metastases of renal cell carcinoma to the adrenal, when low-grade, have a morphology that overlaps with normal or adenomatous adrenal, and when higher-grade, with primary adrenal carcinoma. Diagnostic dilemmas are hardest when based on needle biopsy material. An optimal immunostaining panel, as well as the immunoprofile of the rare Oncocytic adrenal tumor, have not been defined.
Design: We compared 34 cases of clear cell renal cell carcinoma metastatic to adrenal with 49 primary adrenal lesions (16 carcinoma, 22 adenoma, 9 oncocytic tumor, 2 hyperplasia). Normal adrenal was available in 59 cases. Each entity was represented on tissue microarrays by 2 or 3 evaluable spots taken from spatially separate areas. A panel of 12 immunohistochemical stains was used, including the first uses of a steroid receptor coactivator (SRC1) and equilibrative nucleoside transporter 1 (ENT1) for this diagnosis. 2 pathologists evaluated reactivity from 0 -3+. Logistic regression with generalized estimating equations (GEE) was performed. Decision rules were based on sensitivity and specificity using a 2+ cut point.
Results: The most sensitive and specific renal cell carcinoma markers were membranous reactivity for carbonic anhydrase IX (CAIX) and RCC Marker (together: sensitivity 0.82, specificity 0.95, p<0.0001) and nuclear reactivity for Paired box 8 (PAX8). For adrenal cortical carcinoma, best markers were synaptophysin (sensitivity 0.77, specificity 0.68) followed by SRC1, MelanA, and membranous ENT1 (**Fig.**).

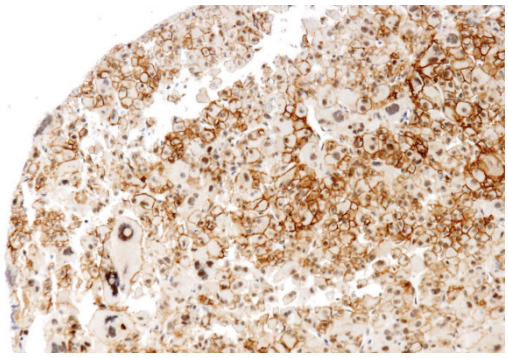

For Oncocytic tumor, synaptophysin (sensitivity 0.44, specificity 0.80) and ENT1 were optimal. Optimal markers for adrenal cortical adenoma and normal adrenal were ENT1 (more specific), and either MelanA or SRC1 (more sensitive). Calretinin, cytokeratin 34βE12 and CAM5.2, inhibin, and steroidogenic factor 1 (SF1) proved less discriminatory.
Conclusions: Tumors with high-grade cytology should be worked up with 2 of the 3 stains: CAIX, PAX8, or RCC Marker; plus synaptophysin, and either SRC1 or Melan-A. To distinguish normal or adenomatous adrenal from low-grade renal cell carcinoma, use ENT1, and either SRC1 or Melan-A, plus CAIX, PAX8, or RCC Marker.

953 Distinct Expression of MicroRNAs in Micropapillary Variant of Urothelial Carcinoma

Yu Liang, Khalida Wani, Yan Wang, Bogdan Czerniak, Charles Guo. University of Texas MD Anderson Cancer Center, Houston, TX.
Background: Micropapillary carcinoma (MPC) is a rare variant of urothelial carcinoma with unique morphology and aggressive biological behavior. MicroRNAs (miRNAs) are small non-coding RNA molecules which regulate RNA silencing and post-transcriptional gene expression. Recent studies have revealed that the aberrant expression of microRNAs (miRNAs) plays an important role in bladder cancer. We aimed to study the expression of miRNA in MPC in comparison with conventional urothelial carcinoma (CVC).
Design: Total RNA was extracted from formalin-fixed and paraffin-embedded tissues of 20 MPCs and 20 CVCs. RNA samples were subjected to miRNA analysis using RT-PCR based microfluidics array cards containing 378 annotated miRNAs. The expression level of each miRNA was compared between MPC and CVC by student t-test with p-value <0.05 being considered statistically significant. The association of differential miRNA expression with patient's survival was evaluated by Kaplan-Meier analysis.
Results: The MPC group included 18 males and 2 females (median age=73 years), and the CVC group included 15 males and 5 females (median age=65 years). All MPCs and CVCs were high grade and invasive. In the miRNA analysis, MPCs had significantly higher levels of 9 miRNAs and lower levels of 74 miRNAs than CVCs. A panel of these differentially expressed miRNAs accurately distinguished MPCs from CVCs. Informatics analysis revealed that these microRNAs were potentially involved in the regulation of multiple signal pathways, including EGFR and TGFB1. Clinical followup information showed that MPC patients with high levels of miR-339-3p had a mean survival of 25 months, which was significantly worse than those with low levels (48 months) (p=0.027).
Conclusions: Our study demonstrates that MPC has a distinct expression pattern of miRNAs from CVC. The differentially expressed miRNAs can be used to accurately distinguish MPC from CVC as well as to predict the outcome of patients with MPC. The distinct expression of miRNAs in MPC also suggests that it may employ different molecular signaling pathways during cancer development and progression.

954 Immunohistochemical Evaluation of NKX3.1 Expression in Human Tumors

Haiyan Liu, Fan Lin. Geisinger Medical Center, Danville, PA.
Background: NKX3.1 is a prostate-specific homeobox gene located on chromosome 8p21. In human tissues, NKX3.1 expression was reported to be highly specific for prostate, testis and breast; however, the data is limited. In this study, we investigated NKX3.1 expression in 1864 tumors from various organs.
Design: Immunohistochemical analysis of NKX3.1 (CP422A,B, Biocare) expression was conducted on tissue microarray sections, including a total of 1864 tumors. In addition, benign prostatic and seminal vesicle tissues (24 cases each) were tested. The nuclear staining was interpreted as negative, 1+, 2+, 3+, and 4+.
Results: The staining results are summarized in the table. One hundred percent of prostatic adenocarcinomas (ADCs) expressed NKX3.1, with diffuse nuclear staining in the majority of cases. The same pattern was seen in benign prostatic tissues, whereas none of the benign seminal vesicle tissues was positive. Eleven percent of invasive lobular carcinomas (CAs) and 33% of invasive ductal CAs of the breast also expressed NKX3.1. All other tumors, except a pulmonary squamous cell carcinoma (SqCC), were negative for NKX3.1, including germ cell tumor of the testis.

NKX3.1 Expression in 1864 Tumors

Tumor	N. of Positive/Total	Percentage
Prostatic ADC, usual type	137/137	100%
Prostatic ADC, foamy gland	22/22	100%
Breast invasive lobular CA	10/90	11%
Breast invasive ductal CA	13/40	32.5%
Uterine CA	0/268	0%
Cervical CA	0/39	0%
PSCa and CCCa	0/110	0%
Pancreatic ADC	0/56	0%
CCRCC/PRCC	0/120	0%
ChRCC/oncocytoma	0/30	0%
Testical germ cell tumor	0/46	0%
Invasive urothelial CA	0/48	0%
Esophageal ADC	0/48	0%
Colorectal ADC	0/126	0%
Hepatocellular CA	0/36	0%
Mesothelioma	0/17	0%
Lung SqCC	1/74	1%
Lung ADC	0/234	0%
Lung NET	0/58	0%
Pancreatic NET	0/34	0%
Skin NET	0/40	0%
Melanoma	0/93	0%
SqCC of ENT	0/50	0%
Papillary thyroid CA	0/48	0%

PSCa:papillary serous carcinoma of ovary; CCCa:clear cell carcinoma of the uterus and ovary; CCRCC:clear cell renal cell carcinoma; PRCC:papillary renal cell carcinoma; ChRCC:chromophobe renal cell carcinoma; NET:neuroendocrine tumor.

Conclusions: These data demonstrate that NKX3.1 is a highly sensitive and relatively specific prostate immunomarker, with the exception of mammary CAs. NKX3.1 should be included in the panel of immunomarkers for the identification of prostate origin when working on metastatic tumors of unknown primary.

955 BK Polyoma Virus Reactivation Is Associated With Increased Risk of Bladder Carcinomas in Solid Organ Transplant Patients

Sandy Liu, Alexander Berrebi, Levi Machado, John Papadimitriou, Cinthia Drachenberg, Allen Burke, Borislav Alexiev. University of Maryland, Baltimore, MD; Universidade Federal do Ceará, Fortaleza, Ceará, Brazil.

Background: The risk for malignancy is increased in transplant patients. Reactivation of latent BK polyomavirus (BKV) infection following renal transplantation is relatively common and causes BKV-associated nephropathy and allograft failure. Although BK virus has been clearly shown to cause cancers in animal models, to date, no study has demonstrated a significant association of BK reactivation in the genitourinary tract with an increased risk of genitourinary cancers in transplant patients.

Design: We conducted a retrospective cohort study, single institution study for BK replication through an electronic search of all kidney biopsies and urine cytologies with "polyoma" over a 16 year period with at least 12 months of follow-up. The inclusion criteria for BK reactivation were one positive kidney biopsy demonstrating BK nephritis, at least two positive urine cytologies, or any positive BK viremia. A total of 402 solid organ transplant patients (401 kidney, 1 heart) had BKV reactivation (BKV+) and were randomly matched with 402 transplant controls (BKV-) (401 kidney, 1 pancreas).

Results: There was a significantly increased risk of bladder cancers in the BKV+ cohort ($p<0.001$, Kaplan-Meier, log-rank), but not other types of cancers. In the BKV+ cohort, seven patients developed a total of 8 primary bladder cancers: 2 high-grade, non-invasive papillary urothelial carcinomas, 5 invasive high-grade urothelial carcinomas, and 1 invasive urothelial carcinoma with clear cell and giant cell features. In 7 of 7 patients, there was positive polyoma urine reactivation and in 6/7 patients, there also was BK nephritis on kidney biopsy. In 5 of 7 bladder cancers, there was polyoma viral LT antigen presence, confirmed by SV-40 immunostain. Zero patients in the control group developed bladder cancers. The mean follow-up time to develop bladder cancer was 94 months. BK reactivation was also significantly associated with older age ($p<0.001$), male gender ($p<0.001$), and Caucasian race ($p=0.002$).

Table 1: Clinical variables by BKV status

	BKV+	BKV-	Total	P value
Count	402	402	804	
Mean clinical f/u (mo)	84.9	94.2	89.6	0.002
Mean Age (yrs)	50.9	47.7	49.3	<0.001
Gender				
Male	300	239	539	<0.001
Female	102	163	265	
Race				
Whites	210	155	365	0.002
Blacks	169	232	401	
Other	23	15	38	
Bladder Cancer (#)	8	0	8	<0.001
Prostate Cancer (#)	1	4	5	0.24
Kidney Cancer (#)	7	7	14	0.97
Other Cancer (#)	8	7	15	0.50

Conclusions: BKV reactivation is significantly associated with urothelial carcinomas and is preceded by BK nephritis and or positive urine viral cytopathic effect.

956 AR-V7, a Splicing Variant of Androgen Receptor, Is Upregulated in High-Grade Urothelial Carcinomav

Xichun Liu, Liang Cheng, Yang Zhan, Yan Dong, Max Kong, Ming Zhou, Jonathan Melamed, Haitao Zhang, Peng Lee, Fang-Ming Deng. Tulane University School of Medicine, New Orleans, LA; Indiana University School of Medicine, Indianapolis, IN; New York University Langone Medical Center, New York, NY.

Background: The androgen receptor (AR) and its pathway have been implicated in tumorigenesis and progression of bladder urothelial cancer (BCa). Recent studies identified at least 15 splicing variants of AR (AR-Vs). Structurally, AR-Vs have insertions of cryptic exons downstream of the exons that encode the DNA-binding domain or deletions of the exons encoding the ligand-binding domain, resulting in a disrupted AR open reading frame and expression of ligand-binding-domain-truncated AR proteins. Some of the AR-Vs including AR-V7 remain constitutively active as a transcription factor and are associated with aggressive disease in prostate cancer. The AR-V expression in human BCa specimens has not been studied. We explored whether the status of AR-V7 associates with divergent biological behaviors and can be used to distinguish low-grade non-invasive from high-grade invasive BCa.

Design: Thirty-two cases consisting of 22 high-grade and 10 low-grade BCa were tested in this preliminary study. Cancer areas were macrodissected from formalin fixed paraffin embedded sections with total RNA extracted using the PureLink® FFPE RNA Isolation Kit (Invitrogen). Reverse transcription was performed by using the SuperScript® III Reverse Transcriptase Kit (Invitrogen). cDNA from reverse-transcription was used for real-time PCR analysis. AR-V7 expression was presented as negative cycle number difference to housekeeping gene (-delta CT).

Results: AR-V7 is expressed in all 10 low-grade BCa cases, at a similar level to normal urothelial mucosa. The expression levels (-delta CT values) of low-grade BCa vary from -15.5 to -1.6 with mean of -8.8±5.0. AR-V7 is detected in 20/22 cases of high-grade BCa, with -delta CT values ranging from -6.8 to 1.7 (-1.7±2.2). The expression level is significantly higher in high-grade BCa ($p<0.0001$). Using -5.0 as cutoff, the positive and negative predictive values for high-grade BCa are 95.5% and 87.5%, respectively.

Conclusions: These data, for the first time, indicate overexpression of AR-V7 in high-grade urothelial carcinoma and warrant future studies in cohorts with large numbers of cases. AR-V7 may serve as a useful biomarker to differentiate high- from low-grade BCa and raise the potential for use as a therapeutic target.

957 Urothelial Carcinoma With Squamous Differentiation in Urinary Bladder Is Associated With High Tumor Stage and Pelvic Lymph Node Metastasis

Yunguang Liu, Bo Xu. Roswell Park Cancer Institute, Buffalo, NY.

Background: Urothelial carcinoma (UC) is well known for its divergent differentiation resulting in distinct morphologic variants. Squamous differentiation occurs in more than 20% of UC of bladder and is thought to be an unfavorable prognostic factor. However, conflicting data were reported regarding the adverse factors associated with squamous differentiation. The aim of this study is to compare tumor pathologic stage and pelvic lymph node metastasis of invasive UC with (UC-Squ) and without (UC-NOS) squamous differentiation.

Design: Cases with diagnosis of UC and treated with cystectomy were selected for past 12 years (2002-2014). Cases with non-invasive carcinoma, without residual tumor, and containing UC variants other than UC-NOS and UC-Squ were excluded. Cases without lymph node dissection were also excluded. Two-tier system is adopted for stage analysis. T1 and T2 disease were grouped into organ-confined category, while T3 and T4 were grouped into high stage. For UC-Squ, the extent of squamous differentiation is semi-quantified as non-extensive (£20%) and extensive (>20%). Two-sample Z-test for the Difference between Proportions was used for statistical analysis.

Results: 195 cases of invasive UC, including 153 UC-NOS and 42 UC-Squ, were identified from 352 radical cystectomy specimens. Squamous differentiation occurs in 21.5% (42/195) of cases and extensive squamous differentiation is noted in 47% (20/42) of UC-Squ cases. Patients with UC-Squ display significant higher rate of high stage disease than those of UC-NOS (79% vs 56%, $p<0.01$). Lymph node dissection was performed on 92% cases (179/195) including 143 UC-NOS, and 36 UC-Squ. Although there is no significant difference of nodal metastasis (N1 to N3) between UC-Squ and UC-NOS (42% vs 29.4%, $p=0.09$), the nodal metastatic rate in UC with extensive squamous differentiation is significantly higher than that in UC-NOS (55% vs 29.4%, $p<0.05$).

Conclusions: Our study demonstrates that advance tumor stage associated with UC-Squ can be one of the contributing factors for its unfavorable clinical outcome. Extent of squamous differentiation in invasive UC should be documented as high rate of pelvic lymph node metastases is associated with UC containing extensive squamous differentiation.

958 TMPRSS2-ERG and SLC45A3-ERG Single and Double Rearrangements in Prostate Cancer: Effects on ERG Overexpression and Relationship With Tumor Grade

Josep Lloreta-Trull, Alba Font, Silvia de Muga, Nuria Juanpere, Marta Lorenzo, Raquel Albero, Ivonne Vazquez, Sergi Serrano, Silvia Hernandez. Hospital del Mar – Parc de Salut Mar, Barcelona, Spain; Universitat Pompeu Fabra, Barcelona, Spain; Autonomous University of Barcelona, Barcelona, Spain.

Background: *SLC45A3* is the second most common 5' partner gene of the *ERG* rearrangements in prostate cancer (PrCa). *TMPRSS2* and *SLC45A3* rearrangements have been reported in the same tumor in a subset of cases, but the meaning of this association is still unknown. The purpose of the present study has been to analyze the prevalence of single and double *SLC45A3-ERG* and *TMPRSS2-ERG* rearrangements and their relationship with *ERG* expression and with tumor grade in PrCa.

Design: A series of 63 PrCa and 3 benign prostate frozen tissue samples (Parc de Salut MAR Biobank, Barcelona, Spain) was used. *TMPRSS2-ERG* and *ERG* were analyzed by qRT-PCR (Applied Biosystems, CA). *SLC45A3-ERG* and *TMPRSS2-ERG* were also assessed by RT-PCR. The concordance among qRT-PCR, RT-PCR and FISH in *TMPRSS2-ERG* detection was tested in a subset of 28 cases. *SLC45A3-ERG* detection by RT-PCR was confirmed by sequencing of the rearrangement amplicons in all cases (Big Dye Terminator Kit v.3.1).

Results: Rearrangements were found in 47 cases (74.6%): a single *TMPRSS2-ERG* rearrangement in 32 cases (50.8%), a single *SLC45A3-ERG* rearrangement in 5 cases (8%), and both rearrangements in 10 cases (15.8%). *ERG* overexpression was found in 39 tumors (62%). *TMPRSS2-ERG* was strongly associated with *ERG* overexpression ($p < 0.0001$), and *SLC45A3-ERG* was not ($p = 0.663$). *TMPRSS2-ERG* was the only rearrangement in 58.3% GS ≤ 7 and 26.7% GS ≥ 8 tumors ($p = 0.032$). *SLC45A3-ERG* was found in 16.6% of GS ≤ 7 and in 46.7% of GS ≥ 8 tumors ($p = 0.033$). Concurrent *TMPRSS2-ERG* and *SLC45A3-ERG* rearrangements were detected in 4.3% of GS = 6; 12% of GS = 7, and 40% of GS ≥ 8 tumors ($p = 0.017$).

Conclusions: Single *TMPRSS2-ERG* rearrangement is associated with GS ≤ 7 PrCa, and concurrent *TMPRSS2/SLC45A3-ERG* with GS ≥ 8 PrCa. *SLC45A3-ERG*, either alone or combined, is also associated with GS ≥ 8 PrCa. These results suggest that *SLC45A3-ERG* rearrangement could be a secondary event in the pathogenesis of PrCa and therefore it could be used as a molecular marker of progression in tumors with the *TMPRSS2-ERG* rearrangement.

Supported by FIS/ Instituto Carlos III/ FEDER PI12/01426, Spanish Ministry of Health.

959 PTEN Status Determination in Prostate Cancer: Comparison of IHC and FISH in a Large Multi-Center Cohort

Tamara Lotan, Carlos Morais, Wei Wei, Dean Troyer, Tamara Jamaspishvili, Ziding Feng, Jesse McKenney, Jeff Simko, James Brooks, Jeremy Squire, CAnary Pathology Team Investigating Tissue Biomarkers (CAPIT). Johns Hopkins School of Medicine, Baltimore, MD; University of Texas MD Anderson Cancer Center, Houston, TX; Eastern Virginia Medical School, Norfolk, VA; Queen's University, Kingston, ON, Canada; Cleveland Clinic, Cleveland, OH; University of California, San Francisco, CA; Stanford University, Stanford, CA; University of São Paulo School of Medicine, São Paulo, Ribeirão Preto, Brazil.

Background: PTEN loss is a promising prognostic and potentially predictive biomarker in prostate cancer. Because PTEN loss in prostate cancer occurs most commonly via gene deletion, we developed and validated an inexpensive immunohistochemical (IHC) assay to detect PTEN protein loss. Here, we studied the sensitivity and specificity of this assay relative to fluorescence *in situ* hybridization (FISH) for detection of *PTEN* gene deletion in prostate cancer.

Design: 1275 primary prostate tumors from the Canary Retrospective Prostate Cancer Tissue Microarray (TMA) cohort were analyzed for PTEN loss by IHC. PTEN IHC was performed by autostaining on the Ventana Discovery Ultra platform using a rabbit monoclonal antibody (Cell Signaling, clone D4.3) and scored by two independent reviewers with very good agreement (96.4% agreement over 2783 spots; $\kappa = 0.905$; 95% CI=0.887-0.923). FISH was previously performed in the same cohort using a four color probe set (CymogenDx) yielding measurable results for 612 tumors.

Results: By IHC, 8% (108/1275) of tumors had homogeneous PTEN loss in all sampled tumor glands, 12% (150/1275) had heterogeneous PTEN loss in a subset of sampled tumor glands, 66% (837/1275) had intact PTEN and 14% (180/1275) had ambiguous or missing immunostaining results. 551 tumors had both IHC and FISH data available for comparison. Intact PTEN immunostaining was 91% specific for absence of *PTEN* gene deletion by FISH, with 413/454 tumors with 2 copies of *PTEN* showing intact PTEN IHC. PTEN IHC loss was 98% sensitive for homozygous *PTEN* deletion by FISH, with homogeneous or heterogeneous PTEN protein loss in 48/49 homozygous tumors. PTEN IHC was 62% sensitive for detection of hemizygous *PTEN* deletion by FISH, with homogeneous or heterogeneous PTEN protein loss in 30/48 tumors with hemizygous deletion. Other inactivating mutations of *PTEN* (not detectable by FISH) may lead to PTEN protein loss in tumors with normal or hemizygous *PTEN* copy number.

Conclusions: Our validated and automated PTEN immunostaining protocol is a simple and relatively inexpensive test that is 91% specific and 98% sensitive for detection of homozygous *PTEN* gene deletions in a large multi-center study of prostate cancer.

960 Hunner Type (Classic) Interstitial Cystitis Is a Distinct Inflammatory Disorder Characterized By Epithelial Denudation and Pancystitis With Frequent Expansion of Clonal B-Cells

Daichi Maeda, Yoshiyuki Akiyama. Graduate School of Medicine, Akita University, Akita-shi, Akita, Japan; University of Tokyo, Bunkyo-ku, Tokyo, Japan; Graduate School of Medicine, The University of Tokyo, Bunkyo-ku, Tokyo, Japan.

Background: Interstitial cystitis (IC) is a chronic bladder disease of unknown etiology. Presence of Hunner lesion is a well-known cystoscopic feature of Hunner type/classic IC (HIC). Those patients presenting with IC symptoms without Hunner lesion are diagnosed as non-Hunner type IC (NHIC). However, such subclassification is not always performed in current clinical practice. In the past, inflammatory cell infiltration, predominantly composed of lymphocytes and plasma cells, and denudation of overlying epithelium had been documented as major pathological findings of IC. But, degrees of lymphoplasmacytic infiltration and epithelial denudation have not been assessed in detail, especially with regards to the difference between HIC and NHIC.

Design: We performed immunohistochemical quantification of T-lymphocytes, B-lymphocytes, plasma cells and amount of residual epithelium in urinary bladder biopsy specimens taken from HIC patients (N=27), NHIC patients (N=39) and non-IC patients (N=26) using image analysis software. In addition, *in situ* hybridization for light chains was performed to examine clonal B-cell expansion. For HIC cases, biopsies from Hunner lesion and background mucosa were evaluated.

Results: Substantial lymphoplasmacytic inflammation (³200cells/mm2) was observed in 93% of HIC specimens, whereas only 8% of NHIC specimens were inflamed. Expansion of light chain-restricted plasma cells was observed in 20% of HIC specimens. The amount of epithelium was decreased in HIC specimens compared with NHIC specimens and non-IC cystitis specimens (P<0.0001). Degrees of inflammation and epithelial denudation did not differ significantly between Hunner lesion and background mucosa in HIC patients.

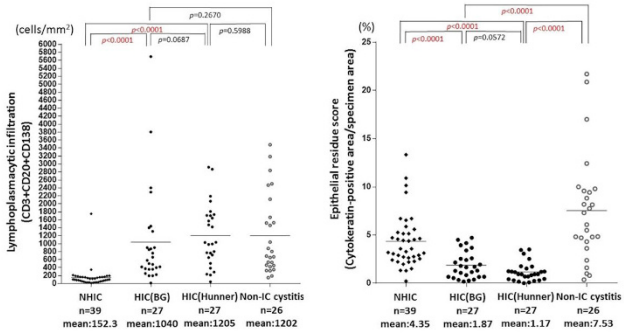

Conclusions: The results of this study suggest that HIC is a distinct inflammatory disorder characterized by epithelial denudation and pancystitis. B-cell abnormality can be associated with pathogenesis of HIC. NHIC is a non-inflammatory entity which should be clearly distinguished from HIC.

961 The Value of Routine Expert Pathology Review in Patients With Bladder Cancer

Chelsea Maedler, Yutong Yang, Wassim Kassouf, Fadi Brimo. McGill University Health Center, Montreal, QC, Canada.

Background: This study investigates the value of routine expert pathology review of bladder biopsies or transurethral resections (TURB) prior to treatment in a major referral center for bladder cancer in the province of Quebec, Canada.

Design: All TURBs performed in community hospitals that were referred by urologists prior to treatment to one tertiary care center for second opinion over a four-year period were included. All slides were reviewed by a specialized Genito-Urinary pathologist. Detailed pathological parameters were recorded and original and secondary reports were compared.

Results: 89 cases were included, 81 of which were urothelial lesions. The pathological stage was discordant in 20% of cases and the main discrepancy occurred in the originally reported T1 urothelial carcinomas (UC) of which 25% were upstaged to T2 upon review.

Original /reviewed	TA	T1	T2?	T2
TA	5	1	1	0
T1	1	16	1	6
T2?	0	1	2	3
T2	0	1	1	42

Similarly, 3 out of 6 cases originally reported as indeterminate for muscularis propria (MP) invasion (T2?) were found to be definitive for MP invasion and one was reclassified as T1. Two out of seven cases originally reported as non-invasive were reclassified as invasive UC. Of the 16 confirmed T1 UCs, 10 (62%), 12 (75%) and 3 (19%) of the original reports did not comment on the presence or absence of lymphovascular invasion, carcinoma in-situ, or muscularis propria, respectively. In 19 (23%) cases, the presence of variants of UC was not included in the original report, five of which were prognostically important such as the sarcomatoid and the micropapillary variants.

Conclusions: Routine expert second opinion is warranted for all TURB specimens of patients referred to large academic centers as major discrepancies exist. Futhermore, our data highlight the under-reporting of MP invasion at initial review, despite it being the most important pathological feature with potential significant clinical impact. Our study reaffirms the need for international pathology guidelines that address an approach to and morphological criteria of MP invasion as well as synoptic reporting of such cases in the community.

962 Anatomical and Immunohistochemical (IHC) Characterization of Testis and Excretory Ducts: A Prospective Study of 25 Autopsies at a Tertiary Care Center

Martin Magers, Aaron Udager, Arul Chinnaiyan, Diana French, Jeffrey Jentzen, Jonathan McHugh, Rohit Mehra. University of Michigan, Ann Arbor, MI.

Background: Testis and excretory duct anatomy and immunophenotype in patients without testicular pathology or exogenous hormonal administration have not been extensively studied. Additionally, testicular (TA) and epididymal (EA) appendages are frequent but without a reported comprehensive morphologic or immunophenotypic study.

Design: Whole mount (WM) sections of testis/paratestis were generated from 25 autopsies of men whose death was not genitourinary-organ related and were not treated hormonally. IHC for multiple markers was performed on full sections of TA, EA, testis, rete testis (RT), ductuli efferentes (DE), epididymis (EP) and vas deferens (VD) from a subset of cases. Intensity (strong: 3, moderate: 2, or weak: 1) and percentage of cells staining were multiplied to give a product score (scale: 0-300; positive staining>50).

Results: Testicular anatomy was well-detailed using WM sections. 20 patients had a TA (80%) and 15 had an EA (60%). TA and EA often coexisted (10 testes). AR was expressed in most EA, TA, sertoli cells (SC), RT, DE, EP, and VD (Table 1). ER and PR had similar patterns, being positive in most EA, TA and DE. PAX8 and WT1 were both expressed in EA, TA and RT, but were differentially expressed in DE, EP and VD (PAX8: positive, WT1: negative).

Table 1	AR	ER	PR	PSA	PSMA
EA	6/6	5/6	6/6	0/6	3/6
TA	9/9	8/9	9/9	0/9	1/9
Germ cells	0/7	0/7	0/7	0/7	2/7
SC	4/7	0/7	0/7	0/7	2/7
Leydig cells	0/7	0/7	0/7	0/7	3/7
Tunica vaginalis	0/7	0/7	0/7	0/7	0/7
RT	7/7	2/7	0/7	0/7	1/7
DE	5/7	7/7	7/7	0/7	0/7
EP	4/6	0/6	0/6	0/6	0/6
VD	3/4	0/4	0/4	0/4	0/4
	PAX8	WT1	Calretinin	CK7	CK20
EA	6/6	6/6	0/6	6/6	0/6
TA	9/9	9/9	0/9	9/9	1/9
Germ cells	0/7	0/7	0/7	0/7	0/7
SC	0/7	1/7	0/7	0/7	0/7
Leydig cells	0/7	0/7	7/7	0/7	0/7
Tunica vaginalis	0/7	1/7	7/7	6/7	0/7
RT	7/7	6/7	7/7	7/7	3/7
DE	6/7	0/7	0/7	7/7	5/7
EP	6/6	0/6	0/6	6/6	4/6
VD	4/4	0/4	0/4	4/4	1/4

Conclusions: Testis and excretory duct structures demonstrate specific IHC patterns and may aid in accurate diagnosis of testicular/paratesticular neoplasms. TA and EA are commonly found structures with reproducible anatomic locations, histomorphology, and immunophenotypic features.

963 Clinicopathological Characteristics of Anterior Prostate Cancers (APC) With Focus on Previous Biopsy Correlation

Martin Magers, Tianyu Zhan, Aaron Udager, Brent Hollenbeck, John Wei, David Miller, Jeffrey Montgomery, Javed Siddiqui, Alon Weizer, Todd Morgan, Arul Chinnaiyan, Ganesh Palapattu, Hui Jiang, Rohit Mehra. University of Michigan, Ann Arbor, MI.

Background: APC is an incompletely understood entity which can be difficult to sample via transrectal biopsy. Seemingly favorable biopsy results belie the potential aggressiveness of these tumors. Here, we attempt to characterize anterior prostate cancer by reviewing the experience at our institution and correlate our findings with previous biopsy data from these patients.

Design: All radical prostatectomy (RP) cases with whole mount sections from 1/2012 to 3/2014 were assessed for APC. APC was defined as the bulk of index tumor (largest size) being anterior to the midpoint of the urethra. Extraprostatic extension (EPE), surgical margin (SM), seminal vesicle invasion (SVI), growth pattern, anatomic location, and Gleason score (GS) of the index tumor and other tumor foci were assessed and compared to non-APC in the same cohort. Previous biopsy information was correlated with RP.

Results: 72 patients with APC were identified in this cohort. 50 APC were located in the anterior peripheral zone (APZ, 69%), 10 in the transitional zone (TZ, 14%), and 12 in both APZ and TZ (17%). 25 APC were single tumors (ST, 35%) and 47 were multifocal tumors (MT, 65%). Of 47 MT, 32 contained smaller posterior foci (67%). Relative to the index tumor, 3 MT with smaller posterior foci were higher GS, 13 were the same GS, and 16 were lower GS. 15 MT were entirely anterior (33%); of these, 6 cases had additional foci lower GS and 9 cases equal GS to the index tumor. 17 cases were identified as "horseshoe" tumors, forming a large horseshoe shaped nodule anterior to the urethra. Overall GS distribution of APC was GS=6 (20%), GS=3+4 (65%), GS=4+3 (10%) and GS=8-10 (6%). 14% of APC demonstrated a positive SM and 21% exhibited EPE. APC had lower GS (p=3.81e-05) and less frequent EPE (21% vs 35%; p=0.0247) than non-APC. SVI was not identified in any patient with APC. 56 APC were preceded by an extended biopsy, 2 by sextant biopsy, while 14 APC were identified after a combination of extended and saturation biopsies. 39 APC had a higher GS at RP than on biopsy (54%).

Conclusions: APC demonstrate distinct growth pattern and clinical features (including absence of SVI) and are frequently under-graded at the time of biopsy. Future long-term studies are needed to determine the outcome of these patients.

964 Utility of S100A1, Caveolin-1, and Napsin A in Distinguishing Chromophobe Renal Cell Carcinoma From Renal Oncocytoma

Abul Ala Syed Rifat Mannan, Songyang Yuan, Beverly Wang, Violette Ghali. Mount Sinai St. Luke's Roosevelt Hospital Center, New York, NY; Mount Sinai Beth Israel Medical Center, New York, NY.

Background: Chromophobe renal cell carcinoma (ChRCC) and renal oncocytoma (RO) often share overlapping morphologic and immunophenotypic features. The differentiation is important, due to their different biologic behaviors. In this study, we investigated the usefulness of S100A1, caveolin-1, and napsin A in differentiating ChRCC from RO.

Design: We selected 15 ChRCCs, and 16 ROs and performed immunohistochemical staining for S100A1, caveolin -1, and napsin A. Immunohistochemistry results were graded as negative, focal positive (<20% positivity) and diffuse positive (³20% positivity).

Results: Caveolin-1 was positive in all 15 ChRCCs (100%), 14 (93%) of which were stained in a diffuse pattern involving >90% of the tumor cells. Expression was moderate to strong, in a granular cytoplasmic pattern with focal membranous accentuation. In contrast, only 4 (25%) of 16 ROs showed focal weak positivity. None of the ROs demonstrated diffuse expression. S100A1 showed diffuse cytoplasmic positivity involving >90% tumor cells in14 (88%) of 16 ROs. Only 3 (20%) of 15 ChRCCs showed positivity for S100A1. In 2 cases S100A1 showed focal positivity in scattered tumor cells. In one case of ChRCC, S100A1 was diffusely positive, with focal positivity for caveolin-1. Napsin A was positive in 7 (45%) of the 16 ROs(2 focal and 5 diffuse), while it was positive in only 2 (14%) of the 15 ChRCCs (1 focal and 1 diffuse). Detailed results are presented in the table.

	S100A1n (%)			Caveolin-1n (%)			Napsin An (%)		
	Negative	Focal positive	Diffuse positive	Negative	Focal positive	Diffuse positive	Negative	Focal positive	Diffuse positive
ChRCC (n=15)	12 (80)	2 (13)	1 (7)	0 (0)	1 (7)	14 (93)	13 (86)	1 (7)	1 (7)
Oncocytoma (n=16)	2 (12)	0 (0)	14 (88)	12 (75)	4 (25)	0 (0)	8 (50)	3 (19)	5 (31)

Conclusions: These results suggest that a panel involving caveolin-1 and S100A1 is very useful in differentiating ChRCC from RO in a problematic case. Strong expression of caveolin-1 with negativity for S100A1 strongly favors a diagnosis of ChRCC over RO. Napsin A appears to be less helpful. Although it was negative in majority of the ChRCCs, only in less than half of the ROs showed napsin A expression.

965 Atypical Renal Cysts: A Morphological, Immunohistochemical, and Molecular Study of 29 Cases

Andres Matoso, B Vishal Rao, Yingbei Chen, Liang Cheng, Jonathan Epstein. Johns Hopkins Hospital, Baltimore, MD; Memorial Sloan Kettering Cancer Center, New York, NY; Indiana University, Indianapolis, IN.

Background: There is a lack of standardized nomenclature for renal cysts lined by multiple cell layers or with short papillary projections. A morphologic, immunophenotypic and molecular characterization of these lesions we have diagnosed as "atypical cysts" is missing in the literature.

Design: 29 cases (15 nephrectomies, 14 partial nephrectomies) were retrieved from our Surgical Pathology files from 1993 to 2014. Immunohistochemistry (IHC) for CK7, racemase, CA9, CD10 and FISH for trisomy 7 and 17 and 3p deletion were performed.

Results: Mean age at excision was 58 years (range 29-80) with 16 males and 13 females. Mean size was 2.9 cm (range: 0.3-7) and were grouped by their morphology into 1) multilayered clear cytoplasm; 2) multilayered eosinophilic cytoplasm; and 3) tufting/short papillary projections. Table 1 summarizes the IHC and molecular results.

	Clear cell stratified	Papillary	Eosinophilic stratified	P value
No/Total (%)	9/29 (31)	14/29 (48)	6/29 (21)	NS
Associated with CCRCC	3/9 (33)	2/14 (14)	3/6 (50)	NS
Associated with PRCC	0/9 (0)	2/14 (14)	0/6 (0)	NS
Multilocular	8/9 (89)	8/14 (57)	1/6 (17)	NS
ADPCKD	0/9 (0)	3/14 (21)	0/6 (0)	NS
CK7	8/9 (89)	14/14 (100)	3/6 (50)	NS
Racemase	3/9 (33)	3/14 (21)	2/6 (33)	NS
CD10	2/9 (22)	2/14 (14)	1/6 (17)	NS
CA9	7/9 (78)	3/14 (21)	1/6 (17)	0.05
Deletion Chr 3	0/8 (0)	1/14 (7)	0/6 (0)	NS
Trisomy Chr 7	2/8 (25)	1/14 (7)	1/5 (20)	NS
Trisomy Chr 17	3/8 (37)	1/14 (7)	2/5 (40)	NS

Clinical follow-up was available in 23 patients; 20 were alive with no evidence of disease after a median follow-up of 20 months (range 3-120), 1 patient was dead due to metastatic lung cancer, 1 of sepsis, 1 of unknown reason.

Conclusions: Atypical renal cysts present as complex radiological lesions, as secondary lesions in patients with a renal mass or in a background of chronic renal disease. These atypical proliferations appear heterogeneous and do not follow in their morphology, immunoprofile, and molecular with more well established renal tumors. The presence of 3p deletion, trisomy 7/17 along with their morphology suggest that in some cases they may be precursors of renal cell carcinoma. Longer follow-up with more cases are needed but based on our data, these lesions should not be diagnosed as carcinoma.

966 Epithelioid Angiosarcoma of the Bladder: A Series of 9 Cases

Andres Matoso, Jonathan Epstein. Johns Hopkins Hospital, Baltimore, MD.

Background: Primary angiosarcoma of the bladder is very rare with approximately 30 cases reported in the literature. Those with epithelioid morphology are even rarer with only single-case reports published.

Design: We describe the histopathologic features and clinical follow-up of 9 patients with epithelioid angiosarcoma (EA) of the bladder retrieved from our Surgical Pathology files from 1998 to 2014. 8 cases were consults.

Results: The mean age at presentation was 65y (range 39-85). The M:F ratio was 8:1. The clinical presentation was hematuria and bladder mass in all cases. 6 patients had a history of radiotherapy to the pelvis, 5 to treat prostate cancer, and 1 to treat uterine cancer. The time from radiotherapy to the diagnosis of EA ranged from 6 to 15 years. The average size of the tumor was 4 cm. (range 1-8 cm.). The submitting diagnoses were poorly differentiated carcinoma (n=5), high-grade invasive urothelial carcinoma (n=3), atypical vascular proliferation (n=1). Morphologically, the tumors were composed of nests and sheets of highly atypical cells with high N/C ratio, occasional intracytoplasmic lumens, and a hemorrhagic background. None of the cases showed any urothelial carcinoma component. 3 patients showed usual angiosarcoma in the resection specimen. By immunohistochemistry, 5/9 cases were positive for cytokeratins, including CK7 (n=3), AE1/AE3 (n=3), and Cam5.2 (n=1). All cases were positive for at least one endothelial marker, including CD31 (n=7), CD34 (n=2), FVIII (n=3) and ERG (n=2). Urothelial markers (p63 and GATA3) were consistently negative. Surgical treatment included TURB only (n=5), TURB followed by cystoprostatectomy (n=2), TURB followed by partial cystectomy (n=1), cystoprostatectomy only (n=1). The tumor involved the muscularis propria in 5/9, the periureteric adipose tissue in 1/9 and the prostate and seminal vesicles in 1/9. 5/9 patients died of disease with a median survival of 7 months (range 6-14). 2 patients were alive with disease at 3 and 6 months of follow-up. 1 patient that underwent radical cystoprostatectomy was alive with no evidence of disease 12 months after surgery.

Conclusions: EA of the bladder is a rare malignancy that is frequently misdiagnosed as high-grade carcinoma, especially due to positive immunostaining for cytokeratins. This tumor is more frequent in older men with history of radiotherapy to the pelvis. Morphologic features that should suggest the vascular origin of the tumor include highly atypical nuclei, hemorrhagic background, and occasional intracytoplasmic lumens. Patients usually present with muscle invasive disease and the prognosis is dismal.

967 Radical Prostatectomy (RP) Findings in Men Who Failed Prostate Cancer Active Surveillance (AS) Based on Repeat Biopsy Progression Versus Those on AS Who Subsequently Underwent RP Due To Anxiety

Andres Matoso, Oudai Hassan, B Vishal Rao, Jonathan Epstein. Johns Hopkins Hospital, Baltimore, MD.

Background: Limited data is available on the RP findings in patients who no longer qualify for AS based on repeat biopsy findings.

Design: 140 patients from our AS program underwent RP. Slides were available in 119, including 84 men with worse findings on repeat biopsy (biopsy progression) and 35 men without worse findings who elected RP due to anxiety (no biopsy progression).

Results: The results are summarized in Table 1.

	Biopsy Progression (N=84)	No Biopsy Progression (N=35)	P
Age (y)	65 (64-74)	63 (49-74)	
Time from biopsy to RP (m)	37 (11-194)	32 (8-97)	
Gleason score No. (%)			
6	28 (33.3)	23 (65.7)	0.002
6 with tertiary pattern 4	10 (11.9)	4 (11.4)	0.81
3+4=7	30 (35.7)	8 (22.8)	0.25
4+3=7	11 (13)	0 (0)	0.06
>7	4 (4.7)	0 (0)	0.45
Organ confined	65 (77.3)	29 (82.8)	0.67
Extraprostatic extension			
Focal	10 (11.9)	4 (11.4)	0.81
Non-focal	8 (9.5)	1 (2.8)	0.38
Seminal vesicle involvement	1 (1.2)	0 (0)	0.65
Lymph node involvement	1 (1.2)	0 (0)	0.65
Positive margin	14 (16.6)	4 (11.4)	0.65
Mean cm3 tumor volume (range)	1.1 (0.04-4.73)	0.98 (0.01-6.43)	
Tumor volume 3 No. (%)	56 (66.6)	27 (77.1)	0.36
Mean cm3 dominant tumor (range)	1.03 (0.03-4.39)	0.6 (0.15-5.45)	
Dominant tumor volume >1 cm3	27 (32.1)	5 (14.2)	0.07
Total tumor volume 3	34 (40.4)	30 (85.7)	
Dominant nodule location			
Anterior	18 (21.4)	9 (25.7)	0.79
Posterior/posterolateral	37 (44)	16 (45.7)	1
Lateral	6 (7.2)	2 (5.7)	0.92
Scattered foci	23 (27.4)	8 (22.9)	0.77
Anterior dominant nodule >1 cm3 No./Total (%)	7/18 (38.9)	2/9 (22.2)	0.66
Posterior/posterolateral dominant nodule 3 No./Total (%)	30/37 (81.1)	15/16 (93.7)	0.009

9/84 (10.7%) in the group with biopsy progression and 6/35 (17.1%) with no progression (p=0.5) had insignificant cancer at RP (TV <0.5 cc., organ confined, Gleason 6).

Conclusions: None of the patients who elected RP had GS 4+3=7 or worse. The large majority of men with biopsy progression on AS who undergo RP still have relatively favorable findings with curable disease, justifying AS a treatment option in selected patients.

968 Elevated PD-L1 (B7-H1) Expression in Cystectomy for Urothelial Carcinoma Following Neoadjuvant Chemotherapy

Andrew McDaniel, Ajjai Alva, Tianyu Zhan, Arul Chinnaiyan, Hui Jiang, Cheryl Lee, Rohit Mehra. University of Michigan, Ann Arbor, MI.

Background: Expression of the costimulatory ligand PD-L1 (B7-H1) on malignant cells has been shown to inhibit anti-tumor T cell mediated immune responses, providing a molecular shield for tumors and an attractive target for immune based therapies. Investigational agents such as the antiPD-L1 antibody MPDL3280A are currently being used in the trial setting for a number of malignancies. PD-L1 expression in urothelial carcinoma (UCA) is associated with high grade disease. However, the expression of PD-L1 in UCA following neoadjuvant chemotherapy prior to cystectomy has not be reported.

Design: Immunohistochemical (IHC) staining for PD-L1 was performed using a murine anti-B7-H1 monoclonal antibody (clone 5H1) on a tissue microarray including matched pre-NAC pT1/T2 transurethral resection and post-NAC cystectomy samples (T0=15, Tis=1, T1=3, T2=7, T3=12, T4=2) from 40 patients. IHC was scored as the product of tumor cell staining intensity (0-3) and percentage of cells positive (0-100) (overall product score range[thinsp]=[thinsp]0-300).

Results: The expression of PD-L1 was significantly higher in post-NAC cystectomy specimens (mean IHC score= 217.5) compared to the matched pre-NAC TUR specimens (mean IHC score= 176.7, p value=0.0196 by Student's paired T test). PD-L1 expression in pre-NAC TUR was not associated with recurrence free or overall survival, progression to LN metastases, or likelihood of T0 cystectomy following NAC.

Conclusions: Patients with residual UCA in cystectomy specimens following NAC have poor outcomes and limited treatment options. The level of PD-L1 expression in the pre-NAC TUR setting does not seem to correlate with outcomes; however, the expression of PD-L1 in post-NAC cystectomy specimens is elevated compared to the pre-NAC samples. The elevation in PD-L1 following post-NAC cystectomy suggests this setting may be a rational timepoint for potentially utilizing immune-based therapies, including MPDL3280A, in these patients.

969 Retinoblastoma Protein Expression Is Associated With PSA-Recurrence in Localized Prostate Cancer and Is Variable in Metastatic Foci

Andrew McDaniel, Nallasivam Palanisamy, Alisa Tubbs, Kassie Smith, Kristina Fields, Javed Siddiqui, Felix Feng, Maha Hussain, Scott Tomlins. University of Michigan Medical School, Ann Arbor, MI; Ventana Medical Systems, Inc., Tucson, AZ.

Background: Retinoblastoma, or Rb (encoded by *RB1*) is tumor suppressor that is frequently lost in prostatic small cell carcinoma. Promising therapies against CDK4/6 are dependent on Rb expression. Here we investigated Rb expression via immunohistochemistry (IHC) in treatment naïve prostate cancer (PCa) and metastatic castration resistant prostate cancer (mCRPC).

Design: Fully automated IHC to detect Rb expression was performed with a mouse anti-Rb monoclonal antibody using the VENTANA BenchMark ULTRA slide staining system on tissue microarrays (TMA) including samples from treatment naïve radical prostatectomies (TNRP) with long term follow up (n= 82). Additionally, visceral and bone metastasis from an autopsy series of patients with mCRPC (105 samples from 45 patients) were evaluated. IHC was evaluated as the product score (PS) of tumor cell staining intensity (0-3) times percentage of cells positive (0-100). Non-tumoral cells were used as internal positive controls. Rb1 expression was dichotomized into low and high groups using the overall median PS.

Results: For TNRP, Rb expression was present in every case with a median PS of 118 (interquartile range [ICR] 70-180). Low Rb expression was significantly associated with worse PSA recurrence free survival (logrank test p=0.03). Along with stage (p=0.004) and Gleason score (p=0.004), the Rb PS (p=0.004) was a significant predictor of PSA recurrence (Cox regression analysis). In mCPRC, median Rb expression (median PS 20, IQR 8-80) was significantly lower than TNRP (p<0.0001, Mann-Whitney). Additionally, heterogeneity in Rb intensity between metastatic foci from the same case was observed. For example, bone and liver metastases from one case showed Rb PS of 270 and 5, respectively.

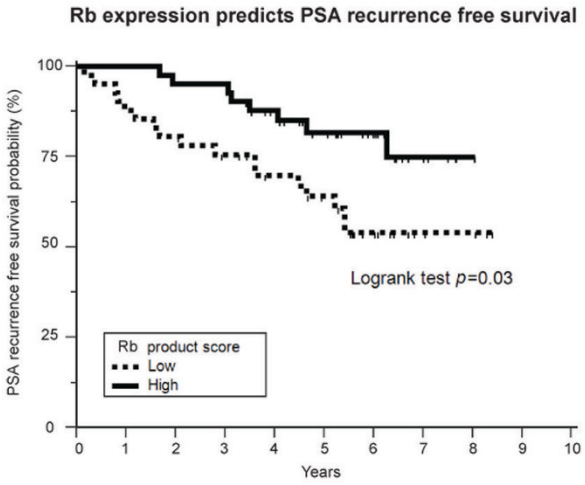

Conclusions: The observation of decreased Rb expression leading to shortened PSA recurrence time and reduced Rb levels in mCRPC compared to TNRP indicates that Rb has a potential role in PCa progression. All TNRP cases had Rb expression, indicating that hormone sensitive PCa is potentially an effective setting for anti-CDK4 therapy, but variability of Rb expression among metastatic foci may limit CDK4 inhibitor efficacy in the CRPC setting.

970 Targeted Genomic Profiling of Penile Squamous Cell Carcinoma Reveals Opportunities for Targeted Therapy

Andrew McDaniel, Daniel Hovelson, Andi Cani, Chia-Jen Liu, Yali Zhai, Yajia Zhang, Seth Sadis, Santhoshi Bandla, Paul WIlliams, Kathleen Cho, Daniel Rhodes, Scott Tomlins. University of Michigan Medical School, Ann Arbor, MI; Thermo Fisher Scientific, Inc., Ann Arbor, MI.

Background: Penile squamous cell carcinoma (PeSCC) is a rare cancer notable for significant morbidity as well as an incomplete understanding of the underlying molecular alterations and lack of effective non-surgical therapies.

Design: A retrospective cohort of 60 formalin fixed, paraffin embedded (FFPE) tumor samples from 44 PeSCC cases (including 14 matched primary/metastasis pairs) was subjected to targeted next generation sequencing (NGS) using the Oncomine Cancer Panel encompassing actionable recurrent somatic alterations in ~125 oncogenes and tumor suppressors identified by analysis across multiple cancer types. HPV infection status for each sample was assessed using additional genomic DNA for PCR with the GP5/6 and My09/11 consensus primer sets for viral detection and typing.

Results: Tissue samples included a variety of morphologic subtypes, including 29 usual, 5 warty, 4 papillary, 3 basaloid, and 3 verrucous PeSCC. The cohort contained a variety of tumor grades (including well, moderate, and poor) and stages (ranging from pT1a to pT4). High risk HPV was detected in five cases (Four with HPV 16, one with HPV 33). Targeted NGS yielded an average of 1,136,032 mapped reads per sample with high coverage (mean >535X) over targeted bases using 20ng of input genomic DNA. An average of 309 variants were called per sample. Frequently altered genes genes included *CDKN2A*, *P53*, *NOTCH1*, *FBXW7*, *PIK3CA*, NFE2L2, and *HRAS*. Notably, four cases harbored amplifications of *EGFR* and one demonstrated *CDK4* amplification; genes for which targeted therapies are available. Importantly, cases with paired primary tumors and metastasis profiled showed heterogeneity for actionable mutations such as *EGFR* amplification in 4 of 14 samples.

Conclusions: We evaluated a cohort of PeSCC FFPE specimens using an NGS panel of recurrently altered cancer-associated somatic variants, providing detailed molecular analysis of this disease for the first time. The scope of mutations identified was similar to squamous cell carcinomas from other locations such as the lung and head and neck region. We identified a subset of cases harboring mutations with immediate therapeutic potential, including *EGFR* amplifications. This research suggests that NGS profiling of PeSCC may have utility as part of a precision medicine approach to aid clinical decision making.

971 ERG Expresion By Immunohistochemistry in Prostate Needle Biopsies and Radical Prostatectomy Specimens in the West of Ireland Prostate Cancer Centre

Teresa McHale, Mary Casey, Frans Colesky. Galway University Hospital, Galway, Ireland.

Background: Galway University Hospital(GUH) provides prostate cancer services for the West Of Ireland as part of the National Cancer Control Program. In the Pathology Dept. at GUH we examined the frequency of ERG expression by immunohistochemistry (IH) in both needle core biopsies (NC) and radical prostatectomy (RP) specimens and its relationship to patient age, PSA level, Gleason score and TNM stage (RP).

Design: 77 consecutive NC biopsies, with prostate cancer foci involving >5% of a core and 28 randomly selected RP specimens were stained with ERG antibody (Dako). Where carcinoma was bilateral or foci of differing Gleason score were identified, each focus was stained. Staining was evaluated as negative, or positive (weak, moderate or strong intensity). ERG+ and ERG- groups were compared with respect to patient age and PSA level at diagnosis (student t test), Gleason score and TNM stage (for RP cases) (X^2 test). Patient ethnicity was noted.

Results: Radical prostatectomies: 22/28 (78.5%) showed strong positive staining of at least one cancer focus. Where more than one cancer focus was tested (N=19), 16 were positive and 8 (50%) of these showed differential staining in different tumour foci. PSA level at diagnosis was significantly lower in RP ERG+ patients (mean PSA 6.52 vs. 11.78; p=0.02). There was no significant difference between the ERG+ and ERG- groups with respect to Gleason score, patient age or TNM stage.

Core biopsies: 50/77 (65%) showed strong positive staining in at least one cancer focus. Where more than one focus of carcinoma was stained (N=28) 9 had differential staining in separate foci. Age at diagnosis was significantly lower in the ERG+ group (mean 64.7 yrs vs. 68 yrs; p=0.046). There was no significant difference between ERG+ and ERG- groups with respect to PSA level at diagnosis or Gleason score. There was no ERG expression in benign prostatic tissue. ERG expression was noted in high grade PIN adjacent to invasive cancer. All patients were of Irish ethnicity.

Conclusions: ERG expression in prostatic adenocarcinoma in this sample of Irish prostate cancer patients is one of the highest reported, compared with other IH studies of ERG expression in various populations. In RP specimens, expression is significantly associated with lower PSA level at diagnosis and, in NC, is significantly associated with younger age at diagnosis. These findings warrant further exploration of the significance of ERG expression (and by implication, the TMPRSS2-ERG gene rearrangement) in prostate cancer in this particular patient population.

972 PDL1 Status in Muscle Invasive Urothelial Bladder Carcinoma (MIBC) in the Context of Neoadjuvant Cisplatin Based Chemotherapy

Maria Angelica Mendoza Rodriguez, Alexander Baras, Gunes Guner, Nilay Gandhi, Enrico Munari, Sheila Faraj, Janis Taube, Trinity Bivalacqua, George Netto. Johns Hopkins, Baltimore, MD.

Background: Post-cystectomy cancer specific survival (CSS) for MIBC that failed to respond to cisplatin based neoadjuvant chemotherapy (cNAC) is poor. The 27% 5-yr CSS in such setting is significantly lower than the ~ 50% 5-yr CSS observed in MIBC treated with cystectomy alone. Given the cNAC response rate of 40-50%, approximately half of MIBC would be amenable to alternative therapy if available.

Programmed death ligand 1 (PDL1) plays a crucial role in suppressing immune response. Anti PDL1 therapy in tumors with proven expression has shown promising results, including advanced stage MIBC. We evaluated PDL1 in MIBC in the context of a cohort annotated for response to cNAC to address the question of whether anti-PDL1 therapy could be a viable an option to test for patients with evidence of non-response to cNAC.

Design: We studied 150 consecutive patients who received cNAC followed by radical cystectomy (RC) from 2000-2013. A cohort of 121 patients treated by RC alone, 2000-2005, was used for comparison. Pathologic response and cancer-specific survival (CSS) were compared. Tissue microarrays (TMAs) of cNAC MIBC specimens were stained with PDL1 and FOXP3 and scored for extent of membranous PDL1 staining of tumor cells and tumoral lymphocyte FOXP3 staining.

Results: The rate of PDL1 positivity in MIUC was the same for cNAC responders and non-responders, 43% and 47% respectively. There was a strong positive correlation of tumoral PDL1 staining with tumoral lymphocytes FOXP3 staining, Goodman-Kruskal gamma=0.71 with p<0.0001, independent of cNAC responder status.

Table 1. *Tabulation of tumoral PDL1 staining in conjunction with intratumoral lymphocyte FOXP3 staining.*

		Intratumoral Lymphocyte FOXP3		
		>15/hpf	1-15/hpf	0/hpf
Tumoral PDL1	>5%	4	6	0
	1-5%	2	9	4
	0%	1	20	22

* A strong Goodman-Kruskal **gamma of 0.71 with p<0.0001** is observed, supporting the correlation of these two ordinal variables.

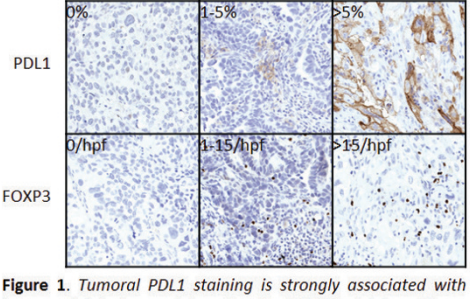

Figure 1. *Tumoral PDL1 staining is strongly associated with increased intratumoral lymphocyte FOXP3 staining.* Three representative cases (columns) are shown, exhibiting the correlation which is tabulated across the entirety of the cohort in Table 1.

Conclusions: Patients with MIBC that are non-responders to cNAC fare worse than patients proceeding directly to RC alone. Interestingly though, 40% of non-responders to cNAC do exhibit PDL1 tumoral staining. Our findings offer a biologic rational in support of future studies to evaluate the role of anti-PDL1 therapy in MIBC patients that fail to respond to cNAC.

973 Significance of a Minor High Grade Component (<5%) in Non-Invasive Papillary Urothelial Carcinoma of Bladder

Maria Angelica Mendoza Rodriguez, Leonardo Reis, Gunes Guner, Stephania Bezerra, Alexander Baras, Trinity Bivalacqua, George Netto. Johns Hopkins Hospital, Baltimore, MD; Johns Hopkins University, Baltimore, MD.

Background: Currently, ISUP grading of non-invasive papillary urothelial carcinoma is assigned based on the highest grade component in a given tumor regardless of its extent. Occasionally, some of tumors contain only a minor (5% or less) high-grade component in otherwise low-grade tumor ("LG/HGTCC"). We assessed the clinicopathologic characteristics, prognostic significance and potential treatment implications of such occurrence.

Design: All archival cases with a diagnosis of "LG/HGTCC" were retrieved (2005-2014). Only patients with initial (de novo) dx of "LG/HGTCC" are included. Patients with close subsequent (£3 months) higher grade (CIS or HGTCC) or stage lesions were excluded. Follow-up data was obtained from medical records.

Results: A total of 31 non-invasive "LG/HGTCC" as defined above are included in the study. The mean tumor size was 3.5 cm (0.6-9). 7 tumors were multifocal (22.6%), the mean patient age at diagnosis was 67.2 (36-87) years. 25 (80.6%) patients were white, 23 (74.2%) were male and 17 (54.8%) reported tobacco use, with a mean follow-up of 35.7 (3-144) months. Progression was documented in 6 (19.3%) cases: 3 (9%) to bona fide high grade non-invasive papillary urothelial carcinoma, 1 (3.2%) to CIS and 2 (6.4%) other cases developed metastases. The mean time to progression was 8 (4-17) months. Cancer specific death occurred in the 2 patients (6.4%) that endured metastatic disease. As summarized in table 1, intravesical treatment (BCG and/or mitomycin) was associated with favorable progression [1/13 (7.7%) versus 5/18 (27.8%)] and cancer specific death rates [0 versus 1/18 (11%)]

Intravesical treatment*	Mean Follow-up (months)	Tumor Mean Size (cm)	Multifocality (%, n)	Progression Rate (%, n)	Metastases & Cancer Specific Death (%, n)
YES(n=13)	45.6	3.11 cm	30.8%(4/13)	7.7%(1/13)	0 (0/13)
NO(n=18)	28.5	3.73 cm	16.75%(3/18)	27.8%(5/18)	11%(2/18)

*BCG and/or mitomycin

Conclusions: Although the 19.3% progression rate in this cohort of LG/HGTCC is comparable to our previously found 18.3% progression rate in LGTCC, the high rate of metastases and favorable outcome of BCG treatment in LG/HGTCC would argue for keeping the category as a distinct group for now. Our finding of advanced stage progression in rare patients strongly suggests TUR undersampling. Larger prospective studies are required to better characterize the biologic behavior of "LG/HGTCC" tumors.

974 Predictive Value of Pathologic Parameters and ERG Oncoprotein Expression in the Stratification of Prostate Cancer Risk Associated With Diagnosis of High-Grade Prostatic Intraepithelial Neoplasia (HGPIN) in Prostate Needle Biopsy

Savvas Mendrinos, Rajal Shah, Monica Hansen. Miraca Life Sciences Research Institute, Irving, TX.

Background: HGPIN diagnosis in prostate needle biopsy (NBX) has traditionally been associated with high predictability of finding a cancer (PCa) in repeat biopsy (~40%); however, the diagnosis rates of PCa after an initial diagnosis of HGPIN have significantly decreased in recent years (~25%) as more aggressive biopsy templates have reduced the number of cancers missed on initial biopsy. However, there is still considerable heterogeneity in practices regarding management of HGPIN. Which patients with the HGPIN diagnosis should be biopsied remain a clinical management dilemma. ERG is a highly prostate-cancer specific marker that is present in ~50% of prostate carcinomas (PCas) and ~20% of high-grade prostatic intraepithelial neoplasia (HGPIN) that intermingle with PCa.

Design: 107 patients with HGPIN in initial biopsy and at least one follow-up biopsy were included. Clinicopathologic features including age, serum PSA, number of cores with HGPIN, laterality of involvement and presence or absence of ERG overexpression by immunostaining (IHC) were analyzed in order to identify parameters that correlate with subsequent detection of PCa.

Results: The mean age was 63 years (range from 46 to 83). At a mean of 5.5 months (range 1 to 26 months) the repeat biopsy was performed. A mean of 10.5 and 10.8 cores for initial and repeat biopsy were obtained (range from 6 up to 24 cores). Twenty five (23%) had cancer, 9 (8.4%) had HGPIN, and 73 (68%) had benign diagnosis on repeat biopsy. ERG expression was present in 9 (8%) patients, in which PCa was found in 7 (77%) subsequent biopsies. Of 98 biopsies with negative ERG staining, PCa was found in 16 (15%) subsequent biopsies. Of 25 patients with subsequent cancer diagnosis, 14 (56%) had >1 site with HGPIN and 11 (44%) had bilateral involvement. Of 82 patients with no cancer on follow-up repeat biopsy, 32 (39%) had >1 site with HGPIN and 12 (15%) had bilateral disease. Only 6 (6%) patients with single site (core) with HGPIN had PCa on repeat biopsy. The combination of > 1 core with HGPIN and/or bilateral involvement with ERG positivity was associated with the presence of PCa in 100% of repeat biopsies.

Conclusions: Our preliminary results support utility of the ERG IHC along with pathological parameters to tailor management of patients with HGPIN on the initial biopsy.

975 Clonal Analysis of Multi-Focal Tumors in Patients With Birt-Hogg-Dube Syndrome

Maria Merino, Arunima Ghosh, Laura Schmidt, Marston Linehan. National Cancer Institute, Bethesda, MD; Frederick National Laboratory, Frederick, MD.

Background: Birt-Hogg-Dubé (BHD) syndrome is an autosomal dominant disorder in which patients are predisposed to develop fibrofolliculomas, pulmonary cysts, spontaneous pneumothorax and kidney tumors. The syndrome is caused by germline mutations in *FLCN,* a novel tumor suppressor gene, that affect the FLCN protein. Kidney tumors associated with BHD show a morphologic spectrum of hybrid, chromophobe, oncocytoma, and, rarely, clear cell. Whether the tumors are clonal or polyclonal is not known. We utilized the HUMARA assay; a methylation based clonal analysis that takes advantage of a highly polymorphic trinucleotide repeat (CAG) within the human androgen receptor gene (HUMARA) on the X chromosome, to investigate the clonality of these tumors. If the alleles are polymorphic, normal tissues will have two alleles of equal intensity, indicating a polyclonal origin. Lesions with a single allele after digestion are considered monoclonal in origin.

Design: Four female patients with Birt-Hogg-Dubé (BHD) syndrome and who had multiple and bilateral hybrid tumors in both kidneys were selected. Normal and tumor cells were manually microdissected from formalin-fixed paraffin-embedded blocks and DNA was purified using a Qiagen DNA isolation kit. For the HUMARA assay, DNA was digested with HpaII or no enzyme. Digestion products were subjected to PCR with standard HUMARA primers and analyzed on the ABI 310 genetic analyzer. For microsatellite analysis, undigested DNA was subjected to PCR with the desired primer pairs and analyzed on the ABI 310 genetic analyzer.

Results: Hybrid tumors from both kidneys of each patient showed methylation of the same lower allele and were considered to be clonal. To provide additional evidence of the clonality of these tumors, microsatellite analysis was performed using markers from chromosomes 1q, 3p, 17p, and 17q; all tumors showed the same pattern of loss of heterozygosity.

Conclusions: Patients with BHD syndrome have a predisposition to develop different histologic types of renal cancer, including hybrid, chromophobe, and oncocytoma. The results of our study with the HUMARA assay supports a clonal origin for these tumors, suggesting that they probably arise from the same cell. The finding of similar heterozygosity patterns using microsatellite analysis supports the monoclonal nature of the tumors.

976 Cyclin D1 Loss Distinguishes Prostatic Small Cell Carcinoma From Usual-Type Adenocarcinoma

Carlos Morais, Harrison Tsai, Jessica Hicks, Nilesh Gupta, Jonathan Epstein, George Netto, William Isaacs, Jun Luo, Rohit Mehra, Angelo De Marzo, Tamara Lotan. Johns Hopkins School of Medicine, Baltimore, MD; Henry Ford Health System, Detroit, MI; University of Michigan Health System, Ann Arbor, MI.

Background: Small cell neuroendocrine differentiation in prostatic carcinoma is an increasingly common mode of resistance to potent androgen deprivation therapy (ADT). Distinguishing small cell carcinoma (SCC) from Gleason score 9-10 prostatic adenocarcinoma (AdCa) can be challenging in limited biopsy specimens, particularly in the context of hybrid tumors developing after ADT, and this distinction is critical for clinical management. We recently reported that Rb protein loss is nearly universal in prostatic SCC and distinguishes it from AdCa. Here, we investigated whether cyclin D1 and p16 expression, widely available immunostains in clinical pathology labs, can serve as surrogate molecular markers for Rb status, distinguishing SCC from AdCa.

Design: We used publically available copy number and gene expression data from patient-derived xenografts, primary and metastatic prostatic AdCa and SCC to show proof-of-principle that a high ratio of p16 to cyclin D1 (*CDKN2A/CCND1*) mRNA expression reflects underlying Rb loss and distinguishes SCC from AdCa. Then, we tested these markers at the protein level in formalin fixed paraffin embedded (FFPE) tissues by immunostaining morphologically identified SCC (n=41), Gleason 7-10 primary AdCa from radical prostatectomy specimens (n=94), Gleason 9-10 primary AdCa from needle biopsies (n=44) and metastatic castrate resistant prostate AdCa (CRPC) from rapid autopsies (n=115 metastases from 39 cases).

Results: Using dichotomous scoring, 88% (36/41) of SCC were cyclin D1-negative by immunostaining compared to 2% (2/94) of primary AdCa from radical prostatectomy specimens, 9% (4/44) of primary AdCa from needle biopsies and 7% (8/115) of CRPC AdCa metastases. Somewhat higher rates of cyclin D1 loss were seen in primary AdCa associated with concurrent SCC (18% or 2/11). Cyclin D1 loss was highly correlated with underlying Rb loss, with 94% (34/36) of cyclin D1-negative SCC cases lacking Rb protein, compared to 79% (11/14) of cyclin D1-negative primary/metastatic AdCa. Despite utility at the mRNA level, p16 immunostaining did not distinguish SCC and AdCa, showing a range of expression intensity across all groups studied.

Conclusions: When combined with morphology, cyclin D1 loss is a promising and widely available immunostain to help identify prostate tumors with small cell neuroendocrine differentiation, both in the primary and metastatic settings.

977 Pre-Analytic and Analytic Validation of Automated PTEN Immunohistochemistry To Detect PTEN Loss in Prostate Cancer

Carlos Morais, Anu Gopalan, Jessica Hicks, Victor Reuter, Howard Scher, Angelo De Marzo, Tamara Lotan, The Precision Medicine Biomarker Validating Center CDMRP Tranformative Impact Award Group. Johns Hopkins School of Medicine, Baltimore, MD; Memorial Sloan Kettering Cancer Center, New York, NY.

Background: We report on the multi-institutional validation of an automated immunohistochemistry (IHC) assay to detect PTEN protein loss in prostate cancer, assessing the effects of pre-analytic and analytic variables on immunostaining results.

Design: PTEN IHC was performed on the Ventana Discovery Ultra, Discovery XT and Benchmark Ultra. Inter-observer reproducibility in scoring was evaluated in 817 prostate

tumor cores on 6 multi-institutional TMAs. Tumors were scored as having PTEN loss (either homogeneous or heterogeneous) or intact PTEN by assessing staining relative to benign glands and stroma as an internal positive control. Benign specimens utilized to test pre-analytic variables were assessed as evaluable or inevaluable based on intact staining in benign glands.
Results: Inter-observer reproducibility in scoring between two urologic pathologists at different institutions was very good, with agreement in 97% of scored tumor spots (including 197 spots with PTEN loss and 592 spots with intact PTEN) and κ=0.911 (95% CI = 0.878 to 0.943). Machine-to-machine variability assessed across 3 Ventana platforms and 2 institutions was negligible in 65 tumors (including 30 with *PTEN* gene loss by FISH), with identical scoring on all platforms. In benign cores taken from radical prostatectomy specimens, delay of fixation for 0-4 hours at room temperature (n=10) and 0-12 hours at 4 degrees (n=3) did not alter the percentage of evaluable specimens, however, staining was appreciably decreased with 24-48 hours of cold ischemia (n=3). Similarly, fixation in 10% formalin for 0-48 hours (n=16) or 0-128 hours (n=2) did not alter the percentage of evaluable specimens and fixation in Hollande's and Bouin's fixatives showed similar staining compared to 10% formalin (n=5 for each fixative). Tissue cores from tumors with PTEN loss (n=2) and intact PTEN (n=1) processed using variable tissue processing protocols at 11 institutions were all evaluable and scored identically. In radical prostatectomy specimens from 1997-2004, >95% of tumors were evaluable for PTEN staining in all sampled spots. Storage of unbaked, unstained slides for 5 years at room temperature prior to immunostaining resulted in equivalent scoring across tumors with PTEN loss (n=2) and intact PTEN (n=1) compared to freshly cut slides from the same tissue blocks.
Conclusions: Automated PTEN immunostaining is robust, with minimal effects of pre-analytic variables on immunostaining results and evaluability and very good inter-observer reproducibility of scoring.

978 Genomic RNAseq From Formalin Fixed Paraffin Embedded (FFPE) Prostate Needle Core Biopsies of Patients With Prostatic Adenocarcinoma

Carlos Moreno, Qi Long, Soma Sannigrahi, Theresa Gillespie, John Petros, Martin Sanda, Adeboye Osunkoya. Emory University School of Medicine, Atlanta, GA; Veterans Affairs Medical Center, Atlanta, GA.
Background: Our recently published set of biomarkers is designed to predict therapeutic response to radical prostatectomy using RNAseq of prostatectomy samples. However, a more pressing clinical need is to discriminate those patients who need active surveillance/deferred treatment from those who need more aggressive therapy, using only RNA obtained from diagnostic prostate needle core biopsies.
Design: We performed global RNA-sequencing on FFPE samples from prostate needle core biopsies to demonstrate the feasibility of large-scale analyses and compare data from biopsies to matched prostatectomy specimens. Whole transcriptome RNAseq was performed on three needle core biopsies per patient for three separate cases. Total RNA was prepared from FFPE biopsies, using the Omega Biotek FFPE RNA methodology in 96-well format on an automated liquid handler. RNAseq libraries were analyzed for QC and average size of inserts were approximately 200-300 bp. Samples were multiplexed into three samples per lane on the Illumina Version 3 Flowcells on the HiSeq2000 platform. Sequencing reads were mapped to the human reference genome (GRCh37) using TopHat software (version 2.0.8) and Bowtie (version 2.1.0), and Cufflinks software will be used to generate fragment per kilobase per million reads (FPKM) values.
Results: Average RNA yield for the three cases was 16.8 ug (range 11.4-26 ug). We obtained high-quality RNAseq data from all sample libraries, with 39-41M reads per sample and 49-74% of the reads uniquely mapped to the human genome, for an average of 23 million mapped reads per biopsy. Correlation analysis of biopsy and prostatectomy-derived RNAseq data indicates that the data from both sources are strongly correlated, both for all detected genes and for the subset of biomarker genes analyzed by TaqMan assay. Log2 transformed FPKM values for 5317 detected genes comparing RNAseq data from a biopsy and prostatectomy sample had a correlation of $\rho = 0.852$. The correlation of log2 transformed FPKM values for 24 biomarker genes was higher at $\rho = 0.946$.
Conclusions: We have demonstrated the feasibility of performing RNAseq on RNA isolated from biopsies, generating on average 23 million mapped reads per biopsy in our pilot studies and demonstrating high correlation between the gene expression observed in prostatectomy and biopsy tissues. We plan to use this approach to identify biomarkers of aggressive prostatic adenocarcinoma from FFPE prostate needle core biopsy samples.

979 New and Old Testicular Lesions Associated With VHL Syndrome

Vanessa Moreno, Adam Metwali, W Marston Linehan, Maria Merino. National Cancer Institute, Bethesda, MD.
Background: Von Hippel-Lindau syndrome (VHL) is an inherited autosomal dominant disorder in which affected individuals are at risk to develop renal cell carcinoma and other tumors. Clear cell papillary cystadenoma (CCPC) of the epididymis are rare benign lesions accounting for only 4% of all epididymal tumors. They may occur sporadically; however, more than 1/3 of the cases have occurred in patients with VHL disease. CCPC are of mesonephric derivation and originate in the efferent ductules of the head of the epididymis in the form of tiny precursor lesions. Intratesticular lesions have not been reported in the literature as part of the VHL syndrome.
Design: We reviewed the clinical histories from UOB of male patients with VHL syndrome that had been followed as part of familial screening. Patients presented with either paratesticular tumors, pain or discomfort.
Results: The most common tumor found was CCPC which were characterized by cystic spaces with intracystic papillary projections lined by clear cells with a resemblance to renal cell carcinoma. New intratesticular lesions were identified composed of a rich capillary network of single-layered flat endothelial cells and stromal cells, the latter demonstrating features suggestive of hemangioblastoma-like tumors. Immunoperoxidase for CD31, AE1/AE3 and CK7 were positive. Other lesions showed sertoli cell hyperplasia with early incipient lesions present in the adjacent parenchyma. Additionally, all these tumors showed loss of the VHL gene by FISH.
Conclusions: Although CCPC are the most common lesions associated with VHL, intraparenchymal tumors with morphology similar to hemangioblastomas and sertoli cell tumors can occur as part of the VHL syndrome. Testicular screening should be recommended in patients with VHL syndrome.

980 MAGE-A Expression, Immune Microenvironment and Prognosis in Upper Urinary Tract Carcinoma

Teppei Morikawa, Naohiro Makise, Takashi Ichimura, Masashi Fukayama. Graduate School of Medicine, The University of Tokyo, Tokyo, Japan.
Background: The melanoma-associated antigen-A (MAGE-A) family comprises cancer-testis antigens that represent promising prognostic biomarkers and immunotherapy targets in several cancer types. However, their significance in upper urinary tract carcinoma remains unknown.
Design: We examined MAGE-A expression by immunohistochemistry and analyzed its correlations with clinicopathological features, Ki-67 proliferation index, immune microenvironment status determined by CD3, CD8, CD20 and CD45RO immunohistochemistry coupled with quantitative digital image analysis, and patient outcome in 171 patients with upper urinary tract urothelial carcinoma. We also examined MAGE-A expression in selected metastatic lesions.
Results: High (≥50% positive cells) and low MAGE-A expression levels were observed in 33 (19%) and 49 (29%) cases, respectively. MAGE-A was negative in 89 (52%) cases. MAGE-A expression was positively correlated with ureteral location, histological grade 3, concomitant carcinoma *in situ*, higher Ki-67 proliferation index, and infiltration of CD3-, CD8- and CD45RO-positive T-lymphocytes, but not with CD20-positive B-lymphocytes. High MAGE-A expression was significantly associated with shorter metastasis-free survival after nephroureterectomy (log-rank P=0.019; multivariate hazard ratio, 1.98; 95% confidence interval, 1.00–3.92). MAGE-A expression in metastatic lymph nodes was highly correlated with its expression in primary lesions. MAGE-A expression was retained in lung metastases of urothelial carcinoma that were resistant to chemotherapy.
Conclusions: Our results suggest that MAGE-A may be a promising prognostic biomarker and potential target of immunotherapy in patients with upper urinary tract urothelial carcinoma.

981 Adrenal Myelolipomas With Associated Adrenal and Extra-Adrenal Lesions: A Clinicopathological Study

Diana Murro, Vijaya Reddy, Pincas Bitterman, Mariachiara Mei, Paolo Gattuso, Lauren Rosen, Smita Patel. Rush University Medical Center, Chicago, IL; Sapienza University of Rome, Rome, Italy.
Background: Myelolipomas are the most common lipomatous tumor of the adrenal gland and have been associated with extra-adrenal malignancies. However, concomitant myelolipomas and adrenocortical lesions have been only sporadically reported in the literature, mainly as case reports. We undertook a retrospective study of adrenal myelolipomas to assess the clinicopathological features and association with adrenal/extra-adrenal lesions.
Design: 21 myelolipomas were diagnosed in the past 22 years (1992-2014) at our institution. The clinical and pathological findings of all cases were reviewed.
Results: A total of 194 adrenalectomies were performed at our institution for a primary adrenal lesion. There were 65 cortical adenomas (34%), 92 pheochromocytomas (47%), 16 myelolipomas (8%), 12 cysts (6%), 5 ganglioneuromas (3%), 2 PEComas (1%), 1 neuroblastoma (0.5%) and 1 teratoma (0.5%). A total of 21 myelolipomas were found including 1 cytology and 4 autopsy specimens. The cases included 13 females and 8 males with mean age of 56 years (range 27-79 years). Twelve occurred on the left side and 9 on the right. Size ranged from 0.6-17 cm with a mean of 6 cm. Seven patients (33%) had concomitant adrenal lesions, including 3 cortical adenomas, 2 cortical hyperplasia and 2 Perivascular Epitheloid Cell tumors (PEComas). In all cases, the concomitant lesions were found in the same adrenal gland. In 6 cases the myelolipoma was found within the lesion and in 1 case the myelolipoma and adenoma were separate. Ten patients (48%) had extra-adrenal lesions (6 synchronous, 4 metachronous) including 2 with renal cell carcinoma (RCC; 1 with concomitant renal medullary fibroma and 1 with renal angiomyolipoma and adrenal PEComa), 1 with multiple tumors (adenosquamous lung carcinoma, renal oncocytoma and renal tubulopapillary adenoma), 2 renal oncocytomas, 1 renal pelvic urothelial cell carcinoma, 1 multiple myeloma, 1 Hodgkin lymphoma, 1 breast cancer and 1 pancreatic islet cell tumor.
Conclusions: A significant percentage of adrenal myelolipomas (7/21, 33%) are associated with other adrenal lesions or extra-adrenal neoplasms (10/21, 48%). The most common extra-adrenal malignancy is RCC, clear cell type. This is the first report of myelolipomas with associated adrenal PEComas (2/21, 10%), suggesting myelolipomas may have a MEN-1 gene defect. Both patients with PEComas had no history of tuberous sclerosis. Though myelolipomas are considered benign, coexistence with other adrenal lesions and extra-adrenal malignancies warrants thorough clinical work-up in these patients.

982 Papillary Renal Cell Carcinoma (PRCC), Type 1: A Single Institutional Study of 199 Cases Addressing Classification, Clinicopathologic Features and Treatment Outcome

Paari Murugan, Yingbei Chen, Sahussapont Sirintrapun, Hikmat Al-Ahmadie, Anuradha Gopalan, Samson Fine, Mariam Imnadze, Melissa Assel, Paul Russo, Satish Tickoo, Victor Reuter. Memorial Sloan Kettering Cancer Center, New York, NY.

Background: WHO divides PRCC into types 1 and 2. This classification remains controversial with growing evidence that type 2 PRCC are a heterogeneous group. The morphologic spectrum of type 1 PRCC has also been poorly defined. We investigated clinicopathological features, including cancer specific (CSS) and progression free survival (PFS) of PRCC with any type 1 component, based on the premise that the presence of even focal typical type 1 morphology would define tumor classification.

Design: We reviewed 199 cases of PRCC with WHO-defined type 1 features, diagnosed at our institution from 1995 to 2008. Tumors with type 2 features were included if any identifiable type 1 areas were present. Type 2 areas were quantified in tumors with mixed histology. Various pathological features were evaluated. Clinical features and follow up (FU) information were obtained from an IRB-approved annotated database. Multiple statistical tests were performed to evaluate outcome and its association with pathological parameters.

Results: Median FU among those not dead of disease was 7.8 yrs (IQR:5.7,10). 12 patients had recurrence, 10 of which died of disease. Kaplan-Meier estimated probability at 15 yrs of FU for recurrence & cancer-specific death was 7% (95%CI 4%,11%) & 6% (95%CI 3%,10%). 95 tumors (48%) contained some type 2 component; median amount of type 2 morphology was 25% (IQR:10%,70%). PFS and CSS showed no significant association with the presence of type 2 morphology (p=0.2&0.2, respectively) or its %age (p=0.052&0.13, respectively). Tumor size, mitotic rate, circumscription, LVI, and sarcomatoid & solid architectures were significantly associated with CSS (p<0.05). All 6 patients with LVI died of disease. While predominant high (3 or 4) Fuhrman or ISUP nucleolar grades were significantly associated with PFS (p=0.007;0.008), & CSS (0.005;0.037), less than predominant (<50%) high nuclear/nucleolar grade did not show association with outcome. pT3 stage had hazards of progression & cancer-specific mortality significantly greater than pT1 (p=0.001;0.0003).

Conclusions: -PRCC with any component of type 1 morphology, regardless of presence or amount of type 2 features, have excellent long-term outcome.

-Both predominant high Fuhrman and ISUP nucleolar grades are significantly associated with clinical outcome, but focal high grade nuclear or nucleolar features are not.

-Tumor size, mitotic rate, tumor circumscription, LVI, sarcomatoid and solid architectures are significantly associated with outcome in type 1 PRCC.

983 Does Hormonal Treatment Affect Gene-Specific Methylation Profiles in Prostate Cancer? A Preliminary Study

Gabriella Nesi, Raffaella Santi, Piera Rizzolo, Gianna Baroni, Monica Pepi, Laura Ottini. University of Florence, Florence, Italy; Sapienza University of Rome, Rome, Italy.

Background: DNA promoter hypermethylation is a frequent epigenetic event in prostate cancer (PCa) and many genes have been found to be aberrantly methylated in PCa.

Design: Using the candidate-gene approach, we performed promoter methylation analysis of a panel of genes involved in hormonal (AR, ESR1, ESR2) and tumor progression (RASSF1, APC, CD44, CDH1, BCL2) pathways. A series of 48 PCa cases were retrospectively collected: 25 patients had surgery alone (non-treated) while 23 had received androgen deprivation therapy for 3 months before surgery (treated). Clinicopathologic data, including age, histology, Gleason score, stage and margin status, were recorded. Biomolecular analysis was performed by pyrosequencing and methylation levels were assessed by calculating the average of methylation for each gene. Kruskal-Wallis test was used for statistical purposes.

Results: No significant differences emerged in methylation levels for the AR, ESR1, ESR2, RASSF1, CDH1, APC, ZEB1 and BCL2 genes in treated and non-treated PCa cases. Mean CD44 methylation levels were significantly higher in treated tumors (p=0.015). A correlation between CDH1 methylation and positive surgical margins was also noted (p=0.03). Gene-specific methylation profiles were not associated with the other prognostic parameters analyzed.

Conclusions: These preliminary findings showed that the methylation profiles of the genes investigated did not significantly vary in relation to hormonal therapy apart from the enhanced expression of the CD44 stem cell-related gene in hormonally treated PCa.

984 Use of Synoptic Pathology Data To Compare Performance of Subspecialist GU Pathologists With General Surgical Pathologists

Colin Newbill, Chris Magnusson, Nicholas Reder, Rodney Schmidt, Lawrence True. University of Washington, Seattle, WA.

Background: Subspecialization of pathologists is increasingly common. An expectation is that consistency in reporting pathologic features will be greater. Gleason grading (ISUP/WHO 2005) of prostate cancer (PrCa) in needle biopsies (NBxs) stratifies patients into management plans, i.e. active surveillance, curative therapy, neoadjuvant therapy, that have different treatments and complication rates. We questioned whether grading by general surgical pathologists (GS) differed from that of genitourinary (GU) pathologists.

Design: Based on records of 2,664 biopsies and of 1,411 prostatectomies spanning a 9 year period, we tabulated the frequency with which each of 19 pathologists graded PrCa as 6, 3+4, 4+3, or 8-10. Of the 19 pathologists reviewing biopsies and RPs, 4 subspecialize in GU pathology. Differences in frequency of grade categories were assessed by chi square analysis, using $p < 0.05$ as the threshold value for significance.

Results: GU pathologists were less likely to grade PrCa in needle biopsies as 4+3

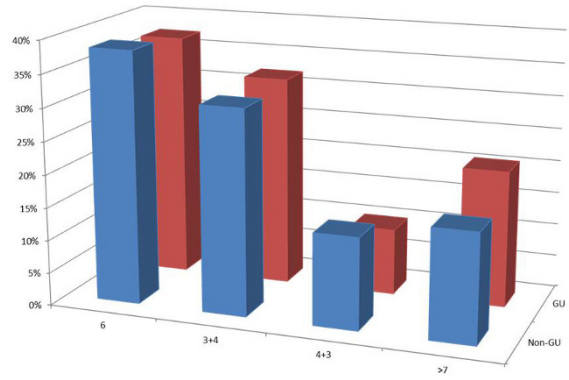

GU pathologists were more likely to grade cancer in both biopsies and RPs as greater than 7. General pathologists graded PrCa in RPs more frequently as grade 6.

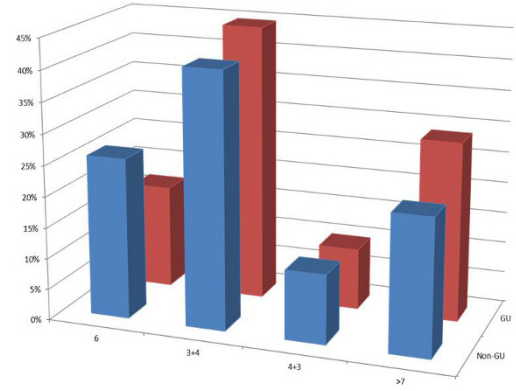

Conclusions: We find that GS pathologists more frequently undergrade PrCA in both NBxs and RP's. It follows that some of our patients undergoing RP are inaccurately assured of a low likelihood of disease progression. Patients with PrCA that is undergraded by NBx may be managed by an overly conservative regimen. While a summative grade of 7 could result in definitive therapy, some clinicians treat grades 3+4 and 4+3 differently. Thus, overestimating the prevalence of grade 4 in a needle biopsy may discourage a more conservative therapeutic approach among some clinicians. It is also possible that the bolus of 4+3 cases in the group of cancers diagnosed by GS pathologists reflects overly conservative evaluation of tumors that would more accurately be graded 8-10.

985 Prognostic Values for ERG, PTEN, CRISP3, and SPINK1 To Predict Biochemical Recurrence in Prostate Cancer

Byeong-Joo Noh, Ji-Youn Sung, Youn-Wha Kim, Sung-Goo Chang, Yong-Koo Park. Kyung Hee University Hospital, Seoul, Korea.

Background: Many studies have been conducted on prostate cancer, but its pathogenesis remains unclear. The established prognostic factors are Gleason score (GS), pathologic T (pT) staging, and serum prostatic-specific-antigen (PSA). However, these prognostic factors alone are not sufficient for predicting prognosis. Herein, the purpose of our study was to simultaneously evaluate the prognostic value and relationship of four biomarkers, ERG, PTEN, CRISP3, and SPINK1, and to conduct risk stratification of prostate cancer for patient management. This study is the first report to research on ERG, PTEN, CRISP3, and SPINK1 expression concurrently in an Asian patient population.

Design: Sixty-eight formalin-fixed, paraffin-embedded, prostate cancer samples from radical prostatectomies were obtained in the Kyung Hee University Hospital and were studied immunohistochemically for ERG, PTEN, CRISP3, and SPINK1. The results were measured for proportion and staining intensity.

Results: ERG fusion has a central role in regulating PTEN, CRISP3, and SPINK1 expression. ERG fusion is an important pathognomonic event in the pathogenesis of prostate cancer. Positive ERG expression can promote the loss of PTEN and increase CRISP3 expression. SPINK1 expression is mutually exclusive of ERG expression.

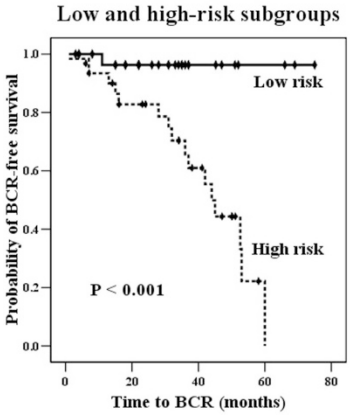

The loss of PTEN and high CRISP3 expression can be unfavorable indicators for prostate cancer because PTEN loss is associated with shorter BCR (biochemical recurrence), and high CRISP3 expression also increases BCR and cancer-related deaths. By using the combination of low PTEN and high CRISP3 expression, we can focus on patients who have a poor prognosis. Subgrouping into high-risk and low-risk is well correlated with BCR-free survival in prostate cancer.

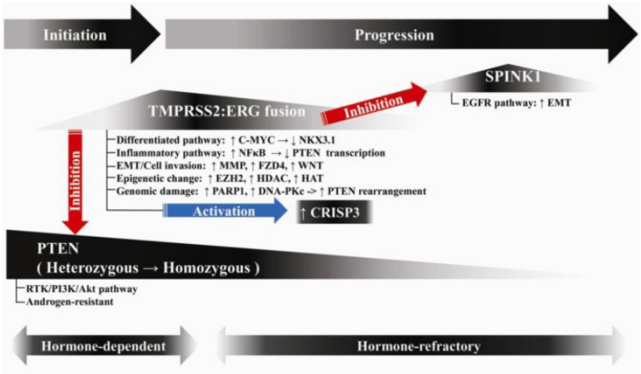

Conclusions: Low PTEN and high CRISP3 expression significantly characterize the subgroups of prostate cancer that have a poor prognosis for BCR.

986 Role of Trefoil Factor-3 Peptide (TFF3) in Prostate Cancer Progression

Michael Nowak, Constanze Merz, Anne von Maessenhausen, Wenzel Vogel, Diana Boehm, Maria Svensson, Jessica Carlsson, Ove Andren, Sven Perner. Institute of Pathology, University Hospital, Bonn, Germany; University Hospital of Örebro, Örebro, Sweden.

Background: Prostate cancer (PCa) is the second most abundant cancer diagnosis in men and accounts for about 10% of cancer-related deaths.

The ability of tumors to metastasize depends on the coordinated expression of extracellular matrix degrading enzymes (MMPs) and adhesion molecules. TFF3 (ITF, intestinal trefoil factor) is a 18 kDa protein with a characteristic trefoil structure containing three conserved cysteine residues. To date, neither the exact function nor its receptors are well defined. Aim of this study was to identify the receptor for TFF3 and its role in prostate cancer progression.

Design: Expression of TFF3 in prostate tumors was semi-automatically assessed by immunohistochemistry using a tissue microarray of the Cohort of Swedish Men, which consisted of primary tumors from radical prostatectomies (n=284 patients). TFF3 expression was furthermore assessed in prostate tumor cell lines DU145, PC-3, and LnCaP as well as the benign prostate cell line BPH-I. Functional assays using these cell lines involved receptor internalization assays, flow cytometry, and Boyden-chamber migration assays.

Results: Expression in prostate tumors positively correlated with PSA levels.Based on the unresolved regulation and receptor for TFF3 we tested the basal expression in cells from benign prostate hyperplasia (BPH-1) and three cell lines from prostate cancer metastasis (DU145, PC3, LnCaP). Among the tested cell lines BPH-1 cells showed the highest expression. LnCaP cells were TFF3 negative, PC3 and DU145 showed intermediate expression within this spectrum. Which soluble factors regulate the expression of TFF3 in prostate cancer cells is not known. Using antibody-mediated blockage of the interleukin-6 receptor (IL-6R), we show that TFF3 expression is driven by autocrine IL-6. Incubation with TFF3 mobilized calcium from intracellular stores and led to phosphorylation of STAT3, independent of the EGFR, which has been discussed as a potential TFF3 receptor. Furthermore, we show that TFF3 is a chemokine, which is mediated by the chemokine receptor CXCR4.

Conclusions: Our results point to a IL-6 mediated regulation of TFF3 in prostate cancer, which effects on migration and proliferation are mediated by the chemokine receptor CXCR4.

987 A Clinicopathologic Analysis of 53 Cases of Renal Cell Carcinoma With Vena Caval Involvement

Ifeoma Nwadei, Adam Lorentz, Viraj Master, Adeboye Osunkoya. Emory University School of Medicine, Atlanta, GA.

Background: Only occasional cases of renal cell carcinoma (RCC) are reported to demonstrate involvement of the vena cava (VC). Despite advances in biological and chemotherapeutic treatment modalities and surgical techniques, 5 year survival in this population continues to be poor. Further studies are needed to better characterize this patient population, especially from the pathologic standpoint.

Design: A retrospective review of RCC with VC involvement diagnosed at our institution from 2006-2014 was performed. Multiple clinicopathologic parameters were examined in our cohort.

Results: Fifty three cases of RCC with VC involvement were identified. All patients underwent radical nephrectomies. Mean patient age was 62 years (range: 40-82 years). The cohort consisted of 36/53 (68%) males and 17/53 (32%) females. Mean primary tumor size was 10.4 cm (range: 2.5-21.0 cm). Several cases demonstrated multifocality (11/53, 20.7%). Tumor stage breakdown was: 37/53 (70%) were pT3b, 14/53 (26%) were pT3c, and 2/53 (4%) were pT4. Histologically, 37/53 (70%) cases were found to have intraluminal inferior VC tumor thrombi (pT3b) and 16/53 (30%) had microinvasion of the inferior VC wall (pT3c, pT4), one of which also demonstrated superior VC wall microinvasion. Most of the tumors were clear cell RCC (45/53, 84.6%) though other RCC variants were also represented. Most cases were Fuhrman nuclear grade 3 (34/53, 64%) or 4 (19/53, 36%) with sarcomatoid differentiation present in 5/53 (9%) cases. Of those cases for which tumor necrosis status was available, 25/37 (68%) demonstrated tumor necrosis. As of the time of initial tumor resection, 11/53 (21%) cases were staged pM1. In these cases, the ipsilateral adrenal gland was the most common site of metastasis though several cases had metastases to unusual sites including the eye and scalp. Of the 15 patients staged pMX at the time of primary tumor resection, 12/15 (80%) presented later with metastasis, most commonly to the lungs. Of all cases, 4/53 (7.5%) had positive vascular resection margins. One of two cases with pT4 disease had positive surgical margins.

Conclusions: This is one of the largest studies to date on the clinicopathologic findings of patients with RCC and VC involvement. Our findings suggest that in a select group of patients with VC involvement may benefit from radical nephrectomy, though tumors staged as pT4 may be more likely to have positive vascular and non-vascular surgical resection margins.

988 MED15 Overexpression Arises During Androgen Deprivation Therapy Via PI3K/mTOR Signaling

Anne Offermann, Zaki Shaikhibrahim, Martin Braun, Isabella Syring, Wenzel Vogel, Christian Ruiz, Tobias Zellweger, Cyrill Rentsch, Lukas Bubendorf, Sven Perner. Institute of Pathology, University Hospital, Bonn, Germany; Institute for Pathology, University Hospital Basel, Basel, Switzerland; St. Claraspital Basel, Basel, Switzerland; University Hospital of Basel, Basel, Switzerland.

Background: Androgen deprivation therapy (ADT) is the main therapeutic option for men with advanced prostate cancer (PCa). After initial regression, most tumors develop into castration-resistant PCa (CRPC). Previously, we found the Mediator complex subunit MED15 to be overexpressed at high frequency in CRPC and to correlate with clinical outcome. We observed that MED15 is implicated in TGFß signaling, a pathway involved in CRPC and linked to PI3K signaling. Therefore, we investigated whether MED15 is implicated in the signaling changes taking place during progression to CRPC.

Design: We performed immunohistochemistry (IHC) for MED15, pAKT and pSMAD3 on 112 PCa samples before and 145 after ADT, as well as on matched samples from same 29 patients before and after ADT. PCa cells were treated with EGF, PI3K-, TGFß- and mTOR- inhibitors. Cell viability and apoptosis of *MED15* knockdown and control cells was measured using MTT and annexinV staining, respectively.

Results: We observed significant increased MED15 expression after ADT in 72% of matched samples, and in CRPC compared to hormone-sensitive tissues. IHC for pAKT and pSMAD3 shows that MED15 correlates with PI3K and TGFß activities, respectively, and that hyper-activation of both pathways simultaneously correlates with highest levels of MED15 expression after ADT. We further show that MED15 expression increases in LNCaP cells under androgen deprivation, and via EGF mediated PI3K hyper-activation. PI3K/mTOR inhibition by LY294002 and Rapamycin resulted in a complete inhibition of MED15 expression, while blocking the TGFß-receptor by SB431542 leads to decreased MED15 expression. Si-RNA mediated *MED15* knockdown reduced LNCaP cell viability and induced apoptosis during androgen deprivation.

Conclusions: Taken together, MED15 overexpression arises during ADT via hyper-activation of PI3K/mTOR signaling, thus MED15 has the potential of serving as a predictive marker for response to PI3K/mTOR inhibitors. Furthermore, MED15 is potentially a more specific and effective therapeutic target for the treatment of CRPC.

989 Comprehensive Genomic Profiling of Collecting Duct Carcinoma of the Kidney Reveals a High Frequency of NF2 Genomic Alterations

Norma Palma, Siraj Ali, Kai Wang, Julia Elvin, Doron Lipson, Mark Rosenzweig, Rachel Erlich, Juliann Chmielecki, Vincent Miller, Doug Lin, Philip Stephens, Jeffrey Ross. Foundation Medicine Inc, Cambridge, MA; Beth Israel Deaconess Medical Center, Boston, MA.

Background: Collecting duct carcinomas (CDC) of the distal renal collecting duct, accounts for than 1% of all renal malignancies. CDC typically presents at an advanced stage and often recurs, frequently metastasizes and has an adverse prognosis relative to other renal carcinomas. We queried whether comprehensive genomic profiling (CGP) would uncover clinically relevant genomic alterations (CRGA) that could lead to targeted therapies for patients with CDC.

Design: DNA was extracted from 40 microns of FFPE sections from 11 CDC cases. Comprehensive genomic profiling (CGP) was performed on hybridization-captured, adaptor ligation based libraries to a mean coverage depth of 748X for 3,769 exons of 236 cancer-related genes plus 47 introns from 19 genes frequently rearranged in cancer. The results were evaluated for all classes of genomic alterations (GA) including base substitutions, short insertions and deletions, copy number changes and gene fusions/rearrangements. CRGA were defined as GA linked to drugs on the market or under evaluation in mechanism driven clinical trials.

Results: There were 10 male and 1 female patients with a median age of 57 years. There were 2 (18%) stage III and 7 (63%) stage IV tumors at the time of sequencing. Staging data was unavailable for 2 samples. All samples were Fuhrman grades 3 and 4. For the 7 cases where PAX8 IHC staining data was available, all seven cases stained positively. CGP revealed 22 total GA (2.0 GA/sample), with 10/11 cases harboring at least one GA. 5(45%) of CDC featured at least 1 CRGA with a total of 6 CRGA identified.*NF2* truncating alterations were the most frequent GA/CRGA in 45% of cases, with 2 cases harboring such an alteration within the N-terminal FERM domain, and 3 cases harboring an *NF2* truncating alterations proximal to moesin domain (aa 510 and 522 twice). The next frequent CRGA included *DNMT3A* (18%), *CDKN2A* (18%), and *HRAS* and *EGFR* both at 9%. Other GA include *STED2* (27%), *ARID2, CSF1R, PBRM1, RB1, SMARCB1,* and *STAG2* (all at 9%).

Conclusions: CGP of CDC reveals a significant number of CRGA, with an enrichment of *NF2* alteration (45%) in contrast to the low frequency of *NF2* alterations (<4%) found in clear cell and chromophobe carcinoma. With the potential of employing targeted therapies such as MAPK pathway inhibitors for *NF2* driven CDC, further studies utilizing CGP in CDC are in progress to verify and expand on this finding.

990 Does the Distance Between Tumor and Margin in the Posterior Half of the Prostate Correlate With Progression After Radical Prostatectomy?

Swetha Paluru, Jonathan Epstein. Johns Hopkins Medical Institutions, Baltimore, MD.

Background: When the urologist performs radical prostatectomy (RP) it is easier to dissect close to the prostate posterioly since the posterior half of the prostate has a smooth well-defined edge unlike the anterior prostate. Often tumor extends close to the posterior margin where the issue is whether pathologists should measure how close the tumor is to the margin, which implies that close margins are at higher risk of post-operative progression. There are conflicting studies on whether the proximity of tumor to the margin in RPs correlates with post-operative progression. However, there is no published data regarding the impact of the closest distance of the tumor to the margin specifically relative to the anatomical location within the RP of the closest margin.

Design: We identified 105 RPs for prostate cancer. Cases were sequential and selected to have the longest follow-up after 2005 so that the modified ISUP grading system was used. The tumor with the closest margin was in the posterior half. All tumor was organ confined, margin negative, and Gleason score 6. Distances were measured with a micrometer.

Results: Eighty seven cases had no progression with a minimum 6 year follow-up (median 8, range: 6-9). Eighteen cases had progression with the median time to progression of 2 years with all men progressing within 6 years after RP. For cases without progression, the median distance was 0.35 mm. (range 0.02-8 mm.). For cases with progression, the median distance was 1.19 mm. (range 0.03-6 mm.). There was no statistically significant difference in the risk of progression based on the proximity of tumor to margin.

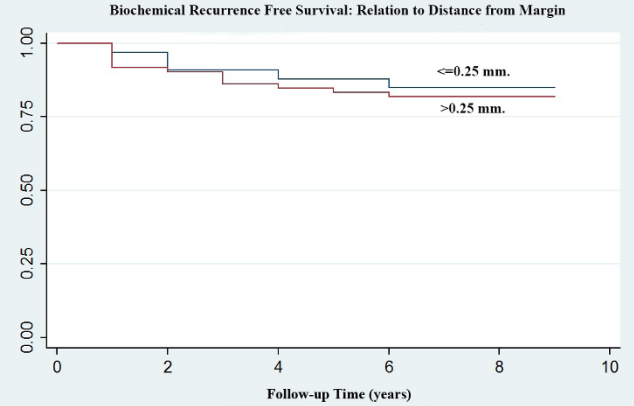

Conclusions: For tumor located posteriorly or posterolaterally, the distance of tumor to the margin has no impact on the progression rate following RP. Ours is the first study to evaluate the impact of closest distance of tumor to the margin relative to location in the RP. The study also has the benefit of the longest follow up for patients without progression. We are in the process of analyzing the impact of distance of tumor to the margin in the anterior half of the prostate, where the closeness of tumor to margin may have different implications given the different anatomy in this area.

991 Institutional Review of Papillary Renal Cell Carcinoma: A Pathologic and Cytogenetic Correlation

Monika Paroder, Lara Harik, Murty Vundavalli. Columbia University Medical Center, New York, NY.

Background: Papillary renal cell carcinoma (PRCC) is the second most common type of renal cell carcinoma. Recent recommendations subdivide PRCC into types 1 and 2. Type 2 PRCC appear to be a heterogeneous combination of tumors with variable immunohistochemical and clinico-pathologic characteristics. We present our institutional experience evaluating these two subtypes of PRCC in conjunction with cytogenetic analysis.

Design: A review of our database was performed for patients with papillary renal cell carcinoma who underwent surgery between 1999 and 2014 with available cytogenetic analysis on those tumors. Cytogenetic results were stratified as compatible with PRCC (comprising of a combination of trisomy 7 and/or 17) or cytogenetic abnormalities that are not known to be typically associated with PRCC, including complex karyotype alterations. In addition, clinical and pathologic data were retrieved and reviewed.

Results: 137 cases of PRCC were identified in our database; complete review was performed on 63 cases. The M:F ratio was 52:11 and the average age was 61.54 (38-89) years. One patient had bilateral disease. 35/63 cases (55.6%) were histologically designated type 1 PRCC, 25/63 (39.7%) type 2 PRCC, and 3/63 (4.76%) cases mixed type 1 and 2. Cytogenetic results were analyzed according to the morphologic types of PRCC, as well as by age cutoff (<50 and >50 years). 31/35 (88.6%) cases of **type 1 PRCC** displayed a cytogenetic profile compatible with PRCC and 4/35 (11.4%) showed cytogenetic abnormalities that are not typically associated with PRCC. 16/25 (64%) cases of **type 2 PRCC** showed karyotypes that are compatible with PRCC and 7/25 (28%) showed cytogenetic abnormalities that are not typically associated with this tumor type. The 3 (100%) cases of mixed type 1 and 2 PRCC showed cytogenetic abnormalities usually observed in PRCC. 8/11(73%) of patients < 50 years of age showed cytogenetic changes that are compatible with PRCC. 3/11 cases (27%) displayed unusual karyotypes and interestingly, these were all classified as type 2 PRCC.

Conclusions: Type 2 PRCC, particularly patients less than 50 years of age, showed a higher rate of cytogenetic abnormalities not typically associated with PRCC. A more detailed morphologic and Immunohistochemical analysis of these tumors might elucidate a subset of tumors with similar features. Our data supports the need for further studies of the cytogenetic profile in PRCC, along with clinical and histologic correlation.

992 Interpretation of Margin Status in Robot-Assisted Laparoscopic Partial Nephrectomy: A Diagnostic Challenge for Pathologists

Viren Patel, Daniel Eun, Andrew Harbin, Varsha Manucha. Temple University Hospital, Philadelphia, PA.

Background: Assessment of truly significant positive surgical margins (PSM) can result in diagnostic and management dilemma after robotic partial nephrectomy(RPN). Incongruent opinions between the pathologist's microscopic findings and the surgeon's intraoperative observations associated with post-extraction or specimen handling artifactual changes contributes to this problem.

Design: A total of 101 RPN cases, performed by the same surgeon (DE) using the daVinci Si Robotic System (Intuitive Inc, Sunnyvale,CA) for 2 years were retreived. Most tumors were enucleated with minimal to no benign parenchyma at the deep margin, and were extracted in an endoscopic specimen retrieval bag after extending one of the incisions. The H&E slides of all cases initially reported as PSM (at or less than 1 mm from resection margin) were reviewed by the pathologist(VM) in conjunction with the operative notes. The operative videos of the surgical procedures were reviewed by the clinicians(AH and DE).

Results: PSM was reported in 9(8.91%) tumors. Six(83%) of these were chromophobe carcinomas. On review, 2 cases had tumor at the inked margin, in 5 cases the tumor was within 1 mm of the margin and in 2 cases the margin was negative (post-extraction disruption of tumor pseudocapsule; technically difficult extraction due to multifocal tumors).

Table.1

Renal cell carcinomas (number of cases)	Positive, initial review	Tumor on ink, second review	Surgeons perception
Clear cell (57)	1	1	Positive
Papillary (16)	1 (incidental along with oncocytoma with negative margin)	0	Negative; did not see the papillary carcinoma (4mm size)
Chromophobe (11)	6	1	1-positive3-visually negative2-complicated operative procedure but tumor extraction complete
Oncocytoma (12)	0	0	Negative
Angiomyolipoma (4)	0	0	Negative
Mucinous Spindle cell (1)	1	0	Negative

Conclusions: The margin assessment in RPN can be challenging in renal tumors that have been surgically enucleated, and may be affected by tumor multifocality and extraction-related disruption. Chromophobe carcinoma margins are more difficult to judge in-situ since their bland color appears similar to normal renal parenchyma. Inspection of the specimen on the back table, correlation of pathology with operative notes, intraoperative video review and surgeon corroboration can be helpful in more accurately assessing PSM.

993 Central Zone Adenocarcinoma of the Prostate Is a Rare Aggressive Tumor, PAX2 and PAX8 Negative

Pallavi Patil, Karen Streator Smith, Paula Carver, Cristina Magi-Galluzzi. Pathology and Laboratory Medicine Institute, Cleveland, OH.

Background: Prostatic central zone (CZ), similarly to seminal vesicles (SV) and ejaculatory duct (ED) is alleged to be of Wolffian duct origin as opposed to endodermal urogenital sinus origin of peripheral (PZ) and transitional zone. Prostatic adenocarcinoma (PCa) involving CZ is rare. PAX2 and PAX8 are lineage specific markers for Wolffian duct origin. We studied the pathologic characteristics of PCa arising in CZ compared to all PCa seen during the same time and their PAX2 and PAX8 expression.

Design: 1579 radical prostatectomy specimens (RP) diagnosed with PCa between 2005-2014 were reviewed by a single pathologist. Tumor outline was mapped to determine the location relative to PZ and CZ. Only tumors involving prostate base and ED region were considered CZ tumors. Age, Gleason score (GS), presence of utricle and intraductal carcinoma (IDC-P), pathologic stage (T2 vs. T3), seminal vesicle (SVI) and ED invasion (EDI), margin status (M+), lymph node metastasis (LN+), biochemical failure (BCF), distant metastasis and death were recorded for all CZ tumors; one representative block per case was stained with PAX2 and PAX8.

Results: 27 (1.7%) tumors involved CZ: 16 were limited to CZ (CZ PCa) and 11 extended into PZ (CZPZ PCa). Patients' mean age was 59 years (range 46-68). Utricle was present in 55% of cases. Pathologic characteristics of all tumors are summarized in Table 1.

	CZ PCa (n=16)	CZPZ PCa (n=11)	PCa (n=1579)
Mean age	58	60	59
GS [%]			
6	0*	0	20
7	12*	36	64
≥8	87*	54*	14
N/A	0	9	1
T2 [%]	0*	0*	64
T3 [%]	100*	100*	36
SVI [%]	69*	91*	7
M+ [%]	44	45	27
LN+, n (%)	0/15	2/9 (22)*	55/963 (6)
IDC-P [%]	50*	82*	3
*statistically significant on comparison with PCa (P			

GS was ≥8 in 74% and IDC-P was present in 63% of CZ cases. All CZ tumors were stage T3, 78% had SVI and EDI, and 44% had M+. LN+ was present in 22% of CZPZ PCa. BCF occurred in 3 patients (11%); 2 (7%) developed skeletal metastasis and 2 (7%) died of disease. All CZ tumors were negative for PAX2 and PAX8; positive nuclear staining was noted in SV/ED tissue. A single normal CZ gland staining for PAX2 was noted in 1 case.

Conclusions: Central zone adenocarcinoma of prostate represents <2% of all PCa, and is a high-grade, high-stage tumor frequently associated with IDC-P and SVI. 7% of patients developed skeletal metastasis and 7% died of disease. Lack of PAX2 and PAX8 expression in CZ PCa does not support a Wolffian origin of this tumor.

994 ERG and SPINK1 Expression in Ductal Adenocarcinoma of the Prostate

Pallavi Patil, Paula Carver, Karen Streator Smith, Cristina Magi-Galluzzi. Cleveland Clinic, Cleveland, OH.

Background: Ductal adenocarcinoma of the prostate (DAC) is an uncommon variant of prostatic carcinoma (PCa). Mixed ductal and acinar carcinoma (MDAC) is more common than pure ductal adenocarcinoma (PDAC). ERG and SPINK1 are molecular alterations frequently studied in acinar PCa (APCa), but not well characterized in DAC. We studied the pathologic characteristics of DAC and its expression of ERG, SPINK1 by immunohistochemistry (IHC).

Design: We queried our PCa database for cases containing DAC in the diagnosis. All slides were reviewed to confirm diagnosis, >10% ductal component, Gleason score (GS) and pathologic stage (T2/T3), and to select a representative block for IHC. Age, GS, stage, margin status (M+), seminal vesicle invasion (SVI), lymph node metastasis (LN+), biochemical failure (BCF), distant metastasis and death were recorded for all DAC. Tumors were classified as positive if staining was present in >5% of tumor cells.

Results: Of 45 DAC included in our study, 22 were PDAC and 23 MDAC. Pattern of growth was papillary in 58%, cribriform and papillary in 31%, and cribriform in 11% of cases. PIN-like features were seen in 3 cases. GS, stage, M+, SVI, and LN+ of all DAC tumors are summarized in Table 1 and compared to all PCa diagnosed on radical prostatectomy (RP) at the same institution.

	PDAC	MDAC	PCa (n=3259)
Mean age, yrs	64	60	60
GS %			
6	0*	0*	22
7	0*	26*	65
≥8	100*	74*	12
T2 %	38*	13*	67
T3 %	62*	87*	33
SVI %	14	39*	6
M+ %	29	35	28
LN+ %	5	33*	4
* statistically significant on comparison with all PCa (p value			

BCF and metastasis occurred in 25% and 14%, respectively, of DAC; 7% of patients died of disease. ERG was expressed in 15% and SPINK1 in 33% of DAC. All MDACs showed concordant expression of SPINK1 in acinar and ductal component, whereas ERG had concordant expression in all except one case positive only in the acinar component. One MDAC contained concordant SPINK1 and ERG expression.

Conclusions: Our study confirms that DAC are high-grade, high-stage tumors with an aggressive clinical course when treated by RP. ERG expression in 15% of DAC is much lower than the rates reported for APCa, and SPINK1 expression in 33% of DAC is much higher. These differences could partly explain the distinct clinicopathological characteristics of DAC, though further studies on prognostic significance are required. Co-expression of ERG and SPINK1 in 1 case confirms that they are not mutually exclusive.

995 Chromophobe Renal Cell Carcinoma With Neuroendocrine Differentiation and Neuroendocrine-Like Features. Morphologic, Immunohistochemical, Ultrastructural, and ArrayCGH Analysis of 18 Cases

Kvetoslava Peckova, Chisato Ohe, Naoto Kuroda, Petr Martinek, Stela Bulimbasic, Delia Perez Montiel, Jose Lopez, Enric Condom-Mundo, Ondrej Daum, Pavla Rotterova, Milan Hora, Michal Michal, Ondrej Hes. Charles University and Charles University Hospital, Plzen, Czech Republic; Kansai Medical University, Osaka, Japan; Red Cross Hospital, Kochi, Japan; University Hospital Dubrava, Zagreb, Croatia; Institute Nacional de Cancerologia, Mexico City, Mexico; Cruces University Hospital, Barakaldo, Spain; Bellvitge University Hospital, Barcelona, Spain.

Background: Chromophobe renal cell carcinoma (CRCC) with neuroendocrine differentiation (CRCND) has been described recently. Among 624 CRCC in our files, 18 cases with morphological features suggestive of neuroendocrine differentiation were selected for further analysis.

Design: Tumors were routinely processed, examined using immunohistochemistry, ultrastructure, and arrayCGH.

Results: Cases were classified as CRCND or CRC with neuroendocrine-like features (CRCND-L) based on the immunohistochemical expression of neuroendocrine markers.

CRCND: 4 cases. Age range 49-79, size ranged from 2.2 to 22 cm.

CRCND-L: 14 cases. Age range 34-74 years, size range 3.8-16.5 cm. Follow up information was available for 11/18 patients, range 0.5-12 years. 2/4 CRCND showed aggressive clinical course with metastatic spreading.

CRCNDs were positive for CD56 (4/4), synaptophysin (4/4) and chromogranin (1/4). All 14 CRCND-L were negative for the above mentioned markers.

All CRDsND and CRCsND-L were positive for CK 7 and CD117. Ultrastructure showed poorly preserved neuroendocrine granules only in 2/4 CRCsND. Losses of chromosomes 1,2,6,10, were found in all analyzable CRCND, while multiple losses (chromosomes 1,2,5,6,8,10,13,17,21) and gains (chromosomes 4,7,11,12,14,15,16,19,20) were found in CRCsND-L.

Conclusions: 1, Morphological features suggesting neuroendocrine differentiation are rarely seen in CRCCs. In the majority of such cases, true neuroendocrine differentiation cannot be demonstrated, thus representing simply an architectural growth pattern variant.
2, True CRCNDs differ from CRCNDs-L by the expression of neuroendocrine markers.
3, Chromosomal losses (chromosomes 1, 2, 6, and 10) are found in CRCND, while CRCND-L cases show both losses and gains of multiple chromosomes.
4, CRCNDs have metastatic potential.

996 Mucinous Spindle and Tubular Renal Cell Carcinoma: Analysis of Chromosomal Aberration Pattern of Low Grade, High Grade and Overlapping Morphologic Variant With Papillary Renal Cell Carcinoma

Kvetoslava Peckova, Petr Martinek, Saul Suster, Delia Perez Montiel, Ondrej Daum, Pavla Rotterova, Milan Hora, Michal Michal, Ondrej Hes. Charles University and Charles University Hospital, Plzen, Czech Republic; Medical College of Wisconsin, Milwaukee, WI; Institute Nacional de Cancerologia, Mexico City, Mexico.

Background: Chromosomal numerical aberration pattern in mucinous spindle and tubular renal cell carcinoma (MSTRCC) is referred as variable with frequent gains and losses. The objective of this study was to map the spectrum of chromosomal aberrations (extent and location) in a large cohort of the cases and relate these findings to the morphologic variants of MSTRCC.

Design: 54 MSTRCC with uniform morphological pattern were selected (out of 133 MSTRCC available in our registry) and divided into 3 groups: classic low grade (CLG)

(Fuhrman grade 2), high grade (HG) (Fuhrman 3), and overlapping MSTRCC with papillary RCC morphology (OPM). ArrayCGH analysis was applied to 17 cases with well-preserved DNA.
Results: 5 analyzable CLG MSTRCC showed multiple losses, mostly of chromosomes 1,4 ,8,9,14,15,22. No gains were found. 7 analyzable HG MSTRCC showed more variable pattern with normal chromosomal status or with losses of chromosomes 1,6,8,9,14,15,22 and gains of 3,7,16,17.
Group of 5 OPM MTSRCC was more uniform in chromosomal aberration pattern with losses of chromosomes 1,4,6,8,9,13,14,15,22. No gains were detected.
Conclusions: 1, MSTRCC low grade: losses of 1,4,15 were present in all analyzable cases.
2, high grade MSTRCC showed more variable pattern with normal chromosomal status, or with both losses and gains, including gains of 7,17 .
3, cases with overlapping morphological features (MSTRCC) and PRCC showed losses of 1,4,6,8,9,13, 4,15,22 and no gains of 7,17. Such chromosomal aberration pattern supports results of previously published morphological and immunohistochemical studies describing broad morphologic spectrum of MTSRCC with changes resembling papillary RCC.

997 Pathological Features of Penile Lichen Sclerosus (LS) According To a Topographical Method of Evaluation in 200 Patients

Adriano Piris, Diego Sanchez, Sofia Canete, Tania Campagnoli, Lorena Gonzalez, Patricia Zarza, Sabrina Oneto, Cecilia Lezcano, Ingrid Rodriguez, Martin Mihm, Antonio Cubilla. Massachusetts General Hospital, Boston, MA; Instituto de Patología e Investigación, Asunción, Paraguay; Facultad de Ciencias Médicas – UNA, Asunción, Paraguay; University of Pittsburgh, Medical Center, Pittsburgh, PA.
Background: Since the seminal study of Hart and Helwig in 1975 there are few detailed pathological studies of lichen sclerosus.
Design: 200 patients with LS (109 with invasive carcinomas, 28 with penile intraepithelial neoplasia (PeIN) and 63 with no atypias) were evaluated. Sites were foreskin (57%), glans (24%) and multiple compartments (19%). We designed a topographical approach of evaluation by anatomical layers as follow: **squamous epithelium** (hyper and parakeratosis, hyperplasia, atrophy, PeIN), **interphase** changes at basal layer (mild, moderate, severe), **lamina propria** superficially and deeply (sclerosis, vascular changes, edema), **dartos and corpus spongiosum (CS)**. Patterns of sclerosis and hyalinization were globular, perivascular, linear and fully developed. Lymphocytic infiltration was evaluated as superficial and dense, spotty or band-like (below sclerosis).
Results: Frequency of histological changes in penile LS and their confidence intervals (CI) are shown in Table 1.

Topography	Changes*	Number of cases (%)	CI 95%
Epithelium	Hyperplasia	163 (82)	76-87
	PeIN	129 (65)	58-71
	Parakeratosis	108 (54)	47-61
Interphase	Basal vacuoles	197 (98.5)	97-100
LP**: Sclerosis	Perivascular	161 (81)	75-86
	Globular	128 (64)	57-71
	Linear	109 (55)	48-61
Dartos/CS Lymphocytes	Rare, spotty	166 (83)	78-88
	Superficial dense	113 (57)	50-63

* More than one change in many specimens. **LP: lamina propria

Conclusions: A topographical anatomical approach from surface to deep layers was useful to document all possible lesions**.** Histological changes were heterogenous and affected multiple layers with variation from patient to patient. Atypia to the histological level of PeIN was a significant finding. Other common features were basal cell vacuolization at the interphase, squamous hyperplasia, perivascular hyalinization and scarcity of lymphocytes. Focal changes such as perivascular, globular or linear hyalinization were sufficient for the diagnosis of LS. Recognition of LS is important because of its frequent association with precancerous and invasive penile carcinomas.

998 Nuclear Size Measurement for Distinguishing Urothelial Carcinoma From Reactive Urothelium on Tissue Sections

Kate Poropatich, Jason Yang, Rajen Goyal, Vamsi Parini, Ximing Yang. Northwestern University, Feinberg School of Medicine, Chicago, IL.
Background: The diagnosis of urothelial carcinoma (UC) is mainly based on cytologic atypia. Because of the lack of background urothelial cells in a section for comparison, lymphocytes are often used as reference cells for size estimate and comparison in practice. It is believed that high grade UC (including UC in situ) cells are 4 times as big as a lymphocyte. However, studies with objective measurements using advanced imaging systems are limited.
Design: We measured the nuclear size (length and width) of individual urothelial cells on digital images from H&E tissue sections, using standard imaging CellSens software. At least 10 urothelial cells were measured in each image. Lymphocytes on the corresponding sections were also measured as the standard. The specimens studied include reactive urothelium (RU; n=5), low grade UC (n=12) and high grade UC (n=7) including carcinoma in situ (CIS, n=4).
Results: The length (L) and width (W) of 289 cells are measured on bladder H&E sections. The area was calculated by WxLx0.8 based on the oval shape of most urothelial cells. Lymphocyte (LC) area and diameter were determined. These data are in the table below:

Cell Type	L mm (mean)	W um (mean)	Area um2 (mean)	# of cells counted	Liner Ratio L/LC & W/LC	Area ratioTarget Cell/LC
Lymphocytes	4.86	4.86	18.54	47	1	1
Reactive Urothelium	10.05	6.08	48.89	57	2.07/1.25	2.64
Low Grade UC	10.39	6.91	57.44	123	2.14/1.42	3.10
High grade UC	13.84	9.19	101.75	79	2.85/1.89	5.49

Linear ratios were generated by cell length/LC diameter and cell width/LC diameter. Area ratios were generated by cell nuclear area/LC nuclear area. A high grade UC cell is 2.8 times as big as a LC in nuclear diameter and 5.49 times as big as a LC in area. This is significantly larger than those of low grade UC or RU cells. Low grade UC cells did not differ significantly from RU cells on these parameters.
Conclusions: High grade urothelial carcinoma including CIS had much greater nuclear enlargement than reactive urothelium. The increased nuclear length, width and mainly surface area, with or without comparison to a lymphocyte, can be potentially used as a reference in clinical practice. Distinguishing low grade UC and reactive urothelial cells requires other measurement methods. Studies with more cases and different measurement parameters are underway.

999 Ecotropic Viral Integration Site 1 as a New Tumor Stem Cell Like Oncogene in Prostate Cancer

Angela Queisser, Susanne Hagedorn, Hui Wang, Wenzel Vogel, Anne von Massenhausen, Claudia Lengerke, Sven Perner. Institute of Pathology, University Hospital, Bonn, Germany; University Hospital of Basel, Basel, Switzerland.
Background: For prostate carcinogenesis, the accumulation of molecular changes is thought to be essential. Mutations in tumor suppressorgenes like *PTEN* as well as in the oncogenes *MYC* and *EGFR* are important for prostate cancer (PCa) progression. However, the role of transcription factors with stem cell marker properties during prostate carcinogenesis is insufficiently examined. Due to gene rearrangements and inversion the stem cell marker *ecotropic viral integration site 1* (EVI1) is often overexpressed in several types of leukaemia but also in solid tumours such as breast cancer. EVI1 is located on 3q26, which has been shown to be amplified in PCa. Thus, the aim of this study was to investigate the role of EVI1 in PCa.
Design: The expression level of EVI1 was investigated on a PCa progression cohort (primary PCa *n=148*, localized lymph node *n=39* and distant metastases *n=32*) using immunohistochemistry. The staining intensity was determined using an image analysis system (Definiens). PCa cell lines were screened for EVI1 protein expression by western blot. To stably down regulate EVI1, cells were transduced with EVI1-shRNA or control shRNA by lentiviral mediated gene transfer. Proliferation was assessed with the MTT assay and the xCELLigence system. The influence on the cell cycle was examined by immunocytochemical stainings for Ki67 and p27. For the investigation of migration, a scratch assay was conducted. Anchorage-independent growth was determined using a soft agar assay.
Results: In primary prostate cancer, EVI1 was heterogeneously expressed. The expression was higher in lymph node and distant metastases compared to primary PCa. Western blot analysis revealed an expression of EVI1 in the PCa cell line PC3. EVI1 inhibited cells showed an impaired proliferation capacity as well as a reduced migratory potential. The number of cells negative for Ki67 was higher in EVI1 knockdown cells indicating a reduction of the growth fraction. The percentage of cells expressing the cell cycle inhibitor p27 was higher in the EVI1 knockdown cells. Moreover, down regulation of EVI1 in PC3 cells using EVI1-shRNA led to smaller and lesser colonies in soft agar assays compared to the control cells.
Conclusions: Our data indicate that EVI1 influences tumor cell proliferation and cell cycle as well as migration. Thus EVI1 is important for PCa progression and could serve as a therapeutic target.

1000 Chromosome 12p Abnormality Evaluation Using Fluorescence In-Situ Hybridization in Morphologically Unusual Germ Cell Tumors

Gabriela Quiroga-Garza, Arivarasan Karunamurthy, Dinesh Pradhan, Carol Sherer, Kathleen Cumbie, Veronica Derrick, Kathleen Cieply, Sheldon Bastacky, Rajiv Dhir, Anil Parwani, Somak Roy. University of Pittsburgh Medical Center, Pittsburgh, PA.
Background: Chromosome 12p abnormalities are considered an early event for germ cell tumor (GCT) development and invasiveness. 12p status evaluation by FISH in formalin-fixed paraffin-embedded tissue (FFPE) can be of extraordinary aid to establish tissue of origin in neoplasms with unusual morphologic features where GCT is a diagnostic consideration.
Design: The institutional archive was searched for GCT cases with unusual morphologic features, where isochromosome 12p (i12p). H&E sections were used to mark area of interest. After deparaffinization, dehydration and pretreatment and digestion, FISH was performed using TelVysion 12p telomeric probe (Spectrum Green) and CEP 12 centromere probe (Spectrum Orange). (Abbott Molecular, Des Plaines, IL) and counterstained with DAPI. Only individual and well-delineated cells were scored. A ratio of 12ptel/CEP12 signal of 1.4 or greater supported the presence of an isochromosome for 12p. IHC was performed using rabbit or mouse monoclonal antibodies against OCT3/4, SALL4, GP3, C-KIT, PLAP, AFP, and CD30.

Results: A total of 13 GCT tumors were evaluated and all patients were male with an average age of 38.6 years (18-70 years). The tumor specimens included retroperitoneal mass or lymph node dissection (n=8), orchidectomy (n=3), pericardial (n=1) and lung (n=1) biopsies. A wide array of morphological features that were unusual in the context of GCTs were seen, such as extensive poorly differentiated solid growth pattern (n=3), carcinomatous features (n=3), extensive adenocarcinoma-like features (n=1), mixed urothelial & trophoblastic-like features (n=1), extensive high-grade neuroendocrine features (n=2), atypical adenomatous growth pattern (n=2), and extensive spindle cell (myogenic) features (n=1). IHC for germ cell markers (OCT3/4, SALL4, GP3, C-KIT, PLAP, AFP, CD30) was not entirely diagnostic for GCT. FISH for i12p demonstrated abnormal signal pattern that was supportive of germ cell origin in all cases.
Conclusions: GCT uncommonly presents with extensive divergent differentiation that precludes definitive morphological diagnosis of GCT, especially in the context of extragonadal tumors without a clear history of GCTs. FISH for 12p abnormalities is a valuable diagnostic tool in this setting to determine germ cell origin with significant therapeutic implications.

1001 Spermatic Cord Liposarcomas: Clinical, Histopathological and Molecular Findings From a Single Academic Institution

Gabriela Quiroga-Garza, Lee Hugar, Dinesh Pradhan, Bruce Jacobs, Rajiv Dhir, Anil Parwani. University of Pittsburgh Medical Center, Pittsburgh, PA.
Background: Paratesticular sarcomas are rare, and liposarcomas (LS) represent the most frequent subtype, usually occurring in elderly patients. Given their variable clinical presentation and radiological appearance, accurate diagnosis is often delayed. Some have reported that the tumors in this location may be more prone to dedifferentiation and hence the local aggressiveness and morbidity.
Design: The institutional archive was searched for cases of paratesticular liposarcoma and corresponding slides were reviewed. Demographic information, histopathological findings and any available ancillary testing were obtained from the pathology report.
Results: Eleven cases of LS were found (five of these were consult cases). Patient's age averaged 71 years (45-89). Location included spermatic cord (7 cases), scrotum (2 cases) and groin/inguinal area (2 cases). Tumor size averaged 12 cm (4.5-23 cm). Dedifferentiated LS was seen in 7/11 cases (63%). Remainder cases included well differentiated LS (3 cases, one lipoma-like, one myxoid and one NOS) and intermediate grade LS (one case). Special features were noted in three cases (predominantly spindle and focally sclerotic pattern, metaplastic bone formation, mixed (myxoid, sclerotic and inflammatory components) and focal myogenic differentiation; one case each). None of the tumors involved the testis, but resection margins were positive (at least focally) in five cases. Morphology was the diagnostic backbone, with occasional use of immunohistochemistry showing non-specific results. In four cases, LS diagnosis was supported by finding MDM2 amplification (three cases) and CHOP translocation (one case) demonstrated by Fluorescence in situ hybridization.
Conclusions: Paratesticular LS are rare most often the diagnosis is associated with significant morbidity, especially in the setting of dedifferentiated tumors. At least in our single institutional case series, the latter presented in more than half of the cases. Surgical excision and radiotherapy are the mainstays of treatment; however optimal management is still controversial.

1002 Validation of SOX2 mRNA Detection in High Grade Urothelial Carcinoma on Formalin Fixed Paraffin Embedded Tissue Using RNAScope In-Situ Hybridization

Gabriela Quiroga-Garza, Alyssa Luvison, Kimberly Fuhrer, Kathleen Cieply, Anil Parwani, Rajiv Dhir, Somak Roy. University of Pittsburgh Medical Center, Pittsburgh, PA.
Background: Evaluation of transcription regulatory mechanisms controlling gene expression and RNA transcripts in tumor tissue may provide relevant biological and clinical information. Degradation makes RNA detection in FFPE tissue challenging. RNAScope technology allows detection and semi-quantitation of RNA molecules in FFPE tissue using in-situ hybridization. We aimed to validate the use of RNAScope in FFPE samples of high-grade urothelial carcinoma (HGUC) targeting the SOX2 gene transcript.
Design: 15 cases of HGUC were included from a larger cohort. Dual-color SOX2 FISH analysis was performed in paraffin sections, identifying target areas on FISH-treated slides. Only individual, well-delineated cells were scored; at least 60 cells for each case and control. IHC was performed using rabbit monoclonal antibody against SOX2, quantitated using a modified H-score. H-score >200 (with >33% 3+ cells) was a surrogate for protein overexpression. For RNAScope analysis, slides were analyzed using a semiquantative scoring (0-4) based on manufacturer's recommendations.
Results: SOX2 gene amplification was not seen in any case of HGUC. SOX2 transcript level, in cases with no protein expression, was considered to be basal expression (0-1). 8/15 cases (53.3%) demonstrated SOX2 protein overexpression. No protein expression was seen in 5 cases (33.3%). When compared to mRNA expression in tumor cells, 7/8 cases (87.5%) with SOX2 overexpression demonstrated elevated intracellular SOX2 transcripts (RNAScope score ³3). Only 1/8 cases demonstrated slightly lower SOX2 transcript expression (RNAScope score 2), however it was higher than the basal mRNA expression score. Cases with H-score between 1-199 showed low levels of intracellular SOX2 transcripts (RNAScope score £2). Interestingly one of the 5 cases with no SOX2 protein expression demonstrated unusual nuclear-restricted expression of SOX2 transcript, the significance of which will require further investigation.
Conclusions: RNAscope can reliably assess SOX2 mRNA expression on FFPE tissue, correlating with protein overexpression with rare exceptions. In our cohort, this technique was helpful in explaining lack of gene amplification and protein overexpression discrepancy in HGUC. This can be a useful tool for assessing biomarkers with theranostic value on FFPE tissue, which may not be possible using conventional reverse transcriptase PCR.

1003 Underreporting of Histologic Variants of Urothelial Carcinoma Is Not Limited To Community Practice

Brian Radlinski, Katrina Salazar, Giovanna Giannico, Omar Hameed, Lan Gellert. Vanderbilt University Medical Center, Nashville, TN.
Background: Urothelial carcinoma has a marked propensity for divergent differentiation, often with significant diagnostic, therapeutic and prognostic implications. A prior study showed underreporting of histologic variants in community practice, but little is known about such reporting at other institutions without a genitourinary subspecialty sign-out model. The goal of this study was to determine whether underreporting is also prevalent in these settings.
Design: Consecutive radical cystectomy cases (n = 449) diagnosed between 2007 and 2010 by general and non-genitourinary pathologists at a single academic institution were reviewed by GU pathologist(s) to determine the nature and extent of any divergent differentiation using strict diagnostic criteria. The findings were compared to those documented in the original pathology reports.
Results: Of the 449 cases, 151 (33%) displayed at least focal variant morphology. Squamous differentiation was most common (54; 12%), followed by glandular (28; 6%), micropapillary (27; 6%), sarcomatoid (17; 4%), plasmacytoid/diffuse (14; 3%), and neuroendocrine/small cell (9; 2%). Variant histology was not reported in 76 (50%) of these cases, representing 17% of the entire cohort. Underreporting was significantly associated with the type of histologic variant (P<.0001, Figure 1), but not with overall extent of variant morphology or the year of diagnosis.

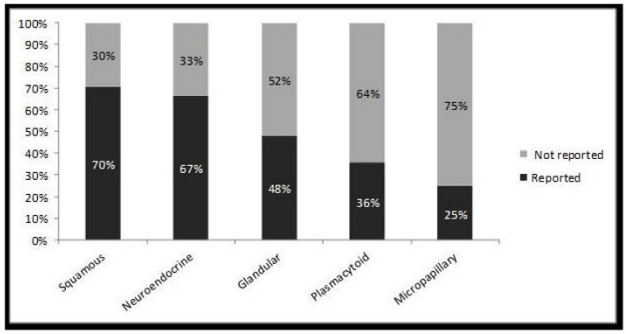

Conclusions: Underreporting of histologic variants of urothelial carcinoma is not limited to community practice and, in the absence of genitourinary subspecialization, can be seen in other institutions with similar prevalence.

1004 Clear Cell Papillary Renal Cell Carcinoma and Papillary Renal Cell Carcinoma: A Comparative Study With Napsin A and Cyclin D1 Staining

Oana Rafael, Guang-Qian Xiao, Adnan Hasanovic, Vira Wolf, Lyubov Kontorovich, Pamela Unger. Lenox Hill Hospital, New York, NY; University of Rochester Medical Center, Rochester, NY.
Background: Clear cell papillary renal cell carcinoma (CPRCC) is a relatively new subtype of renal cell carcinoma (RCC). Initially associated with end-stage renal disease, most cases are in patients with normal renal function. These tumors usually have an indolent course. Papillary renal cell carcinoma (PRCC) is the second most common type of RCC. These tumors may be divided into types 1 and 2; however, many cases have overlapping histologies. Cases could be confused with CPRCC. Prognosis of PRCC depends on stage and nuclear grade. Napsin A is an asparitic protease predominately expressed in type II pneumocytes and proximal renal tubules. Napsin A immunohistochemistry, although associated with lung adenocarcinomas, is known to stain RCC, in particular PRCC and clear cell RCC. Few studies have examined this stain with CPRCC. Cyclin D1, a cell cycle regulator, is known to be overexpressed in many tumors. A few studies have reported its overexpression in RCC. Low protein expression in RCC has been associated with other favorable prognostic factors. One study reported cyclin D1 positivity in CPRCC, while other studies have reported low or no reactivity in PRCC. The aim of the current study was to evaluate Napsin A and cyclin D1 staining in CPRCC and PRCC.
Design: 14 CPRCC and 14 PRCC were retrieved from the Pathology departments at Lenox Hill Hospital, New York, NY and University of Rochester Medical Center, Rochester, NY. Cases were reviewed by a urologic pathologist. Immunohistochemistry for Napsin A and cyclin D1 were performed. Cases were graded as negative if no staining or <5%, +1 if >5% and <25%, +2 if >25% and <50%, and +3 for >50% staining.
Results: Napsin A was negative in 12 of 14 CPRCC. 2 cases had +1 staining. Cyclin D1 was negative in 2/14 cases; 12/14 cases had +3 staining. Napsin A was negative in 1/14 PRCC cases, 4/14 had +1 positivity, 4/14 had +2 positivity, 5/14 had +3 staining. Cyclin D1 was negative in 2/14 cases, 6/14 +1; 3/14 +2, and 3/14 +3 staining.
Conclusions: CPRCC is usually negative for Napsin A staining. Conventional PRCC usually demonstrates reactivity with Napsin A. Cyclin D1 is usually diffusely positive in CPRCC; it has variable staining in PRCC and may reflect heterogeneity of this tumor group. High expression of cyclin D1 in CPRCC is probably not associated with an aggressive clinical course in this tumor. Napsin A immunohistochemistry may be useful in the differential diagnosis of CPRCC and conventional PRCC.

1005 Characterization of GATA3 Expression in Invasive Penile Squamous Cell Carcinoma

Eric Rafla-Yuan, Giovanna Giannico, Omar Hameed, Lan Gellert. Vanderbilt University Medical Center, Nashville, TN.

Background: In the genitourinary tract, GATA3 is commonly used as a marker of urothelial carcinoma for its strong and diffuse expression. The current data on GATA3 in penile squamous cell carcinoma is limited, and the value of GATA3 immunohistochemistry in distinguishing penile invasive squamous versus urothelial carcinoma is uncertain. In this study, we characterized the expression of GATA3 in a large cohort of invasive penile squamous cell carcinoma (SCC).

Design: Immunohistochemical analyses for GATA3 were performed on 88 cases of invasive penile SCC on tissue microarray (TMA) sections. All cases were reviewed by a urologic pathologist according to the current WHO classification on penile SCC and its subtypes. 2 tissue cores of 1 mm each were represented on the TMA. Tumors of penile urethra were excluded from the study. TMA results were compared with and verified on 10 corresponding whole tissue sections (11% of the cohort). GATA3 (clone L50-823) nuclear expression was scored based on staining intensity (0-3) and extent (focal:<25%; moderate: 25-75%; diffuse: >75%). The expression of GATA3 was also compared with P16ink4a immunostain result available from a prior study, in which over-expression of P16ink4a (clone E6H4) is defined as diffuse and strong nuclear and cytoplasmic staining on both tissue cores.

Results: 26 of 88 (30%) cases of invasive penile SCC exhibit GATA3 staining. Of these 26 cases, 12 (46%) exhibit weak and focal staining and 1 (4%) exhibits strong and diffuse staining. Breaking down by histologic subtype, GATA3 expression is most often observed in penile SCC with basaloid component (10 of 16, 63%, p=0.001), compared to warty SCC (5/17, 29%) and usual SCC (8/47, 17%). 43 of 88 (49%) cases exhibit over-expression of P16ink4a. Overall, no correlation was found between expression of GATA3 and P16ink4a. The one case with strong (intensity: 3) and diffuse (extent: ~100%) GATA3 expression is a basaloid SCC and exhibits over-expression of P16ink4a.

Conclusions: A significant portion of invasive penile SCC exhibit some level of GATA3 expression, while only rare case exhibits strong and diffuse immunoreactivity as commonly observed in urothelial carcinoma. GATA3 expression in invasive penile SCC varies by histologic subtype, and it is most commonly seen in the basaloid component. No correlation between the expression of GATA3 and P16ink4a was observed.

1006 Immunohistochemical Expression of SNAI1 Correlates With Tumor Grade, Stage and Biochemical Disease Recurrence in Prostatic Adenocarcinomas (PACs)

Janne Rand, Sanaz Ainechi, Dion Middleton, Tipu Nazeer, Bhaskar Kallakury, Christine Sheehan, Jeffrey Ross. Albany Medical College, Albany, NY; Georgetown University Hospital, Washington, DC.

Background: SNAI1 is a zinc finger protein which down-regulates the expression of ectodermal genes within the mesoderm. In this study we analyzed the expression of SNAI1 in PACs and correlated the results with tumor grade, pathologic stage and biochemical disease recurrence.

Design: Formalin-fixed paraffin-embedded tissue sections from 107 PACs were immunostained by a manual method (DAKO EnVision+ Dual Link System-HRP) using rabbit polyclonal SNAI 1 (Santa Cruz Biotech, Santa Cruz, CA). Cytoplasmic and/or nuclear immunoreactivity was scored based on intensity and percentage of positive cells in both the tumor (T) and adjacent benign (B) epithelium in each case. Cases were assessed as tumor>benign (T>B), tumor=benign (T=B) or tumor<benign (T<B). Results were correlated with clinicopathologic variables.

Results: Cytoplasmic SNAI 1 immunoreactivity was observed as follows: T>B 58%, T=B 30%, T<B 12%; and correlated with high (HG>=Gleason 7) vs low (LG<=Gleason 6) tumor grade [T>B 73% HG vs 48% LG, T=B 17% HG vs 38% LG, T<B 10% HG vs 14% LG; p=0.036], advanced (stage III, IV) vs early (stage I, II) tumor stage [T>B 72% adv vs 47% early, T=B 19% adv vs 38% early, T<B 9% adv vs 15% early; p=0.042]; and biochemical disease recurrence [T>B 72% recurr vs 47% non recurr, T=B 20% recurr vs 38% non, T<B 8% recurr vs 15% non; p=0.034]. On multivariate analysis, advanced tumor stage independently predicted biochemical disease recurrence (p=0.013).

Conclusions: In this study, cytoplasmic immunoreactivity of SNAI1 in PACs directly predicted disease aggressiveness and adverse prognosis. SNAI1 was found to be increased in PACs with high Gleason scores, tumors from patients with advanced stage disease, and those who had disease recurrence. Further study of SNAI1 expression in PACs both as a prognostic factor and potential target for therapy appears warranted.

1007 Renal Cell Carcinoma in Patients Under 30 Years of Age – Clinical Characteristics and Morphologic Features of 80 Cases

Priya Rao, Pheroze Tamboli, Jasreman Dhillon. University of Texas MD Anderson Cancer Center, Houston, TX; Moffitt Cancer Center, Tampa, FL.

Background: RCC in patients under the age of 30 accounts for less than 2% of all new diagnoses each year. As a result, there is limited data available about the clinicopathologic characteristics of RCC when it occurs in this unique age group.

Design: We searched the databases from 1997-2014 of 2 tertiary care cancer centers for RCC diagnosed in pts 30 yrs or younger. Childhood non-epithelial tumors were excluded.

Results: 80 pts (46 males & 34 females) were identified. Mean age at diagnosis was 25 yrs (range 7-30). Tumor types were: Clear cell RCC (CCRCC) n=36; translocation RCC n=11; chromophobe RCC (ChRCC) n=11; Papillary RCC (PRCC) n=7; clear cell papillary RCC (CCPRCC) n=2; collecting duct carcinoma n=2; renal medullary carcinoma (RMC) n=8; mucinous tubular & spindle cell carcinoma (MTSCC) n=2; unclassified RCC n=1. Mean Tsize for CCRCC was 3.3 cm (range 0.8 to 8.5). T stage for pts with CCRCC was as follows: pT1 n=32, pT2 n= 2, pT3a n=1. 2 tumors showed sarcomatoid transformation; both pts died of disease (DOD). In the non-sarcomatoid group 1 pt is AWD & 32 pts showed NED; mean follow up (FU) 47 mos. Cystic change was identified in 68% of CCRCC's, of which 2 pts had documented VHL disease. In the translocation RCC group mean T size was 8.7 cm. 8/11 pts presented with advanced disease. 3 pts in this group were NED at 7, 16 & 24 mos; all 3 pts had pT1 tumors at diagnosis. Mean T size in the ChRCC group was 11 cm (range 4.5 to 17.5). All tumors were pT2/pT3. All pts were NED (mean FU 56 mos). RMC was the most aggressive of all tumor types, mean FU was 10 mos; 6 pts were DOD & 4 AWD. Syndromic associations included VHL; Beckwith-Wiedemann syndrome & Scheurmann's disease. 5 pts with CCRCC had a h/o of chemoradiation for a prior tumor. Only 4 cases showed sarcomatoid dedifferentiation, 1 pT1 tumor in a pt with VHL disease, 1 CCRCC in a pt with no known syndromic association, 1 MTSCC & 1 unclassified RCC.

Conclusions: CCRCC is the most common subtype of RCC arising in young pts, tends to be of low stage & low grade at diagnosis & shows frequent cystic change. In the absence of sarcomatoid transformation CCRCC appears to have a good prognosis in younger pts. ChRCC had a favorable outcome with no adverse events (mean FU interval of 5 yrs). In this age range Translocation RCC & RMC are the most aggressive of the tumor types with a poor outcome, with most patients presenting with high tumor stage at diagnosis. Other less commonly occurring subtypes include PRCC, MTSCC & CDC.

1008 FOXA1 Is Required for Urothelial Differentiation and Its Loss in Bladder Cancer Is Associated With Poor Prognosis

Opal Reddy, Justin Cates, Lan Gellert, Henry Crist, Zhaohai Yang, John Taylor, Joseph Smith, Sam Chang, Michael Cookson, Chaochen You, Daniel Barocas, Magdalena Grabowska, Fei Ye, Xue-Ru Wu, Robert Matusik, Klaus Kaestner, Peter Clark, David DeGraff. University of California, Los Angeles, CA; Vanderbilt University, Nashville, TN; Pennsylvania State University, Hershey, PA; University of Connecticut, Farmington, CT; University of Oklahoma, Oklahoma City, OK; New York University, New York, NY; University of Pennsylvania, Philadelphia, PA.

Background: We previously identified loss of Forkhead box A 1 (FOXA1) expression to be significantly associated with high grade, late stage urothelial carcinoma of the urinary bladder. These findings were recently substantiated by The Cancer Genome Atlas, which showed that FOXA1 is mutated in a subset of bladder cancers. In the present study, we examined the prognostic significance of FOXA1 loss in humans, and determined the impact of inducibly ablating FOXA1 expression in the urothelium of adult mice.

Design: Immunohistochemistry was performed on a tissue microarray constructed using 657 samples from 301 patients undergoing cystectomy for bladder cancer. *In vivo* studies were performed using a tamoxifen-inducible, ubiquitin Cre-driven system to ablate Foxa1 expression in the urothelium of adult mice.

Results: After controlling for tumor stage, patient age, sex, and clinical comorbidities, loss of FOXA1 in human bladder cancer was an independent predictor of decreased overall survival (hazard ratio 1.49, 95% CI 1.04-2.13, p=0.028). Further analysis revealed a statistically significant relationship between loss of FOXA1 and gain of cytokeratin 14 (KRT14) expression (rho=-0.35, p=<0.001).

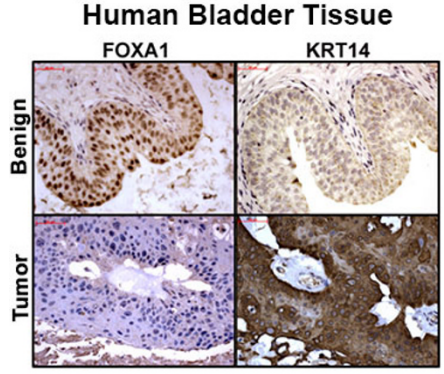

Ablation of Foxa1 expression in the urothelium of adult mice resulted in sex-specific histological alterations, with male mice developing urothelial hyperplasia and female mice developing keratinizing squamous metaplasia.

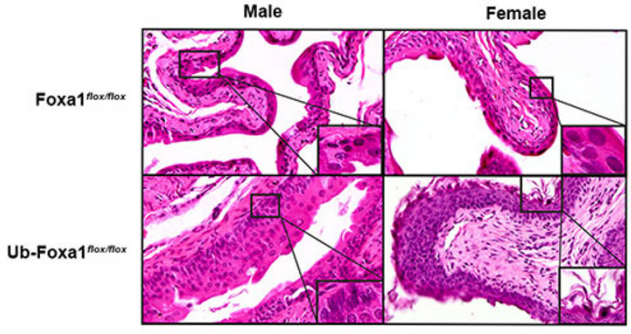

Conclusions: These results show that FOXA1 expression is essential for the maintenance of urothelial differentiation, and loss of FOXA1 expression in urothelial carcinoma is associated with decreased overall survival and increased KRT14 expression.

1009 Quantification of Tumor Heterogeneity in Whole Slide Images of Prostate Cancer Using a Three Biomarker Panel of RHAMM, SIAH2, and SMAD4

Nicholas Reder, Jonathan Henriksen, Anthony Rizzardi, Joseph Koopmeiners, Gregory Metzger, Stephen Schmechel. University of Washington Medical Center, Seattle, WA; University of Minnesota Medical School, Minneapolis, MN; Univeristy of Minnesota School of Public Health, Minneapolis, MN.

Background: Tumor heterogeneity is an important determinant of patient outcomes and treatment response, however it is difficult to quantify by morphological assessment. Prostate cancers (PCa) of intermediate grade have a more variable clinical outcome than indolent low-grade tumors and poorly behaved high-grade tumors. Our group has identified a three-biomarker immunohistochemical (IHC) panel of RHAMM, SIAH2, and SMAD4 correlates with PCa aggressiveness, and developed SigMap software to create IHC spatial heterogeneity maps from whole slide images. We hypothesized that spatial molecular heterogeneity would be higher in tumors of intermediate-grade than in low-grade or high-grade tumors.

Design: Using our database of 16 whole slide scanned PCa cases (37 sections), areas of carcinoma were outlined and Gleason scored using Aperio ImageScope software on H&E stained slides. Using SigMap software, a grid was applied to the H&E stained section, which was then registered with adjacent sections stained with IHC markers for RHAMM, SIAH2, and SMAD4. Spatial heterogeneity was tested by first computing the difference in staining between each grid square and its neighbors for each annotated slide. Then, the spatial heterogeneity scores were grouped by Gleason score, and the Kruskal-Wallis test was used to compare differences between Gleason scores.

Results: Spatial molecular heterogeneity was significant for all three IHC stains, with SIAH2 showing the greatest differences in staining from neighboring grid squares ($p=0.0002$). Gleason scores of 7 and 8 displayed greater spatial molecular heterogeneity than Gleason scores of 6 or 9 for IHC staining with RHAMM, SIAH2, and SMAD4. For example, the standard deviation of RHAMM staining was 0.78 in 3+3 tumor areas, 1.02 in 3+4, 1.15 in 4+3, 1.03 in 4+4, 0.97 in 4+5, and 0.65 in 5+4 ($p=0.046$).

Conclusions: Significant heterogeneity in cancer cell immunophenotype is quantifiable on whole slide images using an IHC panel of RHAMM, SIAH2, and SMAD4. Spatial molecular heterogeneity is greatest in tumors of patterns 3+4, 4+3 and 4+4, and lower in low-grade and higher-grade tumors. These data suggest that variability in clinical outcome with intermediate-grade PCa may be due to underlying spatial molecular heterogeneity in these tumors.

1010 Are Mast Cells Still Good Biomarkers for Bladder Pain Syndrome/Interstitial Cystitis?

Sigrid Regauer, Marianne Gamper, JoEllen Welter, Jakob Eberhard, Volker Viereck. Medical University of Graz, Graz, Austria; Cantonal Hospital Frauenfeld, Frauenfeld, Switzerland.

Background: Clinical diagnosis of bladder pain syndrome/interstitial cystitis (BPS/IC) and overactive bladder syndrome (OAB) is complicated by subjective and overlapping clinical symptoms. The hallmark of OAB is *urgency* and BPS/IC is defined by the key symptom *pain* accompanied by a persistent urge to void or urinary frequency. The guidelines of the European Society for the Study of Interstitial Cystitis (ESSIC) consider infiltrates of >28 mast cell in 1 mm^2 of detrusor muscle as diagnostic histological criterium for BPS/IC, but elevated mast cells are also described for OAB. Considering the proposed importance of mast cells in the distinction of OAB and BPS/IC, we aimed to reassess mast cell counts, type of infiltrates, state of activation and distribution of mast cells in biopsies from painful BPS/IC with and without Hunner's lesion, OAB and bladder-healthy patients.

Design: Bladder biopsies of 12 BPS/IC with Hunner's lesions, 19 BPS/IC without Hunner's lesions, 13 OAB, and 12 control patients were analyzed on HE stains, with immunohistochemistry with antibody to mast cell tryptase, and for WHO criteria for neoplastic mastocytosis (major criterion *increased mast cells* and 3 minor criteria *CD25 expression*, *spindling of mast cells*, *elevated serum tryptase levels.* Statistical analyses included ANOVA, Kruskal-Wallis, Mann Whitney U, Fisher's exact tests, and receiver operating characteristic (ROC) curves for mast cell counts.

Results: 50% BPS/IC patients with Hunner's lesion had concomitant autoimmune diseases. Allergies or drug/food intolerances were found in all patient groups. Lymphocytic infiltration ($p=0.001$), nodular lymphocyte aggregates ($p<0.001$), and urothelial abnormality ($p<0.001$) were identified in biopsies of BPS/IC patients with Hunner's lesion. Subepithelial localization ($p<0.001$) and amount of detrusor mast cells ($p=0.029$), but not mast cell activation ($p=0.21$) or total submucosal mast cell numbers ($p=0.089$) distinguished BPS/IC with Hunner's lesion from the other groups. The optimal cutoff value for detrusor mast cell counts was 32 cells/mm^2. Neoplastic disease was not identified.

Conclusions: We conclude that biopsy recommendations of the ESSIC are too stringent and the use of 'detrusor mast cell counts' as sole histological diagnostic criterion for BPS/IC ought to be critically re-evaluated. Nodular lymphocytic infiltrates, urothelial defects and subepithelial mast cell location were indicative of BPS/IC with Hunner's lesion.

1011 Mucinous Tubular and Spindle Cell Carcinoma (MTSCC): A Genome-Wide Copy Number Analysis of MTSCC and Its Histologic Mimickers

Qinghu Ren, Lu Wang, Anuradha Gopalan, Hikmat Al-Ahmadie, Samson Fine, Satish Tickoo, Victor Reuter, Ying-Bei Chen. Memorial Sloan Kettering Cancer Center, New York, NY.

Background: MTSCC is a rare type of renal cell carcinoma that frequently exhibits histologic and immunophenotypic overlap with type 1 papillary renal cell carcinoma (PRCC). The molecular features defining this entity remain controversial. We sought to delineate the genome-wide copy number alterations (CNA) in tumors displaying classical histologic features of MTSCC in comparison to the solid variant of type 1 PRCC and indeterminate cases with overlapping histologic features to clarify molecular features that can be used for this differential diagnosis.

Design: The study included a total of 24 cases: 10 histologically typical MTSCC (group A), 9 tumors with overlapping features of MTSCC and PRCC (group B) and 5 cases of solid variant of type 1 PRCC (group C). Genomic DNA was extracted from macro- or micro-dissected FFPE material that represented histologically distinct tumor areas. The CNA was investigated using a SNP-array platform (Affymetrix OncoScan) that is suitable for FFPE tissues.

Results: All cases in group A (MTSCC) exhibited an admixture of tubules, spindle cells, and mucinous stroma in variable proportions. Focal papillations and scattered small foci of foamy macrophages were often present. The indeterminate cases in group B had more prominent papillary areas that were either distinct from or intermixed with MTSCC-like areas. We were able to generate high-quality CNA data from an input of only 80ng DNA. Multiple chromosomal losses were observed in the examined group A cases, with 5/5 showing monosomies of 1, 6, 8, 14q, 15q and 22q, and 4/5 displaying additional losses of 4, 9, and 13q. Monosomy of 10 or 18 was also seen in 1/5 cases. No significant gain was observed thus far in cases from this group. Characterizations of remaining cases including micro-dissected areas from the indeterminate cases are ongoing.

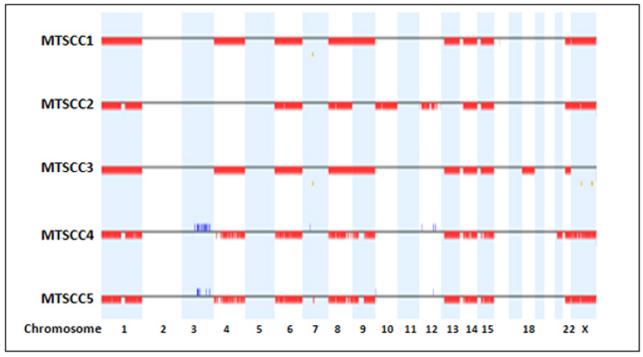

Conclusions: Unlike what is known in PRCC, our preliminary data suggest that MTSCC has multiple chromosomal losses that most frequently involve 1, 4, 6, 8, 9, 13q, 14q, 15q and 22q, while lacking trisomy 7 or 17. OncoScan SNP array can be successfully performed using minimal amount of DNA from clinical archival materials, and it may serve as a helpful ancillary tool for the differential diagnosis of MTSCC and its histologic mimickers.

1012 Upper Tract Urothelial Carcinoma: Genetic Characteristics and Correlation With Morphology and Clinical Outcomes

Qinghu Ren, John Sfakianos, Eugene Cha, Gopa Iyer, Sasinya Scott, Ronak Shah, Philip Kim, Neil Desai, Aditya Bagrodia, Anupama Gandhi, Jonathan Rosenberg, Guido Dalbagni, Dean Bajorin, Ying-Bei Chen, Sahussapont Sirintrapun, Anuradha Gopalan, Samson Fine, Satish Tickoo, Victor Reuter, Michael Berger, Bernard Bochner, David Solit, Jonathan Coleman, Hikmat Al-Ahmadie. Memorial Sloan Kettering Cancer Center, New York, NY.

Background: Urothelial carcinoma (UC) of the upper tract has both epidemiologic and clinical differences from that arising in the bladder, despite their histopathologic similarities. We sought to study the genetic characteristics of a cohort of patients with upper tract UC (UTUC) by next generation sequencing methods and correlate them with clinicopathologic features.

Design: Frozen tumor and germline DNA from patients with UTUC (n=72) treated with radical nephroureterectomy were analyzed using a next -generation exon capture sequencing assay (Integrated Molecular Profiling of Actionable Cancer Targets - IMPACT) to identify point mutations, small insertions and deletions, and copy number alterations in 300 cancer-associated genes. C^2 test was used to evaluate the association between altered genes and tumor grade, stage, and organ-confined (OC) status. Kaplan-Meier and regression analyses were utilized for clinical outcomes.

Results: Pathologic stages in this cohort were Ta (18, 21%), T1 (14, 16%), T2, (8, 9%), T3 (22, 26%), and T4 (10, 12%) patients. Twenty patients (24%) had positive lymph nodes and 27 (31%) had distant recurrences and died of their disease. The most commonly mutated genes in this cohort were *FGFR3* (66%), *KDM6A* (50%), *STAG2* (37%), *CREBBP* (28%), *TP53* (24%), *ATM* (27%), *ARID1A* (21%) and *PIK3CA* (21%). *TP53* and *FGFR3* were the only genes uniformly associated with grade, stage, OC status, recurrence-free survival (RFS), and cancer-specific survival (CSS). *FGFR3* alterations were associated with better outcomes, with an improved 3-year RFS (81% vs 45%, $p<0.001$) and improved 3-year CSS (93% vs 74%, $p=0.007$). On the contrary, *TP53* alterations were associated with adverse outcomes, with a worse 3-year RFS (21% vs 45%, $p<0.001$) and worse CSS (54% vs 74%, $p=0.007$).

FGFR3 alterations were generally associated with exophytic tumors with branching papillary architecture, and were more likely to have low grade morphology.

Conclusions: Upper tract urothelial carcinoma displays a spectrum of somatic alterations similar to high-grade UC of the bladder. The prevalence of these mutations, however, is different from what has been reported in urothelial carcinoma of the bladder. *TP53* mutations are associated with adverse clinicopathologic outcomes whereas *FGFR3* mutations are not. These findings may have future implications on risk stratification and the utility of targeted therapies in this disease.

1013 Urothelial Carcinoma of the Bladder: Identification of Genetic Signatures and Correlation With Clinical Outcomes

Qinghu Ren, Philip Kim, Eugene Cha, John Sfakianos, Gopa Iyer, Sasinya Scott, Anupama Gandhi, Ronak Shah, Dean Bajorin, Jonathan Rosenberg, Nikolaus Schultz, Michael Berger, David Solit, Ying-Bei Chen, Sahussapont Sirintrapun, Anuradha Gopalan, Samson Fine, Satish Tickoo, Victor Reuter, Bernard Bochner, Hikmat Al-Ahmadie. Memorial Sloan Kettering Cancer Center, New York, NY.

Background: Urothelial carcinoma of the bladder (UCB) is genomically heterogeneous, which may contribute to the significant variability in clinical outcomes. Genomic characterization of patients with UCB may allow the identification of new signatures that can predict clinical outcomes. We sought to study a cohort of high-grade UCB to determine the association between unique genomic signatures and clinicopathologic outcomes.

Design: Tumor and germline DNA from patients with high-grade UCB (n=109), 89 of whom were treated with radical cystectomy, were sequenced using a next -generation exon capture sequencing assay (Integrated Molecular Profiling of Actionable Cancer Targets - IMPACT) to identify point mutations, small insertions and deletions and copy number alterations in 300 cancer-associated genes. C^2 test was used to evaluate the association between altered genes and tumor grade, stage, and organ-confined status. Kaplan-Meier and regression analyses were utilized for clinical outcomes.

Results: Mutations were detected in 240 genes, 23 of which were mutated in ≥5% of cases. Mutations in *TP53* were the most common (57%) and were associated with extravesical disease (69% vs 32%, p = 0.005) and lymph node metastasis (77% vs 56%, p = 0.025), but were not significantly associated with outcome in multivariable analyses. Recurrent *PIK3CA* mutations (E453Q, E542K or E545K) were identified in 23 tumors (21%) and were associated with improved recurrence-free survival (RFS) (hazard ratio [HR]: 0.35; p = 0.014) and improved cancer-specific survival (CSS) (HR: 0.35; p = 0.040). *CDKN2A* mutations were identified in 10 cases (12%). In multivariable analyses controlling for tumor stage and nodal status, *PIK3CA* mutations remained associated with better RFS (HR: 0.39; p = 0.032), whereas alterations in *TP53* and *CDKN2A* were associated with worse RFS (HR: 5.76; p < 0.001) and worse CSS (HR: 2.94; p = 0.029). Pathologic review did not reveal specific morphological features that were associated with these mutations.

Conclusions: In patients with high grade urothelial carcinoma of the bladder, the presence of *PIK3CA* mutations is associated with a more favorable clinical outcome whereas mutations in *TP53* and *CDKN2A were* associated with worse outcomes. Genomic profiling may aid in risk stratification, identification of patients at highest risk of recurrence following radical cystectomy, and guide the use of potential targeted therapies in a subgroup of patients with urothelial carcinoma of the bladder.

1014 The Significance of Skeletal Muscle Involvement in Prostatic Adenocarcinoma Gleason Score 3+3=6

Evita Sadimin, Huihui Ye, Jonathan Epstein. Johns Hopkins Medical Institutions, Baltimore, MD; Harvard Medical School, Boston, MA.

Background: Skeletal muscle is seen at the anterior part of the prostate apex, where benign glands may reside as part of normal anatomy and histology. At times, prostatic adenocarcinoma can be seen extending into this region, raising the question of extraprostatic extension. Previously, we have shown that patients who are diagnosed with limited prostatic adenocarcinoma Gleason score 3+3=6 involving skeletal muscle on biopsy did not seem to have increased adverse outcome at radical prostatectomy compared to those without skeletal muscle involvement. In this study, we expanded the criteria to include all patients with Gleason score 3+3=6 with more extensive tumor involvement on biopsy.

Design: We searched our database spanning 10 years from 2003 to 2013 and identified 107 patients that met the criteria. Prostatectomy reports were retrieved. As the control group, we obtained the prostatectomy reports of 85 patients whose biopsies showed prostatic adenocarcinoma Gleason score 3+3=6 without skeletal muscle involvement.

Results: Of the 107 patients in our study, 60 underwent radical prostatectomy, 31 underwent other treatment modalities (brachytherapy, external radiotherapy or cryotherapy), 16 entered surveillance and 9 were lost to follow up. Of the 60 that underwent radical prostatectomy, 56 cases were organ confined (93%), compared to 76 cases (89.4%) in the control group (p=0.2), and 12 cases (20%) had positive margin, compared to 4 cases (4.7%) in the control group (p=0.0001). Of the 12 cases, 6 cases (50%) were in the area of the apex. In 2 of the 6 cases, the apical margin was positive in the area of intraprostatic incision. In another 2 cases, it was not clear whether it was positive in the area of intraprostatic incision or extraprostatic extension due to the ambiguities of the histologic boundaries of the prostate in this region. There were 20% patients in our study who showed higher Gleason scores on the prostatectomy compared to 17.6% in the control group (p=0.5).

Conclusions: This study demonstrated that in patients with skeletal muscle extension of their prostatic adenocarcinoma Gleason score 3+3=6 on biopsies, most patients still had organ confined disease with negative margins and no lymph node involvements on their radical prostatectomies. However, it is important for pathologists to note this finding in the biopsy report so that surgeons performing their radical prostatectomies can ensure adequate excision by extending the dissection of the apical area as much as possible.

1015 Variability in the Diagnosis of Prostate Cancer (PCA) and Atypical/ Premalignant Lesions of the Prostate in the State of Michigan: Improving Diagnostic Consistency towards Better Patient Management

Wael Sakr, Rohit Mehra, Kirk Wojno, Nilesh Gupta, Michael Cher, David Miller, James Montie. Wayne State University and Karmanos Cancer Institute, Detroit, MI; University of Michigan, Ann Arbor, MI; Comprehensive Urology, Royal Oak, MI; Henry Ford Health System, Detroit, MI.

Background: Data suggest variability in the consistency of pathological diagnosis and grading of PCA as well as the frequency of reporting high grade prostatic intraepithelial neoplasia (HGPIN) and atypical small acinar proliferation (ASAP) in needle biopsies. The Michigan Urologic Surgery Improvement Collaborative (MUSIC), is a state-wide initiative supported by Blue Cross Blue Shield of Michigan aimed at collecting data related to PCA diagnosis, staging and management from academic and community urologic practices across the state. This report focuses on the up to- date results of the pathology component of MUSIC and suggests means to improve diagnostic consistency.

Design: Comprehensive data from 36 practices accounting for a total of 225 urologists and representing approximately 90% of urology practices in Michigan continue to be collected for a centralized database at the University of Michigan since March 2012. For this report, parameters related to pathology sampling and the resulting diagnostic categories were tabulated across the participating sites.

Results: To date, the consortium collected data on 11106 biopsies. The cancer detection rate was fairly consistent at approimately 50% (47.6-50.3). The mean and ranges of number of cores obtained, cancer diagnosis rates, proportion of Gleason score (SG), frequency of diagnosing HGPIN and ASAP in biopsies without cancer are shown in the table below.

# of cores	GS=	GS=7	GS=>8	HGPIN	ASAP
8.8 (4-16)	36.3%(13-61)	45.4(20-71)	17.4% (0-35)	15% (0-34)	5.7% (0-10)

Conclusions: The data document considerable variations in the frequency of reporting important pathologic diagnostic categories gleaned from prostate needle biopsies notwithstanding the consistent overall cancer detection rate. It is likely that such variations extend beyond the geographic boundaries of this study. These discrepancies further contribute to a degree of inconsistencies in the approaches to clinical management. Potential reasons for the rather wide range in pathology reporting and means to alleviate them will be discussed.

1016 DOG-1 Immunohistochemical Staining in Testicular Biopsies Is a Reliable Tool for Objective Assessment of Infertility

Rasha Salama, Hany Osman, Thomas Ulbright, Muhammad Idrees. Indiana University, Indianapolis, IN.

Background: Testicular biopsy is common for evaluation of male infertility; however, no reliable diagnostic tools are available for objective quantitative assessment of gonadal cells. DOG1, a calcium-activated chloride channel protein, has shown to be expressed in gastrointestinal Cajal cells and gastrointestinal stromal tumor. Anecdotally, our group has observed differential DOG1 staining of germ cells in seminiferous tubules. We evaluated the utility of DOG1 immunohistochemical stains for the assessment of testicular biopsies submitted for evaluation of infertility.

Design: DOG1 immunostaining was performed on forty testicular biopsies divided into four groups: normal spermatogenesis, Sertoli cell only, hypospermatogenesis and maturation arrest (10 in each group). Additionally 25 cases of benign seminiferous tubules from orchiectomy specimens and four spermatocytic seminomas (SS) were evaluated for DOG1 cytoplasmic expression.

Results: Sertoli cell only cases, where no germ cells are present, were negative for DOG1; while active spermatogenesis specimens and orchiectomy cases displayed cytoplasmic staining in the spermatocytes and spermatids and negative staining in the spermatogonia. Hypospermatogenic tubules displayed staining only in the few remaining spermatocytes and spermatids with no staining in spermatogonia. Maturation arrest specimens either showed severely decreased or negative staining, indicating absence or very few remaining spermatocytes with blockage of normal spermatogenesis at the spermatogonium to spermatocyte transition. No staining was noted in SS.

Conclusions: Evaluation of infertility in testicular biopsies requires assessment of spermatogenesis and maturation of germ cells in a step wise fashion. DOG1 is expressed in spermatocytes and spermatids but not in Sertoli cells and spermatogonia. By using the DOG1 stain we were able to confirm maturation arrest and determine the level at which maturation stops. This may have pathogenetic importance as different processes cause maturation arrest at different levels. Moreover, we could objectively assess the percentage of the testis involved by hypospermatogenesis in mixed patterns. Despite its positivity in normal spermatocytes, DOG1 is negative in SSs.

1017 Pleomorphic Giant Cell Carcinoma of the Urinary Bladder: A Clinicopathological Analysis of 13 Cases

Hemamali Samaratunga, David Hussey, Greg Malone, Kirsten Hoyle, David Kerle, Brett Delahunt. Aquesta Pathology, Brisbane, Queensland, Australia; Brisbane Private Hospital, Brisbane, Queensland, Australia; Greenslopes Hospital, Brisbane, Queensland, Australia; Sunshine Coast Private Hospital, Buderim, Queensland, Australia; Sunshine Coast University Private Hospital, Birtinya, Queensland, Australia; Wellington School of Medicine and Health Sciences, University of Otago, Wellington, Otago, New Zealand.

Background: Pleomorphic giant cell carcinoma (PGCC) of the bladder is a variant of urothelial carcinoma (UC) characterized by highly pleomorphic giant cells. Mentioned in the 2004 WHO classification, <10 cases have been reported in the literature.

Design: The Aquesta Pathology database revealed 13 cases of PGCC of the bladder which were reviewed. We present clinicopathological characteristics of the largest series of this entity to be reported to date.

Results: There were 8 males and 5 females ranging in age from 53-92 years (mean 71). Two patients had a prior history of conventional high-grade UC of the bladder and 1 patient had a ureteric high-grade UC. PGCC was identified in 2 cystoprostatectomy specimens and 11 transurethral resections (TUR) and varied from 40% to 100% of tumor present. Histologically, large bizarre anaplastic mononuclear and multinuclear tumor giant cells were present in all cases. These were within solid expansile masses, infiltrating tumour or as single cells. Mitoses, including atypical mitoses, were numerous in these cases. Associated conventional high grade UC was present in 7 cases including 1 papillary UC, 2 invasive UC and 4 with both. Four cases also had micropapillary UC and 1 each had plasmacytoid UC and choriocarcinoma. UC *in situ* (CIS) was present in 5 cases. Bizarre tumor giant cells were also noted in the surface papillary component in 2 cases and within CIS in 4 cases. Twelve cases (92%) had conventional high grade UC or CIS. Both cystoprostatectomy specimens had pT3 disease, 1 with pN1. Four TUR specimens had pT2 and 7 had pT1 tumor (no muscularis propria in 4). Of 9 patients with follow-up, 4 died within 1 year, 1 is alive with metastases at 17 months and 3 have recurrent pT2 high-grade UC, 28 to 34 months later. 1 patient who had a pT1 tumor treated with a cystectomy is alive and well 46 months later.
Conclusions: PGCC is a highly aggressive variant of UC commonly associated with conventional UC, its variants and urothelial CIS. Identifying these in addition to clinicopathological correlation can be helpful in differentiating this tumor from metastatic malignancy. Pleomorphic giant cell features may also be seen in CIS and surface papillary tumor.

1018 Clear Cell Carcinoma of the Penis. An Unusual and Distinctive HPV-Related Variant of Squamous Cell Carcinoma. A Report of 3 Cases

Diego Sanchez, Ingrid Rodriguez, Adriano Piris, Sofia Canete, Cecilia Lezcano, Elsa Velazquez, Mai Hoang, Antonio Cubilla. Instituto de Patología e Investigación, Asunción, Paraguay; Facultad de Ciencias Médicas – UNA, Asunción, Paraguay; Massachusetts General Hospital and Harvard Medical School, Boston, MA; University of Pittsburgh, Medical Center, Pittsburgh, PA; Miraca Life Sciences and Tufts University, Boston, MA.
Background: Five cases of clear cell carcinoma of the foreskin have been reported and are thought to be originated from sweat glands at that site (Am J Surg Path 2004). Here we report 3 cases of clear cell squamous cell carcinomas arising in the penile glans epithelium.
Design: Clinical and pathological features were evaluated. An average of 15 sections per case were studied. Immunohistochemical stains were GATA 3, cytokeratin 7, cytokeratin 19 and p16. HPV detection by whole tissue section (WTS)-PCR was done in one case.
Results: Patients' ages were 52, 90 and 98 years. Tumors were large (Average: 6.1 cm) and involved glans and sulcus in all cases; foreskin was partially compromised in one case. Microscopically clear cells predominated (>95%). Growth was in solid nests some with comedo-like necrosis. Geographical necrosis was present. Cells were non-keratinizing with a clear cytoplasm. Nuclei were irregular, with numerous mitosis. Focal invasive warty-basaloid or basaloid features were present in 2 cases, both showing warty or basaloid PeIN. There was invasion of corpora cavernosa, lymphatics, veins and perineural spaces. p16 was positive in all 3 cases while CK 7 and CK 19 were positive in only 1 case. GATA 3 stain was negative in the 3 cases. HPV 16 was detected in one. Clinical groin metastases were present in the 3 cases, and pathologically confirmed in one. The youngest patient of the series died from tumor dissemination 12 months after penectomy. The remainder two (recent patients) refused lymph node surgical excision and are alive with disease.
Conclusions: We are reporting 3 morphologically distinctive aggressive penile tumors with prominent clear cell features originated in the glans surface squamous epithelium. The differential diagnosis includes metastatic renal cell carcinoma and sweat gland carcinoma of the shaft, which were previously reported. Features that favor the diagnosis of primary penile clear cell carcinoma are tumor location on the glans mucosa, presence of concomitant warty-basaloid PeIN, and HPV/p16 positivity.

1019 Penile Intraepithelial Neoplasia: A Comparison of p16INK4a and HPV By Laser Capture Microdissection (LCM)-PCR in 122 Lesions From 43 Patients

Diego Sanchez, Maria Jose Fernandez-Nestosa, Nuria Guimera, Patricia Zarza, Sofia Canete, Sabrina Oneto, Elsa Velazquez, David Jenkins, Wim Quint, Antonio Cubilla. Instituto de Patología e Investigación, Asunción, Paraguay; Facultad de Ciencias Médicas – UNA, Asunción, Paraguay; Facultad Politécnica – UNA, San Lorenzo, Paraguay; DDL Diagnostic Laboratory, Rijswijk, Netherlands; Miraca Life Sciences and Tufts University, Boston, MA.
Background: Subtypes of PeIN are classified in differentiated and undifferentiated (basaloid, warty-basaloid and warty). Differentiated PeIN is rarely associated with HPV whereas the virus is prevalent in undifferentiated lesions. $p16^{INK4a}$ immunohistochemical stain is considered a surrogate for high risk Human Papillomavirus (hrHPV) in invasive penile carcinomas. We found no studies comparing $p16^{INK4a}$ and HPV by LCM-PCR technique in PeIN.
Design: Each lesion was evaluated for $p16^{INK4a}$ and HPV with Whole Tissue Section (WTS) and LCM-PCR for selected regions. These were performed by SPF_{10}-DEIA-$LiPA_{25}$ (version 1). DNA quality of all HPV negative cases was confirmed by RNaseP/PhHV qPCR. Full epithelial thickness dense stain was required for a $p16^{INK4a}$ positive result.
Results: Subtypes of hrHPV detected were: 16, 18, 30, 33, 35, 39, 51, 52, 56, 58, 59, 66 and 73. Correspondence of $p16^{INK4a}$ immunostain and hrHPV are summarized in table 1.

PeIN (cases)	hrHPV+/p16+ (%)	hrHPV-/p16- (%)	hrHPV+/ p16- (%)	hrHPV-/p16+ (%)
Differentiated (43)	0	41 (95)	2 (5)	0
Basaloid (23)	19 (83)	2 (9)	1 (4)	1 (4)
Warty-Basaloid (33)	28 (85)	1 (3)	4 (12)	0
Warty (23)	15 (65)	3 (13)	4 (17)	1 (5)
Total (122)	62 (51)	47 (39)	11 (9)	2 (1)

Conclusions: The $p16^{INK4a}$ stain was useful to separate hrHPV positive from hrHPV negative cases. All $p16^{INK4a}$ were negative in differentiated PeIN and 2 of them were positive for HPV 16. The majority of warty/basaloid PeINs were HPV and $p16^{INK4a}$ positive. The stain demonstrated a high sensitivity and specificity for undifferentiated PeINs. The data suggests a role for $p16^{INK4a}$ in the differential diagnosis and as a tissue marker of hrHPV in penile precancerous lesions.

1020 Utility of Uroplakin II and GATA3 for the Diagnosis of Metastatic Urothelial Carcinoma

Angela Sanguino Ramirez, Jan Silverman. Allegheny General Hospital, Pittsburgh, PA.
Background: GATA3, a member of the family of zinc finger transcription factors, is a recent immunohistochemical marker useful to confirm a malignancy of urothelial origin. When used to evaluate metastatic urothelial carcinoma approximately 20% of cases can show negative staining (1). Uroplakin II is a cytoplasmic-membranous protein component of urothelial plaques that been recently identified as a potential marker for urothelial differential. A recent study evaluated a novel uroplakin II antibody having good sensitivity (77%) and excellent specificity (100%) for the evaluation of urothelial carcinoma (2). The objective of this study was to evaluate the utility of uroplakin II in cases of metastatic urothelial carcinoma and compared this new antibody with GATA3.
Design: We selected 29 cases of histologically confirmed metastatic urothelial carcinoma. Most of the cases were metastatic to lymph nodes that were removed at the same time of cystectomy. A small percentage of cases were metastasis to other sites such as colon or omentum in patients with a confirmed histologic diagnosis of urothelial carcinoma. We used the mouse monoclonal uroplakin II antibody [BC21] from Biocare Medical (prediluted) and mouse monoclonal GATA3 antibody (HG3-31) from Santa Cruz Biotechnology, 1:25 dilution.
Results: We defined positivity when at least 5% of the cells show any degree of staining. GATA3 was positive in 83% (24/29) of cases, uroplakin II in 79% (23/29) of cases and combined GATA3 and uroplakin II in 90% (26/29) of cases. There were 21 cases positive for both antibodies, 3 cases only positive for GATA3 and 2 cases only positive for uroplakin II. In addition there we cases with substantial differences in the percentage of cells (more than 50%) that stained positive with each antibody, including 3 cases in which GATA3 performed significantly better and 2 cases in which uroplakin II was superior.
Conclusions: 1) We believe the combine use of GATA3 and uroplakin II has increased sensitivity for the diagnosis of urothelial carcinoma when evaluation metastasis of unknown origin, especially when a possible urothelial primary is considered in the differential diagnosis. 2) Both antibodies are directed to non related proteins explaining why the staining percentage can be different and is enhanced when combined in the immunohistochemistry workup. 3) The use of both markers may be especially useful when assessing small specimens such as core needle biopsies or cytology cell blocks.
References
1. Chang A, et al. Am J Surg Pathol. 2012 Oct;36(10):1472-6
2. Hoang LL, et al. Arch Pathol Lab Med. 2014 Jul;138(7):943-9.

1021 Urothelial-Associated Marker S100P Expression in a Multi-Tumor Cohort: Immunohistochemical (IHC) Evaluation in a Tissue Microarray (TMA) Study of 300 Cases

Julian Sanz, Mukul Divatia, Claudia Zampini, Steven Smith, Mariza de Peralta-Venturina, Daniel Luthringer, Mahul Amin. Hospital Clinico San Carlos, Madrid, Spain; Cedars-Sinai Medical Center, Los Angeles, CA; Virginia Commonwealth University, Richmond, VA.
Background: S100P is an emerging urothelial-associated marker which is reported to be supportive of, and sensitive for the diagnosis of urothelial carcinoma (UCa) and its histologic variants. Though it is generally considered to be less specific than other newer markers (e.g., Uroplakin II, GATA3) due to reported expression in other tumors, comprehensive studies testing S100P expression across a broad cohort of cancers remain lacking.
Design: S100P IHC was evaluated in a TMA panel of 300 cases from 15 different tumor types. Staining was scored using two metrics:1. percentage of tumor with S100P staining (0: no staining; 1: <10; 2: 10-25; 3: 25-50 or 4: >50), and 2. staining intensity. Cytoplasmic and nuclear staining was considered positive.
Results: Our results in (%), listed in Table 1, highlight prevalent expression of S100P in pancreaticobiliary tract lesions. We also report S100P positivity in mesothelioma (50%) and rarely in gastrointestinal stromal tumors (GISTs) (5%). We observed decreased S100P positivity in high grade UCa with squamous differentiation and markedly reduced reactivity in urothelial carcinoma with sarcomatoid differentiation and undifferentiated carcinoma.

Tissue type	0	1	2	3	4	% (+)
Gastric Ca	0	20	15	15	50	100
Pancreas Ca	10	5	0	30	55	85
Bladder Ca	16	5	5	11	63	84
Lung adenoCa	30	20	25	10	15	70
Lung squamous Ca	35	20	30	5	10	65
Breast Ca	44.5	17	11	5.5	22	55
Mesothelioma	50	19	19	6	6	50

Conclusions: This S100P IHC study on a large multi-tumor TMA cohort expands the range of known positivity to include mesotheliomas and GIST while confirming positivity seen previously in lesions in the differential. The advantage of S100P remains its sensitivity for urothelial carcinoma, though we recommend its use in a panel with more specific markers.

1022 TCEB1-Mutated Renal Cell Carcinoma (RCC): An Entity With Clear Cytoplasm and Prominent Fibromuscular Stroma Is Distinct From Clear Cell Renal Cell Carcinoma (ccRCC)

Judy Sarungbam, A Ari Hakimi, Yusuke Sato, Seishi Ogawa, Anders Jacobsen, Yukio Homma, Teppei Morikawa, Haruki Kume, Masahi Fukayama, Yingbei Chen, Anuradha Gopalan, Hikmat Al-Ahmadie, Samson Fine, Sahussapont Sirintrapun, Paul Russo, James Hsieh, Victor Reuter, Satish Tickoo. Memorial Sloan Kettering Cancer Center, New York, NY; Kyoto University, Kyoto, Kansai, Japan; University of Tokyo, Tokyo, Japan.

Background: Multiple recent publications have claimed the uniqueness of RCC with clear cytoplasm and prominent fibromuscular stroma (RCFMS). Such tumors have variably been called CK7+ RCC, renal angioadenoleiomyomatous tumor (RAT), RCC with angioleiomyoma-like stroma, clear cell-papillary RCC, etc. Most of these reported RCFMS also lack 3p losses/*VHL* mutations. Among these, clear cell-papillary RCC is now accepted as a distinct entity. In extensive genetic analysis of ccRCCs, Sato et al. (Nature Genetics 2013;45:860), identified a subset with recurrent *Transcription Elongation Factor B1* (*TCEB1*) hotspot mutation. *TCEB1,* localized to 8q21.11, encodes Elongin C, a vital component of the VHL complex. *TCEB1* and VHL mutations were mutually exclusive. Our initial morphologic evaluation of TCEB1-mutated tumors from Sato cohort suggested a distinct histology and some overlap with RCFMS. We subsequently undertook a detailed morphologic and immunohistochemical (IHC) analysis of these cases.

Design: Morphology on all H&E slides from 8 *TCEB1*-mutated RCCs from the Sato et al, and virtual slide from 1 case in the TCGA database was reviewed. IHC for carbonic anhydrase-IX (CA-IX), hypoxia-inducible factor 1 (HIF1a), CK7, CD10 and HMW cytokeratin (34BE12) was performed on the 8 Sato et al tumors.

Results: All tumors were well circumscribed with at least partial encapsulation. In all, broad bands of fibromuscular septae imparted vaguely nodular appearance to the tumor. Variable cystic changes were seen in all. Combination of architectural patterns present included: acinar and micro- or macro-cystic areas, in 9/9 with thin colloid-like secretions and scalloping of the secretions in 4; branching tubules and papillations in 5. While on low magnification evaluation, the cells appeared to contain abundant clear cytoplasm, higher-power examination revealed small amount of dispersed pink granules or fibrillary strands in the cytoplasm, and prominent cytoplasmic membranes. 8/9 tumors were Fuhrman nuclear grade 2. No necrosis or vascular invasion was identified. All 8 tumors were diffusely positivity for HIF-1a and CA-IX (box-like). Patchy CK7 positivity was seen in 8/8 tumors. CD10 and 34BE12 were focally positive in 5 and 3 tumors.

Conclusions: 1. *TCEB1*-mutated tumors are distinct from clear cell RCC at the morphologic, immunophenotypic and molecular levels.

2. It is highly likely that most, if not all, RCCs with clear cytoplasm, prominent fibromuscular stroma and CK7 positivity, may in fact be *TCEB1*-mutated RCC.

1023 TERT Promoter Mutations and HER2 Overexpression in Upper Urinary Tract Urothelial Carcinoma

Judy Sarungbam, Sabina Babayeva, Jian Zhuge, John Fallon, Minghao Zhong. Memorial Sloan Kettering Cancer Center, New York, NY; New York Medical College at Westchester Medical College, Valhalla, NY.

Background: Upper urinary tract urothelial cell carcinomas (UUT-UCs) are uncommon. Recent studies have suggested *TERT* promoter mutation as a biomarker for urothelial carcinoma (UC). In addition, HER2 overexpression has been demonstrated in a subset of UC. However, there is no study correlating *TERT* promoter mutation and HER2 overexpression in UC, especially UUT-UC. In this study, we investigated *TERT* promoter mutation and HER2 overexpression in UUT-UC.

Design: All cases of UUT-UC with nephrouretrectomy from 2006 to 2012 were retrieved from the archives of pathology department of a tertiary care center. Electronic medical records were reviewed for clinical informations. Slides of all cases were reviewed and also appropriate blocks selected to make sure that the tumor component is at least >20% of all tissue. Macro-dissection was performed in some of cases. gDNA was extracted from those tissue. *TERT* promoter mutations were detected by standard PCR-sequencing. In addition, tissue microarray (TMA) was also constructed from these cases. The TMA slide was subjected to HER2 IHC stain. The level of HER2 protein expression was assessed semi-quantitatively by the intensity and percentage of staining and scored on a scale of 0–3+and only 3+ membranous staining is considered as positive.

Results: A total of 53 cases of UUT-UC (12 cases of low grade and 41 cases of high grade) were identified. TERT promoter mutation was detected in 38 cases (71.7%), of which 7 were low grade and 31 high grades. HER2 was positive in only 11 cases (20.8%) which were all high grade UC. There were 7 cases (13.2%) which were both positive for TERT promoter mutation and HER2 overexpression. HER2 overexpression, but not TERT promoter mutation, was associated with higher stage (>pT2).

Conclusions: 1. *TERT* promoter mutation frequency in UUT-UC is similar to that of bladder UC (~70%). HER2 overexpression is seen in only 20% of UUT-UC and restrict to high grade lesions.

3. This result supports that TERT promoter mutation is an early event in the carcinogenesis of UUT-UC and HER2 amplification contributes to tumor progression at a later stage and is likely independent of TERT promoter mutation.

1024 Suppressive Effect of HDAC Inhibitor, OBP-801, on Prostate Cancer Development, Proliferation, and Invasion In Vivo

Shinya Sato, Shugo Suzuki, Aya Naiki-Ito, Yoriko Yamashita, Toshiya Kuno, Satoru Takahashi. Nagoya City West Medical Center, Nagoya, Japan; Nagoya City University Graduate School of Medical Sciences, Nagoya, Japan.

Background: Histone acetylation changes chromatin structure and gene expression. Histone deacetylase (HDAC) inhibitor promotes histone acetylation and regulate gene expressions associated with cancer development. HDAC inhibitors have been reported to suppress growth of several malignancies, and are expected to treat and prevent prostate cancer. Previously we established two rat models of prostate carcinogenesis and hormone refractory prostate cancer. In this study, we examined suppressive effects of novel selective HDAC inhibitor, OBP-801, on prostate cancer development, proliferation, and invasion in vivo using the two models, human cell lines and surgical pathology specimens.

Design: First, for assessing the effects of OBP-801 (provided by Oncolys biopharma) on prostate carcinogenesis, we prepared male transgenic TRAP rats which develop androgen dependent prostate cancers, and OBP-801 was given intravenously at doses of 0, 0.5, and 2mg/kg once a week for 8 weeks. Second, for assessing the effects of OBP-801 on prostate cancer proliferation and invasion, we transplanted hormone refractory rat prostate cancer (PLS-P) onto the femurs of male F344 rats, and OBP-801 was administered intravenously at doses of 2.5 and 5mg/kg every other day for 2 weeks.

Results: In the first study, incidences of adenocarcinomas in low dose and high dose groups were decreased compared with the control group.

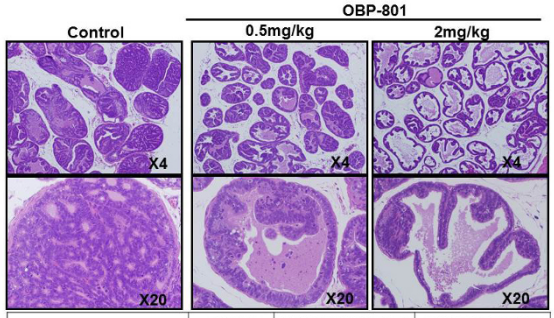

	control	OBP-801 0.5mg/kg	OBP-801 2mg/kg
Adenocarcinoma (n)	10/11	7/11	5/10
Percentage of adenocarcinoma for all prostate glands (%)	4.9±5.3	1.1±1.2	1.1±1.7

Figure. 1 Histopathology, incidence, and percentage of adenocarcinoma in rat prostate glands

The relative number of adenocarcinoma glands in treated groups was significantly decreased compared with those of the control group. Nkx3.1 protein and mRNA levels in the lateral lobe of the high dose group were increased compared with the control group. In the second study, OBP-801 significantly reduced the volume of the transplanted tumor, while inducing cleaved caspase 3 protein expression. OBP-801 also suppressed bone destruction with reduction of osteoclasts.

Conclusions: In conclusion, the obtained data suggests that OBP-801 may be a candidate as a therapeutic or preventative agent for androgen dependent and hormone refractory prostate cancer. Elucidation of mechanisms of HDAC underlying these effects is needed.

1025 Dissimilar Clinicopathological and Biological Characteristics of Anterior/Transition Zone Prostate Cancer With Emphasis of Lower Incidence of ERG Overexpression

Shun Sato, Hiroyuki Takahashi, Takashi Yorozu, Takahiro Kimura, Masahiro Ikegami. Jikei University School of Medicine, Tokyo, Japan.

Background: We have reported the significant prevalence of anterior zone prostate cancer (ANT) in Japanese men at the previous USCAP meeting. The anterior (ANT)/transition zone (TZ) cancer showed unique clinicopathological characteristics from posterior (POST)/peripheral zone (PZ) cancer. In this study, we conducted further clinicopathological analysis based on the locational/zonal aspect.

Design: A total of 211 radical prostatectomy (RP) specimens were utilized. The cases were subclassified into ANT, POST or Non-dominant (ND) cancer by dominant cancer location; into TZ or PZ cancer by zonal origin as previously. Status of core needle biopsy (number of positive core/case, repeat number of biopsy prior to diagnosis), concordance of GS between biopsy and RP specimen, and status of digital rectal exam (DRE) were analyzed. Immunohistochemistry for ERG was performed and evaluated.

Results: Cases were subclassified as 88 (41.7%), 75 (35.5%) and 48 (22.7%) of ANT, POST and ND; 88 (41.7%) and 122 (57.8%) of TZ and PZ, respectively. Proportion of

positive core was significantly lower in ANT/TZ cancers. Patients with ANT cancers have experienced more repeat biopsies than those with POST cancers. The ANT/TZ cancers were likely to be non-palpable than POST/TZ cancers. Overexpression of ERG was significantly more frequent in POST/PZ cancers.

	ANT (%)	POST (%)	p-value	TZ (%)	PZ (%)	p-value
% pos. core (mean)	20.8	38.4		25.0	37.3	0.0002
rate of repeat biopsy (mean)	0.136	0.027	0.0340	0.125	0.049	0.0811
GS concordance: upgrade	28 (32.1)	17 (23.0)	0.2329	26 (29.9)	27 (22.3)	0.4405
concordant	52 (59.8)	46 (62.2)		50 (57.5)	79 (65.3)	
downgrade	7 (8.0)	11 (14.9)		11 (12.6)	15 (12.4)	
DRE: palpable	23 (26.1)	38 (50.7)	0.0019	26 (29.5)	58 (47.5)	0.0102
non-palpable	65 (73.9)	37 (49.3)		62 (70.5)	64 (52.5)	
ERG: positive	3 (3.4)	21 (28.0)		7 (8.0)	26 (21.3)	0.0117
negative	85 (96.6)	54 (72.0)		81 (92.0)	96 (78.7)	

Conclusions: The ANT cancers seem to be more difficult to detect by core needle biopsy and DRE. Urologists should know this fact and further contrivance of biopsy strategy should be considered to detect this type of tumor. The different molecular pathway of carcinogenesis between ANT/TZ and POST/PZ cancers is suggested.

1026 Interobserver Variability in PTEN Immuno-Status on Sections From Radical Prostatectomy Cases

Swati Satturwar, Theodorus Van der Kwast, Michelle Downes. University Health Network, Toronto, ON, Canada.

Background: Loss of the PTEN tumor suppressor gene is a late event in prostate carcinogenesis and identification of this may be used as a biomarker of disease aggression in the context of prostate biopsy samples. PTEN loss can be assessed by FISH or immunohistochemistry. Most immunohistochemical assessments have been performed on biopsy material or TMA's. Our aim was to assess PTEN immuno-status on sections from radical prostatectomy cases to determine the degree of interobserver variation in PTEN interpretation.

Design: A cohort of 57 previously characterized carcinomas (acinar Gleason pattern 3, large cribriform and non-cribriform Gleason pattern 4, intraductal carcinoma) were selected and stained using a mouse monoclonal PTEN antibody (DAKO) on radical prostatectomy sections. PTEN was scored as positive when >90% of tumor showed cytoplasmic staining equal or greater in strength to background benign glands/stroma. Each section was blindly scored by 3 independent observers in a binary fashion (positive/negative). Kappa values were calculated to determine interobserver agreement.

Results: 56 cases were evaluable (1 block missing). There was marked heterogeneity in staining across any given section with most marked variability in the admixed acinar Gleason grade 3 and non-cribriform 4 components. No consistent loss of PTEN was noted in the more aggressive cribriform architecture tumor components. Despite the mixed staining patterns, the overall kappa value was 0.717 (good).

Conclusions: Using a pre-defined cut off with specific scoring instructions results in a good level of inter-observer agreement. The variability in tumor staining in any given section raises concerns about PTEN analysis in biopsy/TMA studies.

1027 A microRNA Profile Identifies a Subset of Bladder Cancers With Favorable Prognosis That Are Enriched for phosS6 Overexpression

Luciana Schultz, Claudia Coutinho-Camillo, Renato Puga, Isac Castro, Gilcy Damm, Samuel Spagnul, Isabela Cunha, Fernando Soares. A.C.Camargo Cancer Center, São Paulo, Brazil; Hospital Israelita Albert Einstein, São Paulo, Brazil; Universidade de São Paulo, São Paulo, Brazil; Instituto de Anatomia Patologica, Santa Barbara d'Oeste, Brazil.

Background: mTOR inhibition is being considered for advanced and cysplatin-resistant bladder cancer. miRNAs have been implicated in mTOR pathway downregulation in a subset of bladder cancers.

Design: The cohort consisted of 74 patients treated by cystectomy for urothelial carcinoma: 10/74 (14%) pTa/pTis/pT1, 21/74 (28%) pT2, and 43/74 (58%) pT3/pT4. Immunohistochemistry was performed for phosS6 (Ser 235/236): 35/74 tumors were negative, 31/74 showed low levels and 8/74 showed high levels (cut-off of 22.5% of positive cells). We applied parametric statistical method t-test with 1000 permutations and p-value <0:05, to identify differentially expressed miRNAs. With these data, we did a hierarchical cluster supported with Pearson correlation that identified two main groups. A miRNA microarray was performed for all tumors.

Results: Cluster analysis revealed 17 diffentially expressed miRNAs, broadly dividing the samples into two groups: one with a miRNA over-expression profile and other with an under-expression signature. Cluster I showed up-regulation of mir-29, mir-130, and mir-518, and Cluster II showed down-regulation of mir-493, mir-125a, mir-320, mir-204 and mir-145. Opposite profiles were observed for mir-382, mir-324, mir-492 and mir-138, which were up-regulated in Cluster I while down-regulated in Cluster II. Seven/8 phosS6 overexpressers belonged to Cluster II. Furthermore, clinic-pathological and outcome differences were significant (p<0.033). Cluster I was composed predominantly of males (75%), 12/42 (29%) patients were younger than 60y, with non-papillary tumors enriched for squamous differentiation. Half (51%) of patients in Cluster II were females, 26/31 (84%) patients were older than 60y, often with multifocal tumors (11/31; 35%) enriched with papillary histology. Pathological stage, perineural or vascular invasion, and node or margin status were not significantly different between the two groups. Mean follow-up time (75 percentile) was 8.15 years. Disease-specific survival in Cluster I was 49% while 74% in Cluster II (p=0.028).

Conclusions: We reveal several miRNAs possibly implicated in mTOR regulation in bladder cancers. Their profile may be able to distinguish a favorable prognostic group, with similar sex distribution and older age group, whose tumors are enriched for phosS6 overexpression, papillary histology and multifocal disease.

1028 Dendrogram Analyses of Relative Expression Between Bladder Cancers and Controls Identify PTEN-HIF1α Association as an Alteration Characteristic of Malignancy

Luciana Schultz, Claudia Coutinho-Camillo, Isac Castro, Gilcy Damm, Samuel Spagnul, Isabela Cunha, Luiz Onuchic, Fernando Soares. A.C.Camargo Cancer Center, São Paulo, Brazil; Universidade de São Paulo, São Paulo, Brazil.

Background: Drugs that target the PIK3/AKT/mTOR pathway are been considered for advanced or post-cysplatin bladder cancer. Clinical trials have shown long term response in some patients but resistance is not infrequent and relates to PTEN loss. Here we compare and measure intrinsic associations between mTOR pathway members and their main known interactions, in malignant and non-malignant urothelial tissue.

Design: Samples from 101 bladder tumors resected by cystectomy and adjacent histologically-benign urothelium (paired control) were collected. Markers (proteins/genes) of cell cycle, mTOR and hypoxia-inducible pathway were analyzed by immunohistochemistry (IHC) and RT-PCR. Relative expression of tumors and controls was obtained by subtraction (IHC) or division (RT-PCR). Dendrograms were constructed to compare and measure intrinsic associations. A discriminatory multivariate analysis was used to separate variables (Wilks Lambda test) and measure centroid distances (Mahalanobis test). Cluster analysis was then used to determine the associations and categorize groups. The markers were organized by median connection within groups as elements of a tree, where the leaves represent patients and the length between knots represent distance by Pearson correlation. An $\alpha \leq 5\%$ was adopted for type I error and $\beta \leq 20\%$ for type II.

Results: The dendrogram of immunoexpression in controls followed a physiological array, discriminating the different pathways and linking hypoxia with cell cycle proteins before connection with the mTOR branch. In tumors, dendrograms of relative expression showed significant association between PTEN and HIF1α, both at the protein and gene expression levels. The imbalance included association between pRB and the pS6/pAKT duet displayed by IHC. The finding of association between caspase-3 and AKT3 mRNA expression was also suggestive of pathway deregulation. Analysis of absolute expression in tumor samples did not reveal association between PTEN and HIF1α.

Conclusions: mTOR and hypoxia pathways are deregulated in bladder tumors and a PTEN-HIF1α association may play a pivotal role. Analizing the relative expression between tumors samples and adjacent histologically-benign urothelium seems more robust than tumor expression alone. Our results are in line with targeted-therapy for mTOR and hypoxia pathways in bladder cancer and further suggest that combined inhibition might be beneficial.

1029 Overexpression of mTOR Pathway Members Reveals Different microRNA Backgrounds That Can Be Linked By pS6

Luciana Schultz, Claudia Coutinho-Camillo, Renato Puga, Isac Castro, Gilcy Damm, Samuel Spagnul, Isabela Cunha, Fernando Soares. A.C.Camargo Cancer Center, São Paulo, Brazil; Hospital Israelita Albert Einstein, São Paulo, Brazil; Universidade de São Paulo, São Paulo, Brazil; Instituto de Anatomia Patologica, Santa Barbara d'Oeste, Brazil.

Background: PI(3)K/AKT/mTOR/CCND1 pathway alterations have been reported to be frequent and mutually exclusive in urothelial cancer. microRNAs (miRNA) are implicated in mTOR pathway down-regulation in a subset of bladder tumors.

Design: Immunohistochemistry for pAKT(Ser473), cyclin D1 and pS6 (Ser235/236) was conducted on a well-characterized cohort of 74 urothelial tumors of patients treated by cystectomy and paired peripheral histologically-benign urothelium. Each maker was scored as percent of positive cells and relative expression between malignant and benign samples was calculated by subtraction. A cut-off was reached by ROC curve for the positive tumor samples and higher levels were considered overexpression (high) for pAKT (n=6), cyclin D1 (n=14) and pS6 (n=8). Within this subset, we applied the parametric statistical method t-test with 1000 permutations and p-value <0:05, to identify differentially expressed miRNAs. With these data, we did a hierarchical cluster supported with Pearson correlation. This cluster showed three distinct groups, one been negative expression. A miRNA microarray was then performed.

Results: Overexpression of pAKT and cyclin D1 were mutually exclusive events, accurately classified by unsupervised cluster analysis (n=20) of the miRNA matrix. Five/8 pS6-high belonged to this group and most of them (4/5) coincided with cyclin D1-high. There were 21 differentially expressed miRNAs, mainly related to tissue differentiation, and also to epithelial-mesenchymal transition, apoptosis and immune response. Up-regulated miRNAs included mir-200 family, mir-20, mir-10 and mir-90 and down-regulated miRNAs included mir-199 family, mir-146 family and mir-150. Cyclin D-high samples were broadly divided into two halfs, one of them having a profile that was more similar to that of pAKT-high than the remaining samples, and this subset included all 5 pS6-high tumors.

Conclusions: Our findings suggest that overexpression of cyclin D1 and pAKT are mutually exclusive in bladder cancer and bare different miRNA epigenetic background. Overexpression of pS6 is frequent in this scenario and more often coincide with overexpression of cyclin D1. This event seems to approach the miRNA profiles of cyclin D1 and pAKT in up-regulated tumors.

1030 Imaging Mass Spectrometry Reveals New Insights Into Prostate Cancer Pathology

Kristina Schwamborn, Peter Wild, Richard Caprioli. TU Munich, Munich, Germany; University Hospital of Zurich, Zurich, Switzerland; Vanderbilt University, Nashville, TN.

Background: Imaging Mass Spectrometry (IMS) is a molecular analytical technology capable of simultaneously measuring multiple analytes directly from intact tissue sections. Applied to prostate cancer tissue biopsies IMS enables the visualization of the spatial distribution and the relative abundance of tissue specific protein/peptide expression profiles in correlation with histological features. The aim of this study was to identify disease related markers by comparing benign prostatic hyperplasia, prostate cancer, hormone refractory prostate cancer, and prostate cancer metastases utilizing tissue microarrays (TMA).

Design: Four different TMAs were subjected to on-tissue tryptic digestion and IMS comprising tissue cores from the following samples: 115 benign prostatic hyperplasia, 535 prostate adenocarcinomas, 57 hormone refractory prostate adenocarcinomas, and 46 metastases. Briefly, sections were mounted onto conductive glass slides and underwent paraffin removal well as antigen retrieval. On-tissue digestion was achieved by spotting trypsin onto the tissue in an array pattern using a Portrait 630 reagent multi-spotter. Following digestion, matrix was spotted directly onto the array of tryptic spots. Samples were analyzed utilizing an UltrafleXtreme MALDI-TOF/TOF mass spectrometer. Additionally, MS/MS measurements of selected peptides were acquired. Data analysis was performed by using the ClinProTools 2.2 and FlexImaging 2.1 software.

Results: On-tissue tryptic digestion of prostate tissue revealed on average hundreds of tryptic peptides in the mass range from *m/z* 600-3000. Supervised classification analysis comparing prostate cancer and benign prostatic hyperplasia resulted in a classifier composed of 25 peptides that could predict the class of cancer and benign samples achieving a sensitivity and specificity of 94.8% and 81.1%, respectively. Similarly, utilizing a different classifier, 94.5% of all hormone naïve and 70.4% of all hormone refractory prostate cancer samples could be classified correctly. In total 73 peptides form 34 different proteins could be identified. For example, fatty acid binding protein, epidermal, glutathione S-transferase P and heat shock protein beta-1 were differentially expressed between prostate cancer and benign hyperplasia. Immunhistochemical validation analyses are ongoing.

Conclusions: These results could provide insight into the discovery of novel biomarkers for prostate cancer.

1031 Interobserver Reproducibility in the Diagnosis of Gleason Pattern 5 Prostate Adenocarcinoma Among Urologic Pathologists

Rajal Shah, Jianbo Li, Liang Cheng, Fang-Ming Deng, Lars Egevad, Samson Fine, Lakshmi Kunju, Jonathan Melamed, Rohit Mehra, Adeboye Osunkoya, Gladell Paner, Steven Shen, Toyonori Tsuzuki, Kiril Trpkov, Tian Wei, Ximing Yang, Ming Zhou. Gleason Grading Collaborative Group, Irving, TX; Cleveland Clinic, Cleveland, OH.

Background: Accurate recognition of Gleason pattern 5 (GP5) prostate adenocarcinoma (PCa) in needle biopsy (NBX) is critical as it is associated with disease progression and adverse clinical outcomes. Previous studies have demonstrated that GP5 PCa in NBXs is underdiagnosed by pathologists.

Design: Digital images of 50 PCa that potentially contained a GP5 component were distributed to 16 urologic pathologists who were asked to classify whether GP5 was present or not. Each image was initially classified into one of 4 morphologic subpatterns by two study authors (RBS and MZ): solid nests (8), comedocarcinoma (4), single cells and/or cords of cells (35), and variant morphology (3). Additional features captured included: size (large>20 cells, medium 10-20 cells, and small <10 cells) and distribution of nuclei (uniform vs non-uniform) for nest; coagulative necrosis, karyorrhectic debris and amorphous secretions for comedocarcinoma; and quantity (<5, 5-10 and >10) and distribution (clustered vs intermixed with adjacent well-formed glands) for single cell and cords of cell patterns. Interobserver reproducibility was assessed and the morphologic subpatterns and features were correlated with the consensus diagnosis (defined as 75% agreement within participants).

Results: Interobserver reproducibility for overall diagnostic agreement was fair (k=0.369). Amongst subpatterns, variant morphology had highest reproducibility (k=0.547) followed by comedocarcinoma (k=0.526), single cells and cords of cells (k=0.369) and nests (k=0.340). The following features had high consensus for GP5: large nests with uniformly distributed nuclei; coagulative necrosis with or without karyorrhectic debris; single cells and/or cords >10 or 5-10 in a cluster; and signet ring-like cells. The following features had high consensus for not being classified as GP5: small nests or medium nests with non-uniformly distributed nuclei; amorphous secretions only; single cells and/or cords <5 and intermixed with adjacent well-formed glands; and Paneth cell change. The majority (86%) of participants would classify small focus of GP5 only when it is present in more than one level (average 2 to 3).

Conclusions: Some morphological features are highly reproducible for and against GP5. However, the diagnostic reproducibility of GP5 PCa is only fair among urologic pathologists. These findings suggest that additional studies are needed, testing highly reproducible features of GP5 with documented aggressive clinical outcomes.

1032 PTEN Protein Loss and Genomic Deletions in Prostate Cancer: A Comparative Study of Immunohistochemistry and Four-Color FISH Assay

Rajal Shah, Alex Nicolau, Thomas Moss, Savvas Mendrinos. Miraca Life Sciences Research Institute, Irving, TX; Cymogen, Irvine, CA.

Background: The loss of a PTEN tumor suppressor gene is increasingly being analyzedon prostate core biopsies (NBXs) due to its prognostic relevance in cancer (PCa) risk stratification. Yet, there is no standardized approach for interrogation of this biomarker in laboratories. Immunohistochemistry (IHC) may miss cases that have small clusters of cells with deletion and FISH may miss cases where PTEN is inactivated due to very small deletions or single-nucleotide polymorphism. The purpose of this study was to use a four-color FISH assay which reduces false positivity due to nuclear truncation and IHC on prostate biopsies to evaluate the potential of a developing standardized approach to PTEN evaluation.

Design: Sixty-one PCa NBXs (Gleason score 3+3 (36); 3+4 (20); ≥4+3 (6)) were analyzed by both IHC (clone D4.3, Cell Signaling) and four-color FISH assay(CymGen Dx, CA). PTEN loss by IHC was defined as complete (entire tumor) or partial (any amount of tumor) loss and by FISH as hemizygous (loss of one copy) or homozygous (loss of both copies). Tumors with a minimum of five cells demonstrating hemi or homozygous loss were considered positive. For IHC benign glands and stroma were used as an internal control, and for FISH CEP10 was used to enumerate chromosome 10 and the inclusion of flanking probes to separate "pseudo deletion." Results of the two methods were blinded.

Results: The overall rate of PTEN loss by IHC was 17 (28%), FISH was 19 (31%), and a combined rate of 25 (41%). FISH did not detect a deletion in 6 of 17 IHC positive cases (35%) and IHC did not detect inactivation (loss) in 6 of 19 FISH positive cases (32%). In addition, IHC missed homozygous deletions in 6 of 10 cases, whereas complete PTEN loss was not associated with homozygous deletion in 5 of 9 cases. PTEN loss/inactivation by both IHC and FISH methods were associated with an increasing Gleason score.

Conclusions: To most accurately identify PTEN deletion/inactivation, a FISH/IHC integrated model needs to be developed. This model may involve FISH as a reflex test for cases where IHC is intact or reduced. In addition, a comprehensive study combining IHC and FISH detection of PTEN deletion/inactivation results with clinical outcome is in order to determine if combining the two tests in an integrated model is superior to one method or the other.

1033 Solitary Fibrous Tumor of the Genitourinary Tract: A Clinicopathologic Study of 11 Cases and Their Association With the NAB2-STAT6 Fusion Gene

Novae Simper, Shaoxiong Chen, Sean Williamson, David Grignon, John Eble, Gregory MacLennan, Rodolfo Montironi, Antonio Lopez-Beltran, Shaobo Zhang, Mingsheng Wang, Thu Tran, Maria Monn, Constantinos Linos, Liang Cheng. Indiana University, Indianapolis, IN; Henry Ford Health System, Detroit, MI; Case Western Reserve University, Cleveland, OH; Polytechnic University of the Marche Region, Ancona, Italy; Cordoba University Medical School, Cordoba, Spain; Dartmouth-Hitchcock Medical Center, Hanover, NH.

Background: Solitary fibrous tumor (SFT) is a rare lesion in the genitourinary tract. Its recognition is challenging, as it is one of a number of spindle cell lesions, some of which share partly overlapping immunohistochemical profiles. Although most SFTs follow a less aggressive clinical course, local recurrence or metastatic disease has been observed in almost 10% of cases. Recently, several studies have reported a recurrent intrachromosomal fusion between the *NAB2* and *STAT6* genes on chromosome 12q13 in a majority of SFTs. We examined 11 genitourinary tract SFTs for the presence of the *NAB2-STAT6* gene fusion using a novel breakapart fluorescence in situ hybridization (FISH) probe and correlated with the clinicopathologic features.

Design: Eleven SFTs of the genitourinary tract were accrued from the authors' institutional files. Demographic and clinical information were obtained from medical records. Hematoxylin and eosin-stained slides for all tumors were reviewed to confirm the diagnosis. All showed positive CD34 immunohistochemistry. FISH analysis for *NAB2-STAT6* gene fusion was performed using a probe cocktail with BAC clones for *STAT6* and *NAB2*.

Results: Eleven SFTs were identified in 3 female patients and 8 male patients with an average age of 52 years (range 29 to 80 years). Sites were as follows: kidney (4), prostate (2), bladder (2), adrenal gland (1), testicle (1), and retroperitoneum (1). Five of the tumors (45%) had malignant histologic features. Clinical outcome data were available for 8 patients with a mean follow up time of 38 months (range 2 to 72 months). Of these, 7 of the 8 patients had no residual or recurrent disease, and one developed recurrence. The *NAB2-STAT6* gene fusion was detected in 6 of the 11 tumors (55%) and was present in 3 of the 5 tumors with malignant features (60%) including the single tumor with recurrence.

Conclusions: Our findings suggest that SFTs of the genitourinary tract tend to be clinically indolent lesions despite a relatively high percentage of cases with malignant histologic features. Using a new breakapart FISH probe cocktail, we found the *NAB2-STAT6* gene fusion in 55% of SFTs of the genitourinary tract. However, the *NAB2-STAT6* fusion status was not useful in discriminating between low or high risk tumors.

1034 Intratumoral Morphologic and Molecular Heterogeneity of Rhabdoid Renal Cell Carcinoma Pose a Challenge for Personalized Cancer Therapy

Rajesh Singh, Pheroze Tamboli, Bogdan A Czerniak, L Jeffery Medeiros, Rajyalakshmi Luthra, Kanishka Sircar. University of Texas MD Anderson Cancer Center, Houston, TX.

Background: The behavior of clear cell renal cell carcinoma (RCC) may be stratified based on molecular alterations. However, molecular analysis of RCCs needs to account for the histologic and genomic diversity of each tumor which can possess different regional tumor grades and genetically distinct subclones. Our aim was to evaluate morphologic heterogeneity within cases of rhabdoid clear cell RCC with respect to known driver genes using archival tissues and a clinical next generation sequencing (NGS) platform.

Design: We evaluated 16 discrete regions from 8 cases of clear cell RCC with rhabdoid features (stage IV, n=6; stage III, n=2) that showed extreme intratumoral morphologic heterogeneity. Using formalin-fixed paraffin-embedded specimens, we microdissected the rhabdoid (R) and typical clear cell/epithelioid tumor components (ISUP nucleolar grades G2, G3 and G4). Common driver mutations in clear cell RCC were assessed by NGS of 409 cancer-related genes according to clinical thresholds and correlated to histology.

Results: Six of 8 tumors showed genotypic differences between the rhabdoid and epithelioid components in terms of cancer related mutations. The mutational profile of the different components with respect to common RCC drivers is shown in the table below.

VHL showed an identical mutation in all regions from the same tumor. BAP1 and PBRM1 mutations were mutually exclusive and discordant between epithelioid and rhabdoid components in 3/3 cases and 1 case, respectively, with mutations called only in the rhabdoid component. SETD2 mutations were concordant in 3/4 cases, with the discordant case showing a mutation in the epithelioid component only. No mutations in mTOR, PIK3CA, KDM5C, TP53, PTEN or TCEB1 were detected in this cohort.

	Regional histologic grade				Patients
Gene	Rhabdoid	Clear Cell/Epithelioid			(n=8)
	R (n=8)	G2 (n=5)	G3 (n=2)	G4 (n=1)	
VHL	5 (63%)	4 (80%)	1 (50%)	0 (0%)	5 (63%)
PBRM1	1 (13%)	0 (0%)	0 (0%)	0 (0%)	1 (13%)
SETD2	3 (38%)	1 (20%)	2 (100%)	1 (100%)	4 (50%)
BAP1	3 (38%)	0 (0%)	0 (0%)	0 (0%)	3 (38%)

Conclusions: Aggressive clear cell rhabdoid RCC are characterized by a high rate of SETD2 and BAP1 mutations. However, driver mutations in RCC are distributed across different morphologic regional tumor grades and cannot be reliably captured with single biopsy sampling. Pathologists may need to select tumor foci from different regions and of different histologic patterns for molecular profiling of RCC for prognostic or predictive purposes.

1035 Is Tubulocystic Carcinoma With Dedifferentiation a form of HLRCC/ Fumarate Hydratase-Deficient RCC?

Steven Smith, Kiril Trpkov, Rohit Mehra, Mukul Divatia, Ondrej Hes, Santosh Menon, Sergio Tripodi, Jonathan McHugh, Fadi Brimo, Anthony Gill, Cristina Magi-Galluzzi, Mathilde Sibony, Sean Williamson, Gabriella Nesi, Maria Picken, Liang Cheng, Victor Reuter, Jonathan Epstein, Satish Tickoo, Scott Tomlins, Ying-Bei Chen, Mahul Amin. Virginia Commonwealth University Health System, Richmond, VA; Cedars-Sinai Medical Center, Los Angeles, CA; Memorial Sloan Kettering Cancer Center, New York, NY; University of Michigan, Ann Arbor, MI; Johns Hopkins Medical Institutions, Baltimore, MD; IU School of Medicine, Indianapolis, IN; University of Siena, Siena, Italy; University of Florence, Florence, Italy; Calgary Laboratory Services, Calgary, Canada; McGill University, Montreal, Canada; Cleveland Clinic, Cleveland, OH; Royal North Shore Hospital, Sydney, Australia; Hopital Cochin, Paris, France; Charles University, Plzen, Czech Republic; Tata Memorial Hospital, Mumbai, India; Loyola University, Maywood, IL.

Background: We hypothesized that tubulocystic carcinomas with focal dedifferentiation (TC-D) may be a possible histologic pattern of fumarate hydratase *(*FH*)*-deficient RCC because of similarities in morphology, immunohistochemistry (IHC), and outcomes shared with hereditary leiomyomatosis-RCC syndrome associated carcinoma (HLRCC).

Design: We used complementary prospective and retrospective approaches to determine if there is a relationship between TC-D and FH-deficient RCC. First, 16 cases with morphology of TC-D were collected and studied by IHC for expression of FH and aberrant succination (2SC). Second, 29 cases showing loss of *FH* and expression of 2SC, with molecular confirmation of FH mutation, were evaluated for presence of TC-D morphology.

Results: Cases with *a priori* TC-D morphology had M:F ratio of 1.6; median age 52y, median size 7.3cm, and stage pT3a. In 10/13 cases with follow-up, there was a persistent disease, metastasis, or demise at <16 months. Syndromal stigmata were identified in only 1/16 cases of TC-D. Of these, FH loss was detected in 6/16 and 2SC expression in 10/14. Of cases with data for both, an aberrant FH-/2SC+ pattern was seen in 5/14, normal FH+/2SC- pattern seen in 4/14, and 5/14 had intermediate findings (FH+-/2SC +). Among *a priori* FH-deficient RCCs, TC-D morphology was found in 10/29, with M:F ratio of 3.5; median age 44y; median size 7.25cm; and stage pT3a. In 7/9 cases there was persistent disease or demise at <24 months.

Conclusions: The overlapping features between TC-D and FH-deficient carcinoma suggest that a substantial subset of TC-D represents FH-deficient RCC. TC-D morphology in this setting should prompt further patient workup. Cases with intermediate IHC findings raise intriguing questions of novel FH-related pathways. Next generation sequencing is underway to further delineate the relationship between TC-D with and without FH loss by IHC.

1036 Incidental Lymphomas in Genito-Urinary Resection Specimens: A Multi-Institutional Study

Payal Sojitra, Neval Ozkaya, Tatjana Antic, Nukhet Tuzune, Milind Velankar, Maria Picken, Girish Venkataraman, Vijayalakshmi Ananthanarayanan. Loyola University Medical Center, Maywood, IL; University of Chicago, Chicago, IL; Istanbul University, Istanbul, Turkey.

Background: Lymphomas of the genitourinary (GU) tract are uncommon malignancies. Furthermore, lymphomas discovered incidentally during work-up of GU lesions are even less frequent. Aim of this study was to assess frequency of incidentally found lymphomas (IL) in GU resection specimens.

Design: Pathology databases at three tertiary health care institutions were searched for a diagnosis of IL in GU resection specimens (2004-2014). All primary GU lymphomas were excluded. Parameters abstracted from the pathology reports were: primary diagnosis, presence of concurrent IL and its sub-classificationnodal or extra-nodal involvement.

Results: A total of 22 patients (9 females, 13 males) with IL were identified. Of these, 3 patients were noted to have a prior history of lymphoma. Summary regarding the site, procedure, primary diagnosis, IL and its sub-classification is provided in Table 1. Eleven cases had concurrent lymph node dissections, of which 8 cases showed nodal lymphoma without primary organ involvement. Three cases showed both nodal and primary organ involvement by IL.

Primary site(n)	Procedure	Primary diagnosis(n)	Incidental lymphomas(n)
Adrenal (2)	Adrenalectomy	Pheochromocytoma(2)	CLL/SLL(1);Low grade BCL(1)
Urinary Bladder (6)	Cystectomy and Cystoprostatectomy	Urothelial Carcinoma(6)	CLL/SLL(5); FL(1)
Kidney (4)	Nephrectomy	Clear cell carcinoma(2); Urothelial Carcinoma(1); Angiomyolipoma(1)	CLL/SLL(2); MZL(2)
Prostate (11)	Prostatectomy	Prostatic adenocarcinoma(6); Benign(5)	CLL/SLL(4); FL(1); CD5- low grade BCL(1)
Ureter(1)	Ureterectomy	Benign(1)	CLL/SLL(1)

CLL/SLL, Chronic lymphocytic leukemia/small lymphocytic lymphoma; FL, Follicular lymphoma; BCL, B-cell lymphoma; MZL, Marginal zone/MALT lymphoma.

Conclusions: The incidence of IL was noted to be 0.3% at our institution (8/2566). Majority of them are low-grade lymphomas with either nodal or extra-nodal involvement. Presence of IL merits a close patient follow-up. Awareness of these malignancies is necessary while evaluating GU resection specimens.

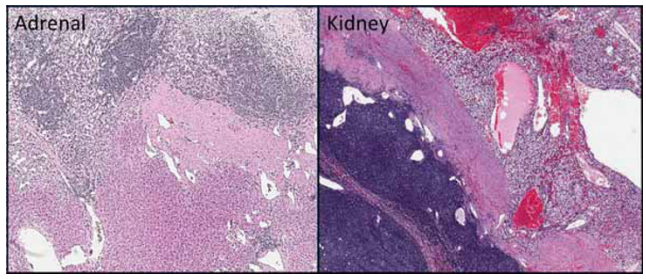

1037 Loss of PLZF Expression in Prostate Cancer By Immunohistochemistry Correlates With Metastasis

Bibiana Steinbauer, David Burstein, Qi Yang, Yayoi Kinoshita, Pamela Unger, Faqian Li, Guang-Qian Xiao. University of Rochester Medical Center, Rochester, NY; Mount Sinai Medical Center, New York, NY; Lenox Hill Hospital, New York, NY.

Background: The metastatic potential of Prostate cancer (PCa), a mostly indolent and non-lethal disease, is a key prognostic factor that until now, has not been shown to be accurately predictable with available biomarkers. Promyelocytic leukemia zinc finger protein (PLZF), a zinc finger transcription repressor, plays a critical role in embryonic development, spermatogenesis and oncogenesis. The expression of PLZF in prostate tissue has not been well studied. The aim of this study was to investigate the expression of PLZF in primary as well as metastatic PCa by immunohistochemistry and to correlate the alteration of PLZF expression with PCa aggressiveness as well as metastasis.

Design: A total of 83 different prostate biopsies with primary PCas of different grades (Gleason patterns 3, 4, and 5), and a total of 43 different metastatic PCas were studied. The anatomic sites for the metastasis include the following: bone (22), lymph node (11), liver (7), and lung (3). By immunohistochemistry, nuclear stain was considered positive. The intensity of nuclear expression of PLZF was graded as negative (0), weak (+1), moderate (+2) and strong (+3).

Results: PLZF was strongly expressed in almost all (~100%) coexisting benign luminal cells (n=77) in the biopsies.Of the 83 biopsies with primary prostate cancer, 65 (78%) stained positive (all Gleason pattern 3 and most 4 and 5), and 18 (22%) stained negative (all Gleason pattern 4 and 5). Of the 43 metastasis, 7 of the 43 were positive, while the vast majority (84%) showed a significant decrease or loss of PLZF.

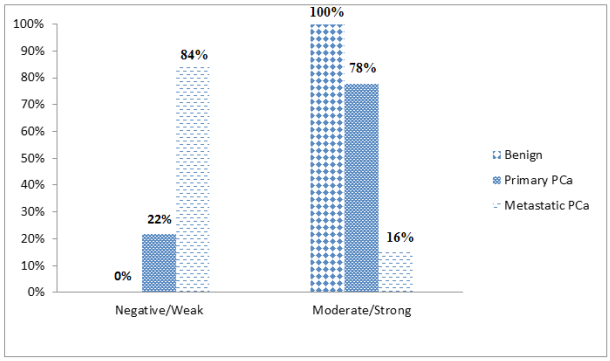

The PLZF expression patterns are significantly different between benign, primary PCa and metastasis. There is a significant decrease in high-grade PCa, particularly in metastatic PCa.

Conclusions: The data demonstrates that downregulation of PLZF is strongly correlated with aggressive/metastatic prostatic cancer. A loss of PLZF expression detected by routine immunohistochemistry is a promising and valuable biomarker for PCa aggressiveness and metastatic predictability and ought to be used to provide clinical decision support.

1038 RBFOX 1 Immunoexpression in Renal Tumors

Cristina Storoz, Oluyomi Ajise, Myriam Chevarie-Davis, Yasser Riazalhosseini, Bin Xu, Fadi Brimo. McGill University Health Center, Montreal, QC, Canada.

Background: RNA - binding proteins (RBPs) govern gene expression patterns through post-transcriptional regulation of mRNA stability and alternative splicing procedure. Preliminary data showed that RBFOX1, an RBP, can play a role in down regulation of tumoral activity in clear cell renal cell carcinoma (CCRCC).

Design: Immunoexpression of RBFOX1 protein in 491 renal samples (197 CCRCCs , 136 papillary (P) RCCs, 35 chromophobe (Ch) RCCs , 51 oncocytomas and 72 benign renal tissue) was evaluated in nine tissue microarrays using a monoclonal RBFOX1 antibody. Nuclear immunoreactivity which was recorded as number of cases staining, highest intensity, % of stained cells and H-score (HS) (staining intensity X % of positive cells) was correlated with multiple clinical and pathological parameters.

Results: Renal tumors significantly under-expressed the marker in comparison to benign tissue ($p<0.001$). There was no significant difference in % of positive cases among different tumor types except for ChRCC which expressed the marker only rarely (20%). Among primary tumors, HS was significantly higher in PRCC (64.5%) in comparison to CCRCC (29.2%), oncocytoma (24.5%), and ChRCC (4.2%).

RBFOX1 and CCRCC: There was significant RBFOX1 overexpression in metastatic versus primary tumors in terms of % of positive cases, staining intensity and HS ($p<0.001$). This difference was confirmed in a separate set of 18 matched primary and metastatic samples. Overall ISUP grade correlated with RBFOX1 overexpression, but no significant different expression was detected in terms of the pathological stage of the primary tumor (£T2 versus ³T3). Survival analysis using Cox proportional hazards regression models performed on 111 CCRCCs (67 primary and 44 metastases) with clinical follow-up showed that disease specific survival (DSS) was significantly shorter in patients expressing RBFOX1 overall ($p=0.03$) and in the metastases ($p=0.04$). Moreover, patients with high HS had significantly shorter DSS those under-expressing the marker ($p=0.05$).

Conclusions: Although RBFOX1 is generally under-regulated in renal tumors in comparison to benign renal tissue, it seems to become activated in metastatic CRCC. The data also points to a potential independent prognostic role of RBFOX1 immunoreactivity that warrants further investigations.

1039 The Role of BCBP2 in Renal Tumors

Cristina Storoz, Oluyomi Ajise, Myriam Chevarie-Davis, Yutong Yang, Yasser Riazalhosseini, Bin Xu, Fadi Brimo. McGill University Health Center, Montreal, QC, Canada.

Background: RNA - binding proteins (RBPs) are known to govern gene expression patterns through post-transcriptional regulation of mRNA stability and alternative splicing procedure. Preliminary data showed that BCBP2, an RBP, can play a role in down regulation of tumoral activity in clear cell renal cell carcinoma (CCRCC). This is the first study to evaluate the prognostic role of BCBP2 immunoexpression in a large cohort of renal tumors.

Design: Immunoexpression of BCBP2 in 491 renal samples (197 CCRCC , 136 papillary (P) RCCs, 35 chromophobe (Ch) RCCs , 51 oncocytomas (ONC) and 72 benign renal tissue) was evaluated in nine tissue microarrays using a monoclonal antibody. Immunoexpression which was recorded as number of cases staining, highest intensity, % of stained cells (nuclear) and H-score (HS) (staining intensity X % of positive cells) was correlated with multiple clinical and pathological parameters.

Results: Benign tissue, ONC and ChRCC showed very low expression of BCBP2 (HS of 13.9, 5.3, 4.1, respectively). In contrast, CCRCC significantly overexpressed the marker in comparison to benign tissue and to all other tumor types ($p<0.001$). BCBP2 and CCRCC: There was significant BCBP2 overexpression in metastatic versus primary tumors in terms of % of cells staining (74% versus 53%) as well as HS (104.5 versus 80.2) ($p<0.001$). This difference was confirmed in a separate set of 18 matched primary and metastatic samples. No significant different expression was detected in terms of nuclear grade (low-grade versus high-grade) ($p=0.1$) and primary pathological stage (£T2 versus ³T3) ($p=0.8$). Survival analysis using logistic regression models performed on 111 CCRCCs (67 primary and 44 metastases) in which follow-up information was available showed no significant difference between primary and metastatic CCRCC in terms of disease-specific survival and disease-free survival ($p > 0.05$).

Conclusions: BCBP2 is overexpressed in CCRCC and PRCC in comparison to benign renal tissue, and is significantly associated with metastasis in CCRCCs, indicating a potential key role in driving oncogenesis. However, BCBP2 overexpression does not seem to correlate with local tumor characteristics nor with overall clinical outcome.

1040 Preferential Expression of PLZF in Benign Prostatic Epithelium and Low Grade Prostate Cancer

Shana Straub, Pamela Unger, Qi Yang, Yayoi Kinoshita, David Burstein, Mary Beth Beasley, Hongfa Zhu, Faqian Li, Jonathan Yao, Loralee McMahon, Guang-Qian Xiao. University of Rochester, Rochester, NY; Mount Sinai Medical Center, New York, NY; Lenox Hill Hospital, New York, NY.

Background: Promyelocytic leukemia zinc finger (PLZF) protein, a transcriptional repressor, is involved in many developmental processes as well as oncogenesis. PLZF expression has been reported to be lost or down-regulated in some cancer cell lines. However, there have been almost no studies on the distribution of PLZF expression in different human tissues as well as neoplasms, particularly in the prostate.

Design: A range of human neoplasms and their corresponding benign tissues were immunohistochemically stained with PLZF antibody, including 83 different prostate cancer (PCa) cases (13 Gleason score 6 and 70 Gleason score 7-10). Benign prostatic epithelium was present in 77 of these biopsies. Other tissue/tumors included 13 renal, 13 testicular, 16 urinary, 18 gastrointestinal, 34 hepatobiliary and pancreatic, 6 breast, 4 soft tissue, 3 thymic, 42 thyroid, 6 adrenal, 3 melanomas, 22 lung high grade neuroendocrine tumors, 10 lung squamous carcinomas, and 68 lung adenocarcinomas. Nuclear staining was considered positive and graded in intensity from 1 (weak) to 3 (strong).

Results: Negative staining for PLZF was appreciated in the vast majority of the benign and malignant tissues, including renal, testicular, urinary, gastrointestinal, billiary and pancreatic, breast, thymic, melanoma, soft tissue and aforementioned lung tumors. The non-neoplastic spermatogonium showed strong nuclear positivity. Focal nuclear staining was also found in some of thyroid follicular cells (5/42 cases, 12%), benign hepatocytes (2/9 cases, 22%), and adrenal cortical cells (3/6 cases, 50%). 9 of 68 lung adenocarcinomas (13%) showed weak to moderate cytoplasmic staining for *PLZF*, but no nuclear staining. In contrast, moderate to strong nuclear staining for PLZF was seen in the luminal cells of all the benign prostate epithelium (77/77 cases), all low grade PCa (13/13 cases), and 74% of high grade PCa (52/70 cases), however, basal cells and a portion (26%) of high grade PCa showed weak or negative staining for PLZF.

Conclusions: Our results demonstrate that PLZF is preferentially expressed in benign prostatic luminal cells and low grade PCa, and absent in the vast majority of other neoplasms. Loss of PLZF is noted in a portion of high grade PCa, which may well represent those with aggressive behavior. Further validation and correlation studies of PLZF as a specific biomarker for aggressive PCa are warranted.

1041 ERG Oncoprotein Inhibits ANXA2 Expression and Function in Prostate Cancer

Shyh-Han Tan, Nicholas Griner, Denise Young, Pankaj Chaudhary, Ahmed Mohamed, Wei Huang, Yongmei Chen, Taduru Sreenath, Albert Dobi, Gyorgy Petrovics, Jamboor Vishwanatha, Isabell Sesterhenn, Shiv Srivastava. Uniformed Services University of the Health Sciences Center for Prostate Disease Research, Rockville, MD; University of North Texas Health Science Center, Fort Worth, TX; Joint Pathology Center, Silver Spring, MD.

Background: ERG overexpression due to *TMPRSS2:ERG* fusion contributes to prostate cancer (CaP) progression by inhibiting differentiation and promoting epithelial mesenchymal transition. ANXA2, a Ca2+-dependent phospholipid binding protein with many functions, including the maintenance of epithelial cell polarity, is inversely correlated to ERG expression. It also helps to convert plasminogen to plasmin, which stimulates the production of metalloproteinases that drives metastasis. ANXA2 is expressed in normal prostate glands, becomes lost in moderately differentiated tumors, but is detected in high-grade adenocarcinomas.

Design: The immunohistochemistry (IHC) staining of ERG and ANXA2 was evaluated on whole-mounted prostate sections of 40 patients. ERG and ANXA2 expression was correlated to adverse pathology and clinical end-points of biochemical recurrence (BCR) and patient survival. Based on results obtained, the study is being extended to cover an additional 40 cases and a tissue microarray of 99 patients. The regulation of ANXA2 transcription by ERG was also evaluated in cell lines by ERG siRNA knockdown followed by chromatin IP and luciferase assays.

Results: Our results established a reciprocal relationship of ANXA2 and ERG expression in 80% (32/40) of cases analyzed. ANXA2 was absent or markedly reduced in well-differentiated ERG(+) tumors (19/26). ERG(-) tumors, meanwhile, expressed moderate to high levels of ANXA2, and were either poorly-differentiated (PD) (6/11) or displayed subsets of PD cells (5/11). We observed a poorer BCR-free survival in patients with ERG(-)/ANXA2(+).

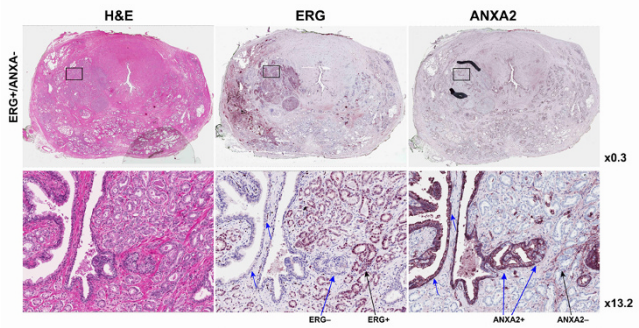

Conclusions: We conclude that the inverse corrleation of ERG and ANXA2 expression in WD tumors of ERG(+)/ANXA2(-) status is mainly the result of transcriptional repression of ANXA2 by ERG. In contrast, the moderate to high levels of ANXA2 in PD tumors is due to either the loss of ERG expression or other yet to be determined mechanisms. Taken together, our results support the potential utility of ANXA2/ERG status to enhance biological stratification for CaP treatment.

1042 Mutational Profiling of Recurrent and Non-Recurrent Non-Invasive Papillary Urothelial Carcinoma of the Bladder

David Terrano, Jennifer Oliver-Krasinski, Aesis Luna, Jorge Sepulveda, Antonia Sepulveda, Lara Harik. Columbia University College of Physicians & Surgeons, New York, NY.

Background: Around 54% of non-invasive low-grade papillary urothelial carcinoma (LGUC) recur within 2 years, 18% of which progress to high-grade tumors. Identifying which LGUC patients will recur could potentially impact clinical care and follow up (FU). Our aim is to identify genomic differences between LGUC tumors in patients with recurrence (R) and patients without recurrence (NR).

Design: We studied 13 male patients with LGUC: 7 with no evidence of clinical recurrence (NR) and 6 with episodes of recurrence (R). Both groups had FU ≥ 24 months. Representative areas of carcinoma were micro-dissected from FFPE biopsy/TURBT specimens. Genomic DNA was sequenced with the TrueSeq Amplicon Cancer Panel (Illumina) in the MiSeq platform. Sequences were aligned against the hg19 human reference genome. Variant calling was annotated by comparison with dbSNP version 145, dbNSFP (v.2.1) and COSMIC (v.67) databases. Only non-synonymous SNV with allele frequencies > 5% were considered in regions with coverage > 150 reads.

Results: The median age was 69 years with a median FU of 41.1 months. There was no significant difference in FU time between the R and NR groups. All cases in the R group had a SNV in at least one gene and a higher mutation load among the queried genes (median = 3.5 mutations/case) compared to the NR group (median = 2.0 mutations/case, p = 0.56). Unexpectedly several genes with SNVs in the R group (APC, ERBB2, ERBB4, JAK3, KDR, KIT, PTEN, SMARCB1, and STK11) were not present in the NR cases. None of these unique SNVs has been reported in genitourinary tumors and thus may represent general hypermutability rather than oncogenic driver mutations. Interestingly, SNVs in the FGFR3 gene, which is commonly mutated in LGUC, were present in 86% (6/7) of the NR cases compared to 17% (1/6) of the R cases, (p = 0.029, Fisher's exact test). The FGFR3 SNV found in the single R case, a C>T transversion (minor allelic frequency = 22%) leading to an amino acid change of R248C, has been reported in a case of bladder and also in lung carcinoma. However, this amino acid is located between two immunoglobulin domains, making the biological significance questionable.

Conclusions: The present study shows that recurrent (R) cases of LGUC have several unexpected mutations not found in cases that do not recur (NR). Furthermore, the NR cases more frequently have mutations in FGFR3. Further studies are required to determine the biologic and functional significance of these genomic changes.

1043 In Situ expression Profiling of microRNA in Different Grades of Prostate Cancer

Suresh Thakur, Krishan Kalra. BioGenex, Fremont, CA.

Background: Prostate cancer (P Ca) is the most frequently diagnosed form of male cancer in the USA. Prostate cancer can be managed successfully if diagnosed at an early stage, however due to non-specific symptoms and slow progression, diagnosis is often missed. microRNAs (miRNAs) are small non-coding RNA molecules that have tissue-specific and cancer-specific expression patterns. In this study we have attempted a miRNA expression profile in the different grades of P Ca, including benign prostatic hyperplasia (BPH).

Design: A total of 166 FFPE cases of different grades of prostate cancer and BPH were used in this study [table 1]The miRNA expression profile was carried out by *in situ* hybridization (ISH). miRNA probes and detection system (DF400-50KE) available from BioGenex were used. Stained slides were scored as negative (N), weak (W), moderate (M) and strong (S).

Results: miR-17 was up-regulated in 50% (13/26) cases of high grade prostate cancer (P Ca IV) but did not show any significant expression pattern in P Ca II and P Ca III. miR-125b was up-regulated in 77% (20/26) and 72% (21/29) of the cases of P Ca IV and P Ca III, respectively, in comparison to paired normal lung tissue. miR-205 was significantly up-regulated in 90% (18/20) of the cases of BPH (BPH not shown in table 1). miR-144 (not shown here) did not show any sigficant expression pattern.

	miR-17					
Pattern	P Normal (n=18)	P Ca II (n=18)	P Normal (n=29)	P Ca III (n=29)	P Normal (n=26)	P Ca IV (n=26)
N	6	3	10	4	10	2
W	2	1	4	1	4	0
M	8	7	13	14	10	11
S	2	7	2	10	2	13
	miR-125b					
N	3	1	1	0	1	0
W	5	3	17	5	14	2
M	6	3	3	3	6	4
S	4	11	8	21	5	20
	miR-205					
N	2	0	0	0	0	0
W	3	2	13	3	14	4
M	2	0	2	0	0	0
S	11	16	14	26	12	22

Conclusions: *In situ* visualization of miRNA provides a benefit of localization of miRNA inside a tumor cell. Differential expression of miR-17 and miR-125b in high grade P Ca and miR-205 in BPH needs to be verified in larger sample cohort and should also be evaluated in collaboration with treatment response.

1044 Invasive Low-Grade Urothelial Carcinoma: Immunohistochemical Studies of 26 Cases

Wei Tian, Jonathan Epstein. Johns Hopkins Hospital, Baltimore, MD.

Background: Invasive low-grade papillary urothelial carcinoma (Inv LGUC) is a rare diagnostic entity in routine pathology practice. This is the largest series to study the immunohistochemical characteristics.

Design: We identified 66 cases of Inv LGUC at our institution (1998-2013) (nested and large nested urothelial carcinoma were excluded), of which 26 cases had tissue available for immunohistochemical (IHC) studies (21 were consults). P53 and CK20 were scored as follows: 0, negative; 1, weak and patchy (10-<50%); 2, moderate and patchy (<50%), or weak and diffuse (>50%); and 3, moderate or strong and diffuse (>50%). For p53, we required score 2 and above to be considered positive. Only moderate to strong Ki67 nuclear stains were counted as positive.

Results: The median age was 65(45-92), 23 males and 3 females. 2 cases had muscularis propria (MP) invasion and 24 had lamina propria invasion, 2 of which had uncertain MP invasion. 2 cases were nephrectomy involving renal pelvis, 1 cystoprostatectomy, and the rest were TURBs. CK20 expression was present in 22 cases (85%), of which 16 (61%) scored 2 and 3. Comparing CK20 expression in noninvasive vs invasive component: unchanged (n=14), decreased (n=7), slightly increased (n=1). For p53 labeling, positive (n=15, score 2-3 with score 3, n=5; score 2, n=9), negative (n=11, score 0-1). Comparing p53 expression in noninvasive versus invasive component: unchanged (n=24), significantly increased (n=2, score 0 to 3). There was a wide range of Ki67 labeling from <5% to 70%. Ki67 <=5% (n=11), 6-30% (n=8), 31-70% (n=7). 2 showed increased (from <5% in the noninvasive to 20% and 40% respectively in the invasive component); 2 showed decrease (20 to 10%, 50 to 30% respectively). All cases had intact PTEN except one showed focal clonal PTEN loss in both noninvasive and adjacent invasive component. All cases had preserved strong and diffuse E-cadherin expression in both noninvasive and invasive component.

Conclusions: 7/22 (31%) showed decreased CK20 expression in the invasive component of low grade urothelial carcinoma. p53, PTEN, E-cadherin, and Ki67 proliferation index showed no significant change in the noninvasive versus invasive component. High Ki67 labeling was present in a significant portion of Inv LGUC cases in both noninvasive and invasive component, much higher than previous studies of noninvasive LGUC. IHC is not helpful in general in identifying invasion in LGUC. Whether higher ki67 in these cases is associated with more aggressive disease warrants further study.

1045 Utility of Uroplakin II Expression as a Marker of Urothelial Carcinoma

Wei Tian, Gunes Guner, Hiroshi Miyamoto, Ashley Cimino-Mathews, Nilda Gonzalez-Roibon, Pedram Argani, Xuan Li, Rajni Sharma, Andrea Subhawong, Katayoon Rezaei, Trinity Bivalacqua, Jonathan Epstein, Justin Bishop, George Netto. Johns Hopkins Hospital, Baltimore, MD; George Washington University, Washington, DC.

Background: Uroplakins are markers of terminally differentiated urothelium. Uroplakin II (UPII) is newly described sensitive marker for urothelial carcinoma (UC). The expression profile of UPII in different types of urothelial carcinoma and its utility in diagnostic setting is needed.

Design: We evaluated UPII expression in bladder tissue microarrays, including urothelial neoplasm of low malignant potential (LMP, n=8), low-grade papillary urothelial carcinoma (LGUC, n=72),noninvasive high-grade papillary urothelial carcinoma (HGUC, n=77), urothelial carcinoma in situ (CIS, n=27), and invasive high-grade urothelial carcinoma (INVUC, n=122). UPII expression in 52 breast carcinomas and 38 high-grade prostate adenocarcinomas was also assessed. UPII expression was compared to GATA binding protein 3 (GATA3) and estrogen receptor (ER) in regards to its role in facilitating the differential diagnosis of the above three types of malignancy.

Results: UPII labeling was seen in 83.0% of UC overall, including 95.7% of noninvasive UC and 65.6% of INVUC. UPII labeling was not found in any breast and prostate carcinomas. In comparison, GATA3 labeling was seen in 91.6% of all UCs, including 96.4% of noninvasive UCs and 85.1% of INVUC, with stronger intensity and extent compared to UPII($p<0.005$). GATA3 labeled 2 of 38 (5%) high-grade prostate adenocarcinoma. ER nuclear labeling was seen in 13.0% of UCs and 12.5% of prostate carcinomas.

Conclusions: UPII demonstrated moderate sensitivity but 100% specificity for UC, and can potentially be a useful marker to identify urothelial differentiation in metastatic sites and to distinguish UC from prostate cancer or, in conjunction with GATA3, metastatic breast cancer.

1046 Correcting the Shrinkage Effects of Formalin Fixation and Tissue Processing for Renal Tumors and Its Implications for Pathologic Staging: Toward Standardization of Pathological Reporting of Tumor Size

Thu Tran, Chandru Sundaram, Clinton Bahler, John Eble, David Grignon, Maria Monn, Novae Simper, Liang Cheng. Indiana University, Indianapolis, IN.

Background: The current tumor, nodes, and metastasis (TNM) staging of renal cell carcinomas is based on tumor size, with T1a tumors being 4 cm or less in greatest dimension and T1b between 4 and 7 cm. Larger renal cell carcinomas included in the T1b category are known to have decreased 5-year survival rates. Given the importance of correctly staging renal cell carcinomas, specific guidelines should be in place for tumor measurement. We sought to assess the accuracy of postfixation and microscopic measurements of renal tumor size, as compared to fresh measurements.

Design: From the period of October 2013 to August 2014, 25 nephrectomy cases performed by a single surgeon were prospectively measured at different time points. At the end of surgery, the fresh specimen was sectioned and measurements of the tumor's three dimensions were taken. After formalin fixation, another set of measurements were recorded. A whole mount slide was prepared from the most representative cross-section, and two-dimensional tumor size was measured. In addition, computerized tomography and magnetic resonance images were retrospectively reviewed, and three dimensional tumor measurements were recorded.
Results: The renal cases included 15 clear cell renal cell carcinomas, 6 papillary renal cell carcinomas, 1 chromophobe renal cell carcinoma, 1 translocation-associated renal cell carcinoma, and 2 oncocytomas. Radiologic tumors were 10.0% larger in diameter than fresh tumors (P<0.001). Furthermore, fresh specimens were 5.2% larger than formalin fixed specimens (P<0.001), and postfixation measurements were 6.3% greater than microscopic measurements (P<0.001). The overall mean percent shrinkage between fresh and histological specimens was 11.2% (P<0.001). Histological processing would cause a tumor stage shift from pT1b to pT1a for one tumor.
Conclusions: While a standard means of renal tumor measurement has not been established, intuitively, tumor size should be based on fresh measurements. The shrinkage effects of formalin fixation and histological processing may result in understaging of renal cell carcinomas. Reporting of tumor size should consider the shrinking factor.

1047 Ki67 Prognostic Value: Multi-Institutional Case-Control Study of >1,000 Prostatectomies

Maria Tretiakova, Hilary Boyer, Wei Wei, Lisa Newcomb, Funda Vakar-Lopez, Ziding Feng, James Brooks, Canary Prostate Investigators. University of Washington, Seattle, WA.
Background: The Canary Foundation Retrospective Prostate Tissue Microarray (TMA) Resource contains tissue samples from over 1,000 participants treated for prostate cancer (PC) by radical prostatectomy at 6 US and Canadian hospitals between 1994-2005. These 33 TMAs were designed to balance recurrence (case) and non-recurrence (control) cases across all Gleason scores (GS) allowing identification of prognostic markers independent of GS. Our goal was to correlate Ki-67 expression in these TMAs with clinico-pathologic features and to validate its utility in predicting cancer-specific outcome.
Design: TMA slides were immunostained for Ki67, scanned as digital image files. The Ki67 proliferation index (PI) of tumor areas of each core was analyzed using nuclear quantification algorithm (Aperio). Ki67-PI was statistically correlated with recurrence free survival (RFS) including biochemical, clinical, radiological, metastasis or PC death (7 y median follow-up).
Results: In 1004 PCs (~4,000 tissue cores) Ki67-PI showed significantly higher inter-tumor (0.68) than intra-tumor variation (0.39). Significant associations were found between Ki67-PI and stage (p<.0001), seminal vesicle invasion (SVI, p=0.02), extraprostatic extension (EPE) and GS (p<.0001), but not with margin status (p=0.21) or pre-op PSA (p=0.36). Since no obvious cut-off point for Ki67-PI was detected on Martingale residual plot, a continuous variable was fitted in the survival models in addition to dichotomized classes by median average (PI=2.19) and maximum Ki67 positivity per case (PI=3.11). By both univariate and multivariate logistic regression analyses Ki67 significantly correlated with 5-year RFS status as continuous outcome and in dichotomized classes. A univariate weighted Cox proportional hazard model revealed significant Ki67-PI correlation with RFS both as continuous outcome and dichotomized by median class; maximum Ki67-PI was associated with RFS only as continuous outcome. Higher weighted average or maximum Ki67-PI (HR=1.12-2.78) significantly correlated with worse RFS after adjusting for other clinical factors (margin, SVI, GS, pre-op PSA) in multivariate Cox proportional hazard models (p=0.01-0.0001).
Conclusions: Higher Ki67-PI is strongly associated with a higher GS and stage, SVI and EPE, and a greater probability of 5-year recurrence, confirming its independent prognostic value. We also found substantial intra- and inter-tumoral heterogeneity of Ki67 expression, and lack of a suitable cut-off point, thus discouraging routine clinical use. Therefore, we advocate for pre- and post-analytic standardization of Ki67 analysis of PCs.

1048 IHC Screening of Unclassified RCC Detects Tumors Associated With HLRCC

Kiril Trpkov, Ondrej Hes, Abbas Agaimy, Petr Martinek, Cristina Magi-Galluzzi, Fadi Brimo, Glen Kristiansen, Gabriella Nesi, Eva Comperat, Mathilde Sibony, Rohit Mehra, Michael Bonert, Daniel Berney, Kirsten Hills, Fiona Maclean, Norma Frizzell, Anthony Gill. Calgary Laboratory Services, Calgary, Canada; Charles University, Plzen, Czech Republic; McGill University, Montreal, Canada; Cleveland Clinic, Cleveland, OH; University of Bonn, Bonn, Germany; Carregi Hospital, Florence, Italy; Pitié-Salpêtrière Hospital, Paris, France; Pathology Institute, Erlangen, Germany; University of Michigan, IL; Sydney, Australia; Bart's Cancer Institute, London, United Kingdom; University of Southern California School of Medicine, Columbia, SC.
Background: RCC associated with HLRCC syndrome are rare and difficult to diagnose. Two recent studies used IHC, either positive S-(2-succino)-cystein (2SC+) or negative fumarate hydratase (FH-), to screen for such tumors, but a combined approach has not been done.
Design: RCC labelled "unclassified, high grade" or "unclassified with papillary pattern", with at least focal prominent nucleoli, were retrieved from multiple institutional archives. In 112 cases, IHC for FH and 2SC was done on a whole slide. We also evaluated 3 TMA with 776 RCC (with 381 papillary RCC). Clinicopathologic data and follow-up were collected in **positive** cases (FH-, 2SC+) and molecular test for FH alterations was performed on the available tissue.
Results: Positive result (FH-, 2SC+) was found in 16% (18/112) cases evaluated on whole slide; 6 were confirmed by molecular test. 25% (28/112) cases were **equivocal** (FH+, 2SC+ or +/-) and 59% (66/112) were **negative** (FH+, 2SC-). No FH alteration was detected in all 19 cases tested in the **equivocal** and **negative** group. On TMA, **positive result** (FH-, 2SC+) was found in 0.5% (2/381) papillary RCC. All other tumorson TMA were **negative** (FH+, 2SC-): clear cell RCC (232), ChRCC (21), oncocytoma (25), other RCC (39), and urothelial carcinoma (78). In the 20 **positive** cases (FH-, 2SC+), detected on whole slide and TMA, the mean age was 43y (range 21-65), with M:F ratio 2.3:1. Mean tumor size was 9cm (range 1-18); 61% patients had stage ^{3}pT3 and 50% had positive nodes at surgery. In 90% (18/20) **positive** cases, mixed histologic patterns were found, most commonly: papillary 70% (14), solid 45% (9), tubular 35% (7) and tubulocystic 30% (6). Lack of foam cells and hyalinized stalks were frequent in cases with papillary pattern. On follow-up (mean 26 mo, range 1-114), 45% (9) patients were dead of disease and 20% (4) had disease progression.
Conclusions: Negative FH on IHC strongly correlates with FH gene alterations, morphology compatible with HLRCC, and aggressive behavior. It can be used to identify cases for genetic testing. Given the lower specificity of 2SC and difficulty in interpretation, negative FH appears to be a more specific and equally sensitive test.

1049 Solid and Cystic Eosinophilic Renal Cell Carcinoma With Frequent Cytokeratin 20 Reactivity: Clinicopathologic Study of 13 Unique Tumors Occurring in Women

Kiril Trpkov, Ondrej Hes, Stephen Bonsib, Gabriella Nesi, Eva Comperat, Mathilde Sibony, Jose Lopez, Daniel Berney, Jesse McKenney. Calgary Laboratory Services, Calgary, Canada; Charles University, Plzen, Czech Republic; Nephropath, Little Rock, AR; Carregi Hospital, Florence, Italy; Pitié-Salpêtrière Hospital, Paris, France; Hopital Cochin, Paris, France; Cruces University Hospital, Barakaldo, Spain; Bart's Cancer Center, London, United Kingdom; Cleveland Clinic, Cleveland, OH.
Background: Recent studies report a unique renal tumor with solid and cystic eosinophilic morphology, found in female patients with Tuberosus Sclerosis Complex (TSC). To date, similar renal tumors have not been documented in patients without TSC.
Design: Renal tumors labelled "unclassifed, oncocytic/eosinophilic" were searched in multiple institutional archives. All cases were reviewed by two GU pathologists, comparing the features with index cases. Clinicopathologic and follow-up data were collected and immunochemistry was performed for: CK7, CK20, PAX-8, C-kit, AMACR, Pan-CK, CD10, CA9, Vimentin, Hamartin and Tuberin.
Results: A total of 13 cases were identified, all in females without clinical features of TSC. Median age was 56 y (range 44-74). Grossly, all tumors were yellow-gray and had solid and cystic (10) or only solid appearance (3). Median tumor size was 44 mm (range 15-135). Kidney side: 7 right, 6 left. On microscopy, all tumors showed variably sized solid areas, composed of tightly packed acini. The cells had voluminous eosinophilic cytoplasm and often showed basophilic stippling. Solid areas were admixed with variable size cysts, lined by cells often showing hobnail features. Cells had round to oval nuclei with prominent nucleoli (ISUP nucleolar grade 3). Scattered multinucleated cells were common and collections of foam cells and lymphocytes were invariably present. Stage pT1 (1a in 7, 1b in 4) was found in 11 patients; 1 patient each had pT2 and pT3a. Immunochemistry findings were: CK20 positive (11/13), CK7 positive (3/13), PAX-8 positive (11/11), Pan-CK positive (11/11), CD10 positive (7/10), C-kit positive (1/10), AMACR positive (3/12), CA9 positive (2/9) and Vimentin positive (8/11). Tuberin was retained (10/10), while Hamartin was lost in all tested cases (10/10). Follow-up was available for 11 patients (median 32 mo, range 1-130); 10 patients were alive without evidence of disease (1 died of other causes).
Conclusions: Solid and cystic eosinophilic RCC is a distinct renal tumor found in females, that shows typical morphology, frequent CK20 reactivity, and indolent behaviour. These tumors are similar to a subset seen in TSC patients, but in this study, they were found in a sporadic setting.

1050 Relationship of Pathological Factors To Efficacy of Sorafenib Treatment in Patients With Metastatic Clear Cell Renal Cell Carcinoma

Toyonori Tsuzuki, Hidemori Araki, Tohru Kimura, Kuniaki Tanaka, Shin Yamada, Naoto Sassa, Yasushi Yoshino, Ryohei Hattori, Momokazu Gotoh. Japanese Red Cross Nagoya Daini Hospital, Nagoya, Japan; Toyohashi Municipal Hospital, Toyohashi, Japan; Shakaihoken Chukyo Hospital, Nagoya, Japan; Kariya Toyota General Hospital, Kariya, Japan; Okazaki Municipal Hospital, Okazaki, Japan; Nagoya University Graduate School of Medicine, Nagoya, Japan; Japanese Red Cross Nagoya Daiichi Hospital, Nagoya, Japan.
Background: We have demonstrated that growth pattern, a pathological parameter, is an independently predictive of the outcomes of patients clear cell renal cell carcinoma (CCRCC). We aimed to evaluate the predictive value of growth patterns in patients undergoing sorafenib treatment for metastatic CCRCCs.
Design: 48 patients were analyzed, each of whom underwent nephrectomy and received sorafenib treatment for metastatic CCRCC. Progression-free survival (PFS) was predicted using pathological parameters, including pathological stage, Fuhrman nuclear grade (FNG), the presence of a sarcomatoid component, lymphovascular invasion, tumor necrosis, and growth pattern. Expansive pattern was defined as a well-circumscribed tumor margin without the presence of normal renal tissue in the tumor, and infiltrating pattern was defined as an ill-circumscribed tumor margin with cancer cells that were extensively infiltrating normal renal tissues.

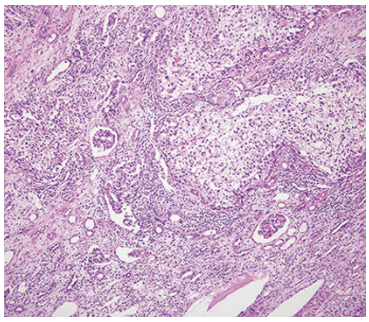

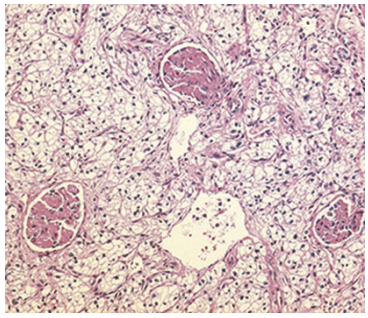

Results: Three patients showed partial response (6%), 20 patients showed stable disease (42%), and 25 patients showed progressive disease (52%). nivariate analyses demonstrated that FNG (p=0.001), the presence of a sarcomatoid component (p=0.011), tumor necrosis (p=0.005), and growth pattern (p=0.005) were significantly associated with PFS. In the multivariate analysis, growth pattern was the only parameter that was significantly and independently predictive of PFS (p=0.019).
Conclusions: As a novel histological prognostic parameter, growth pattern may be useful for predicting response to sorafenib treatment.

1051 The Presence of Intraductal Carcinoma of the Prostate in Needle Biopsy Is a Significant Prognostic Parameter for Prostate Cancer Patients With Distant Metastasis

Toyonori Tsuzuki, Masashi Katoh, Kyosuke Kimura, Ryo Ishida, Naoto Sassa, Yasushi Yoshino, Ryohei Hattori, Momokazu Gotoh. Japanese Red Cross Nagoya Daini Hospital, Nagoya, Japan; Nagoya University Hospital, Nagoya, Japan; Nagoya Medical Center, Nagoya, Japan; Japanese Red Cross Nagoya Daiichi Hospital, Nagoya, Japan.
Background: The presence of intraductal carcinoma of the prostate (IDC-P) is an adverse prognostic factor for prostate-specific antigen (PSA) failure, progression-free survival, and cancer-specific survival (CSS) in localized prostate cancer patients. However, there is no data indicating whether the presence of IDC-P can influence patient outcome in prostate cancer patients with distant metastasis at presentation. We aimed to evaluate whether IDC-P in needle biopsies is also an adverse prognostic parameter for CSS in prostate cancer patients with distant metastasis.
Design: We retrospectively evaluated 159 prostate cancer patients with distant metastasis who presented at the hospitals that the authors are affiliated with between 2002 and 2012 and reviewed the slides prepared from prostate needle biopsy specimens. Data on the patients' age, performance status, clinical T stage, serum PSA, C-reactive protein, alkaline phosphatase (ALP), hemoglobin (Hb), albumin, serum calcium, biopsy Gleason score (> 8 or not), the presence of Gleason pattern 5, the percent of the core involved with cancer, and the maximum percent of a core involved with cancer were analyzed. The patient characteristics were analyzed using the Fisher's exact test. Multivariate Cox proportional hazard regression models were developed to predict CSS.
Results: The median age of the patients was 73 years (range 47–90 years). The median serum PSA was 290 ng/mL (range 4.18–10,992 ng/mL). The median follow-up period was 36 months (range 3–120 months). IDC-P component was detected in 103 (64.8%) patients. There were 82 patients who died of the disease and 6 patients who died of other causes. Using univariate analysis, IDC-P (p = 0.0001), the presence of Gleason pattern 5 (p = 0.005), the percent of the core involved with cancer (p = 0.002), Hb (p = 0.001), and high ALP (p = 0.002) were all shown to be significantly associated with CSS. In the multivariate analysis, only IDC-P (p = 0.016; hazard ratio, 2.187) was significantly associated with CSS.
Conclusions: The presence of IDC-P in needle biopsy is a prognostic parameter for CSS in patients with distant metastasis at the presentation.

1052 Correlation Between Transperineal Mapping Template Prostate Biopsy and Radical Prostatectomy in 53 Patients at a Large Academic Institution

Aaron Udager, Angela Wu, John Wei, Todd Morgan, Ganesh Palapattu, Lakshmi Kunju. University of Michigan Health System, Ann Arbor, MI.
Background: Transperineal mapping template prostate biopsy (TMPB) allows for systematic sampling, detection, and mapping of prostate cancer (PCa) and may be helpful during selection of patients for active surveillance or for patients with previous negative transrectal biopsies. The clinicopathologic aspects of radical prostatectomy (RP) specimens in patients after TMPB have not been extensively characterized. In this study, we correlated TMPB results with mapped PCa foci in a large cohort of RP specimens.
Design: A prospectively maintained database at a single large academic institution identified patients who underwent TMPB and subsequent RP between 1/2007 and 8/2014. TMPB was performed through the perineum using a brachytherapy grid to sample the prostate gland. RP specimens were reviewed, and all PCa foci were mapped, measured, and assigned a Gleason score (GS). The location of the index nodule (defined as the largest nodule) and all multifocal tumor foci were recorded in octants (i.e., right anterior proximal, left posterior distal, etc.). Anterior-predominant tumors, defined as index nodules located predominantly anterior to the midpoint of the urethra, were identified. TMPB results were compared to RP maps to determine the sensitivity for detection and localization of tumor foci.
Results: Of the 235 patients who underwent TMPB, 61 subsequently underwent RP, of which 53 patients (median age = 65 years, median pre-biopsy serum PSA = 7.3 ng/dL) had all RP tissue available for review. PCa was bilateral in 33 (62%) and 44 (83%) TMPB and RP specimens, respectively. Highest TMPB GS was ≥7 in 47 (89%) cases, and the index nodule GS was ≥7 in 49 (92%) cases. PCa was multifocal and anterior-predominant in 46 (87%) and 32 (60%) RP specimens, respectively. The index nodule was identified by TMPB in 52 (98%) cases; median index nodule size was 1.7 cm (range = 0.3-3.4 cm). All index nodules 0.4 cm or larger were detected by TMPB; one case of multifocal PCa with a 0.3 cm anterior-based index nodule (GS 6) was not detected by TMPB.
Conclusions: TMPB has very high sensitivity (98%) for the detection and localization of index nodules. Anterior-predominant tumors comprise a majority (60%) of the RP specimens in this cohort. All index nodules 0.4 cm or larger were detected by TMPB.

1053 Nuclear ERG and MYC Protein Overexpression Is Positively Correlated in Prostate Cancer

Aaron Udager, Yang Shi, Hui Jiang, Saravana Dhanasekaran, Arul Chinnaiyan, Rohit Mehra. University of Michigan Health System, Ann Arbor, MI.
Background: *TMPRSS2-ERG*, the most common recurrent gene fusion in prostate cancer, results in overexpression of the nuclear transcription factor ERG, which can be detected with high sensitivity and specificity by IHC in clinically localized prostate cancer (PCa). The nuclear transcription factor MYC may play a role in tumor initiation and progression in prostate cancer. MYC protein is overexpressed in the majority of HGPIN and PCa, however, the relationship between ERG and MYC protein overexpression in PCa is poorly understood.
Design: Tissue microarrays (TMA) comprised of benign prostatic glands (BPG; n = 77), HGPIN (n = 12), and PCa (n = 150) from radical prostatectomy specimens were examined for ERG and MYC protein overexpression by IHC using primary antibodies against ERG (Ventana Medical Systems, EPR3864; Tucson, AZ, USA) and MYC (Epitomics, clone Y69; Burlingame, CA, USA). For each evaluable core, IHC was scored semi-quantitatively based on nuclear staining intensity (0-3; i.e., negative, weak, moderate, or strong) and percentage of positive tumor cells (0-100), and an IHC product score was calculated (range = 0-300).
Results: MYC protein expression was significantly increased in HPGIN and PCa (mean IHC product score = 47.5 and 54.9, respectively), compared to BPG (mean IHC product score = 17.9; $P < 0.05$). ERG protein expression was similarly increased in PCa (median IHC product score = 95.4), compared to BPG (mean IHC product score = 0; $P < 0.05$). ERG and MYC protein overexpression demonstrated moderate positive correlation in PCa (Pearson correlation coefficient = 0.219; $P < 0.05$), however, there was no significant association between ERG or MYC protein overexpression and time to biochemical recurrence after radical prostatectomy (as determined by serum PSA levels) in this cohort.
Conclusions: Nuclear ERG and MYC protein overexpression is positively correlated in PCa. Despite a lack of prognostic significance for nuclear ERG or MYC protein overexpression in our cohort, our data suggest that ERG and MYC may have synergistic roles in PCa initiation and/or progression.

1054 Spectrum of RCC in Patients 30 Years of Age and Younger: A 28-Year Retrospective Experience at a Single Tertiary Clinical Institution With Updated RCC Classification

Aaron Udager, Hong Xiao, Lina Shao, Ganesh Palapattu, Jeffrey Montgomery, Todd Morgan, Javed Siddiqui, Xuhong Cao, David Miller, Alon Weizer, J Stuart Wolf, Khaled Hafez, Arul Chinnaiyan, Diane Roulston, Rohit Mehra. University of Michigan Health System, Ann Arbor, MI.
Background: Renal cell carcinoma (RCC) is the most common renal malignancy in adults, and clear cell RCC (CCRCC) is the predominant subtype in older patients. Recent molecular studies have expanded the spectrum of RCC subtypes to include syndrome-associated tumors (i.e., VHL, HLRCC, TSC, SDH deficiency, etc.), as well as sporadic tumors with recurrent genetic abnormalities [i.e., *TFE3* and *TFEB* translocation-associated RCC (t-RCC)]. To explore the spectrum of RCC subtypes in children and younger adults, we sought to retrospectively evaluate a large cohort of RCC in patients 30 years of age and younger.
Design: A retrospective search of the pathology records database of a single large tertiary clinical institution identified all in-house cases of RCC in patients 30 years of age and younger between January 1986 and December 2013. Available cases were re-reviewed in light of current WHO diagnostic criteria for renal tumors, and additional clinicopathologic information was obtained from the electronic medical record.
Results: 55 specimens from 51 unique patients were available for review, including: CCRCC (n = 43); TSC-associated RCC (n = 4); type I papillary RCC (n = 3); chromophobe RCC (n = 3); type II papillary RCC (n = 1); confirmed *TFE3* t-RCC (n = 1); confirmed *TFEB* t-RCC (n = 1); medullary RCC (n = 1); an RCC occurring in an HLRCC patient (n = 1); and, RCC which could not be further classified upon initial screening (n = 13). Of these unclassifiable RCC, 9 (69%) were morphologically suspicious for t-RCC, including 2 from patients with a history of prior chemotherapy;

an additional 2 tumors were morphologically suspicious for SDH-deficient RCC. 11 specimens from 9 unique VHL patients had at least 26 distinct tumors, all of which were CCRCC. There were 4 tumors from 3 unique TSC patients, including 1 with renal angiomyoadenomatous tumor (RAT)-like morphology and 3 with granular eosinophilic-macrocystic morphology.

Conclusions: In patients 30 years of age and younger, there is a diverse spectrum of RCC subtypes, including syndrome-associated RCC (i.e., VHL, TSC); this patient population also frequently includes candidates for *TFE3* and *TFEB* t-RCC. FISH for *TFE3* and *TFEB* aberrations and additional IHC studies are currently underway to characterize tumors which were morphologically suspicious for t-RCC.

1055 TERT Promoter Mutations in Urinary Bladder Glandular Lesions

Eric Vail, Esther Yoon, Jian Zhuge, Ximing Yang, Ming Zhou, John Fallon, Minghao Zhong. New York Medical College at Westchester Medical Center, Valhalla, NY; Northwestern University, Feinberg School of Medicine, Chicago, IL; New York University School of Medicine, New York, NY.

Background: Glandular lesions of the urinary bladder include a broad spectrum of entities ranging from completely benign to primary and secondary malignancies. The accurate diagnosis of these lesions is important yet challenging. Recent studies suggest that TERT promoter mutations is a biomarker for urothelial carcinoma (UC). We hypothesized that these mutations can distinguish UC with glandular differentiation from nephrogenic adenoma, primary adenocarcinoma of the urinary bladder (PAUB) or secondary malignancies.

Design: 20 Cases of UC with glandular differentiation, 10 cases of primary adenocarcinoma of the urinary bladder, 5 cases of nephrogenic adenoma and 10 cases of metastatic colon cancer, prostatic carcinoma and carcinoma from Müllerian origin were collected. Slides were reviewed and selected to make sure the lesion was at least 20% of all tissue. Macro-dissection was performed in some of cases and gDNA was extracted from the tissue. TERT promoter mutations were determined by standard PCR-sequencing.

Results: Glandular component of UC with glandular differentiation was 5-50% of whole tumor mass in our specimens. Main tumors were predominantly located in bladder (with few from kidney and ureter). Other divergent components were squamous, sarcomatoid differentiation and small cell carcinoma. 15 cases (75%) of UC with glandular differentiation including the glandular component were positive for TERT promoter mutations. However, none of the remaining cases (total 45 cases of nephrogenic adenoma, primary adenocarcinoma of the urinary bladder, metastatic colon cancer, prostatic carcinoma and carcinoma from Müllerian origin) were positive for TERT promoter mutation.

Conclusions: TERT promoter mutations were strongly associated with UC with glandular differentiation, but not other glandular lesions of bladder. Therefore, In conjunction with morphological features and clinical information, TERT promoter mutations could distinguish UC with glandular differentiation from other bladder glandular lesion. Lack of TERT promoter mutations in primary adenocarcinoma of bladder suggests that this entity may have different origin or carcinogenesis from urothelial carcinoma.

1056 Gene Expression Analysis of Normal Urinary Bladder: Does the Muscularis Propria Differ From the Muscularis Mucosa?

Funda Vakar-Lopez, Dapei Li, Ilsa Coleman, Peter Nelson, Lawrence True. University of Washington, Seattle, WA; Fred Hutchinson Cancer Research Center, Seattle, WA.

Background: The anatomical layers of urinary bladder, i.e. urothelium (U), lamina propria (LP), muscularis mucosa (MM), submucosa (SM) and muscularis propria (MP) are landmarks for staging bladder cancer. Distinguishing muscularis mucosa from muscularis propria differentiates superficially invasive carcinoma (pT1) from more deeply cancer (pT2). Although often readily distinguished, distinction can be problematic in TUR specimens due to uncertain orientation, cautery effect and/or prominent stromal/inflammatory cell reactions. Layer-specific immunohistochemical stains (IHC) could resolve such cases. Smoothelin, a putative marker for MP, does not reliably distinguish these muscle layers. Transcript profiles specific for the bladder layers could identifiy IHC markers to more accurately stage invasive bladder carcinoma.

Design: Fresh tissue obtained from the bladders of 8 patients who underwent cystectomy for non-urothelial lesions were macrodissected by layer and frozen. Layer-specific cells were laser microdissected. Amplified RNA from these cells was hybridized onto Agilent 44K whole human genome expression oligonucleotide microarrays. Only genes highly expressed in one layer, but not the other, were selected for analysis.

Results: Transcript profiles of the most differentially expressed genes distinguish the five layers of the bladder. Candidate genes for IHC, by layer, are LP-sparc, MM-collagen, type X, SM-vitrin, MP-FBX032.

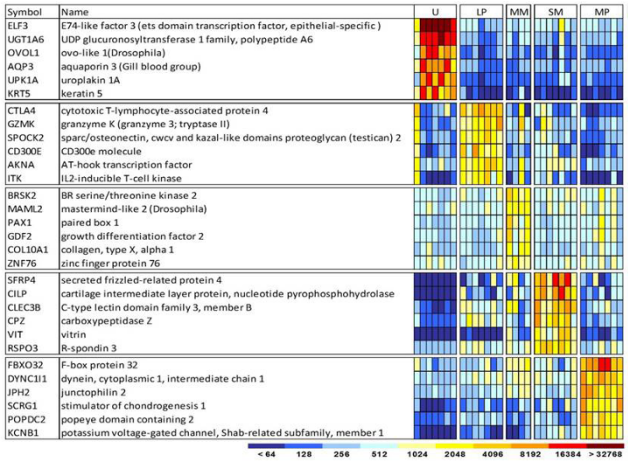

Rank ordering transcripts only from the MP and MM reveal specific gene products that can distinguish these layers of muscle, i.e. MM - HHIP, IGF2; MP - SCRG1, POPDC2.

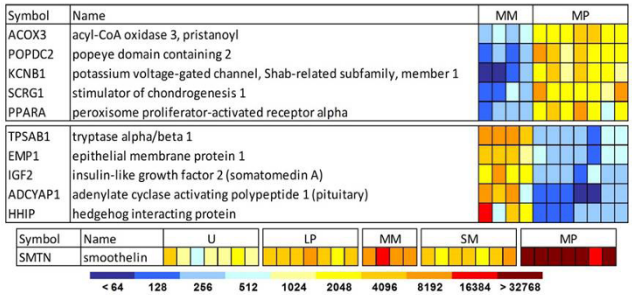

Conclusions: Distinct transcript profiles potentially provide both muscle layer-specific IHC markers and markers for the 4 stromal layers - LP, MM, SM and MP. Substaging superficially invasive carcinoma (pT1) based on 3 compartments - LP, MM, SM - might further guide therapy.

1057 Epigenetic Alterations in Prostate Carcinoma Glands With Cribriform Architecture or Intraductal Carcinoma

Theodorus Van der Kwast, Ekaterina Olkhov, Farshid Siadat, Dominique Trudel, Bharati Bapat. University Health Network, Toronto, ON, Canada; Centre Hospitalier de l'Université de Montréal, Montreal, QC, Canada; Samuel Lunenfeld Research Institute, Toronto, ON, Canada.

Background: Gleason grade 4 prostate cancer comprises several distinct morphological patterns, including those with cribriform architecture, and may be associated with intraductal carcinoma (IDC). Cribriform architecture and IDC are thought to represent independent unfavourable prognostic markers for metastatic disease. We previously demonstrated that DNA-methylation of CpG islands in promoter regions of *APC* and *HOXD3* may be associated with prostate cancer aggressiveness.

Design: We compared DNA methylation levels of *APC* and *HOXD3* in Gleason grade 4 carcinoma glands with and without small and large cribriform architecture / IDC in a series of 91 prostatectomy specimens with a Gleason score 7 prostate cancer, using the semi-quantitative MethyLight assay on bisulphite-treated DNA extracted from paraffin blocks. Association between percentage of methylation reference (PMR) values and architectural pattern / IDC was analyzed using the Mann-Whitney U-test.

Results: Presence of any amount of cribriform architecture / IDC within Gleason grade 4 carcinoma areas was associated with elevated median PMR values for *APC* (p=0.045), but not for *HOXD3*. Stratification of cribriform architecture revealed median PMR in large cribriform versus no cribriform of 66% versus 39%, p=0.008 and in small cribriform versus no cribriform of 49% versus 33%, p=0.033). *APC* methylation levels did show a stepwise increase with percentage of carcinoma involvement by cribriform architecture / IDC.

Conclusions: The findings suggest for the first time that among the various morphological Gleason grade 4 patterns, those with cribriform architecture / IDC have a unique epigenetic profile which may be explored further for clinical use. The mere presence of cribriform architecture or IDC seems to be sufficient to promote the observed increase in APC methylation and would be in line with an epigenetic cancer field alteration.

1058 Intraductal Carcinoma of Prostate (IDCP) Reporting Practice: A Survey of Expert European Uropathologists

Murali Varma, Lars Egevad, Ferran Algaba, Daniel Berney, Lukas Bubendorf, Philippe Camparo, Eva Comperat, Andreas Erbersdobler, David Griffiths, Rainer Grobholz, Andrea Haitel, Christina Hulsbergen-VandeKaa, Cord Langner, Barbara Loftus, Antonio Lopez-Beltran, Nick Mayer, Gabriella Nesi, Pedro Oliveira, Jon Oxley, Nathalie Rioux-Leclercq, Gerhard Seitz, Jonathan Shanks, Glen Kristiansen. University Hospital Wales, Cardiff, United Kingdom; Karolinska Institutet, Stockholm, Sweden; Universitat Autonoma Barcelona, Barcelona, Spain; Queen Mary University Hospital, London, United Kingdom; University Hospital of Basel, Basel, Switzerland; Centre de Pathologie, Amiens, France; Hôpital La Pitié-Salpêtrière, Paris, France; Universität Rostock, Rostock, Germany; Kantonsspital, Aarau, Switzerland; Medical University Vienna, Vienna, Austria; Radboud UMC, Nijmegen, Netherlands; Medical University, Graz, Austria; Tallaght Hospital, Dublin, Ireland; Champalimaud Clinical Center, Lisbon, Portugal; Cork University Hospital, Cork, Ireland; University of Florence, Florence, Italy; Hospital da Luz, Lisboa, Portugal; Southmead Hospital, Westbury-on-Trym, United Kingdom; Rennes Hospital, Rennes, France; Sozialstiftung Bamberg, Bamberg, Germany; Christie Hospital, Manchester, United Kingdom; University of Bonn, Bonn, Germany.

Background: In addition to the intrinsic subjectivity of morphologic interpretation, variation in IDCP reporting may be due to differences in diagnostic criteria or reporting protocols. However, there is limited data on how IDCP is reported in prostate needle biopsies (PNBx) in current clinical practice.

Design: A survey of diagnostic criteria and reporting practice of IDCP in PNBx [pure or associated with invasive prostate cancer (IDC+inv)] was circulated to 23 expert uropathologists from 11 European countries.

Results: Criteria used for diagnosis of IDCP included solid intraductal growth (100%), dense cribriform (96%), loose cribriform/micropapillary with nuclear size >6x normal (83%) or comedonecrosis (74%) and dilated ducts >2x normal (39%). Nuclear "size" was interpreted as nuclear area by 74% and nuclear diameter by 21%.

Pure IDCP was reported by 100% and Gleason graded by 30%.

In cases of IDC+inv, IDCP component was included in estimation of tumour extent and number of cores involved by 74% and 83% respectively.

All respondents would report presence of definite IDCP in IDC+inv and 52% would include IDCP component when grading IDC+inv. 48% perform immunohistochemistry (IHC) in solid or cribriform nests with comedonecrosis to exclude IDCP (17% routinely, 30% if the focus appeared to have basal cells on H&E). 48% graded such foci as Gleason pattern 5 even if IHC had shown presence of basal cells.

Conclusions: There is a high level of agreement among experts regarding diagnostic criteria for IDCP. However, there are significant differences in IDCP reporting practice (especially grading of IDC+inv) highlighting a need for greater consensus.

1059 A Clinico-Pathologic Study of 17 Patients With Renal Cell Carcinoma Associated With Leiomyomatous Stroma Identifies a Strong Association With Tuberous Sclerosis

Virginie Verkarre, Aurore Mensah, Xavier Leroy, Mathilde Sibony, Viorel Vasiliu, Eva Comperat, Stephane Richard, Arnaud Mejean. CHU Necker, Paris, France; CHU HEGP, Paris, France; AP-HP, Paris, France; CHU Bicetre, Le Kremlin-Bicêtre, France; CHRU, Lille, France.

Background: Renal cell carcinoma (RCC) associated with leiomyomatous stroma (RCCALS) is a rare newly described subtype of RCC poorly characterized. A recent study has found a subtype of "renal angiomyoadenomatous tumor" in 37% of RCC occuring in Tuberous sclerosis complex (TSC). We describe a large clinicopathologic series of RCCALS in order to better characterize this entity.

Design: 17 patients with a diagnosis of RCCALS with the specific immunophenotype CK7+, AMACR- were collected from multiple institutions between 2009 and 2014. All cases with past history of RCC were reviewed. Clinical data, pathological features, immunohistochemical findings (CK7, cytokeratin 34bE12, AMACR, CD10, HMB45, Melan-A, TFE3, desmin, caldesmon) were analyzed.

Results: Mean age at the first diagnosis of RCCALS was 51 years (range from 28 to 72y) (11 females, 6 males); 7/17 (41%) occurred before 50 years old. 6/17 patients (35%) had multiple RCCALS (range; 2 to 18 tumors) and 8/17 were associated with other renal tumors mostly angiomyolipomas (5/8). 5/6 patients with multiple renal tumors had TSC and one patient with unique isolated RCCALS had germline TSC2 mutation. In 3 cases, renal neoplasm was the first manisfestation of TSC. Tumor sizes were comprised between 0.9-5.5 cm. 85% were pT1a, 15% pT1b and 2 cases had metastatic lymph nodes at time of first diagnosis (N2). All Tumors were mainly solid with a tubulopapillary pattern lined by large cells with mixed clear to eosinophilic cytoplasm. Tumors cells expressed CK7, CD10, 34bE12 but were negative for AMCR, TFE3, HMB45 and Melan-A. 64% had nuclear grade 3 and 36% grade 2. Tumors were surrounded and lobulated by a leiomyomatous stroma desmine + caldesmone + HMB45- and Melan-A-. Clinical follow-up was available for 14 patients (mean 40 months –range : 5-204 months). All patients were alive without progression of disease at last follow-up (24 to 120 months for two N+ patients).

Conclusions: Our study has identified a high proportion of TSC in RCC-ALS (35%). This suggests that TSC screening should be considered for patients with RCCALS and that the mTOR pathway could be involved in the pathogenesis of this subtype. The presence of metastatic lymph nodes detected in 11% of cases also prompt us to a long monitoring.

1060 Ankyrin G Expression Is Associated With Androgen Receptor Stability and Is of Prognostic Value in Men with Prostate Cancer

Tingting Wang, Michael Dolph, Bryan Donnelly, Tarek Bismar. University of Calgary and Calgary Laboratory Services, Calgary, AB, Canada; University of Calgary, Calgary, AB, Canada.

Background: Despite availability of various therapis for prostate cancer (PCA), tumor metastasis and castrate resistant disease remain as primary causes of mortality. Identification of new prognostic markers and targets that involved in this process is of paramount importance. Ankyrin G belongs to Ankyrins family, which function to provide cellular stability by anchoring cytoskeleton to the plasma membrane. The aim of the study was to investigate the expression and function of the Ankyrin G in PCA.

Design: Protein expression of human PCA tissues was assessed and correlated to patients' outcome. Invitro studies were carried out to assess Ankyrin G role on cell invasion and proliferation, in addition to exploring potential mechanisms and pathways.

Results: Silencing Ankyrin G resulted in a statistically significant decrease of cell proliferation in both AR dependent cells (LNCaP and VCAP cells, p=0.0083 and P=0.079 respectively) and AR independent cell (PC-3 cell, P=0.0047). Decreased Ankyrin G expression inhibited CyclinA and CyclinB expression, thus delaying cells in G1/S phase transition. Unexpectedly, Ankyrin G knockdown cells exhibited significant increase in cancer cell invasion in LNCaP (p=0.0059) and VCaP (P=0.0077) cells, but not in PC-3 cells. These results suggested that Ankyrin G mediated invasion may require AR. Interestingly, we found that knockdown of Ankyrin G was associated with increased AR protein stability. Within 48 hours of treatment, AR protein level was reduced ~ 40% in Ankyrin G knockdown LNCaP cells. However, control siRNA LNCaP cells were more sensitive to cycloheximide (CHX) treatment, where AR protein level was reduced ~90% (P<0.001). Similar effects were noted in VCaP cells (P<0.001). To explore whether the above findings are clinically relevant in PCA patients, we analyzed Ankyrin G expression in a cohort of 225 men with PCA. Consistent with in vitro data, Ankyrin G intensity levels were associated with disease progression and were inversely related to AR expression (P<0.0001) and Gleason Score (P<0.0001). Furthermore, lower Ankyrin G expression showed significant association with cancer specific mortality (P=0.012).

Conclusions: Our results suggest opposite roles for Ankyrin G on cell growth and motility and confirm the prognostic role for Ankyrin G expression in men with PCA. This support Ankyrin G role in PCA progression and patinets prognosis. Targeting Ankyrin G may be of potential theraputic value.

1061 Utility of PAX8, GATA3, P40 and Uroplakin III Expression in Sarcomatoid Carcinomas of the Upper Urinary Tract

Xiaoyan Wang, Darrell Davidson, Antonio Lopez-Beltran, Rodolfo Montironi, Robert Emerson, Sean Williamson, Puay-Hoon Tan, Lee Ann Baldridge, Gregory MacLennan, Liang Cheng. Indiana University School of Medicine, Indianapolis, IN; Cordoba University, Cordoba, Spain; Institute of Pathological Anatomy and Histopathology, Polytechnic University of the Marche Region (Ancona), United Hospitals, Ancona, Italy; Henry Ford Health System, Detroit, MI; Singapore General Hospital, Singapore, Singapore; Case Western Reserve University, Cleveland, OH.

Background: Sarcomatoid carcinoma (carcinosarcoma) of the upper urinary collecting system is a rare aggressive malignancy composed of malignant epithelial and stromal components. Recently, positive immunohistochemical staining for PAX8 has been observed in a majority of renal epithelial neoplasms, whereas GATA3 (GATA-binding protein 3) and p40, a truncated isoform of p63, have been found to have high specificity for urothelial carcinoma and pulmonary squamous cell carcinoma, respectively. Uroplakin III is an urothelium-specific marker of terminal differentiation. Due to the paucity of reported cases, little is known about the expression of PAX8, GATA3, p40 and uroplakin III in the upper urinary tract sarcomatoid carcinoma.

Design: Nine sarcomatoid urothelial carcinomas involving the renal pelvis, calyces, or upper ureter were included in this study. Immunohistochemical expression of PAX8, GATA3, p40 and uroplakin III was analyzed on paraffin-embedded tissue sections for each case.

Results: The patients included 6 female and 3 male patients with an age range of 56 to 78 years (mean 68 years). Presenting symptoms included gross hematuria, fever, sepsis and flank mass. Radical nephroureterectomy was performed on all patients. Moderate to strong PAX8 expression was demonstrable in 2 of 9 (22%) tumors. GATA3 yielded moderate positivity in 1 of 9 (11%) tumors. Three of 9 (33%) cases revealed moderate immunoreactivity for p40. Staining for uroplakin III was entirely absent in all 9 tumors (0%).

Conclusions: There is limited expression of PAX8, GATA3 and p40 in the upper urinary tract sarcomatoid urothelial carcinomas. Expression of PAX8 in 22% of sarcomatoid carcinomas of the upper urinary tract indicates that PAX8 cannot reliably distinguish these urothelium-derived malignancies from renal cell carcinomas. Although p40, uroplakin III and GATA3 are frequently expressed in urothelial carcinoma, sensitivity for confirming the urothelial origin of sarcomatoid carcinoma of the upper urinary tract is low.

1062 Cytogenetic and Pathologic Characteristics of Subtypes of Papillary Renal Cell Carcinoma

Fang Wen, Anthony Sisk, Nagesh Rao, Allan Pantuck, Jiaoti Huang. University of California, Los Angeles, CA.

Background: Papillary renal cell carcinoma (PRCC) is classified as type 1 and type 2 with different morphologic features and biological behavior. Although cytogenetic changes for type 1 tumors have been reported, type 2 tumors have not been well characterized cytogenetically.

Design: Ninety-one cases of PRCC from 80 patients (M:F 5:2) were received at our institution 2008-2014. Forty-seven tumors were type 1 (52%), and 38 were type 2 (42%), while 6 (7%) showed mixed type 1 and 2 features. Cytogenetic analyses were performed prospectively.

Results: While the male patients showed equal distribution of type 1 and 2 PRCCs (36/48% and 35/47%, respectively), the female patients were 3 times more likely to develop type 1 than type 2 PRCC (11/69% vs 3/19%). Type 2 PRCCs were associated with older age (mean 68 vs 62, P = 0.02), larger tumor size (mean 6.2 vs 3.2 cm, P = 0.004), higher nuclear grade (P < 0.0001), a higher percentage with sarcomatous component (11% vs 0%, P = 0.04), higher rate of positive margins (11% vs 0%, P = 0.04), and higher pT stage (P = 0.0009). Cytogenetic results were available on 62 tumors (31 type 1 and 28 type 2). Loss of Y and gains of chromosomes 7, 16 and 17 were seen in >50% of both type 1 and 2 tumors. While the most frequent chromosomal abnormality in type 2 PRCC was loss of Y (92% in males), gains of chromosome 17 was the most common and was significantly more prevalent in type1 compared with type 2 PRCC (84% vs 54%, P = 0.02). Type 2 PRCC showed more complex karyotype abnormalities (mean 7.6 vs 5.7, P = 0.04). In particular, loss of chromosome 14 was only seen in type 2 PRCC (18% vs 0%, P = 0.02), associated with the presence of sarcomatous component (40% vs overall 11% in all type 2, P = 0.03) and a more complex pattern of cytogenetic abnormality (mean 15.0 vs 7.6 in all type 2, P = 0.003). Loss of chromosomes 11,18 and 22 and gains of chromosome 21 were also more prevalent in type 2 compared with type 1 PRCC (11% vs 0%, 14% vs 3%, 18% vs 6%, 11% vs 3%, respectively), although the differences were not statistically significant in this cohort.

Conclusions: 1. The two PRCC subtypes show both overlapping and distinct cytogenetic alterations; 2. Type 2 PRCC has more cytogenetic abnormalities, consistent with their more aggressive behavior; 3). The novel observations can form the basis of studying the molecular basis of PRCC subtypes; 4. Cytogenetics can be useful in subclassification of difficult cases of PRCC.

1063 Pathologic Evaluation of Renal Core Needle Biopsies and Its Role in Clinical Management: A Single Institution Experience

Elizabeth Whittington, Oleksandr Kryvenko, Raymond Leveillee, Merce Jorda. University of Miami Miller School of Medicine, Jackson Memorial Hospital, Miami, FL.

Background: Renal core needle biopsies are frequently used in the diagnosis of renal masses and often present a diagnostic challenge. This is a retrospective study to evaluate the diagnostic accuracy of renal core needle biopsies and the impact in clinical management.

Design: The pathologic diagnosis of 399 consecutive renal biopsies from 358 patients between 2003-2013 was reviewed along with the available subsequent resection specimens and the clinical/radiologic data.

Results: The patients consisted of 222 (62%) men and 136 (38%) women with a median age of 67 (4-92). 372 (93.2%) renal masses were diagnostic and 27 (6.8%) were non diagnostic. Diagnosed samples included 83 (22.3%) benign, 41 (11%) oncocytic neoplasms, and 248 (66.6%) malignant diagnoses. The benign diagnoses included 11 angiomyolipomas (AML), 1 ganglioneuroma, and 71 other negative for malignancy. The malignant cases included 109 clear cell renal cell carcinoma (CCRCC), 35 papillary renal cell carcinoma (PRCC), 31 urothelial cell carcinoma (UCC), 8 chromophobe RCC (chRCC), 18 RCC not further classified (uRCC), 2 mixed CCRCC & PRCC, and 30 other. Subsequent nephrectomy diagnoses were available for 68 (17.0%) of cases. Of these, the diagnosis was the same in 34 (50%) cases, while 8 (11.8%) had a change in histologic subtype, 15 (22.0%) had a change in grade, and 11 (16.2%) changed from non-diagnostic/negative to neoplastic. Therefore, the diagnostic accuracy of renal core needle biopsy was 83.8% in determining malignancy and 72% in determining subtype. Clinical data was available for 285 (71.4%) cases. Clinical management varied within the different diagnostic categories (see table). Mean tumor size was 3.61 cm (0-16 cm).

Clinical Management According to Renal Lesion Diagnosis

	CCRC	PRCC	UCC	chRCC	URCC	Oncocytic	Benign
Nephrectomy	20	7	15	1	2	3	0
Ablation	66	20	0	4	6	19	8
Chemo	8	1	4	2	3	0	0
Radiation	0	1	1	0	0	0	0
Surveillance	3	2	2	0	1	3	4
Total	97	31	22	7	12	25	12

Conclusions: Most (93.2%) of the renal mass core needle biopsies were diagnostic. The diagnostic accuracy of renal core needle biopsies was 83.8% in determining malignancy and 72% in determining subtype. Ultimately, pathologic diagnosis is useful in establishing patient treatment plans and impacts patient management.

1064 Renal Cell Carcinoma With Angioleiomyoma-Like Stroma: Exploring SDHB Protein Immunohistochemistry and the Relationship To Tuberous Sclerosis Complex

Sean Williamson, Jason Hornick, John Eble, Nilesh Gupta, Craig Rogers, Lawrence True, David Grignon, Liang Cheng. Henry Ford Health System, Detroit, MI; Brigham & Women's Hospital, Boston, MA; Indiana University, Indianapolis, IN; University of Washington, Seattle, WA.

Background: Renal cell carcinoma (RCC) with angioleiomyoma-like stroma appears to be molecularly and immunohistochemically distinct from clear cell RCC; however, its relationship to clear cell papillary RCC remains debated. Two recent studies found that tumors with similar morphology sometimes occur in patients with tuberous sclerosis complex (TSC), and one study found such tumors to be unexpectedly negative for succinate dehydrogenase B (SDHB) protein immunohistochemistry.

Design: We evaluated immunohistochemistry for SDHB in 12 apparently sporadic RCCs with angioleiomyoma-like stroma and correlated with clinical information for evidence of TSC. Tumors were compared to a group of 16 clear cell papillary RCCs and 8 unclassified tumors with borderline features.

Results: In RCC with angioleiomyoma-like stroma and clear cell papillary RCC, SDHB immunohistochemical staining appeared near-negative when performed at usual antibody concentration. However, examination at high magnification and repeated analysis with increased antibody concentration revealed at least focal fine cytoplasmic granular staining in all tumors. Detailed clinical, imaging, and family history information was available for 9 of 11 patients with RCC with angieiomyoma-like stroma and revealed no angiomyolipomas or other findings to suggest undiagnosed TSC. Family histories revealed renal cysts and renal cancer in 2 patients and end-stage renal disease in 1. Staining remained equivocal in 1 unclassified tumor (CK7+ with clear cell morphology and chromosome 3p deletion), even at higher antibody concentration. Follow-up imaging in this patient revealed a solitary renal angiomyolipoma but no other lesions to suggest TSC, including negative brain MRI. Electron microscopy performed on 1 tumor revealed mitochondria to be very sparse, potentially accounting for the weak immunohistochemical labeling for SDHB protein.

Conclusions: SDHB immunohistochemistry often reveals weak labeling of RCC with angioleiomyoma-like stroma and clear cell papillary RCC, likely due to sparse distribution of mitochondria within the cytoplasm. Similar tumors have been recently reported in patients with TSC; however, absence of staining in this setting may not be specific for TSC. In tumors with pale or clear cytoplasm, scant SDHB immunohistochemical staining should be interpreted with caution, as it may not reflect an abnormality in SDH genes or proteins.

1065 Clear Cell Renal Cell Carcinoma With Borderline Features of Clear Cell Papillary Renal Cell Carcinoma: Combined Morphologic, Immunohistochemical, and Cytogenetic Analysis

Sean R Williamson, Nilesh Gupta, John Eble, Craig Rogers, Susan Michalowski, Shaobo Zhang, Mingsheng Wang, David Grignon, Liang Cheng. Henry Ford Health System, Detroit, MI; Indiana University, Indianapolis, IN.

Background: Clear cell papillary renal cell carcinoma is regarded as a unique neoplasm in the 2012 International Society of Urological Pathology Vancouver Classification of Renal Neoplasia. Despite its resemblance to clear cell renal cell carcinoma, to date we are aware of no report of metastasis or aggressive behavior. Immunohistochemical and molecular features also differ, including positive immunohistochemical staining for cytokeratin (CK) 7, high molecular weight CK, absent staining for alpha-methyl-acyl-coA-racemase (AMACR/p504s) and CD10, and absence of chromosome 3p deletion and *VHL* gene mutation.

Design: We correlated immunohistochemical staining results with chromosome 3p fluorescence in situ hybridization or karyotyping in tumors with partial but incomplete morphology of clear cell papillary renal cell carcinoma.

Results: Tumors from 22 patients (ages 33-82 years) were analyzed. The percentage of the tumor resembling clear cell papillary renal cell carcinoma ranged from 10-90% (median 25%). Sources of resemblance included: branched glandular architecture (95%), nuclear alignment (68%), small papillary tufts in cystic spaces (32%), focal branching papillae (27%), and prominent papillary structures (14%). Carbonic anhydrase IX uniformly yielded diffuse strong positivity. Staining for CK7 was often negative (18%) or focal (64%); however, >50% labeling was present in 4 tumors (18%). Reactivity for both CD10 and AMACR was usually present (median 80% and 60% of cells, respectively). Seven tumors were at least focally reactive for high molecular weight CK (32%). Loss of material from chromosome 3p was confirmed in 15 tumors (68%), including 4 of the 7 tumors with labeling for high molecular weight CK or diffuse (>50%) reactivity for CK7. Intratumoral variation in morphologic patterns did not parallel variation in staining or cytogenetic findings.

Conclusions: A discordant immunohistochemical staining pattern typically correlates with loss of material from chromosome 3p in tumors with partial but incomplete morphology of clear cell papillary renal cell carcinoma, supporting the hypothesis that these tumors are best classified as clear cell renal cell carcinomas. Diffuse labeling for CK7 can uncommonly be observed in clear cell renal cell carcinomas confirmed to have chromosome 3p loss, but the immunohistochemical profile is usually discordant with that expected of clear cell papillary renal cell carcinoma, including CD10 and AMACR positivity.

1066 Clear Cell Adenocarcinomas of the Urinary Tract: GATA-3 Immunohistochemical Expression and Review of Other Relevant Immunomarkers

Angela Wu, Nallasivam Palanisamy, Javed Siddiqui, L Priya Kunju. University of Michigan, Ann Arbor, MI.

Background: Primary clear cell adenocarcinomas of the urinary tract (CA-U) are rare tumors, and the origin of such tumors as urothelial versus Mullerian is controversial. The majority of CA-U in the literature have been reported to be negative for p63 and positive for PAX-8. To the best of our knowledge, there is no literature on the expression of GATA-3, a promising new biomarker which is highly sensitive for urothelial carcinoma, in CA-U.

Design: All CA-U diagnosed at our institution from 1/1990-6/2013 were reviewed, and representative whole tissue blocks were immunostained for GATA-3 (Santa Cruz mouse monoclonal antibody, 1:100). Percentage of cells with nuclear staining as well as intensity (weak, moderate and strong) were recorded. GATA-3 staining in surface urothelium acted as an internal control.

Results: Nine cases of CA-U were included (median age 56; Female: Male=8:1), accounting for <0.1% of all urinary tract carcinomas diagnosed at our institution over this time period. The primary sites included urethra and urinary bladder (5), bladder only (2), urethra only (1), and ureter (1). No cases showed a component of conventional urothelial carcinoma and/or urothelial carcinoma in-situ, and a Mullerian primary was excluded in all cases. GATA-3 was not expressed in any cases of CA-U. PAX-8 was performed in 5/9 cases at time of diagnosis and was positive in all cases. P63 was performed in 5/9 cases at time of diagnosis and was negative in all cases.

Conclusions: GATA-3 is not expressed in primary clear cell adenocarcinoma of the urinary tract. These rare carcinomas are generally negative for p63 and positive for PAX8. This adds evidence that clear cell adenocarcinomas do not generally stain with urothelial markers.

1067 Utility of GATA-3 and ERG Immunohistochemistry in Distinguishing Between Intraductal Urothelial Carcinoma in the Prostate and Intraductal Carcinoma of the Prostate

Angela Wu, Nallasivam Palanisamy, Javed Siddiqui, L Priya Kunju. University of Michigan, Ann Arbor, MI.

Background: Distinguishing intraductal urothelial carcinoma in the prostate (IUC) and intraductal carcinoma of the prostate (IDC-P) is critical due to differing clinical and therapeutic implications; however, these intraductal lesions can be challenging, particularly in limited biopsies when surface urothelium cannot be evaluated and/or when the growth pattern is predominantly or exclusively intraductal. We evaluated the utility of GATA-3 and ERG immunostains, markers which have shown promise in distinguishing between urothelial and prostatic carcinoma, in the differential diagnosis between IUC and IDC-P.

Design: Representative whole tissue blocks from 20 cases (12 cystoprostatectomies and 8 TURPs) of IUC (which included both high grade urothelial carcinoma and flat urothelial carcinoma in situ) and 20 cases (12 prostatic biopsies and 8 prostatectomies) of IDC-P from our archives were stained for GATA-3 (Santa Cruz mouse monoclonal, 1:100) and ERG (Epitomics rabbit monoclonal, 1:100). We recorded the percentage of cells staining and scored the nuclear expression of GATA-3 and ERG as 1-3+. Cases showing 2-3+ staining in >15% of the intraductal carcinoma cells were counted as positive for GATA-3 or ERG expression. GATA-3 expression within prostatic basal cells and surface urothelium/urothelial carcinoma was also recorded.

Results: GATA-3 was expressed in 80% (16/20) of IUC; the positive cases had a median percentage of GATA-3+ cells of 55% and 94% (15) had strong nuclear staining. GATA-3 was absent in all IDC-P cases. GATA-3 expression was present in surface urothelium/urothelial carcinoma in 35% (7/20) of IUC cases and in prostatic basal cells and atrophic prostatic glands in 55% (11/20) of IDC-P cases. ERG was expressed in 40% (8/20) of IDC-P; the positive cases had a median percentage of ERG+ cells of 100% and 75% (6) had strong nuclear staining. ERG was absent in all IUC cases.

Conclusions: GATA-3 is a highly sensitive and specific marker for IUC. ERG is a highly specific but not a very sensitive marker for IDC-P. A panel including these markers may be helpful in distinguishing between IUC and IDC-P, particularly in high grade carcinomas in which other routinely used immunomarkers (p63, CK903, PSA) may be negative. Lack of ERG expression does not exclude IDC-P. It is also important to distinguish GATA-3 staining in prostatic basal cells from staining within the intraductal carcinoma.

1068 The Prognostic Impact of Rhabdoid Differentiation in Renal Cell Carcinoma

Xuemei Wu, Rafael Jimenez, Loren Herrera Hernandez, Christine Lohse, Robert Thompson, Stephen Boorjian, Brian Costello, John Cheville. Mayo Clinic, Rochester, MN.

Background: Renal Cell Carcinoma (RCC) with rhabdoid differentiation is associated with poor prognosis, and the ISUP grading system classifies both rhabdoid and sarcomatoid RCC as grade 4. The objective of this study was to determine the prognostic significance of rhabdoid differentiation in comparison to grade 3 RCC and RCC with sarcomatoid differentiation.

Design: The study consisted of 406 patients with grade 4 RCC and 1758 patients with grade 3 RCC. All cases were reviewed by a urologic pathologist for the presence of sarcomatoid and rhabdoid differentiation. Associations of clinical and pathologic features with death from RCC were evaluated using Cox models.

Results: Among the 406 grade 4 RCCs, 111 (27%) showed rhabdoid differentiation and 189 (47%) had sarcomatoid differentiation. In multivariable analysis of grade 4 RCC, there was not a statistically significant association between rhabdoid differentiation and death from RCC (hazard ratio 0.95, p=0.75), in contrast to sarcomatoid differentiation (hazard ratio 1.63, p<0.001). Using grade 4 RCC without rhabdoid or sarcomatoid differentiation as the reference, the presence of rhabdoid differentiation did not have a statistically significant impact on death from RCC (hazard ratio 1.03, p=0.88). Patients with RCC with rhabdoid differentiation were significantly more likely to die of RCC than patients with grade 3 RCC (hazard ratio 2.45, p<0.001) and grade 3 RCC with necrosis (hazard ratio 1.62, p<0.001).

Conclusions: The presence of rhabdoid differentiation in grade 4 RCC is not associated with an increased risk of death from RCC in contrast to sarcomatoid RCC. Therefore rhabdoid and sarcomatoid differentiation should not be grouped together when assessing risk in a patient with grade 4 RCC. Patients with RCC and rhabdoid differentiation do significantly worse than patients with grade 3 RCC, confirming that RCC with rhabdoid differentiation is grade 4.

1069 Polyoma Virus Is Prevalent in Urothelial Carcinoma Post Kidney Transplant

Ling Yan, Mohamed Salama, Linh Matsumura, Megan Troxell. Oregon Health & Science University, Portland, OR; University of Utah and ARUP Laboratories, Salt Lake City, UT.

Background: Polyoma virus is a potential causative agent of genitourinary (GU) tract cancer in post kidney transplant patients due to its re-activation following immunosuppression. The exact tumorigenic mechanism of polyoma virus in this setting is controversial. Human papilloma virus (HPV) is generally not implicated in GU cancers, but data is scarce in transplant populations. A better understanding of viral associated GU cancer has important clinical implications for monitoring, early detection and patient outcome.

Design: With IRB approval, pathology records were searched for GU cancer in kidney transplant patients. Tumor morphology, clinical history and follow up were reviewed. Immunostains for SV40 (polyoma), p16, and in situ hybridization (ISH) for high-risk HPV were performed.

Results: Over the last 20 years, 2345 kidney transplants were performed at our center. 14 cases of GU cancer were identified (0.6%) including 8 bladder/ureter carcinoma (mean 10 years post transplant), 5 renal cell carcinoma (RCC, mean 17 years post transplant) and 1 prostate carcinoma. Among 8 bladder/ureter cases, 2 were high grade papillary non-invasive urothelial carcinoma (UC), 5 high-grade invasive UC (one with focal squamous differentiation), and 1 pure squamous cell carcinoma. Three invasive UCs (38%) were positive for SV40. All SV40+ bladder cancers developed at ≥9 years post-transplant with history of BK polyoma viremia, high creatinine level at diagnosis and after surgical treatment. Two patients with SV40 positive UC had renal failure due to reflux/obstruction, and were young at the time of transplant and cancer diagnosis (early 30's). One of these two patients died of metastatic UC (SV40+ in metastatic sites) 13 months after initial diagnosis. Seven bladder cancers were positive for p16 (including all 3 SV40+); of 4 tested for high-risk HPV-ISH, all were negative. All cases of RCC (1 clear, 3 papillary, 1 clear-papillary) were negative for both SV40 and p16; one patient had both SV40+ UC and SV40- RCC. The prostate cancer was SV40- and partially positive for p16.

Conclusions: Our study shows high incidence of polyoma virus positivity in bladder UC post kidney transplant (38%). RCC was negative. Interestingly, we noted an association of positive BK viremia and poorer allograft function with polyoma virus positive UC. Although sample size is small, young patients with obstructive disease may be at particular risk. Overall, our data further support the necessities of close monitoring and early detection for these patients.

1070 Optimization of Nanostring Platform for Evaluation of Prostate Cancer Biomarkers and Therapeutic Targes in FFPE Specimens

Wusheng Yan, Denise Young, Yingjie Song, Yongmei Chen, Shilpa Katta, Lakshmi Ravindranath, Jocelyn Lee, Alagarsamy Srinivasan, Jennifer Cullen, Jacob Kagan, Sudhir Srivastava, Albert Dobi, Inger Rosner, David McLeod, Isabell Sesterhenn, Shiv Srivastava, Gyorgy Petrovics. Uniformed Services University of the Health Sciences, Rockville, MD; National Cancer Institute, Rockville, MD; Walter Reed National Military Medical Center, Bethesda, MD; Joint Pathology Center, Silver Spring, MD.

Background: Identification of prognostic indicators of disease progression is one of the highest priorities in prostate cancer (CaP) research. The majority of CaP tissue specimens available for biomarker discovery and validation are formalin fixed paraffin embedded (FFPE) specimens. The RNA quality of these tissues for traditional gene expression analysis approaches is not adequate, especially of cases with long term- follow up necessary for prognostic marker studies. We systemically evaluated and optimized the NanoString platform for CaP gene expression analysis in FFPE whole mounted prostate specimens with up to 15 years follow up.

Design: NanoString readouts were compared between a series of input total RNA prepared through different tissue dissection methods. We then performed NanoString analysis of 151-CaP probe set on 63 archived CaP samples to evaluate this modified protocol. ERG gene expression was validated by immunohistochemistry (IHC) assay using CPDR ERG-MAb (9FY).

Results: We have performed NanoString analysis of CPDR designed 151- CaP gene panel on whole-mounted prostate tissue specimens using our optimized protocol. The prostate epithelial cell markers *KLK3, MSMB* and *PAP* had the highest signals in all samples reflecting the prostate epithelial origin of the specimens. Established CaP specific genes, such as *AMACR, PCA3* and *PSGR* were most highly over-expressed in tumors compared to matched benign prostate epithelium. ERG positive tumors had strong expression of both *TMPRSS2-ERG* fusion probes and probes for several *ERG* splice forms (*ERG 1,2,3* and *8*), with no signals in the matched benign samples. The *ERG* gene expression status was consistent with blinded ERG IHC results.

Conclusions: The feasibility of NanoString profiling in archived whole mounted FFPE prostate specimens was demonstrated. This approach is well suited for a medium throughput evaluation and validation of prognostic biomarker and therapeutic target candidates in CaP.

1071 Atypical Diagnosis in Prostate Needle Biopsies From a Developing Country (Philippines): The Essential Role of a Urological Pathologist

Cecille Yanez, Jeffrey So. St. Luke's Medical Center, Quezon City and Global City, Philippines.

Background: Borderline prostatic lesions, with insufficient histomorphologic features, to be definitely diagnosed as Prostatic adenocarcinoma (PCa) are often signed out as "atypical glands suspicious for carcinoma" or Atypical Small Acinar Proliferation (ASAP). These findings that eventually warrant either immunohistochemistry or a repeat biopsy, prove to be more burdensome to patients in developing countries (such as the Philippines), where healthcare is not as progressive nor is it an utmost priority. At the same time,in these countries, there is a shortage of urological pathologists.

Design: In this study, we compared the Transrectal Ultrasound-Guided Prostate (TRUS) Biopsies signed out by general pathologists in St. Luke's Medical Center Quezon City from 2008-2010, and the TRUS Biopsies primarily signed out by a uropathologist in both St. Luke's Medical Center Quezon City and Global City from July 2013 to July 2014 and September 2013 to July 2014 respectively.

Results: From 2008 to 2010, 30.6% (129 of 421) of the cases were signed out as atypical. Of these, 79 underwent IHC staining, 21 (26.6%) of which were eventually signed out as PCa. Compared to those signed out in 2013 to 2014 by our GU pathologist, only 16.6% (39 of 235) of the cases were signed out as atypical.

	Total TRUS	Total ATYP
2008-2010	421	129(30.6%)
2013-2014	235	39(16.6%)

Of these, 16 underwent IHC staining, with 15 (93%) of them being definitely diagnosed as PCa. Among the 21 cases wherein a repeat biopsy was recommended, only 3 followed and 2 of these had findings of PCa on repeat biopsy. Looking at our 16.6% rate of atypicals and subtracting those that were eventually established as PCa after IHC's, our atypicals would be down to 10% (24/235) in 2013-2014 compared to 25.7% (108/421) in 2008-2010.

	ATYP w/ IHC	PCa after IHC	Total ATYP after IHC	W/ rpt Bx suggestion	With rpt Bx	PCa after rpt Bx
2008-2010	79	21(26.6%)	108(25.7%)	0	0	0
2013-2014	16	15(93%)	24(10%)	21	3	2

Conclusions: These results highlight the critical role a specialist has in the field of Urological pathology, especially in developing countries. It is in the diagnosis of PCa in needle biopsies that a uropathologist impacts the use of an atypical diagnosis, by ensuring its judicious use. This ultimately benefits the patients, by lessening unwarranted expenses through the decreased dependence on immunohistochemical staining and if unnecessary, a repeat biopsy.

1072 microRNA Profiling of Prostate Cancer in Young and Older Man, One or Two Diseases?

Zhiming Yang, Ang Li, Peter Pinto, Maria Merino. National Institutes of Health, Bethesda, MD.

Background: Early-onset prostate cancer, that is prostate cancer diagnosed before age of 50, is associated with aggressive biological behavior, higher Gleason score, and poor prognosis. The genetic risk and underlying mechanisms of early-onset disease remain largely unknown. MiRNA profiling alteration has been reported to play significant roles in prostatic oncogenesis. We investigated and compared the miRNA profiling of prostate cancer occurring in younger and older patients to identify differences and similarities as well to identify miRNA's with possible role as novel biomarkers or new therapeutic agents.

Design: Patients with prostate cancer diagnosed at age 43-49 (Gleason score 3+3 to 4+4) were compared with cases diagnosed at age 64-72 (Gleason score 3+3 to 4+4). Pure population of tumor cells was extracted from manually microdissected and normal adjacent epithelium and was assayed by PCR array for miRNA profiling in all cases. Differentially expressed miRNAs were used to comparatively study early-onset vs. late-onset diseases.

Results: Upregulation of 16 miRNAs (e.g. miR-575, miR-93-5p, and miR-630) and downregulation of 9 miRNAs (e.g. miR-548ai, miR-21, and miR-205-5p) were identified in early-onset group ($p<0.01$). Among these, miR-21 which is known to be related to androgen receptor signaling pathway. A different signature was found in the older age group. Upregulation of 11 miRNAs (e.g. miR-198 and miRNA-663a) and downregulation of 8 miRNAs (e.g. miR-221 and miRNA-143) were identified in the late-onset group.

Conclusions: Our study reveals different miRNA signatures for prostate cancers occurring in the younger and older male populations. These differentially expressed miRNA profiles may be helpful in understanding the molecular events leading to early-onset prostate cancer among different age groups. These differentially expressed miRNA may not only be a novel and prognostic tool, targeting these miRNAs may be a new therapeutic strategy in prostate cancer treatment.

1073 Hilar Invasion in Testicular Germ Cell Tumors: A Potential Understaging Pitfall

Asli Yilmaz, Kiril Trpkov. University of Calgary, Calgary, Canada.

Background: Hilum is the most common site of extratesticular extension (ETE) in germ cell tumors (GCT). Testicular hilum is composed of rete testis and extratesticular hilar soft tissues. A recent study (Yilmaz et al. Modern Pathol 2013;26:579-86) demonstrated that hilar invasion in nonseminomatous GCT is associated with advanced clinical stage at presentation. However, tumor invasion into the testicular hilum is currently not addressed in the pTNM system, which creates staging difficulty in cases showing hilar ETE.

Design: We investigated the presence of hilar invasion in 447 consecutive GCT, resected over a 10-year period (10/1999 to 12/2010) in our institution. All slides were reviewed with a particular attention to the hilar status. Hilar invasion was defined as tumor extension into the rete testis and/or hilar soft tissues. Invasion into tunica vaginalis, epididymis, spermatic cord and the recorded pT stage were also documented.

Results: Of the 447 GCT, there were 270 (60%) seminomas and 177 (40%) nonseminomatous GCT. The pT stage distribution was as follows: 352 (79%) pT1, 82 (18%) pT2, 13 (3%) pT3 and pT4. Rete testis invasion was found in 50% (225/447) and hilar ETE was identified in 25% (113/447) cases. Overall, hilar (including rete testis and/or hilar soft tissues) invasion was found in 55% (246/447) GCT. Of these, 91% (225) showed rete invasion and in 46% (113) had hilar ETE. Among the cases with hilar ETE (113), in 81% (92) rete invasion was found in the sampled blocks and it likely preceded the ETE into hilar soft tissues. In 19% (21) rete testis invasion was not identified, because it was likely not sampled. The pT staging of 113 cases with hilar ETE was as follows: 57 (50%) pT1, 44 (39%) pT2, 12 (11%) pT3 and pT4. In the study cohort overall, we also found invasion into epididymis in 6% (26) and spermatic cord in 3% (14) cases. Tunica vaginalis invasion was rare and it was only identified in 2% (9) of all cases.

Conclusions: Invasion into hilar soft tissues of the testis is the most common site of ETE in both seminomatous and nonseminomatous germ cell tumors. In this study, half of the cases showing hilar ETE were staged pT1, which may represent a potential understaging. We found that hilar ETE is invariably associated with rete testis invasion. Tunica vaginalis invasion is rarely found in GCT. This study underscores the importance of the proper testicular hilum evaluation in GCT, which requires a targeted sampling.

1074 HER2 Overexpression in Metastasizing Urothelial Carcinoma of Urinary Bladder and Upper Urinary Tracts

Takashi Yorozu, Hiroyuki Takahashi, Shun Sato, Jun Miki, Masahiro Ikegami. Jikei University School of Medicine, Tokyo, Japan.

Background: A certain percentage of patients undergoing excision and lymphadenectomy for clinically staged N0M0 urothelial carcinoma reveal lymph node metastases on histologic examination and the majority of those patients will die of the disease. The benefit of chemotherapy for metastasizing urothelial carcinoma is limited, and new therapeutic options are urgently needed. Molecular target drugs such as trastuzumab, a monoclonal antibody against human epidermal growth factor receptor 2 (HER2), might be an attractive candidate to overwhelm the metastasized tumor. In this study, we investigated the HER2 status of urothelial carcinomas with or without lymph node metastases. Our goal is to verify the difference of HER2 status between cases with and without lymph node metastases, and variability between primary tumor and metastatic site.

Design: A total of 104 cases (72 of urinary bladder, 18 of renal pelvis, and 14 of ureter) were analyzed for HER2 overexpression using immunohistochemistry (IHC). Of those patients, 45 had lymph node metastasis to compare primary and metastatic tumors. The scoring system proposed by the ASCO/CAP was used.

Results: Out of 104 primary tumors, 61 patients had a HER2 score-0 or score-1 (58.7%), 25 a score-2 (24.0%), and 18 a score-3 (17.3%) with IHC. A score-3 was observed in 19.4% (14/72) of urinary bladder cancer, 21.4% (3/14) of ureteral cancer, and 5.6% (1/18) of renal pelvic cancer, respectively. A score-3 was observed more frequent in primary tumors with lymph node metastasis (10/45, 22.2%) than tumors without metastasis (8/59, 13.6%). The concordance of HER2 between primary and metastatic sites was observed in 33/45 cases (73.3%).

Conclusions: HER2 overexpression in urothelial carcinoma, particularly the cases showing lymph node metastasis is relatively frequent. HER2 status of primary tumors is generally preserved in their metastatic sites. The molecular target therapy with trastuzumab is suggested to be a potential therapeutic candidate for the cases with HER2 overexpression by IHC.

1075 Atypical Cribriform Lesions of the Prostate Are Often Localized in the Vicinity of High Grade Cancer and Have a Similar Clinical and Pathological Significance as Intraductal Carcinoma of the Prostate

Hui Yu, Max Kong, Richard Hickman, Ming Zhou, Jonathan Melamed, Fang-Ming Deng. New York University Langone Medical Center, New York, NY.

Background: Atypical cribriform lesion (ACL) of the prostate is characterized by a loose cribriform proliferation, with greater architectural complexity and/or nuclear atypia than high grade prostate intraepithelial neoplasia (HGPIN), however insufficient for the diagnosis of intraductal carcinoma (IDC). The clinical and pathological characteristics of ACL have not been formally addressed. This study evaluated the relationship of ACL and invasive carcinoma and compared the clinical and pathological features of ACL with classic IDC on radical prostatectomy specimens.

Design: 210 radical prostatectomy specimens received from July 2013 until June 2014 were reviewed. IDC and HGPIN were classified on hematoxylin and eosin stained sections with the aid of PIN4 stains using previously published criteria. Lesions that failed to fulfil the criteria for IDC, but appeared more ominous than HGPIN, were classified as ACL. Such lesions require the presence of : (1) loose cribriform pattern, in which punched-out luminal spaces account for >50% of the central cellular mass;

and (2) relatively uniform nuclei that lack the nuclear features characteristic of classic IDC. ERG immunohistochemistry was performed on all blocks with cribriform lesions that met the criteria described above.

Results: Of the 210 cases, 35 cases were identified to have intraductal cribriform lesions. Of these cases, 13 had only ACL, 4 had only IDC and 18 had both ACL and IDC. The number of ACL foci ranged from 0- 20 per case. The number of IDC foci ranged from 0-11 per case. All ACL and IDC foci except 1 ACL focus are localized near invasive carcinoma (within 3 mm from the invasive component). In all 35 cases, the ERG status of all (100%) ACL and IDC was concordant with the ERG status of the coexisting invasive carcinoma. In contrast, the ERG status of only 46% HGPIN was concordant with the ERG status of the coexisting invasive carcinoma. ACL associated carcinoma (13 ACL only cases) and IDC associated carcinoma (22 IDC with or without ACL cases) had similar clinical and pathologic features, including preoperative PSA level, Gleason Score, tumor volume, index tumor size, extra-prostatic extension, seminal vesicle invasion and lymph node metastasis. .

Conclusions: ACL is often localized in proximity to high grade invasive carcinoma and has similar clinical and pathological significance as IDC. The existence of ACL on prostate biopsy samples may warrant similar clinical attention as IDC.

1076 Pitfalls in the Diagnostic Application of S100A1 as a Marker of Renal Neoplasia in Metastatic Settings

Claudia Zampini, Mukul Divatia, Steven Smith, Mariza de Peralta-Venturina, Bonnie Balzer, Mahul Amin. Cedars-Sinai Medical Center, Los Angeles, CA; Virginia Commonwealth University, Richmond, VA.

Background: Several histologic subtypes of renal cell carcinoma (RCC) can metastasize to any body site and immunohistochemical (IHC) studies play a major diagnostic role in this setting. mRNA expression and IHC of S100A1 has been demonstrated in different neoplastic tissues including RCC (clear cell, papillary and chromophobe) and renal oncocytoma, in carcinomas of breast, ovary, endometrium and melanoma. We have recently shown that >90% of high grade distal nephron-related carcinomas of the kidney (collecting duct carcinoma, renal medullary carcinoma and Fumarate Hydratase-deficient RCC) with marked proclivity for metastatic disease, are positive for S100A1. S100A1 has great potential diagnostic utility as a marker for renal neoplasia in metastatic settings, but its true utility is limited by the lack of comprehensive IHC data in a large cohort of cancers.

Design: S100A1 IHC was evaluated in a tissue microarray (TMA) panel of 300 cases (20 cases of 15 tumor types). Each core was scored using two metrics for IHC staining: % staining (0: negative; 1: <10; 2: 10-25; 3: 25-50 or 4: >50) and staining intensity.

Results: Results in (%), listed below in Table 1.

Tissue type	0	1	2	3	4	% (+)
Melanoma	0	5	10.5	10.5	74	100
Ovarian Ca	10	5	10	25	50	90
Breast Ca	26	26	11	11	26	74
Clear Cell RCC	40	0	5	20	35	60
Endometrial Ca	70	20	5	5	0	30
Gastric Ca	75	20	0	5	0	25
Soft Tissue tumors	75	5	5	0	15	25
Hepatocellular Ca	90	5	5	0	0	10
Lung Adeno Ca	95	5	0	0	0	5
Pancreas Ca	95	5	0	0	0	5
Lymphoma	95	0	5	0	0	5
Lung Squamous Ca	100	0	0	0	0	0
Mesothelioma	100	0	0	0	0	0
Prostate Ca	100	0	0	0	0	0
Bladder Ca	100	0	0	0	0	0

Conclusions: 1. This first study of S100A1 expression on a multi-tumor TMA cohort expands the range of known positivity to include gastric, hepatocellular, pancreatic and lung adenocarcinomas; soft tissue tumors (liposarcoma, synovial sarcoma, gastrointestinal stromal tumor) and splenic marginal zone lymphoma. 2. It confirms previous separately reported positivity in select tumor types. 3. In the diagnosis of metastatic RCC, which has significant therapeutic and prognostic implications, S100A1 IHC adds value to a panel of PAX8 and RCC, as all 3 markers individually are restricted by absolute lack of sensitivity or specificity.

1077 Clinical Utility of Molecular Inversion Probe (MIP) Array in the Diagnosis of Chromophobe Renal Cell Carcinoma From Formalin-Fixed, Paraffin-Embedded Material

Shabnam Zarei, William R Sukov, Jeannette G Rustin, Anne E Wiktor. Mayo Clinic, Rochester, MN.

Background: Renal cell carcinomas (RCC) are a heterogeneous group of tumors by morphology and clinical outcome. Chromophobe renal cell carcinoma (ChRCC) can show significant morphologic overlap with oncocytoma and variants of clear cell RCC and papillary RCC. Due to the difference in clinical behavior associated with each subtype, differentiation is important. RCC subtypes have been shown to exhibit specific recurrent chromosomal abnormalities. By routine cytogenetic studies, ChRCC is characterized by loss of chromosomes 1, 2, 6, 10, 13, 17 and 21. The main disadvantage of chromosomal studies is the requirement of fresh tissue given the fact that most tissue obtained for diagnosis has been formalin-fixed and paraffin-embedded (FFPE). Molecular Inversion Probe (MIP) array is a technique that can be used in identifying genomic copy number alterations, loss of heterozygosity and mutations. It can be performed on FFPE tissue with a small amount of DNA, and is a promising method for differentiating RCC subtypes.

Design: We identified 13 cases of ChRCC diagnosed at Mayo Clinic from 1996-2006. DNA was isolated from FFPE kidney tissue following standard FFPE DNA extraction methods. The DNA was then processed using the Affymetrix OncoScan FFPE Assay (MIP technology). The copy number and Loss of Heterozygosity (LOH) analysis was performed using the Chromosome Analysis Suite (ChAS) Software (Affymetrix).

Results: By MIP array analysis, 10 of 13 (85%) ChRCCs showed consistent chromosomal abnormalities including loss of chromosomes: 1 (10/13), 2 (9/13), 6 (9/13), 10 (10/13), 17(9/13) and 21 (5/13). Each tumor had four or more of these abnormalities. Pathogenic mutation of TP53 was detected in two tumors that also showed loss of chromosome 17. One case showed only deletion of chromosomes 1p and 6p. On re-review of H&E slides, this tumor showed a largely sarcomatoid morphology. One case only showed a small deletion of chromosome 7q33. On re-review, histologic features were not characteristic of ChRCC and based on patient age and gender likely represented a translocation associated tumor. One case showed no abnormality.

Conclusions: ChRCCs demonstrate specific and consistent chromosomal losses. These can be detected on FFPE material by MIP array. Due to small tissue requirement and specificity, MIP array testing may be useful in differentiating ChRCCs from other tumors in diagnostically challenging scenarios and offer an alternative to extensive immunohistochemical panels.

1078 Immunohistochemical Profiles of Molecular Subtypes of Bladder Cancer

Miao Zhang, Charles Guo, Tadeusz Majewski, Vipulkumar Dadhania, Maciej Sykulski, Weronika Wronowska, Woonyoung Choi, David McConkey, Colin Dinney, Anna Gambin, Bogdan Czerniak. University of Texas MD Anderson Cancer Center, Houston, TX; University of Warsaw, Warsaw, Poland.

Background: We recently demonstrated that muscle invasive bladder urothelial carcinoma (UC) can be subdivided into two major molecular subtypes, basal and luminal. The luminal subtype also contains a p53-like subset with upregulation of the p53 pathway genes. These molecular subtypes are characterized by distinct clinical behavior and different sensitivities to neoadjuvant therapy. The purpose of this study was to verify whether the molecular subtypes based on genomic profiling can be identified by immunohistochemical analysis of limited biomarkers.

Design: The studies were conducted on paraffin embedded tissue from muscle invasive urothelial carcinomas from 94 patients. Areas containing more than 50% of intact tumor tissue were marked for RNA extraction and preparation of parallel tissue microarrays. Illumina HumanHT12 V3 chips were used to analyze the gene expression profiles and to sub-classify the tumors into molecular subtypes using previously described analytical algorithms. The following markers that were previously shown to be preferentially upregulated in molecular subtypes of bladder cancer were selected for the analysis: CK18, CK20, uroplakin, GATA3, ER, and HER-2 for luminal subtype; p16, Bcl-2, desmin, SMA, myosin, and calponin for p53-like subtype; and CK5/6, CK14, CD44, cyclinD1, p63, and vimentin for basal subtype. The immunohistochemical results were semi-quantitatively assessed and were scored as follows: 0, negative; 1+, weak; 2+, moderate; and 3+, strong. The differences in the expression levels among the molecular subtypes were assessed by two-tailed t-test.

Results: The gene expression profiles identified three subsets of bladder cancer: luminal (n=25), p-53-like (n=37); and basal (n=32). Immunohistochemical analysis disclosed that 12 of the 18 selected markers showed distinctive staining in molecular subtypes while the remaining 6 markers showed no positive staining and were excluded. Seven of the 12 markers showed statistically significant expression patterns among the molecular subtypes. Luminal cancers were characterized by the co-expression of CK20 (12/25) (48%) and GATA3 (21/25) (84%). The p53-like cancers were characterized by co-expression of uroplakin (12/37) (32.4%) and Her-2 (4/33) (10%). Basal cancers were characterized by co-expression of CK5/6 (29/31) (93.5 %), CK14 (24/32 (75%), and CD44 (31/31) (100%).

Conclusions: The three molecular subtypes of conventional UCs showed distinct immunohistochemical staining patterns and can be identified with limited number of biomarkers.

1079 Primary Carcinomas of the Urethra: A Clinical and Pathological Analysis of 119 Cases

Miao Zhang, Adebowale Adeniran, Curtis Pettaway, Bogdan Czerniak, Pheroze Tamboli. University of Texas MD Anderson Cancer Center, Houston, TX; Yale University, New Haven, CT.

Background: Primary urethral carcinomas (PUCs) are rare. The morphologic, immunohistochemical and clinical features are not well elucidated.

Design: We identified 119 PUCs from 1986-2014. PUCs were defined as tumors arising primarily in the urethra. Secondary involvement of the urethra by urinary bladder carcinomas were excluded. All cases were re-reviewed to confirm the diagnoses. Immunohistochemical stains were performed on 82 tumors as follows: CK7, CK20, CK5/6, CK903, p63, CDX2 and thrombomodulin. P16 and GATA-3 were performed on a subset (n=18). Four urothelial carcinomas (UCs) secondarily involving the urethra were stained as controls.

Results: The mean age at diagnosis was 61 years (range: 29-85 years). The male: female ratio was 3:2. Median tumor size: 4 cm (range: 0.5-6.5cm). 98 tumors had overlapping morphologic features of UC and squamous cell carcinoma (SCC), which we propose calling Urethral Carcinoma (UCa); 17 adenocarcinoma; 2

sarcomatoid carcinoma; 1 lymphoepithelioma-like carcinoma and 1 adenoid cystic carcinoma. Immunohistochemical profile for the UCa was CK7, CK5/6, CK903, p63, Thrombomodulin positive; CK20, CDX2 negative. P16 was positive in 67% (12/18) of UCas; GATA-3 was negative in 78% (14/18) of UCas. The 4 UCs were all positive for GATA-3 and two were positive for p16. Adenocarcinomas (8) have different immunohistochemical profiles: CK7 positive in all 8 cases; CK20 in 6; CDX2 in 5 and thrombomodulin in 2 cases. CK5/6 and p63 were negative in all 8 cases. All patients underwent surgical excision. 22 patients had lymph node metastases (17 UCa; 5 adenocarcinoma). 15 patients had distant metastases (12 UCa and 3 adenocarcinoma), with lung as the most common site. In addition to surgery, 22 patients had chemotherapy, 8 had radiation and 12 had chemoradiation. 114 patients had clinical outcome data, with follow-up of 0.03 to 236.8 months (median: 19.7 months). 24 patients were alive with no disease (median: 17 months); 35 patients were alive with disease (median: 20 months); 28 patients died of disease (median survival: 11 months); 2 patients died of other causes; 25 patients died of unknown causes.

Conclusions: Primary urethra carcinomas are rare, a majority having overlapping morphological features and immunohistochemical profiles of UC and SCC. We propose these should be called Urethral Carcinoma, rather than UC or SCC. PUC may behave aggressively with lymph node and distant metastases with a short median survival time.

1080 Detecting Additional Chromosomal Translocations in TFE3 Translocation Renal Cell RCC By RNA-Seq

Xiaoyong Zheng, Yong Mao, Weihua Huang, Sitharthan Kamalakaran, Youfeng Yang, W Marston Linehan, Maria J Merino, Minghao Zhong, Nevenka Dimitrova, John Fallon. New York Medical College at Westchester Medical Center, Valhalla, NY; Philips Research North America, Briarcliff Manor, NY; National Cancer Institute, Bethesda, MD.

Background: *TFE3* translocation renal cell carcinoma (RCC), officially accepted as distinct subtype by 2004 WHO classification, is characterized by chromosomal translocations involving *TFE3* gene (Xp11). As such, *TFE3* translocation RCC has worse prognosis than other RCC subtypes. However, little is known about other chromosomal translocations or fusions in this particular RCC subtype. Therefore, it was investigated if any other recurrent chromosomal translocations or fusions are associated with *TFE3* translocation RCC.

Design: RNA-seq has been performed on *TFE3* translocation RCC cell lines: UOK109 and UOK145 for unbiased detection of chromosomal translocations including *TFE3*. All potential translocations were detected with SOAPf------use [1] fusion detection pipeline (Version 1.26) plus several layers of additional filters. More *TFE3* translocation RCC samples in TCGA (The Cancer Genome Atlas) RNA-seq database have been analyzed for additional translocations/fusions by the same method.

Results: *PSF-TFE3* and *NONO-TFE3* translocations have been detected in UOK 145 and UOK109 cell lines, respectively. Onaverage, 1-2 translocations/fusions have been identified in the cell lines and 7 cases from TCGA RNA-seq database. Among these translocations/fusions, none of them are recurrent except *TFE3* related translocations/fusions.

Conclusions: There are on average 1-2 translocations in *TFE3* translocation RCC. However, except *TFE3* related translocations, none of them are recurrent. These translocations may be more likely to be secondary/passenger events during the carcinogenesis. This study further elucidates the important carcinogenic role of *TFE3* in this subtype RCC.

[1]. Jia W, Qiu K, He M, Song P, Zhou Q, Zhou F, Yu Y, Zhu D, Nickerson ML, Wan S, Liao X, Zhu X, Peng S, Li Y, Wang J, Guo G: SOAPfuse: an algorithm for identifying fusion transcripts from paired-end RNA-Seq data. Genome biology 2013, 14:R12.

1081 Distinguish Sarcomatoid Urothelial Carcinoma and Inflammatory Myofibroblastic Tumor By TERT Promoter Mutations

Xiaoyong Zheng, Jian Zhuge, John Fallon, Ximing Yang, Minghao Zhong. New York Medical College at Westchester Medical Center, Valhalla, NY; Northwestern University, Feinberg School of Medicine, Chicago, IL.

Background: Inflammatory myofibroblastic tumor (IMT) of the urinary bladder is an unusual spindle cell lesion that exhibits cytologic atypia, infiltrative growth, and mitotic activity mimicking malignant tumors, such as sarcomatoid urothelial carcinoma (UC). Most IMT are positive for cytokeratin. ALK reactivity was seen in 56% of cases. In addition, Absent ALK expression was associated with a higher age overall, subtle histologic differences, and death from disease or distant metastases (in a younger subset). Recently, *TERT* promoter mutations appear as marker of urothelial carcinoma. Therefore, it was investigated if *TERT* promoter mutations could be used to distinguish sarcomatoid UC from IMT.

Design: Cases of sarcomatoid UC and IMTs were collected. Slides were reviewed and selected to make sure that the lesion is at least >20% of all tissue. Macro-dissection was performed in some of cases. gDNA was extracted from those tissue. *TERT* promoter mutations were detected by standard PCR-sequencing.

Results: 20 cases of sarcomatoid UC were collected for this study. Sarcomatoid component were 5-90% of whole tumor. Most of tumors were predominantly located at bladder (with few from kidney and ureter). Other diversion components were squamous, glandular differentiation and small cell carcinoma. 17 cases (85%) were found to have *TERT* promoter mutations. In 9 cases of IMTs were collected for this study, 3 of them come from bladder; the others come from different body sits including Liver, lung and soft tissue. Most of the IMTs were positive for cytokeratin, negative for ALK. However, None of IMT was positive for *TERT* promoter mutation.

Conclusions: *TERT* promoter mutation could be a biomarker for sarcomatoid UC to distinguish from IMT. This assay can be potentially useful in some clinical setting, such as small biopsy specimen.

1082 Spatial-Temporal Analysis of Urothelial Carcinoma for TERT Promoter Mutations

Xiaoyong Zheng, Jian Zhuge, John Fallon, Minghao Zhong. New York Medical College at Westchester Medical Center, Valhalla, NY.

Background: Urothelial carcinomas (UC) are well known for multifocality and recurrence. Recent studies suggest that *TERT* promoter mutations could be a biomarker for the diagnosis or follow up urothelial carcinoma in urine. Therefore, the *TERT* promoter mutation status in those recurrent and multifocal urothelial carcinoma are important information for the utility of *TERT* promoter mutations as urothelial carcinoma biomarker.

Design: For recurrent UC, we collected cases from 10 patients, 23 specimens. For multifocal UC, we collected cases from another 10 patients, 25 different tumor sits. All slides were reviewed and selected to make sure that at least 20% of UC components are present. Macro-dissection was performed in some of cases. gDNA was extracted from those tissue. *TERT* promoter mutations were detected by standard PCR-sequencing.

Results: For recurrent UC, specimens from 8/10 patients were positive for *TERT* promoter mutations, the rest of 2 were negative for the mutations. Importantly, the mutation status were maintained in the recurrent UC. For multifocal UC, specimens from 7/10 patients were positive for *TERT* promoter mutations, the rest of 3 were negative for the mutations. Again, the mutation status were maintained in theses multifocal UCs, too.

Conclusions: We found that *TERT* promoter mutations status keeps consistently in recurrent and multifocal UC of the same individual. This indicates that carcinogenesis of recurrent and multifocal UC from the same individual are probably the same. Importantly, *TERT* promoter mutation would be a good biomarker for the patient whose previous UC were positive for the mutations.

1083 Interobserver Reproducibility in Grading "Poorly Formed Glands" as Gleason Pattern 4 Prostate Cancer Among Urologic Pathologists

Ming Zhou, Jianbo Li, Liang Cheng, Lars Egevad, Fang-Ming Deng, Lakshmi Kunju, Cristina Magi-Galluzzi, Rohit Mehra, Jonathan Melamed, Savvas Mendrinos, Adeboye Osunkoya, Gladell Paner, Steven Shen, Kiril Trpkov, Toyonori Tsuzuki, Tian Wei, Ximing Yang, Rajal Shah. Gleason Grading Collaborative Group, New York, NY.

Background: Gleason pattern 4 (GP4) prostate cancer (PCa) in needle biopsy is critical for patient management and prognostication. The 2005 ISUP modified Gleason grading system regards "poorly formed glands" as GP4. The diagnostic reproducibility is unknown.

Design: Digital images of 8 PCas representing a spectrum of well to poorly formed glands were used to query 17 urologic pathologists for the definition of "poorly formed glands". They were then asked to grade additional 23 PCa cases with poorly formed glands as GP4 or not. These cases were classified into 9 sub-groups based on the number of poorly formed glands (<5, 5-10, >10 in each focus) and location (immediately adjacent to, between and away from other well formed PCa glands) by two study authors before the study. A consensus diagnosis was defined as agreement by 75% participants.

Results: Of 8 images queried for the definition of "poorly formed" glands, 5 attained consensus. Small cancer glands with rigid but well-formed lumens were not considered "poorly formed". Small glands with no discernible lumens, elongated glands with compressed lumen and elongated small nests/cords with no discernible lumen were considered "poorly formed glands". The interobserver agreement for the definition of "poorly formed glands" is fair (kappa=0.35). The diagnostic agreement in 23 ases was fair (kappa=0.34) with 16 (70%) attained consensus. Focus with < 5 poorly formed glands regardless of their locations attained a consensus diagnosis of "not GP4" with a sensitivity, specificity and accuracy of 67% (4/6), 100% (10/10) and 88%, respectively. Focus with >10 poorly formed glands that are not immediately adjacent to other well-formed glands attained a consensus diagnosis of GP4 with a sensitivity, specificity and accuracy of 60% (6/10), 100% (6/6) and 75% (12/16), respectively. The last 3 cases did not achieve a consensus as the poorly formed glands were at the edge of the biopsy specimens. Majority of participants (15/17) would grade poorly formed glands as GP4 only when they retained poorly formed morphology in at least 2 levels.

Conclusions: The agreement for grading "poorly formed" PCa glands as GP4 is only fair among urologic pathologists. More studies are needed to better define "poorly formed" PCa glands. Focus with < 5 poorly formed glands regardless of their locations is not diagnostic of GP 4. Focus with >10 poorly formed glands that are not immediately adjacent to other well-formed glands are diagnostic of GP4.

Gynecologic and Obstetric Pathology

1084 Application of Standardised Tumour Regression Scoring Systems To Post-Neoadjuvant Serous Ovarian Carcinoma

Laura Aalto, Sine Phelan. University Hospital of Galway, Galway, Ireland.

Background: There is no standardised method for assessment of chemotherapeutic response in epithelial ovarian cancer (EOC). EOC is increasingly treated with neo-adjuvant chemotherapy (NAC), with interval debulking. The presence of more viable disease is a negative prognostic factor in advanced EOC post- NAC and there is a need for a reproducible method for the assessment of treatment response.

Design: The archive at UCHG was searched for cases of serous adenocarcinoma of ovarian/primary peritoneal origin resected from 2009 - 2013. 21 post-NAC resections were identified. Histology was reviewed and two well-established tumour regression grade (TRG) systems, usually applied to Gastrointestinal malignancies, were applied;- Mandard TRG and Dworak TRG,